Optimisation of multi-scale ventilated package design for next-generation cold chain strategies of horticultural produce

by
Tarl Michael Berry

Dissertation presented for the degree of Doctor of Philosophy in the Faculty of Engineering at Stellenbosch University

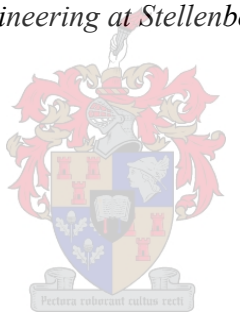

Supervisors: Prof. Umezuruike Linus Opara
Dr. Corné Coetzee

March 2017

DECLARATION

By submitting this dissertation electronically, I declare that the entirety of the work contained therein is my own, original work, that I am the sole author thereof (save to the extent explicitly otherwise stated), that reproduction and publication thereof by Stellenbosch University will not infringe any third party rights and that I have not previously in its entirety or in part submitted it for obtaining any qualification.

Date: .....March 2017.....

ABSTRACT

Corrugated fibreboard boxes (cartons) are used extensively in the cold chain to transport fresh produce from growers to consumers. These ventilated packaging systems have multi-scale structures and should facilitate suitable cooling of produce to preserve quality, protect against mechanical damage and enable efficient handling and transport. However, current designs often do not incorporate these factors and improved designs have been identified as part of new strategies to reduce postharvest losses and enhance overall cold chain efficiency.

The aim of this thesis was to develop improved fresh produce packaging designs through the use of a novel multi-parameter evaluation approach, within the scope of a multi-scaled packaging system. To this end, computational fluid dynamics (CFD) models and experimental box compression tests were used to evaluate new packaging designs, to quantify spatio-temporal moisture distributions in cartons during shipping and to increase packing densities in refrigerated freight containers (RFC).

Three new vent hole configurations were proposed and compared against an existing carton used for handling pome fruit. Results showed that the presence of trays reduced cooling efficiency by 31% in the standard commercial design. Conversely, the use of the newly proposed vent designs considerably improved both cooling efficiency and cooling uniformity by 48% and 79%, respectively.

Next, the effect of vent hole area and board material was investigated. Results demonstrated that significant improvements in both cooling efficiency and carton strength are possible, using alternative vent hole designs. Additionally, a significant interaction, with respect to mechanical strength, was observed between board material properties (board type) and the vent hole design. This finding indicates that high humidity conditions (i.e. refrigerated transport) can substantially influence the expected mode of failure in cartons (mechanical performance).

Furthermore, a CFD model was developed to predict spatio-temporal moisture distribution in cartons loaded in a RFC. The study of a standard shipping scenario showed that moisture gradients were relatively small, indicating that mechano-sorptive creep is likely not a major factor in this case. However, larger gradients are expected during less desirable conditions. These findings can be used as baseline conditioning treatments for future carton compression protocols.

Lastly, two unique packaging system strategies were proposed and evaluated for cooling efficiency. Although both showed generally improved performance, the “Tes” design increased packing density by 12% and forced-air cooling efficiency by 29%, compared to standard designs. Findings also showed improvements in vent hole design for vertical flow (RFC) are still possible.

Overall, research reported in this thesis contributes towards the development of a more optimal ventilated packaging design for use in the fresh produce cold chain. Significant advancements were also made with respect to the implementation of a multi-parameter evaluation approach, which should be further extended to future assessments of fresh produce supply chains both in academia and in commercial practice. Finally, significant knowledge gaps were revealed with respect to the mechanical performance of cartons under high humidity conditions. Future studies should therefore concentrate on the development of new predictive approaches to better assess the integrated performance of cartons under cold chain conditions.

OPSOMMING

Geriffelde veselbord bokse (kartonne) word op groot skaal in die koue ketting gebruik om varsprodukte te vervoer vanaf produsente na verbruikers. Geventileerde verpakkingstelsels het multi-skaal strukture en moet geskikte verkoeling van die produkte fasiliteer om gehalte te bewaar, die produkte te beskerm teen meganiese beskadiging en doeltreffende hantering en vervoer van die produkte in staat te stel. Huidige ontwerpe neem egter dikwels nie hierdie faktore in ag nie en verbeterde ontwerpe is geïdentifiseer as deel van nuwe strategieë om na-oes verliese te verminder en die algehele koue ketting doeltreffendheid te verbeter.

Die doel van hierdie tesis was om verbeterde verpakkingsontwerpe te ontwikkel deur die gebruik van 'n unieke multi-parameter benadering. Vir hierdie doel, is berekeningsvloeidinamika (BVD) modelle en eksperimentele boks druktoetse gebruik om nuwe verpakkingsontwerpe te evalueer, tydruimtelike vog verspreidings in bokse te kwantifiseer tydens vervoer en verpakkingsdigthede in verkoelde vraghouers (VVH) te verhoog.

Drie nuwe ventilasie gatkonfigurasies is voorgestel en vergelyk teen 'n bestaande boksontwerp. Resultate het getoon dat die teenwoordigheid van rakkies die doeltreffendheid van verkoeling in die standaard kommersiële ontwerp verminder met 31%. Aan die ander kant, het die gebruik van die nuwe voorgestelde ontwerpe verkoelingsdoeltreffendheid en verkoelingseenvormigheid onderskeidelik verbeter met 48% en 79%.

Die effek van ventilasie gat area en boks materiaal is ondersoek. Resultate het getoon dat beduidende verbeterings in beide verkoelingsdoeltreffendheid en bokssterkte moontlik is, deur alternatiewe ventilasie gat ontwerpe te gebruik. Daarbenewens is 'n beduidende interaksie, met betrekking tot meganiese sterkte, waargeneem tussen boks materiaal eienskappe en die ventilasie gat ontwerp. Hierdie bevinding dui daarop dat hoë lugvog toestande die verwagte wyse van meganiese faling in bokse aansienlik kan beïnvloed.

Verder is 'n BVD model ontwikkel om tydruimtelike voginhoud verspreidings te voorspel binne kartonne wat verpak is in 'n VVH. Die studie van 'n standaard verskeping scenario het getoon dat vog gradiënte relatief klein was, wat daarop aandui dat megano-sorptiewe kruip waarskynlik nie 'n belangrike faktor in hierdie geval is nie. Tog is groter gradiënte tydens minder wenslike toestande verwag. Hierdie bevindinge kan gebruik word as 'n basislyn kondisionering behandeling vir toekomstige boks druktoets protokolle.

Laastens, is twee unieke verpakkingstelsel strategieë voorgestel en geëvalueer vir verkoelingsdoeltreffendheid. Alhoewel beide oor die algemeen goeie resultate getoon het, het die "Tes" ontwerp in vergelyking met die standaard ontwerpe, die verpakkingsdigtheid met 12% en gevorseerde lugverkoelingsdoeltreffendheid met 29% verhoog. Bevindinge het getoon dat verbeterings in ventilasie gat ontwerp vir vertikale vloei steeds moontlik is.

Algehele navorsing berig in hierdie tesis dra by tot die ontwikkeling van 'n meer optimale ontwerp vir gebruik in die varsprodukte koue ketting. Beduidende vooruitgang is gemaak met betrekking tot die implementering van 'n multi-parameter evaluering benadering, wat verder uitgebrei moet word tot toekomstige assessering van varsprodukte voorsieningskettings beide in die akademie en kommersiëel. Ten slotte, is groot leemtes in bestaande kennis geïdentifiseer met betrekking tot die meganiese verrigting van bokse onder toestande van hoë humiditeit. Toekomstige studies behoort dus te konsentreer op die ontwikkeling van nuwe voorspellende benaderings om die geïntegreerde werkverrigting van bokse beter onder koue ketting toestande te evalueer.

ACKNOWLEDGEMENTS

I thank the South African National Research Foundation (NRF) for the award of postgraduate scholarship through the DST/NRF South African Research Chair in Postharvest Technology at Stellenbosch University.

I would also like to thank my supervisors Prof. Umezuruike Linus Opara and Dr. Corne Coetzee. A special thanks to Prof. Opara for this opportunity, your mentorship, inspiration and encouragement over the course of this PhD (and before). To Dr. Alemayehu Ambaw, thank you for your extensive help with the moisture transport modelling. In addition to Dr. Thijs Defraeye, who acted as a co-supervisor from the start of this project. He was always available for advice and encouragement, as well as input and support for the various challenges that arose. He has contributed considerably to this work and it is greatly valued.

I would also like to express my gratitude to the Department of Horticulture, where I initially started this research journey. Specifically, to Dr. Lynn Hoffman, who has shared advice and encouragement from before a MSc was even a possibility.

Most of all, I would like to thank my wife, Esmari, for your love, support and many late nights working on and reading through this thesis, none of it would have been possible without you. Also to my wonderful parents, Lynne and Mike Berry, as well as my younger sister, Kyla, for your support, encouragement and faith in me.

I would like to further express gratitude to the following organizations and people for sharing their assistance, technical advice and experience: Paper Sciences (Sappi Technology Centre), APL-Cartons, Tru-Cape, Two-a-day and NAMPAK. To Mr Jason Knock and Rene van der Westhuizen from Paper Sciences (Sappi Technology Centre), thank you for hosting our mechanical evaluation experiments and for all your advice. To Mr Henk Griessel from Tru-Cape, thank you for all your support, extensive advice and assistance with experiments. To Roche' Kenny and Dewald Grobbelaar from APL Carton for carton manufacturing. To Mr Isgaaq Adams from Two-a-day, for providing fruit and packaging used during this research. To Mr John Jones and Mr Florence Antoides from NAMPAK, for your advice and input. To Shelley Johnson and Renate Smit for your help with the controlled atmosphere and temperature chamber. To Jan Taljaard, for helping me with some late night model troubleshooting. And last but not least, to all my colleagues at SARChI Postharvest Technology, thank you my friends.

This work was based upon research supported by the South African Research Chairs Initiative of the Department of Science and Technology and National Research Foundation.

To my wife Esmari Berry, for all your love, encouragement and support; you are truly wonderful. To my parents for giving me the opportunity, and to the Lord for all Your grace, blessings and direction.

'Men became scientific because they expected Law in Nature, and they expected Law in Nature because they believed in a Legislator.'

Lewis, C.S., Miracles: a preliminary study,

Table of Contents

List of Figures

List of Tables

NOTE

This thesis presents a compilation of manuscripts where each chapter is an individual entity and some repetition between chapters, therefore, has been unavoidable.

List of contributions

A. Publications – Peer-reviewed journal papers

1. Defraeye, T., Cronjé, P., **Berry, T.M.**, Opara, U.L., East, A.R., Hertog, M.L.A.T.M., Verboven, P., Nicolaï, B.M., 2015a. Towards integrated performance evaluation of future packaging for fresh produce in the cold chain. *Trends Food Sci. Technol*. 44, 201–225.
2. **Berry, T.M.**, Defraeye, T., Nicolaï, B.M., Opara, U.L., 2016. Multiparameter analysis of cooling efficiency of ventilated fruit cartons using CFD: Impact of vent hole design and internal packaging. *Food Bioprocess Technol*. 9, 1481–1493.
3. **Berry, T.M.**, Fadiji, T.S., Defraeye, T., Opara, U.L., 2017. The role of horticultural carton vent hole design on cooling efficiency and compression strength: A multi-parameter approach. *Postharvest Biol. Technol*. 124, 62–74.

B. Publications - Peer-reviewed conference proceedings

Berry, T.M., Fadiji, T.S., Defraeye, T., Opara, U.L., 2016. Effects of horticultural carton vent hole design on cooling efficiency and compression strength. Proceedings of the 8th International Postharvest Symposium: Enhancing Supply Chain and Consumer Benefits - Ethical and Technological Issues conference: Cartagena, Spain. Submitted.

C. Conferences - Posters/Presentations

1. **Berry, T.M.**, Opara, U.L., 2016. Future design strategies for horticultural packaging and cold chain systems. Presentation at the HORTGRO Science Technical Symposium: Stellenbosch, South Africa, 2 June 2016.
2. **Berry, T.M.**, Fadiji, T.S., Defraeye, T., Opara, U.L., 2016. Effects of horticultural carton vent hole design on cooling efficiency and compression strength. Presentation at the 8th International Postharvest Symposium: Enhancing Supply Chain and Consumer Benefits - Ethical and Technological Issues conference: Cartagena, Spain, 21-24 June 2016.
3. **Berry, T.M.**, Fadiji, T.S., Defraeye, T., Ambaw, A., Opara, U.L., 2016. Impact of vent hole design on fruit cooling rate and carton strength: A multi-parameter evaluation. Poster presentation at Engineering and Technology Innovation for Global Food Security: An ASABE Global Initiative Conference: Stellenbosch, South Africa, 24-27 October 2016.

Chapter 1. General Introduction

1. Background

The South African fresh produce industry represents more than 3% of the country's gross national income, with over 3 million pallet stacks dispatched for long-haul export each year (PPECB, 2013). However, rapidly growing world populations, which are estimated to reach 9.1 billion by 2050, have highlighted an important need to increase the food availability. One method to achieve this goal is through significant reductions of postharvest losses, which are estimated to be around 15-30% worldwide (Fox and Fimeche, 2013; Gustavsson et al., 2011) and 20-25% in South Africa (Oelofse and Nahman, 2013). The development of improved packaging systems that better protect fruit from physical damage, such as bruising, and that facilitate improved cooling management are thus expected to play an essential role in reducing these losses (Opara and Pathare, 2014; Pathare et al., 2012).

Horticultural packaging is structured into multiple hierarchical components (multi-scale packaging) based on the level of packing complexity. At the most basic scale, fruit are packed using internal packaging, such as trays or liner bags. The next scale occurs when fruit and the internal packaging are packed into ventilated cartons. The individual cartons are subsequently stacked to form large pallet stacks, which are then loaded into holding areas (Ngcobo et al., 2013a; Robertson, 2013). Although these multi-scaled packaging systems increase packing density for more cost efficient shipping, it also increases the potential for excessive compression forces at the bottom cartons (Fadiji et al., 2016b). Furthermore, the multi-scaled packaging system creates additional barriers between the packed fruit and the surrounding refrigerated environment (Berry et al., 2015), reducing rates of heat transfer during pre-cooling (Pathare et al., 2012). Vent-holes are therefore regularly added to the cartons to improve air permeability into the pallet stacks (Opara, 2011). However, the use of more vent holes on a carton is limited, as the added open area severely compromises mechanical strength of the corrugated fibreboard cartons (Singh et al., 2008). Carton manufacturers thus often make use of additional material to increase strength, but this can significantly increase production costs, which is another important design restriction.

The maintenance of low fruit temperatures is one of the most important factors determining fresh produce quality preservation and therefore the produce shelf-life at the consumer end. Forced-air cooling (FAC) is commonly implemented to rapidly remove field heat from fruit packed in pallet stacks. Some countries, such as the USA also require a longer (> 3 days) secondary FAC treatment at low temperatures immediately before shipment, as a phytosanitary measure against invasive pests such as fruit fly (*Ceratitis capitata, C. rosa*). FAC treatment entails airflow being drawn horizontally through pallets using a fan system (Brosnan and Sun, 2001). The efficiency of the FAC process is influenced by the carton vent-hole design, which should be configured to minimise resistance to airflow and uniformly cool

produce (Defraeye et al., 2013a; Sevillano et al., 2009). Fruit cooling rate and uniformity is typically a function of the airflow rate and air temperature, as well as the resulting airflow distribution in the carton. These parameters are determined by interactions between the vent-hole design and the physical geometry within the carton, such as fruit size, fruit shape, packing configuration and use of internal packaging (Anderson et al., 2004; van der Sman, 2002). FAC is further an energy and time-intensive process that is mainly applied within a short harvest period (2-3 months). This places a high demand on the limited FAC facilities, which can result in fruit not being adequately pre-cooled. Packaging systems should therefore facilitate rapid cooling, while minimising power consumption in the FAC system.

After FAC treatment, palletised fruit may spend a significant period (1-5 weeks) being transported in refrigerated freight containers (RFCs). RFC transport is a critical step in the cold chain, presenting conditions that are considerably more challenging than during cold storage. RFCs also have smaller refrigeration units, as well as more challenging flow distribution systems and are thus less able to precool produce that has been loaded warm (Defraeye et al., 2016). This can result in high respiration rates and early fruit senescence in temperature sensitive fruit (e.g. pome fruit). Additionally, RFCs are substantially more susceptible to temperature fluctuations than cold rooms, for instance as a result of cold chain breaks, refrigeration cooling cycles (defrost cycles) and warm tropic areas. Packaging systems must consequently facilitate efficient vertical airflow through the respective pallet stacks.

Mechanical failure in the pallet stack is also usually reported during RFC shipping. This is often caused by one of the bottom carton(s) in a pallet stack failing under the large compression forces and can be triggered by the ships rocking motion or varying moisture contents (Twede and Selke, 2005a). An important parameter that is often not considered in package design, is thus the interaction between the corrugated fibreboard cartons and the high humidity conditions maintained in the cold chain. Although moisture loss from fruit has been considered in previous studies (Ferrua and Singh, 2009a; Sousa-Gallagher et al., 2013; Veraverbeke et al., 2003), no work has yet explored moisture adsorption and desorption into corrugated fibreboard cartons under cold chain conditions. This is a critical factor of carton mechanical strength, which is influenced by the spatio-temporal moisture content distribution in the corrugated fibreboard (Parker et al., 2006).

The design of packaging systems can also have important implications with respect to cold chain efficiency and transport logistics. For example, current packaging systems only utilise about 90% of the RFC floor area. The introduction of packaging designs that improve packing density could therefore significantly reduce transport costs as well as decrease carbon emissions during transit.

The discussion above highlights a rather dynamic cold chain, for which packaging systems perform multiple functions (packaging functionalities) across various cold chain steps. Previous studies examining improved ventilated package designs have mostly focused on one performance parameter per study, such as cooling rate (de Castro et al., 2004a; Dehghannya et al., 2008), resistance to airflow (Ngcobo et al., 2012a; Vigneault et al., 2004b) or mechanical strength (Han and Park, 2007; Singh et al., 2008). Many of these studies also do not include the presence of internal packaging (Dehghannya et al., 2008; Delele et al., 2008) and often only evaluate a single carton, without considering the impact of larger packaging scales (e.g. pallet stacking, RFCs). Alternatively, studies evaluating cold chains at larger scales (porous media), frequently ignore the geometrical details of packaging material (Ambaw et al., 2013a; Zhao et al., 2016). This has made the implementation of improved packaging designs challenging at commercial levels, resulting in effectively no developments in the standard vent hole design (central oblong vent hole) over the last few decades.

Similarly, commercial evaluation also often relies on a single performance parameter (usually mechanical strength). Most package designs used in the fresh produce industry have originated from a process of trial and error, resulting in carton designs which are frequently not optimized for the dynamic needs of the fresh produce cold chain (Berry et al., 2015). The South African fresh produce industry could therefore also benefit significantly from a more integrated multi-parameter approach.

Ventilated cartons packed with fruit generally have confined geometries making the simultaneous monitoring of multiple performance parameters such as cooling and airflow characteristics challenging, as in these cases the presence of the measurement apparatus can significantly alter the results (Ngcobo et al., 2013a, 2012c). Furthermore, manufacturing and experimental setup of multiple package designs can be resource and time intensive. Computational fluid dynamics (CFD) modelling therefore provides a convenient alternative, capable of producing data at high resolutions in combination with performance parameters that would not normally be possible to derive experimentally (Defraeye et al., 2013a). An example is the convective heat transfer coefficient, which can be useful for the identification of areas where fruit may be more susceptible to chilling injury or where fruit cool slower.

The above discussions shows the value of a multi-parameter design approach. Where multiple performance parameters are used to quantify the value of a specific package design and therefore guide decisions regarding trade-offs. To this end, next generation packaging should be optimised so that the cost of manufacturing and handling is appropriately balanced to the benefits of factors such as fruit packing density, mechanical protection and maintenance of temperature to preserve fruit quality.

2. Objectives and contributions

The aim of this PhD thesis was, therefore, to gain a better insight into the cooling efficiency of the produce-packaging system at different levels of multi-scale packaging. To this end, a more optimised design of ventilated packaging was pursued based on a multi-parameter approach, which integrated the effects of the various packaging components (multi-scale packaging) to evaluate cooling performance, FAC energy consumption and fruit quality preservation.

The specific objectives were to:

a) Develop a validated computational fluid dynamics (CFD) model capable of predicting transfer processes (airflow, heat and moisture) in multi-scale structured horticultural packaging systems.

b) Apply CFD modelling to analyse the performance of cooling operations and packaging design using a multi-parameter approach.

c) Investigate moisture properties in packaging during long term transport under high humidity conditions.

d) Based on the insights gained from the above objectives, design next-generation optimal multi-scale ventilated packaging for postharvest handling of fresh produce, under improved utilisation of refrigerated freight container space.

Chapter 2. Factors Affecting Design and Performance of Ventilated Carton in the Fresh Produce Cold Chain – An Interpretive Review*

Abstract

Horticultural packaging is an important component in the cold chain and influences both the preservation of fresh produce quality, as well as overall cold chain efficiency. Many package related studies, however, are currently missing a method to incorporate the numerous challenges influencing package design. This article provides a summary of the current approaches used to design packaging systems and investigates some of the main interactions, mainly between cooling and mechanical strength, affecting design decisions. Consequently, recent studies towards an optimised package design were reviewed, within the scope of the various cold chain steps. Multiple knowledge gaps in the areas of cooling and mechanical strength were identified, particularly for stacked packages and cartons packed with internal packaging. Future prospects indicate the use of a multi-parameter evaluation (cooling, energy, strength, cost, packing density, produce quality preservation) approach. Furthermore, assessments will also be guided by a clearly defined design space (multi-scale packaging), with an emphasis on meeting all packaging requirements for each of the anticipated cold chain steps.

*Sections of this work have been published in:

Defraeye, T., Cronjé, P., **Berry, T.M.**, Opara, U.L., East, A.R., Hertog, M.L.A.T.M., Verboven, P., Nicolaï, B.M., 2015a. Towards integrated performance evaluation of future packaging for fresh produce in the cold chain. *Trends Food Sci. Technol*. 44, 201–225.

1. Introduction

The challenge of reducing postharvest losses of fresh produce has been gaining attention as a result of the ecological, economical and societal impacts. Studies by the Food and Agricultural Organisation (FAO, 2013, 2009) have shown that due to postharvest losses, over one-third of all food that is grown is not consumed. Furthermore, in South Africa, processing and packaging-related fresh produce losses equal 20-25% (Oelofse and Nahman, 2013). According to the United Nations (2015), it is a reduction in these postharvest losses and not an increased production that will play a greater role in sustainably feeding the world's population in the future. Improvements in cold chain techniques and technologies are, therefore, vital to reduce postharvest losses, as well as to improve fresh produce quality preservation in the cold chain so that more produce is actually consumed.

The cold chain, which is a part of the overall supply chain, is defined as a sequence of steps that fresh produce are subjected to under refrigerated conditions, from production to consumer. These respective steps can be categorised into either pre-cooling, storage, handling or transport. Most postharvest losses can be attributed either directly or indirectly to unfavourable conditions within the cold chain. This includes inadequate temperature regulation, inappropriate atmospheric conditions (modified atmosphere) or physical abuse (vibration, impacts and compression). Furthermore, combinations of these inappropriate conditions can be accumulative, with respect to reduced quality preservation. This indicates that if the product is not immediately lost, it will likely have a reduced shelf-life period or reduced consumer acceptance level (Kader, 2002).

In the cold chain, horticultural packaging must perform many functions under diverse physical and environmental conditions. The specific performance criteria of a packaging system is to facilitate temperature treatments, protect produce from mechanical damage, create desirable atmospheres around the produce by ventilation and expedite fresh produce packaging, processing and handling in the supply chain (Robertson, 2013). Furthermore, the requirements for each performance criterion are unique and depend on the produce type, region of production/distribution and the available infrastructure. The many packaging requirements and performance criteria have resulted in a plethora of different packaging designs on the market, for example, over 11 unique designs (several sub-designs of each) for pome fruit in South Africa alone (Berry et al., 2015). However, despite the many available designs, there is still considerable room for improvement, namely to reduce postharvest losses, energy consumption and packaging material (Ambaw et al., 2013a; Defraeye et al., 2015a; Jedermann et al., 2014).

Many studies have investigated package design for the horticultural industry. However, most focused on individual package functionalities and included: (i) product pre-cooling performance (de Castro et al., 2005a), (ii) package ventilation, (iii) energy consumption (Thompson et al., 2010), (iv) mechanical strength (Frank,

2014; Pathare et al., 2012; Pathare and Opara, 2014) and (v) product quality. Although these topics are of critical importance to the horticultural industry, they are often examined separately and lead to recommendations that can neglect other important performance parameters. The performance of a packaging design in each respective cold chain step should be considered before settling on a final design (Defraeye et al., 2015a). The result of studies lacking in this synergetic approach can be credited as the source of many differences in recommendations between past research (1960-1980) and current studies in various package design areas, as noted by Maltenfort (1989), Van Zeebroeck et al. (2007) and Frank (2014).

The purpose of this study was to identify the current design considerations used to design horticultural packaging systems, to identify factors affecting design decisions within complex and dynamic cold chain systems and to identify research opportunities. To this end, first, a review of current package design approaches was performed. Second, factors affecting fresh produce package designs within the overall cold chain were examined, with a specific focus on packaging systems using corrugated fibreboard cartons, which is one of the most common packaging types used for export (Berry et al., 2015). Third, a review of recent studies concerning carton design was performed within the scope of the listed design approaches and previously mentioned design factors, which raises knowledge gaps and emphasises future research directions.

2. A packaging design framework

Various approaches have been applied to investigate horticultural package design in the cold chain. However, a challenge to the development of more optimal package designs has been the difficulty of up-scaling findings to commercial levels and linking findings between related studies. Often, this is simply a result of a study being too specific, which can limit further development into other areas. An important approach that can aid in this regard, is the use of a multi-scale packaging perspective, which delineates the packaging systems and components into several levels of increasing complexity (Ngcobo et al., 2012a). However, before addressing this approach, the horticultural packaging nomenclature is defined.

2.1 Packaging nomenclature

The nomenclature for the various types and components of horticultural multi-scale packaging is extensive. It is common to find the same term being used to describe many different packaging components, for example, “container” when referring to cartons, plastic crates and shipping containers (Jedermann et al., 2013; Laniel et al., 2011; Vigneault and Goyette, 2002). Furthermore, the use of nomenclature systems from other packaging industries are often not appropriate (Hellström and Saghir, 2007; Schuur, 1988), due to the additional complexity (e.g. internal packaging) present in many fresh produce packaging structures. The following system of nomenclature is defined to clearly distinguish between the various components in the cold chain.

The term "horticultural-box" (Figure 2.1) is proposed here and defined as a quadrilateral prism (usually rectangular) intended for stacking on pallet bases to form "pallet stacks" (Figure 2.1). The pallet stacks are further packed into "refrigerated freight containers" (RFC) for extended journeys by either sea (ship), road (truck) or rail. The various horticultural-boxes encompass plastic crates and cartons (usually with vent holes) and exclude all packages incompatible with pallet stacking (e.g. bags and baskets). The packaging types inside a horticultural-box are further defined as "internal packaging" (Linke and Geyer, 2013; Thompson et al., 2010) and include "trays", "carry bags", "clamshells" and "liner bags" (Figure 2.1).

2.2 Multi-scale approaches

The components making up fresh produce related structures are arranged in specific patterns of organisation and span multiple scales (multi-scale). For example, fresh produce such as a pome fruit consists of various tissue types (mesocarp, endocarp, epicarp, seed), which are made up of various differentiated cells and in turn consist of intracellular organelles. Finally, the individual organelles each consist of many micro- and macro-molecules, which together perform the biochemical processes in the fruit. The use of a multi-scale modelling approach has been discussed extensively by Ho et al. (2013), to reduce computational complexity when modelling food structures. This entails features at the micro-scale (e.g. cells) not being modelled explicitly, but incorporated through an averaging procedure into a macro-scale (e.g. whole apple) model. A multi-scale modelling approach thus models a complex structure into an interconnected hierarchy of components.

At the opposite end of the scale, packaging systems used to handle and transport fresh produce also follow a multi-scale structure. Figure 2.1 shows the five main levels in a multi-scale packaging system:

1. A single fruit, which can be packaged individually by wrapping
2. Multiple fruit packed either in bulk (loose) or in/on internal packaging (e.g. carry bags, liner bags, trays)
3. Horticultural-box (e.g. carton, plastic crate)
4. Pallet stack
5. Holding area for the individual pallet stacks (e.g. cold room or RFC).

With respect to packaging systems, multi-scale modelling has most frequently been used to model pallet stacks and fruit bins in large refrigerated holds, such as refrigerated transport (Hoang et al., 2012) and cold rooms (Ambaw et al., 2014; Delele et al., 2009) using porous media approaches. Multi-scale modelling, therefore, provides a valuable approach to assess large packaging structures, with complex interactions.

Aside from modelling, the multi-scale approach should also be extended to evaluations at lower scales, so that the effects at higher scales are included. For instance, many studies have investigated forced-air cooling through either

individual cartons (Delele et al., 2013a, 2012) or a single layer of a pallet stack (Defraeye et al., 2013a; Ngcobo et al., 2012a). This approach provides useful insight into how a package may perform at larger scales (holding area). However, recommendations from this approach should always be made in the context that unforeseen interactions may occur at higher scales, such as vent misalignment during stacking, pallet slats blocking vent holes at the bottom of a pallet stack (Figure 2.2) or uneven air distribution in the holding area (e.g. RFC).

A similar challenge is found in the assessment of pallet stack compression resistance, which is often done by evaluating individual empty cartons (box compression tests; BCT). This approach is used since compression tests on fully loaded pallet stacks are rarely feasible. However, the compression resistance and failure pattern of an individual carton is generally very different compared to a carton stacked in a pallet stack (Frank, 2014; Opara and Pathare, 2014; Pathare and Opara, 2014). This is attributed to how the individual carton walls support each other inside the stack, but not along the pallet sides. Furthermore, pallet stacks usually fail through a tipping motion, resulting in large forces at one of the cartons corners (Kellicutt, 1963). Box compression tests on individual, empty cartons are currently the most widely accepted method for testing a pallet stack's performance (ASTM, 2010; TAPPI, 2012). However, no reliable method is available that can accurately link BCT results to performance at higher scales (Frank, 2014). The use of a multi-scale method in the design and evaluation of packages is an important approach, as each packaging scale can significantly influence factors at both higher and lower scales.

Future studies relating to fresh produce packaging, therefore, need to better incorporate the effects of higher scales (stacking or holding area) into evaluations at lower scales (individual cartons), as well as the effects of lower scales in large scales.

2.3 **Multi-parameter approach**

Past studies investigating packaging design have typically focused on only a few package functionalities at a time, which can result in designs with contradictory requirements. For example, increasing carton vent hole sizes can improve cooling rate performance, but as a result may have compromised mechanical strength. Trade-offs between the various packaging functionalities are an important aspect of package design and an optimal balance can thus only be determined by assessing all applicable package functionalities at the same time (multi-parameter evaluation). Table 2.1 lists the most relevant packaging functionalities and corresponding performance parameters. Some of the main parameters relating to the discussions above are addressed in the sub-sections below. For conciseness, the packaging functionalities and performance parameters are discussed in the context of a single package, although, most can be extended to larger scales (pallet, cold room, RFC).

2.3.1 Fresh product cooling

Packaging should facilitate rapid (within produce tolerances) and uniform precooling treatments, to quickly remove undesirable heat from fresh produce after harvest or after a break in the cold chain. Quantifying the duration and rate of cooling is particularly relevant for precooling, as this determines how fast field heat can be removed (Brosnan and Sun, 2001). These quantities not only affect product quality and shelf life, but also the functional time the precooling equipment needs to run, and thus the related operational costs and total product throughput.

Cooling time

Product cooling is usually evaluated by the fractional unaccomplished temperature change *Y(t)*, as determined from the temperature-time profile (Eq. (2.1)) of the internal product (pulp) temperature (T_f; °C):

$$Y = \frac{T_f - T_a}{T_i - T_a} \tag{2.1}$$

T_i and T_a (°C) are the initial product temperature and the set cooling air temperature, respectively. Different temperatures T_f can be used to define Y: the pulp temperature in the centre of the product ($T_{f,c}$), which is often obtained experimentally from thermocouple measurements or the volume-average product temperature of an entire fruit ($T_{f,avg}$), which can be obtained from numerical modelling (computational fluid dynamics; CFD). The choice of T_f critically affects the value of Y, as typically $T_{f,c} > T_{f,avg}$, although a breaks in cooling may result in $T_{f,avg} \geq T_{f,c}$ (ASHRAE, 2000a; Berry et al., 2016; Brosnan and Sun, 2001).

The cooling time is evaluated based on the dimensionless cooling curve *Y(t)* by determining the half cooling time (HCT, $t_{½}$; Eq. (2.2)) or seven-eighths cooling time (SECT, $t_{⅞}$; Eq. (2.2)) (Table 2.1). These are the times required to reduce the temperature difference between the product and the cooling air by half ($Y = 0.5$) or seven eighths ($Y = 0.125$). In principle, the HCT and SECT can be assumed independent of the temperature difference (T_i - T_a), but in practice, slight differences in HCT and SECT will occur (Berry et al., 2016; Defraeye et al., 2014).

$$t_{7/8} = \frac{\ln(8j)}{C};\ t_{1/2} = \frac{\ln(2j)}{C} \tag{2.2}$$

where j is the lag factor and C is the cooling coefficient.

Cooling rate

A more indirect measure of the cooling rate is the convective heat transfer coefficient (CHTC; W m^{-2} K^{-1}) at the surface of the produce (Kondjoyan, 2006). In this context, the CHTC is a defined parameter, which relates the convective heat flux normal to the surface ($q_{c,w}$; W m^{-2}), i.e., at the air-product interface, to the difference between the surface temperature (T_w; °C) and a reference temperature (T_{ref}; °C), for which often the set air temperature (T_a) is taken: CHTC = $q_{c,w}/(T_w - T_{ref})$. An advantage of CHTCs is that the value is relatively independent of the heat transfer rate magnitude, as it incorporates the temperature difference (T_w - T_a). It should be noted, other T_{ref} values can be used, which will influence the CHTC outputs (Defraeye et al., 2013a).

Cooling uniformity

Cooling uniformity (i.e. homogeneity) between individual products within a box, stacked boxes on a pallet or between pallets in a RFC is critical for ensuring uniform fruit quality preservation throughout the cold chain. Cooling uniformity has mainly been quantified by evaluating variation in cooling time across a packed product (de Castro et al., 2004b; Defraeye et al., 2014) or across the CHTC distribution (Defraeye et al., 2013a). Several methods have been used in past studies, for example, a heterogeneity index (Dehghannya et al., 2011). However, they all generally use a similar approach, which is to calculate the relative standard deviation (RSD), either for a single location or for the whole system. The RSD relates the standard deviation to the mean, is expressed as a percentage and can be calculated with either the cooling time or CHTC. Is should be noted that airflow uniformity/heterogeneity have been quantified using similar approaches (de Castro et al., 2005a, 2005b; Dehghannya et al., 2008; Vigneault et al., 2007).

2.3.2 Package ventilation

The package ventilation potential is mainly determined by the “accessibility” of airflow to the produce. In practice, box ventilation is facilitated by ventilation openings (vent holes) on individual boxes and vent hole alignment during pallet stacking.

Ventilation potential

The airflow rate through a box or pallet stack is widely used and is preferably expressed in L s^{-1} kg^{-1} of the produce. These units make the airflow rate independent of the fruit quantity. Airflow rates typically range from 1 to 3 L s^{-1} kg^{-1} for FAC (Brosnan and Sun, 2001; Thompson, 2004; Thompson et al., 2008) and 0.02-0.06 L s^{-1} kg^{-1} for refrigerated containers (Defraeye et al., 2015c).

The total ventilation area percentage (TVA; %) is frequently used in guidelines on packaging design as a measure for the ventilation potential. It is the amount of vent area relative to the total area of that specific side of the box. More detailed vent

opening characteristics, such as size, shape, number and position, are inherently related to the TVA. The TVA is often correlated to the flow resistance of the box (pressure drop), cooling efficiency (de Castro et al., 2004b; Vigneault et al., 2004b; Vigneault and Goyette, 2002) and mechanical strength of boxes (Singh et al., 2008).

Bypass flow

Preferential airflow pathways, where air bypasses sections of the produce or packaging, can occur due to obstructive internal packaging inside boxes, improper stacking (vent hole misalignment), the packaging system itself (Defraeye et al., 2013a; Ferrua and Singh, 2009b; Vigneault and Goyette, 2003) or inadequate sealing of gaps in RFCs (Fraser and Eng, 1998). For example, preferential airflow pathways can occur in the open air space between the pallets and the container door (section 4.3.1). Airflow bypass is not always a negative phenomenon, since ratios of the colder air can potentially reach packed produce further downstream and therefore improve cooling uniformity (Defraeye et al., 2015b; Ferrua and Singh, 2011a). Additionally, air bypass can also reduce fan power consumption, by decreasing the systems airflow resistance. Air bypass can be quantified as the percentage of air bypassing the produce, ($kg_{air,byp}/kg_{air}$; air loss ratio) (Vigneault and Goyette, 2003).

2.3.3 Energy consumption related to package design

One way to optimise energy efficiency of the cold chain is to design more energy-efficient packaging systems. In this review, it relates to the energy consumed by the ventilation system (fan) to maintain airflow through the boxes during precooling, transport and storage. Other package-related energy-efficient measures can be used in packaging production, transport and recyclability (Opara and Mditshwa, 2013), but are not covered here.

The largest energy savings in refrigerated containers are currently expected to lie in optimising fan operation (GDV, 2014). For instance, Thompson et al. (2010) showed that the forced-air cooling process consumes about 45% of electricity usage, whereas electricity relating to fruit refrigeration is equivalent to 36%. Additionally, during long-haul transport in refrigerated containers, fans often run continuously at a relatively high power (e.g. ≈ 2 kW for a 40’ refrigerated container with a total consumption of roughly 7-15 kW).

Aerodynamic resistance

The aerodynamic (airflow) resistance of the produce-packaging system (Eq. (2.3)) is expressed as the relation between the total pressure drop over the packaging (ΔP; Pa) and the volumetric airflow rate through it (G; $m^3\ s^{-1}$):

$$\Delta P = \xi G^2 \tag{2.3}$$

where ξ is the pressure loss coefficient ($kg\ m^{-7}$). This pressure drop only accounts for inertial effects (Forchheimer term). The viscous effects (Darcy term, ~ G) only become important at very low flow speeds (typically ~ 0.0001 $m\ s^{-1}$ for refrigeration applications) and were found to be negligible for most horticultural cold chain applications (ASHRAE, 2009; Verboven et al., 2006).

The power required to push air through the packaging (w ; Eq. (2.4); W) can be determined as (Defraeye et al., 2014; Ferrua and Singh, 2011a):

$$w = \Delta P G = \xi G^3 \tag{2.4}$$

The power usage (w) only contains the contribution of the packaging. The aerodynamic resistance of other system components, therefore, has to be accounted to determine the system curve (Eq. (2.3); (ASHRAE, 2009, 2000b)). Packaging is often a major contributor to the system curve, particularly in FAC cases (de Castro et al., 2005a), where the packaging substantially increases airflow resistance. The working point of the system is determined by the intersection of the system curve and fan performance curve. The total fan power consumption also depends on the fan and motor efficiencies (η_{fan} and η_{motor}; (Baird et al., 1988)). However, fan types vary considerably between cooling facilities. Studies, therefore, usually do not consider the power usage contributions for particular systems.

Package-related energy consumption

The package-related energy consumption (E; J; (Defraeye et al., 2014; Ferrua and Singh, 2011a)) is defined here as the energy required to force airflow through a box or a palate stack. It is calculated by multiplying the corresponding power w (Eq. (2.5)) with the required (pre)cooling time (e.g., $t_{⅞}$).

$$E = wt = \Delta P G t \tag{2.5}$$

E only accounts for the contribution of the packaging and not of other system components or fan efficiency. This enables a direct comparison of the energy efficiency of different package designs, the amount of boxes or the stacking pattern that contributes to package-related energy consumption. *E* can thus be quantified throughout all cold-chain unit operations (precooling, transport and storage).

2.3.4 Fresh produce quality preservation

Packaging systems should facilitate appropriate conditions to preserve fresh produce quality and enhance shelf-life periods. For instance, limiting conditions prone to decay (e.g. condensation) or physiological disorders (e.g. chilling injury) and reducing moisture loss (Maguire et al., 2001) which can lead to shrivel. In contrast to most package functionalities (Table 2.1), inappropriate cold chain conditions can have an accumulative effect with respect to reduced quality preservation and thus potential increases in postharvest losses. The rate of produce maturation (i.e. the development towards a ripened state) is also directly related to the respiration rate and therefore product temperature over the course of the cold chain. Fruit maturity is often monitored using total soluble solids content (°Brix), titratable acidity, flesh firmness (N, kg) or skin colour (Laguerre et al., 2013).

2.3.5 Carton mechanical strength

Boxes need to be sufficiently strong to protect the produce during handling, transport and storage. This strength requirement limits the amount of vent holes that can be used (TVA) in a box made out of a given material (e.g. corrugated fibreboard), and also affects their size, shape and position.

Compression strength and stacking strength

The compression strength is measured using box compression tests (BCTs). BCTs evaluate the compressive force (N) versus the cross-head displacement (m) in a load-deflection curve (Frank, 2014). The compression strength is then defined as the peak force (N) or the peak force up till a pre-specified deformation distance. The latter is relevant as the position of produce in a box determines the maximum allowable deformation before compression causes damage to the produce.

Package cushioning

Packaging provides protection from shocks and vibrations during transport and handling. The resilience to shocks, so sudden increases and decreases in acceleration, is often quantified. This is done by evaluating the peak acceleration as a function of the static load (Pa) for different drop heights, which leads to an ensemble of so called dynamic cushioning curves (Guo et al., 2011, 2010; Wang, 2009).

Fruit abrasion and bruising damage as a result of vibration often occurs at a specific vibration resonance frequency. It is therefore necessary to perform vibration evaluations across a range of frequencies. Resilience to vibrations is mostly quantified by evaluating the vibration transmissibility (dimensionless) versus frequency (Hz) for different static loads (weight; Pa) (Guo et al., 2011). As an alternative, the power density (m s^{-2} Hz^{-1}) versus frequency (Hz) has also been used (Jarimopas et al., 2005).

2.3.6 Multi-parameter evaluations and trade-offs

A multi-parameter evaluation is achieved by assessing all relevant package functionalities simultaneously, using associated performance parameters as determined from experimental or numerical assessments. The sections above briefly addressed some of the more prominent performance parameters and is more extensively addressed by Defraeye et al. (2015a). Table 2.1 also provides a more extensive list of packaging functionalities and corresponding performance parameters, some of which have been used in previous studies. One packaging functionality very rarely approached is that of packaging logistics. In this case, functionalities such as ergonomics, RFC floor usage, packing density and manufacturing costs are listed and highlight important aspects that need to be addressed in future studies.

3. The cold chain design space

The various unit operations making up a cold chain each have unique conditions and different challenges. For instance, fresh produce undergoing precooling are often exposed to conditions that can induce chilling injury. Furthermore, packages undergoing transport related unit operations are often subjected to mechanical loads (impacts and vibration). Packaging systems must, therefore, be designed to cope with each of these different conditions. An example of the apple fruit cold chain is briefly discussed below to better emphasise these different conditions.

Figure 2.3 shows a simplified schematic of the possible steps used in the apple fruit cold chain. The figure also highlights steps where cold chain breaks can occur and is usually a result of handling in unrefrigerated conditions or from a loss of power. Initially, fruit is harvested into bins and then transported to refrigerated storage rooms (de Vries et al., 2003; Kader, 2002; Thompson et al., 2008). Precooling is often carried out to remove the remaining field heat using room cooling (produce type and cultivar dependent), after which apple fruit can be stored for extended durations (Thompson et al., 2002). After initial storage, fruit are transported to a packhouse where they are sorted, graded, packaged and then palletised. Packhouse operations are typically performed in a non-refrigerated environment and this represents a significant break in the cold chain. Packaging forms a thermal barrier around the produce, which necessitates the use of forced-air cooling (horizontal airflow; section 4.1) to rapidly remove excess heat. After cooling, the pallet stacks are transported to another refrigerated storage room (section 4.2), where they are

kept until transport. Pallet stacks are then packed into RFC (vertical airflow; section 4.3) and transported by truck/rail to the next link in the cold chain. This is often a wholesale or retail distribution facility (section 4.4), alternatively the produce are taken directly to a harbour and shipped to another region. After delivery to the retail distribution area, fruit may be re-packed into appropriate units and distributed to individual retail outlets for sale to consumers (Thompson et al., 2002).

Optimal carton designs are guided by three main competing factors as depicted in Figure 2.4. Namely, (i) ventilation, for cooling and to maintain desirable conditions; (ii) mechanical performance, for protection of produce against mechanical forces (compression, impacts and vibration) and; (iii) cost, which includes factors such as power consumption and manufacturing/material costs (Robertson, 2013; Thompson et al., 2008, 2002). An additional factor is ergonomics, whereby design features needed for package compatibility with a specific cold chain, may compete with the three factors listed above. The identification of an optimal box design is thus only possible when the requirements for each of these factors are met, as indicated by the "improved design" region (Figure 2.4). As an example, vent holes are essential to regulate environmental conditions but can significantly compromise package mechanical strength. Although thicker corrugated fibreboard can enhance the strength, this can significantly increase manufacturing costs (e.g. quantity or quality of material). Design decisions should, therefore, always be made within the context of cost, while still facilitating the desired conditions around the produce.

3.1 **Role of packaging in preserving produce quality**

3.1.1 Respiration and senescence

The effect of package design on produce temperature is one of the most important factors influencing overall design. Maintaining low-temperature conditions is critical to minimise fruit respiration rate and thereby preserve quality. Fruit respiration rates can increase by a order of 2 to 3 (depending on fruit type) for every 10 ºC increase in temperature (Salisbury and Ross, 1991). This exponential relationship between temperature and respiration rate means that fruit kept at field temperatures after harvest will respire more in a few hours than they would over several weeks at optimal storage temperatures. To this end, packaging should enable the cooling of produce, which can increase in temperature as a result of breaks in the cold chain, environment and fruit respiration.

Insufficient package ventilation can result in inadequate cooling and increases the risk of fresh produce decaying by microorganisms. Various microorganisms such as bacteria (e.g. *Botrytis cinerea*) and fungi (e.g. *Penicillium*) propagate more quickly at higher temperatures and in produce that have been damaged as a result of freezing or mechanical damage (Simko et al., 2015). Proliferation of these opportunistic decay-causing organisms can occur due to "hot spots" inside the package as a result of uneven cooling (East et al., 2007). Packed produce should, therefore, be well ventilated to enable rapid evaporation of condensed moisture, as this can induce microbial growth (Larsen et al., 2015).

3.1.2 Physiological disorders

Although low-temperature storage is an important component to preserve fruit quality, the temperature should be carefully regulated, as excessive cooling rates and storage temperatures can induce chilling injury. Qualitatively, chilling injury can cause poor aroma, off-flavour development and impaired ripening. The physiological effects of chilling injury are diverse and often more prominent in certain produce types (Wang, 1990). While the mechanisms are not yet fully understood, low-temperature stress conditions can lead to various physiological disorders linked to damage of the lipid cell membrane. Consequent damage to the cell membrane results in secondary damage due to increased reactive oxidative species in the cell (Kratsch and Wise, 2000; Vigh et al., 1998). Symptoms can include internal and external (scald) browning, uncharacteristic yellow colouring, depressions in the skin, water infiltration into intercellular spaces, woolly or dry pulp texture, decreased mechanical resistance (softening) and increased susceptibility to microbial decay (Sevillano et al., 2009).

Chilling injury has severe economic repercussions on commercial export markets that make extensive use of long-haul cold chain systems to reach distant markets. To avoid conditions prone to chilling injury, package designs should be configured to evenly distribute cooling airflow throughout a pallet stack to minimise possible "cold spots". Additionally, vent hole designs that direct incoming air into high velocity air jets should be avoided if sub-optimal temperatures are being used, as this can potentially over chill nearby fruit (Defraeye et al., 2014). This is particularly true for packages near refrigeration outlets of holding areas, where air is coldest (Moureh et al., 2009b).

Chilling injury sensitive fruit are often shipped at below optimal temperatures to reduce respiration rates over the transit period and thus attain acceptable shelf life periods at retail. However, exposure to low-temperatures for extended durations can result in higher incidences of chilling injury. As a solution, the use of specific dual temperature (intermittent warming) treatments during transit have been shown to both repair damage as a result of chilling injury and improve cell membrane resistance against further damage. These temperature regimes work by stressing the fruit and encourage the production of stress proteins and higher quantities of unsaturated fatty acids in the cell membranes (Wang, 1990). However, treatments

must be implemented for extended durations, often during transit, for example, increasing temperatures from 5°C to 20°C for 24 hours every week of storage (Xi et al., 2012). Packaging systems should, therefore, be matched to the available cooling facilities so that cooling rates do not exceed tolerable rates and produce are cooled evenly. Additionally, packaging systems used for intermittent warming will require a higher emphasis on ventilation design so that the fresh produce can be properly heated and cooled to meet the treatment requirements.

3.1.3 Phytosanitary treatments

The elimination of pests being exported with packaged produce is of high concern for fresh produce export. Accidental introduction of a foreign pest into other production regions could cause considerable damage to local crops and ecology due to a lack of natural protection mechanisms. Many countries have introduced strict guidelines that require phytosanitary treatments for fresh produce being imported from high risk areas (Melo et al., 2014). Typically, regulations avoid the use of chemicals and instead prefer the use of temperature treatments (Birla et al., 2005). The South African citrus industry, for example, regularly makes use of low-temperature treatments for the disinfection of false codling moth larvae (*Thaumatotibia leucotreta*) and fruit flies (*Ceratitis capitata* and C. *rosa*). The treatment incorporates the use of sub-zero temperatures (~-0.5 ºC) for periods of about 18-days. This is considerably lower than normal storage conditions (~4-7 ºC) and so increases susceptibility of chilling injury in fruit (Defraeye et al., 2016; Wang et al., 2001). However, such temperature treatments make it more difficult to cool the fruit, due to the additional field heat that must be removed (Defraeye et al., 2014). Packaging systems used in conjunction with phytosanitary treatments must, therefore, promote proper ventilation for enhanced heat removal, as well as precise temperature control to avoid failed pest sterilisation, chilling injury or low-quality preservation due to inadequate cooling.

3.2 **Corrugated fibreboard packaging materials**

Corrugated fibreboard cartons are the most common form of fresh produce packaging used for export and represented over 99% of all South African pome fruit exports between 2008 and 2012 (Berry et al., 2015). The unique properties of Fibreboard make it a convenient, recyclable and robust packaging material. However, fibreboard materials are notoriously variable with respect to mechanical performance. Variability can be attributed to multiple factors including the source of material, such as wood, fibrous crops and waste paper, each of which has different properties. Additionally, the fibreboard manufacturing process can also add variations (Frank, 2014). For instance, processing water content and temperature, bleaching, beating, fibre alignment, drying conditions and the addition of rosin to block pores for reduced moisture sorption, all influence the end product's performance (Galotto and Ulloa, 2010; Parker et al., 2006; Rahman and Abubakr, 2004; Seaborg et al., 1936).

Corrugated fibreboard is a sandwiched structure made from a middle fluted fibreboard sheet, layered with liner fibreboard sheets. Mechanical characteristics in literature are often indicated by the fluting type (A, B, C, E, F) and the "grammage" (g m^{-2}) for each of the individual sheets (Frank, 2014; Twede and Selke, 2005b). Although these properties provide an indication of board strength, the high variability discussed above can result in different performances from boards with the same specification, but made by different manufacturers. Cellulose based materials such as fibreboard should, therefore, always be characterised with both physical (grammage, fluting) and performance properties.

Edge compression tests (ECTs) are a valuable indicator of corrugated fibreboard compression performance, experimentally measuring the force needed to crush a corrugated board sample (100 × 25 mm) in the direction of the fluting (McKee et al., 1963, 1962; TAPPI, 2007a). However, many studies often neglect to include any performance values for repeatability (Han and Park, 2007; Jinkarn et al., 2006). Future studies should set a precedent to always include ECT results, in addition to any other specification data, so that results and recommendations can be interpreted and applied to future package design developments.

3.2.1 Mechano-sorptive creep

A significant challenge to carton design is that the high and varying relative humidity conditions (80-95%) found in the cold chain can substantially reduce carton mechanical strength. Fluctuations in RH are often introduced due to handling from one cold chain unit operation to another and the on/off cycle of refrigeration units. The combination of large compression loads from the weight of carton stacking and creep is referred to as mechano-sorptive creep, and is a significant contributor to pallet stack failure in the cold chain (Haslach, 2000). Creep presents itself as gradual carton weakening and deformation over time (Haslach, 2000; Hung et al., 2010; Wang et al., 1991).

Although many of the aspects of mechano-sorptive creep have been discussed in various studies and reviews, the underlying mechanisms are poorly understood. Some of the suggested mechanisms include transient hydrogen bonding, molecular mobility and stress gradients (hydro-expansion) as a result of moisture gradients (Hanhijarvi, 1998; Hunt and Gril, 1996; Navi et al., 2002).

Another factor that can further accelerate (mechano-sorptive) creep in fibreboard materials is the effect of hysteresis, whereby the moisture content history of the fibreboard determines the equilibrium moisture content (EMC). The EMC typically has a sigmoidal relationship with the temperature dependent water-activity ($a_w \approx$ RH/100; RH = relative humidity) and is generally characterised using the Guggenheim-Anderson de Boer (GAB) isotherm model (Eagleton and Marcondes, 1994; Galotto and Ulloa, 2010). According to the GAB model, initial water uptake at low RH values, first occurs at the surface polar groups (e.g. hydroxyl sites) of the cellulose fibres, forming a water mono-layer across the respective material. Further

water saturation at about RH > 80% is attributed to capillary condensation (Chatterjee et al., 1997; Galotto and Ulloa, 2010). The complexity of these mechanisms results in sorption isotherms being smaller than desorption isotherms (Figure 2.5). That is, EMCs are higher when a board is equilibrated from a higher relative humidity than from a lower RH (Peralta, 1995). Changes in RH thus result in sorption and desorption values that are dependent on the moisture content history of the board. These hysteresis loops are limited by boundary isotherms as depicted in Figure 2.5 and are well explained by Everett's theory of independent domains (Chatterjee, 2001; Everett, 1967; Mualem, 1974; Peralta and Bangi, 1998; Rojas et al., 2001).

The combined effects of varying moisture contents, hysteresis and creep result in a larger reduction in carton strength, once used in the fresh produce cold chain. According to Pathare et al. (2016) cartons can lose more than 47% of their total strength in the first 2 days of high humidity cold storage. Even larger rates of strength loss are expected over several weeks or even months of cold chain storage. Furthermore, Alfthan (2004) showed that weakening is accelerated by larger moisture content amplitudes. Saha et al. (2010) recommended the use of fibreboard packaging materials with moisture resistant coatings to limit this process. One of the challenges to carton design, is that mechanical evaluations are performed at standard (23 °C; 50 RH) atmospheric conditions (ASTM, 2010, 2006; TAPPI, 2012). A safety factor is, therefore, added to carton strength requirements to address the anticipated loss in strength. Depending on the cold chain conditions, cartons can require between 3 and 8 times more compression strength than the expected carrying load (Twede and Selke, 2005a). A clear analytical method to determine an accurate safety factor is, therefore, an important future goal. This will likely involve predictive methods using finite element analysis techniques to incorporate the various conditions cartons are exposed to in the cold chain (Bandyopadhyay et al., 2002; Biancolini and Brutti, 2003; Djilali Hammou et al., 2012; Rahman et al., 2006).

3.2.2 Mechanical loading and palletising in transport and handling

Packaging performs an important role in protecting fresh produce from mechanical forces (compression, impact or vibration), which can cause fresh produce damage like bruising (Opara and Pathare, 2014; Van Zeebroeck et al., 2007). Packaging systems should be designed to absorb these forces, using combinations of specific fresh produce packing configurations, internal packaging and complementary carton designs.

Vibration

Packaged produce are often exposed to vibrational forces during transport by plane, rail or road. Produce damage occurs depending on the duration and intensity of the vibration and can result in both bruising and abrasion damage. The transport distance and quality (roughness, pot holes, bumps) of a road (transit surface) significantly affect produce damage as a result of the vibration forces (Berardinelli et al., 2005).

Packaging material performs an essential function during transport by absorbing vibration forces and reducing produce damage (Fadiji et al., 2016a). In the case of figs, which are highly susceptible to vibration damage, Çakmak et al. (2010) observed that expanded polystyrene packaging considerably reduced fruit damage compared to cartons. The position of a package in a stack can also influence produce susceptibility to vibration damage. For example, both Jarimopas et al. (2005) and Hinsch et al. (Hinsch et al., 1993) observed that produce packed in horticultural-boxes at the top of a pallet stack showed more damages than produce in boxes lower down. Similar results were observed by Van Zeebroeck et al. (2006) who additionally demonstrated that fresh produce near the top of the individual boxes absorb most of the mechanical energy.

Impact

The behaviour of a carton during impact, for example, when dropped, is often expressed by the peak acceleration versus the static stress curve. Lower acceleration values indicate less possibility of damage to produce. The impact absorbing properties of a paper-based packaging material can be significantly affected by the geometry of the packaging, the type of impact and the physical properties of the packaging material (Frank, 2014). When exposed to an impact force, some of the kinetic energy is absorbed by the packaging and the remaining energy is dissipated into the produce. Repeated impacts will alter the shock absorbing properties of the carton as it is deformed and fibres in the paperboard are damaged. Furthermore, damage to a carton as a result of impacts causes significant reductions in compression strength (Crofts, 1989). However, bruising can be significantly reduced by using packaging with higher energy absorption properties. For example, Lu et al. (2010) showed that double-wall cartons significantly reduced fruit bruising compared to single-wall cartons.

Internal packaging can also significantly reduce bruising of fresh produce and is influenced by the design and properties of the material used (Wang, 2009). However, without internal packaging, produce will absorb a large amount of the impact kinetic energy, irrespective of how the produce are arranged (Holt et al., 1981; Schoorl and Holt, 1982). Internal packaging is consequently used inside horticultural-boxes to reduce produce damage. Fadiji et al. (2016c) showed that the use of trays in cartons packed with apples reduced both bruise incidence and susceptibility by more than 50% compared to apples packed loose in carry bags.

Furthermore, Jarimopas et al. (2007) investigated the effectiveness of plastic foam nets and corrugated fibreboard wrapping to protect individual fruit during impact. The study showed that single face corrugated fibreboard with the fluting facing outwards provided the best protection. Currently, no standardised criteria or recommendation for carton design, with respect to carton impact resistance are available. Future studies, therefore, need to focus on identifying relationships between carton design (vent hole design, board type, carton dimensions) and resistance against impact forces.

Compression

Vent hole design (configuration, size and position) can have a considerable effect on a carton's compression resistance. Figure 2.6 shows a simplified stress distribution in a corrugated fibreboard wall as predicted by Peterson and Fox (1989). The results show stress lines, which represent areas of high tension or compression across a corrugated board, during uniform load and top-to-bottom compression. Specifically, vent holes should avoid stress lines between the centre and corner areas as well as the middle horizontal axis, which are critical for strength preservation (Peters and Kellicutt, 1965; Peterson and Fox, 1989). Peters and Kellicutt (1965) further showed that strength reductions are lowest when vent holes are placed away from the vertical and horizontal edges and the importance of vent hole position versus vent hole area. For example, vent holes with a total ventilated area percentage (TVA) across the carton walls of 3.6% can have similar reductions (22.5%) in strength as a TVA of 24.8% depending on how the vent holes are configured (Han and Park, 2007; Jinkarn et al., 2006; Singh et al., 2008). Although relatively dated, these studies illustrate very clearly the challenges with respect to carton strength that have been reported in more recent work.

3.2.3 Stacking efficiency

Both cartons and the fruit can be exposed to compression, vibration and impact forces during handling, storage and transport, leading to physical damage of the carton and fruit bruising (Fadiji et al., 2016c; Opara and Pathare, 2014). Stacking patterns have a considerable influence on how a carton design will perform with respect to mechanical strength. Interlocking stacking patterns (Figure 2.2) are often used to improve pallet stack stability (Boyette et al., 2000). The majority of a carton's weight is supported along the corners (Maltenfort, 1996). The use of an interlocking stacking pattern results in misalignments of the corners (Figure 2.2), which can reduce stack compression strength by up to 40% (Koning and Moody, 1989). Another negative consequence of the cross stacking method is that the vertical ventilation holes are often obstructed, which increases resistance to airflow and decreases cooling rates. Parsons et al. (1972) compared different stacking configurations with respect to produce cooling rates. The study showed that a carton stacking arrangement, which forms a central duct allowing air to flow freely vertically up and down the stack, had similar cooling rates to pallet stacks without interlocking stacking patterns (Parsons et al., 1972). However, its use significantly

reduces packing density in shipping containers and is not routinely implemented in commercial export (Berry et al., 2015). Despite the importance and widespread use of pallet stacking, no recent work exploring these aspects were found by the authors.

The sections above show that fresh produce package performance can be influenced by multiple factors, many of which are dependent on each other. Changes to a package design affecting one factor, must, therefore, always include an assessment of the remaining factors. Furthermore, the conditions of each cold chain step are unique and must also be included in package assessments.

4. Carton design for dynamic cold chains

Studies addressing the various package functionalities for each cold chain step are often made in isolation of one another. The sections below review recent studies over the past decade examining carton designs in each of the fresh produce cold chain operations. The majority of the studies focused on forced-air cooling (FAC), cold storage and refrigerated transport. Table 2.2, Table 2.3 and Table 2.4 list some of the respective work in these categories and is discussed within the scope of a multi-parameter and multi-scale framework in the section below.

4.1 Forced-air cooling

As shown in Figure 2.7, FAC makes use of fan(s) to generate a pressure difference over packaged produce. This results in refrigerated air being drawn through the packaging, significantly accelerating cooling rates through convection (Brosnan and Sun, 2001; Thompson et al., 2008). Depending on the package design (size and ventilation) and contents, the airflow can be turbulent. This results in improved air mixing in the cartons, as well as enhanced heat transfer rates across the fruit surfaces (Tutar et al., 2009). However, achieving high flow rates through packed produce with large air resistances increases fan power requirements.

FAC efficiency of packaged produce is influenced by the ventilation design of a package (Berry et al., 2017; Pathare et al., 2012). Vent holes configurations should be designed to evenly distribute cooling air through the packed produce and be positioned to ensure ventilation alignment when stacked (Defraeye et al., 2013a; Ladaniya and Singh, 2000). Furthermore, vent hole TVA must be large enough to enable efficient power usage by the FAC fans, but not compromise the mechanical strength of the cartons (Pathare and Opara, 2014). Many different types of packaging systems (multi-scale; section 2.2) are in use, due to the numerous package combinations that are possible. The interactions between box design (geometry), internal packaging, produce varieties and pallet stack configurations make it challenging to generalise recommendations. The sub-sections below have, therefore, been grouped with respect to the internal packaging type (Figure 2.1).

4.1.1 Loose (bulk)

The use of loose packing schemes is typically reserved for fresh produce with a resilience to physical damage, such as some citrus varieties (Kader, 2002). Airflow characteristics through loose packed produce are mainly influenced by the packing configuration and physical properties of the fruit. These include packing porosity, produce shape, tortuosity, surface texture and size (Vigneault et al., 2004b).

TVA (total ventilation area) has been studied extensively in research and can significantly influence both cooling and airflow properties during FAC. Larger vent holes have been shown to both increase airflow distribution and improve cooling uniformity. This can be attributed to the increased air circulation in the individual cartons that better mix incoming cold air with warm air in the carton. According to a study by Tutar et al. (2009), TVAs under 10% had the largest effect on cooling uniformity, with only small improvements at 20%. Similar results have been observed by Dehghannya et al. (2012, 2011, 2008), who examined the effect of vent hole design (size, position, number) and showed improvements in air uniformity between TVAs of 2.4% and 7.2%, but little improvement when increased to 12.1%. The studies additionally observed that changes in TVA were most effective when combined with an appropriate vent hole configuration (shape, position).

Further investigations into vent hole design (size, configuration, shape and position) were performed by Delele et al. (2013a, 2013b). As with previous findings, cooling homogeneity and resistance to airflow improved as the TVA was increased. Furthermore, the study showed that increasing TVA from 1 to 7%, improved cooling rates by 184%. In contrast, larger vent holes (7-100%) only improved cooling by 62%. With respect to vent hole shape, Delele et al. (2013a) observed almost no difference between square and round vent holes on airflow resistance or cooling performance. Finally, the effect of vent hole configuration (position and number) significantly influenced resistance to airflow and cooling rates (Delele et al., 2013a). The study observed the best performance with vent holes placed near the centre, compared to the top and bottom. Additionally, improvements were also observed with increasing vent number and distribution.

The effect on FAC efficiency for two different citrus fruit carton designs was examined by Defraeye et al. (2014, 2013a). Each carton design was evaluated under stacked conditions, with respect to cooling performance and energy efficiency. The results showed that vent holes placed at the top and bottom of the carton produced more uniform cooling in each individual carton. Furthermore, the cartons produced a lower resistance to airflow compared to cartons with centrally positioned vent holes, which enabled more energy efficient cooling. The study emphasised the importance of stacking and vent hole alignment (multi-scale perspective) when designing ventilated cartons.

Most studies examining package design with respect to FAC performance have concentrated on loose packing schemes (Pathare et al., 2012) and recommendations in this area are well covered. With respect to TVA, most studies agreed that a TVA of 7-10% is sufficient to cool produce packed loose (for the various individual parameters). Many fruit types, however, require the addition of internal packaging, which significantly influence air distribution in the carton. More work is therefore needed to develop similar recommendations for alternative packaging combinations.

4.1.2 Trays

The presence of trays in cartons can significantly reduce bruising in fruit, such as apples and pears (Fadiji et al., 2016c). Figure 2.8 shows a typical tray packing configuration, whereby four fruit layers are separated by four individual trays. An important consideration, is that trays compartmentalise a carton's volume. Vent holes must be designed so that air can sufficiently access each fruit layer (Opara and Zou, 2007; Zou et al., 2006a, 2006b). An important variable affecting FAC performance is the number of trays packed in a carton and has been different in each respective study. Han et al. (2015) examined a carton packed with two trays, with ventilation (two round holes) only at the top layer. The study added two vent holes to the bottom layer and observed a twofold reduction in both cooling time and heterogeneity. A later study by Lu et al. (2016), investigated the effect of various distributions of circular and oblong vent holes (TVA = 11.2%) in a carton with three trays. The study observed a 66.5% improvement in uniformity and a reduction of 2.5 °C in the slowest cooling fruit, for cartons using circular vents with a more vertical distribution compared to a linear horizontal distribution.

A study by Berry et al. (2016) investigated the effect of three vent hole designs (TVA = 4%) against a commercially used vertically oblong design in cartons packed with five trays. Vent holes were positioned to allow for alignment during stacking, thus making the findings more relevant to higher packaging scales (pallet stacks). The results showed that the use of multiple short oblong vents reduced energy consumption by 58%, compared to the commercial design. Vent holes along the top and bottom edges increased energy usage by a factor of 7 compared to the commercial design. Furthermore, it was shown that the combined use of trays and the correct vent hole design could actually improve cooling efficiency compared to fruit packed loose, by more evenly distributing airflow to the individual fruit in the carton. The above literature showed that cartons packed with trays require vent hole schemes that ensure uniform airflow distribution to each respective fruit layer, but do not necessarily require larger TVAs than cartons packed loose.

4.1.3 Liner and carry bags

Liner bags are a common packaging method used for many fruit varieties to modify conditions locally around fruit. This usually involves achieving a more desirable humidity to reduce fruit moisture loss. Furthermore, liner bags can also be used for modified atmosphere packaging (MAP; section 4.1.3). The atmospheric (N_2, O_2 and CO_2) concentration around the produce are altered to reduce respiration rates and improve overall quality preservation. Most of the research examining liner bags and carry bags in cartons have been performed on table grape fruit, which are non-climacteric and are harvested ripe off the tree. As a result, table grapes require a very sophisticated packaging system. Some of the components included in this system are moisture absorption pads, SO_2 releasing pads and bags (liner or carry) with various types of perforations (Ngcobo et al., 2013a).

Ngcobo et al. (2012a) investigated the effect of different produce and packaging components present in a fully packed commercially used table grape carton, with vents along the top and bottom edges (TVA: 2.8% = 300 mm side; 6.7% = 400 mm sides). The results showed that for various configurations of a fully packed carton (table grapes, carton, liner, carry bag), the inner liner bags frequently blocked ventilation holes, resulting in high RTA values. The small plastic liner carry bags (several per container) contributed 8%, the micro-perforated liner bags contributed 40%, the non-perforated liner bags contributed 83% and the various perforated liner bags contributed between 40% and 69% of the total pressure drop in a pallet stack. For cooling, Ngcobo et al. (2013b) showed fruit packed in carry bags and liner bags increased seven-eighths cooling time up to 97% and 185%, respectively, compared to fruit packed loose.

Unlike fruit packed loose or on trays, few studies have utilised CFD to optimise carton designs when packing with liner bags. The use of liner bags to reduce moisture loss or as a MAP is an important component of extending fruit quality preservation and is utilised extensively in the fresh produce export industry. Recently a CFD model was proposed by O'Sullivan et al. (2016) and showed good predictions compared to experiments. Future work should, therefore, be focused on identifying vent positions that are less obstructed by liner bags or carry bags and vent hole areas that optimise energy usage by the FAC system.

4.1.4 Clamshells

Strawberries are frequently packed into clamshell tubs, which are then packed in cartons. Strawberries are highly susceptible to microbial growth and decay, making rapid and homogenous cooling important if quality is to be preserved. Since the geometrical shape of clamshell containers are so complex, researchers used numerical simulations to investigate the airflow and heat transfer properties taking place during FAC for several clamshell designs (Ferrua and Singh, 2009a, 2009c, 2009d). The study showed that alternative vent holes in the clamshells could improve cooling rate, but had little effect on cooling homogeneity. It was shown

that the clamshell designs allowed more than half of the airflow to circumvent the tubs. However, vent hole ratios (clamshell) allowing more than 25% airflow penetration did not significantly improve strawberry cooling rates. Additionally, the study showed that cooling rates could be significantly improved by periodically reversing the airflow direction during FAC (Ferrua and Singh, 2009b). A later study by Ferrua and Singh (Ferrua and Singh, 2011a) recommended the use of a by-pass FAC setup in combination with a perforated board in the downwind carton. This setup maintained similar cooling rates as traditional setups, but decreased pressure drop by 70%.

Similar to liner bags and carry bags, more work is needed in the areas of identifying optimal vent hole designs (area, positions and shape) when using clamshells. Additionally, the same vent hole designs are often used in cartons when packing different internal packaging types. Future work, therefore, needs to identify if a more versatile and generic vent hole design is possible.

4.2 **Cold storage**

Cold storage is shown in Figure 2.3 as the step performed after FAC, however, in reality storage can occur at various other points in the cold chain. Furthermore, many studies have grouped both storage steps and refrigerated transport into the same category when investigating use of MAP and liner bags for quality preservation (Table 2.3). It is within this extended cold storage environment that the use of various MAP, such as carry bags, liner bags and clam shells can significantly improve quality preservation (Caleb et al., 2013, 2012; Henriod, 2006; Ngcobo et al., 2013b). For example, Ngcobo et al. (2012b) showed that with the aid of liner bags, moisture loss in table grapes could be reduced to just 10% over a 75 day storage period, compared to 49% and 89% when using perforated and non-perforated liner bags, respectively. An important component of MAP is the proper control of temperatures during storage, since suboptimal conditions can cause reductions in quality preservation as a result of accelerated respiration and undesirable gas concentration in the MAP.

Most cold stores make use of refrigeration units positioned at the top wall of an insulated room (Delele et al., 2012). These units blow air along the ceiling, which then flows down the opposite wall, proceeding along the floor and then flowing back into the unit. Pallets outside this air stream are thus cooled less, which can result in temperature heterogeneity across the room (Hoang et al., 2015). Duret et al. (2014) observed pallets near the cold room centre were cooled less, resulting in warmer temperatures and larger moisture loss rates in fruit.

The effect of ventilation and overall carton design can significantly influence a pallet stacks porosity to airflow and its cooling rate in cold storage, however, no studies were found by the authors examining this phenomenon. Future studies in this area consequently need to link package design to airflow distribution and cooling in the pallet stacks during extended storage periods

4.3 **Refrigerated transport**

4.3.1 Refrigeration

RFCs (Figure 2.1) have a standardised layout and are used by many different industries for reliable, cost efficient and long-haul shipping (Table 2.4). With respect to design, the RFC is, therefore critical, since it is one of the few cold chain components that cannot easily be modified. Fresh produce packaging systems should be designed to make optimal use of the RFC system and available space. The use of RFC in transportation of fresh produce has grown considerably in the last few decades, replacing the conventional vessel shipping system, which made use of large refrigerated storage holds (Cargo Systems International, 1989; Parvini, 2011). Typically, RFC make use of vertical airflow systems. For instance, RFCs have grated floors that deliver cold airflow at low velocities vertically upwards. Cooling is usually more effective near the front of a container, as air temperatures are lower and pressure differences are the highest (Tapsoba et al., 2006).

Although RFCs have been successfully applied in the commercial export of fresh produce, shipments are often afflicted with cooling heterogeneity in the form of hot and cold spots within the pallet stacks (Jiménez-Ariza et al., 2014; Rodríguez-Bermejo et al., 2007; Smale et al., 2006). Hot spots can result in high respiration rates which then further increase produce temperatures, causing undesirable ripening, senescence and even decay. Conversely, cold spots can result in chilling injuries making produce unsatisfactory for retail sale (Heap, 2006). Cooling heterogeneity in these circumstances is primarily a result of packaging designs not being optimised. This is due to incorrect/suboptimal vent hole alignment in the RFC cooling system (Jedermann et al., 2013). Airflow consequently bypasses portions of the packed RFC or is too concentrated in others. One factor attributed to this phenomenon is the presence of gaps between the pallet stacks in the RFC, where floor space has not been utilised. Both Jedermann et al. (2013) and Defraeye et al. (2015c) investigated ambient cooling of standard sized pallets (1.2 × 1.0 m), which is a common size for fresh produce export (Berry et al., 2015). The studies showed that the pallets do not fully exploit the containers floor area, leaving significant gaps between the pallets. Jedermann et al. (2013) showed that gaps significantly influenced cooling heterogeneity over the whole container, by increasing fruit cooling rates in areas adjacent to the gaps, whereas overall cooling rates in other areas were considerably reduced. Similar results were observed by Defraeye et al. (2015b), who showed that increasing the width of gaps improved cooling homogeneity across the vertical axis of the stack. However, overall cooling rates were significantly reduced, due to airflow short-circuiting the packed fruit. Future carton designs should thus aim to better utilise the available floor space of RFCs, which will limit gaps in the container floor. This will consequently improve both produce cooling rates and energy efficiency during RFC shipping.

Refrigerated containers are generally not used to precool produce, but to rather maintain set temperature, though many RFC actually have sufficient refrigeration capacity to precool a fully packed container. The use of RFCs to precool produce is referred to as “ambient loading” (Defraeye et al., 2015c). However, containers are often unable to achieve this goal as a result of uneven cooling patterns, which could potentially result in chilling injury or hot spots that never reach a satisfactory temperature (Defraeye et al., 2015c; Jedermann et al., 2013). The possibility of altering airflow distribution inside RFC packed with pallets of fruit was investigated by Defraeye et al. (2016). The study revealed that improving vertical air penetration into the various pallet stacks decreased moisture loss and extended shelf life conditions, compared to other strategies. Compared to FAC, very little work has been done in this area. Future studies should, therefore, focus on developing a carton design that facilitates lower vertical airflow resistance and improved airflow distribution in pallet stacks. Improved packaging designs would reduce energy consumption during shipping and enable the use of treatments such as ambient loading and phytosanitary sterilisation, allowing the fruit to bypass cold storage steps and reach consumers earlier and in a fresher state.

4.3.2 Compression strength

Impacts and vibrations are often associated with transportation and can act as the trigger causing a pallet stack to fail under its own weight (compression force). The use of vent holes significantly reduce a pallet stack’s resistance to compression and typically range between 1.9% and 8.8% TVA in pome fruit packaging (Berry et al., 2015). These values are close to 5%, as recommended in literature (Pathare et al., 2012; Pathare and Opara, 2014; Thompson et al., 2002) and has been adopted by the South African pome fruit industry (Hortgro, 2013) to achieve a compromise between cooling efficiency and compression strength.

A strong relationship exists between the size of ventilation openings and the overall mechanical strength of a carton. Singh et al. (2008) observed that the relationship between strength loss and TVA is linear up to 40% TVA. However, depending on the configuration, the initial addition of any vent hole to a carton can result in a strength loss of between 20% and 50%. The shape of a ventilation opening can also significantly influence the box strength. Singh et al. (2008) observed that vertical rectangular or parallelogram-shaped holes reduced mechanical strength less than circular openings. In contrast, earlier research by Jinkarn et al. (2006) showed that circular openings reduced mechanical strength less than eclipse shapes. However, Han & Park (2007) showed that vertical oblong holes reduced mechanical strength the least of all, which is consistent with vent hole designs used in commercial practice (Berry et al., 2015). Additionally, Han & Park (2007) suggested a modified hand hold design, as well as various vent hole ratios that should not be exceeded for minimal strength loss.

Many of the above-mentioned recommendations are contradictory, which can be attributed to the different methodologies used. Specifically, mechanical strength has been performed on either single sheets of corrugated board (Jinkarn et al., 2006; Peterson and Fox, 1989) or on regular slotted cartons (Han and Park, 2007; Koning and Moody, 1989; Peters and Kellicutt, 1965; Singh et al., 2008). Recommendations from these studies should be applied with care, since most fresh produce cartons, as depicted in Figure 2.9, use either telescopic or retail display design types (Berry et al., 2015; FEFCO and ESBO, 2007). Future research should, therefore, include more realistic carton designs in evaluations, to better understand the effect of carton type.

4.4 **Other design considerations**

4.4.1 Retail and consumer aspects

With respect to carton types (manufacturing design), cartons can be produced as either regular slotted, telescopic or retail display (Figure 2.9). Most mechanical performance evaluations have been targeted at regular slotted carton types (Frank, 2014). However, as illustrated in Figure 2.10, the majority of cartons manufactured in South Africa are either telescopic or retail display. This is attributed to these types having a considerably larger resistance to mechanical loads. Conversely, the type of carton manufactured has very little influence on cooling performance, as all the designs essentially form similar enclosed rectangular prisms when stacked.

Many packaging systems must function at the retail and even at the consumer level. From a marketing and logistics perspective, package designs such as retail display cartons (Figure 2.9) can be placed directly on retail shelves “as is”, to display either loose or pre-packaged (internal packaging) produce. Packaging systems can also incorporate the use of innovative package designs or new materials (e.g. biodegradable plastics) into the manufacturing process. The main motivation behind these changes is often to make the packages more aesthetically pleasing to consumers or reduce the cold chains overall carbon footprint and the environmental impact (Babalis et al., 2013). Retail display cartons represented up to 30% of the pome fruit exports in South Africa (Figure 2.10) and are used in all the same cold chain steps (FAC, storage, refrigerated transport) as telescopic designs (over 60% of cartons used for export). However, few mechanical strength related recommendations are available for retail display designs, which have unique failure patterns (compared to telescopic designs). Future studies need to target these alternative designs, as they make up a significant portion of the fresh produce export industry.

4.4.2 Compatibility with supply chain logistics

Packaging is a dynamic component of the fresh produce cold chain and must function in union with several treatments, technologies and equipment. One aspect of fresh produce package design is the integration of ergonomics so that labourers can effectively handle packages. This is a relevant parameter in South Africa, as

cartons are still packed and palletised by hand in many packhouses (Ladaniya, 2008). Individual packages should be designed to only pack volumes that does not exceed safe handling weights or guidelines (Dieter and Schmidt, 2009). Fresh produce packages are often designed with openings to function as both ventilation holes and handles (Opara, 2011). However, the placement of a convenient hand hole often does not facilitate ventilation alignment for effective airflow distribution (cooling) or carton mechanical strength preservation (Han and Park, 2007).

Another important aspect of package design is that of compatibility between horticultural packaging and regulated pallets footprint designs. For instance, both the South African deciduous and citrus industries have regulated the use of 1.2 × 1.0 m pallets for export (Berry et al., 2015; Groenewald and Bester, 2010). Curiously, there is enough floor area to accommodate a little over 22 pallets in a 40-foot container (RFC floor area = 11.59 ×2.29 m). However, due to incompatibilities between the pallets and container dimensions, only 20 or 21 pallets are loaded.

A future priority will be to alter pallet footprints, and thus also carton footprints (packaging systems), so more fruit can be transported in containers. Such a design would both improve fruit packing density and reduced carbon emissions. However, any change to pallet stack design must be compatible with equipment such as forklifts, as well as other cold chain infrastructure.

5. Conclusions

Cartons are the most common form of packaging used in the fresh produce cold chain and significantly influence both cold chain performance, as well as fresh produce quality preservation. This review dealt with the various interactions and approaches used to study and design horticultural cartons, within the various steps of the cold chain. Approaches included a multi-scale approach and multi-parameter evaluation. Specifically, the multi-scale packaging approach was defined as the use of a hierarchical packaging perspective to more effectively interpret and evaluate package designs. The multi-parameter approach makes use of multiple evaluation techniques (performance parameters) for a comprehensive and holistic packaging assessment.

Three main factors affecting carton design were identified, namely, material/manufacturing costs, mechanical performance and efficacy of ventilation (e.g. cooling). For cartons, these factors typically require contradictory design features and have often been addressed individually in literature. However, fresh produce packages have quite complex structures, which operate in many conditions and consist of multiple different packaging components. The use of generalised carton design recommendations are thus not practical and future recommendations should be more case specific to the fresh produce type and available cold chain. The development of an optimal carton design requires a clear delineation of the respective cold chain unit operations and a well-defined program with respect to

treatments and conditions needed to preserve the fresh produce. This information can then be used to select appropriate evaluation methods and the respective performance parameter benchmarks can be set. A considerable amount of work has already been done in the areas of carton performance evaluations. Current outputs are mainly used to compare different designs to each other and are not generally relatable to actual performance values in commercial practice. Future studies, therefore, need to develop relationships between evaluation techniques, which often only examine an individual package component (e.g. single carton) at a time, to performance at larger scales. This will require further investigations into the effects of pallet stacking, mechano-sorptive creep, and handling practices on both ventilation and mechanical parameters.

With respect to ventilation, many studies have investigated the optimisation of carton vent hole designs when packed loose or with trays. However, little has been done for cartons packed with liner bags, carry bags and clamshells and should, therefore, be addressed in the future, as they are commonly implemented in fresh produce export. Furthermore, no clear guidelines are available with respect to optimising cartons designs for use in RFC, which is of considerable importance as they are used extensively for long haul transport. Future cartons should, therefore, make better use of the RFC floor space, to improve packing density during transport and also facilitate uniform airflow distribution through the use of improved vent hole designs and stacking arrangements.

Table 2.1: List of performance parameters to evaluate packaging functionalities.

Category	Package functionality	Index	unit	Comments	References
Fresh produce cooling	Time	1/2 and 7/8 cooling time	h, s	Only for transient cooling problems (e.g., precooling)	Dincer, 1995
	Rate	Momentary cooling rate	K h^{-1}	Only for transient cooling problems (e.g., precooling)	Zhao et al., 2016
		Cooling coefficient	h^{-1}	Only for transient cooling problems (e.g., precooling)	ASHRAE 2000a
		Convective heat transfer coefficient	W m^{-2} K^{-1}	Can be correlated to system air speed	Defraeye et al., 2013a
	Temperature uniformity	Heterogeneity index (temperature)	%	Location and time dependant	Dehghannya et al., 2011
		Distribution (spread) of CHTC over products	W m^{-2} K^{-1}	Relative standard deviation	Defraeye et al., 2013a
		Distribution (spread) of 1/2 or 7/8 cooling time over products	h s	Only for transient cooling problems (e.g., precooling)	Dehghannya et al., 2011
Package ventilation	Ventilation potential/rate	Airflow rate	L s^{-1} kg^{-1}	Per kg of produce	Brosnan and Sun, 2001
			m^3 s^{-1}		Brosnan and Sun, 2001
		Total ventilation area (TVA)	%	Relevant in other packaging functionalities	Vigneault and Goyette, 2002
	Airflow uniformity	Coefficient of variance	-		Vigneault et al., 2004a
		Heterogeneity index (air speed)	%	Location and time dependant	Dehghannya et al., 2012
	Bypass flow	Bypass ratio	%	Also called air loss ratio	Defraeye et al., 2015a
		Effective TVA	%	TVA after considering blocked vent holes	Berry, 2013

Fresh produce	Quality	Moisture loss	kg	Factor of fruit skin permeance, conditions and mass transfer coefficient	Maguire et al., 2001
		Chilling injury index	-	Varies by fruit type and industry	Thompson et al.,2008
		Fruit maturity (colour development)	-	Varies by fruit type and industry	Thompson et al.,2008
		Fruit maturity (firmness)	N m^{-2} and kg	Varies by fruit type and industry	Thompson et al.,2008
		Fruit maturity (total soluble solids)	°Brix	Often associated with starch breakdown during ripening	Thompson et al.,2008
		Fruit maturity (total acids)	-	Often associated with phenolic production	Thompson et al.,2008
		Infestation	%	Rejected by international markets	Melo et al., 2014
		Shelf life	days	Expected quality duration at retail	Thompson et al.,2008
Mechanical strength	Compression strength	Peak force	N	Maximum carton strength	Frank, 2014
		Peak force up till predefined displacement	N	Before fruit bruising	Frank, 2014
	Package cushioning	Peak acceleration (Impacts)	-	Function of static load and drop height	Fadiji et al., 2016a
		Vibration transmissibility	-	Function of peak frequency and static load	Fadiji et al., 2016a

Energy consumption	Resistance to airflow	Pressure loss coefficient	Pa s^2 m^{-6}	Relates pressure drop to airflow rate (ΔP and G)	Verboven et al., 2006
	Package-related energy consumption	Package-related energy consumption	J	Fan related energy usage	Thompson et al., 2010
	System energy consumption	Energy added ratio	-	Only for transient cooling problems (e.g. precooling)	de Castro et al., 2005b
		Energy coefficient	-	Only for transient cooling problems (e.g. precooling)	Thompson et al., 2010
Packaging logistics	Ergonomics	Hand holds/vents	%	Hand hole design (area, shape, position) on carton for carrying	Vigneault and Goyette, 2002
		Mass limitations	kg	Allowable mass per a carton for safe manual lifting	Dieter and Schmidt, 2009
	Utilisation	RFC floor usage	%	The ratio of the RFC floor used by the packaging design (i.e. unused area)	Groenewald and Bester, 2010
		Packing porosity	%	Ratio of the carton volume used by fruit (function of packing configurations and internal packing)	Chau et al., 1985
	Manufacturing	Equipment design and manufacturing	currency	Cost of designing, implementing and manufacturing the respective packaging system	-
		Material costs	currency	Cost of specific materials needed per a package	-

Table 2.2: Summary of recent studies (2006-2016) investigating carton design relating to forced-air cooling.

Performance parameters and multi-scale perspective*	Research focus and conclusion	Reference
Individual package (IP: trays); CR, RTA	Used a CFD model to predict airflow distribution and cooling rates of apples in cartons packed with trays. Study developed a user friendly software package to evaluate carton designs.	(Opara and Zou, 2007; Zou et al., 2006a, 2006b)
Individual carton (loose); CR, CU, RTA	Used a CFD model to investigate the effect of vent hole number, positioning and size on cooling efficiency using CFD. The study emphasised the importance of correct vent hole number and positioning over just increasing ventilation area.	(Dehghannya et al., 2012, 2011, 2008)
Individual carton (realistic loose); CR, CU, AD, RTA	Study used a validated CFD model to show the significance of fruit diameter, porosity, packing pattern, confinement ratio and box vent hole design.	(Delele et al., 2008)
Pallet scale, focus on individual carton (IP: Multiple clamshells); CR, CU, AD	Used a CFD model to develop clamshell designs for Strawberries in cartons. Results showed cooling rates could be considerably improved by modifying the clamshell vent hole configuration.	(Ferrua and Singh, 2009a, 2009b, 2009c, 2009d, 2008)
Individual carton (IP: loose); CR, CU, AD	Investigated various CFD model methods to predict fruit cooling efficiency in a carton. Study emphasised the importance of high flow speeds, which cause small scale eddies near fruit surfaces for improved heat transfer.	(Tutar et al., 2009)
Holding area; EU	Examined overall energy usage of FAC facilities using a survey method. Results showed no significant improvement in efficiency over the last 20 years.	(Thompson et al., 2010)
Pallet scale, focus on individual carton (IP: clamshells); CR, CU, AD, EU	Proposed a new carton design and FAC setup for improved cooling efficiency. This improved energy usage, while maintaining cooling rates compared to previous designs.	(Ferrua and Singh, 2011a)
Pallet stack (IP: various liner bags and pads); RTA, CR, CU, AD	Experimentally and numerically (CFD) investigated the effect of various perforated liner bags and pads in table grape cartons on FAC performance.	(Delele et al., 2013c; Ngcobo et al., 2013a, 2013b, 2012a)

Pallet stack (IP: loose); CR, CU, AD, RTA, EU	Experimentally and numerically compared three citrus package designs for FAC performance. The studies also examined the effect of FAC set temperature on system efficiency.	(Defraeye et al., 2014, 2013a)
Individual carton (IP: loose); CR, CU, AD, RTA	Used a CFD model to investigate the effect of vent hole designs in citrus cartons on FAC performance. The study showed that vent hole TVAs larger than 7% did not significantly improve cooling rates.	(Delele et al., 2013a, 2013b)
Individual carton (IP: trays); CR, CU	Used a CFD model to investigate the effectiveness of adding additional vent holes to an apple carton with trays.	(Han et al., 2015)
Pallet scale, focus on individual carton (IP: loose and trays); CR,CU, RTA, EU	CFD study proposing three new vent hole designs (configurations) which align during pallet stacking and comparing them against a currently implemented design.	(Berry et al., 2016)
Individual carton (IP: tray); CR, CU	CFD study examining the effect of fruit packing configuration, vent hole shape (oblong and circular) and vent hole position.	(Lu et al., 2016)
Pallet stack (IP: liner bag); CR, CU	CFD study examining the effect of airflow rate on cooling performance in cartons packed with kiwi fruit in liner bags.	(O'Sullivan et al., 2016)

*AD = Airflow distribution; CR = Cooling rate; CU = cooling uniformity; EU = Energy usage; IP = Internal packaging; RTA = Resistance to airflow.

Table 2.3: Summary of recent studies (2006-2016) investigating carton design relating to cold storage.

Performance parameters and multi-scale perspective*	Research focus and conclusion	Reference
Board samples; SC, ST, ML	Experimental investigation of nano-sized mists to generate high humidity conditions during fruit storage and its effect on corrugated fibreboard strength and fruit moisture loss.	(Hung et al., 2011, 2010)
Individual carton (IP: liner bags, carry bags, pads); CR, CU, ML, QA	Experiments and CFD to investigate the effect of table grape cartons packed with various internal packing types.	(Delele et al., 2012; Ngcobo et al., 2013c, 2012b, 2012c)
Holding area and individual bins; AD, CA	Developed and validated a CFD model to predict 1-MCP absorption in apple fruit in storage bins. Although the study focused mainly on plastic and wooden bins, its scope also covered 1-MCP absorption into corrugated fibreboard.	(Ambaw et al., 2014, 2013b, 2013c, 2013d, 2011)
Holding area (pallet stacks in cold room); CR, CU, ML	Air, heat and moisture properties were evaluated in a cold room holding four pallet stacks.	(Duret et al., 2014; Hoang et al., 2015)
Individual carton (empty); SC	Experimental study examining the effect of high humidity on carton strength during cold storage.	(Pathare et al., 2016)

*AD = Airflow distribution; CA = Chemical application; CR = Cooling rate; CU = cooling uniformity; IP = Internal packaging; ML = Moisture loss; QA = Quality attributes; SC = compression strength; ST= Tensile strength.

Table 2.4: Summary of recent studies (2006-2016) investigating carton design relating to refrigerated transport.

Performance parameters and multi-scale perspective*	Research focus and conclusion	Reference
Individual board samples; SC	Examined vent hole size, shape and position on compression resistance and showed circular vents placed away from corners reduced strength the least.	(Jinkarn et al., 2006)
Individual regular slotted cartons (empty); SC	Used a numerical model to examine vent hole size, shape and position on carton compression resistance. Study recommended the use of oblong shaped vents, and suggested several vent hole ratios with respect to carton geometry for reduced strength loss.	(Han and Park, 2007)
Holding area; CR, CU	Investigated the effectiveness of a RFC full of pallet stacks when using various refrigeration approaches (cooling modes, set point, defrost system and load level).	(Rodríguez-Bermejo et al., 2007)
Holding area and pallet stacks; AD	Used a CFD model to predict flow distribution in a ceiling-slot ventilated enclosure loaded with ventilated pallet stacks.	(Moureh et al., 2009a, 2009b; Tapsoba et al., 2007)
Holding area; CR, CU	Used a simplified model to predict heat transfer in a refrigerated truck containing pallets	(Hoang et al., 2012)
Holding area; CR, CU	Examined cooling heterogeneity, with respect to quality preservation, in a RFC during shipping.	(Jedermann et al., 2013)
Holding area; CR, RH	Proposed the use of phase diagrams to evaluate temperature and humidity gradients in a refer container packed with pallet stacks.	(Jiménez-Ariza et al., 2014)
Holding area; CR, CU, EU, ML, QA	Explored the use of RFC and various method to precool citrus fruit packed in cartons	(Defraeye et al., 2016, 2015c)
Individual cartons; CR, CU, EU	Investigated the effect of gap width between vertically stacked cartons	(Defraeye et al., 2015b)

*AD = Airflow distribution; CR = Cooling rate; CU = cooling uniformity; EU = Energy usage; ML = Moisture loss; QA = Quality attributes; RH = humidity conditions; SC = compression strength.

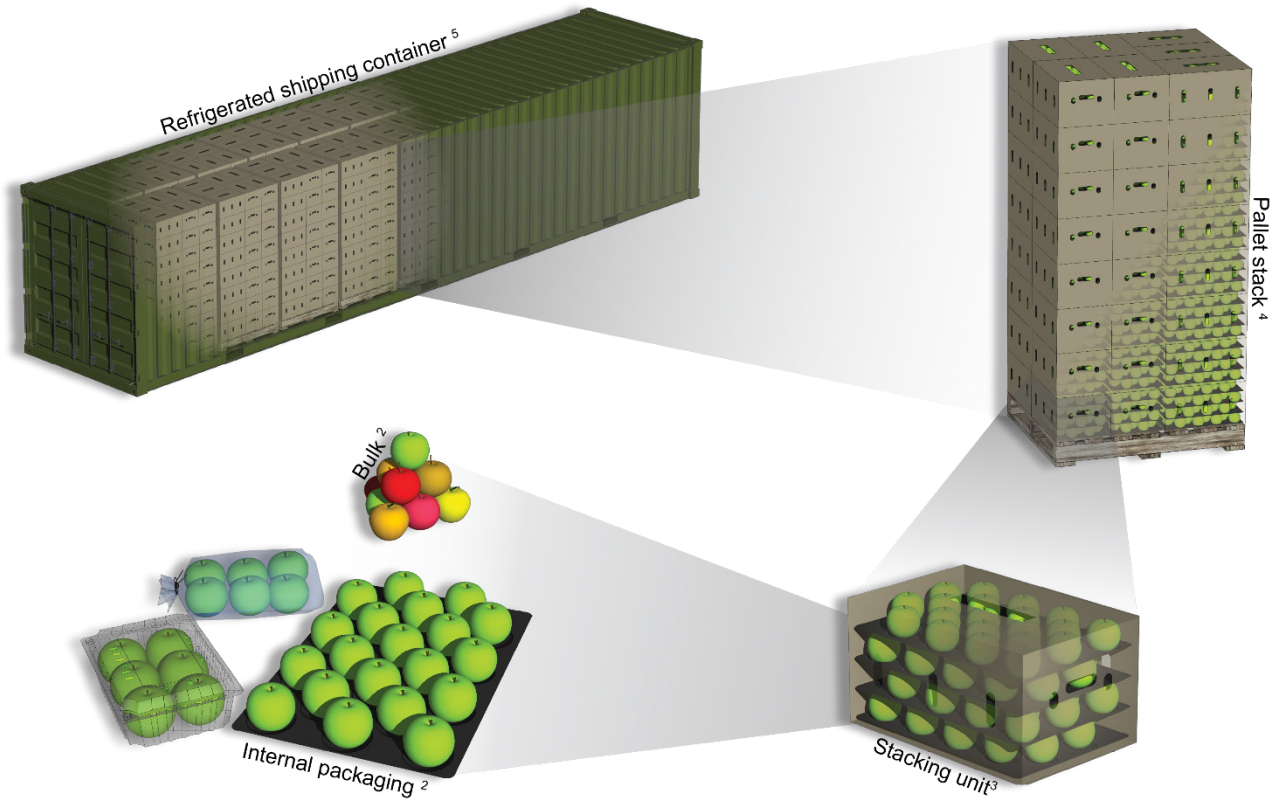

Figure 2.1: Schematic showing the various hierarchical levels of packaging comprised in a multi-scale packaging perspective. Superscript numbers indicates level of scale.

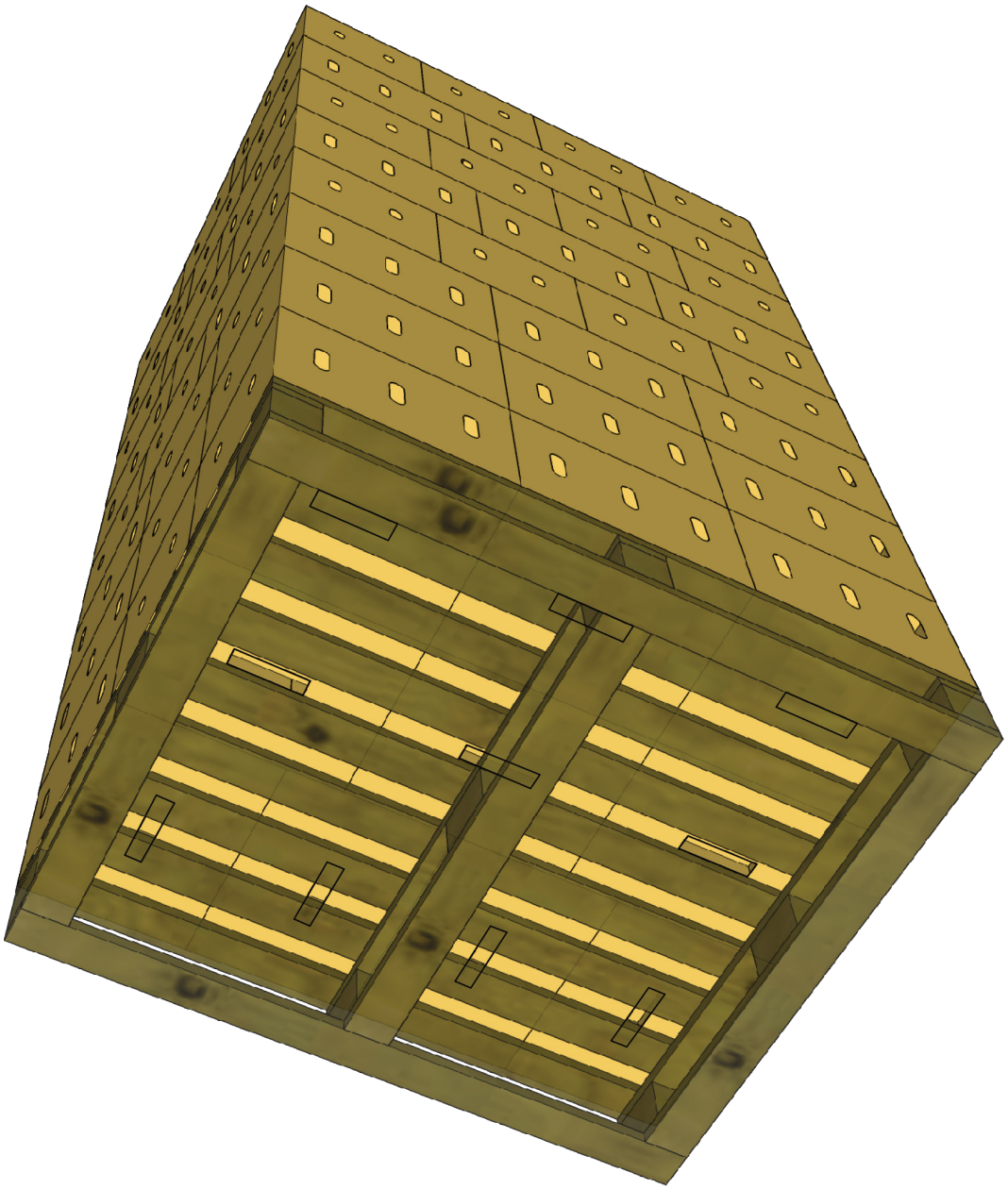

Figure 2.2: Schematic of pallet stack viewed from below, demonstrating cross stacking, with some tiers layered 180 degrees from each other. The schematic also emphasises the location of vent holes at the bottom of stack, as well as the areas obstructed by the pallet.

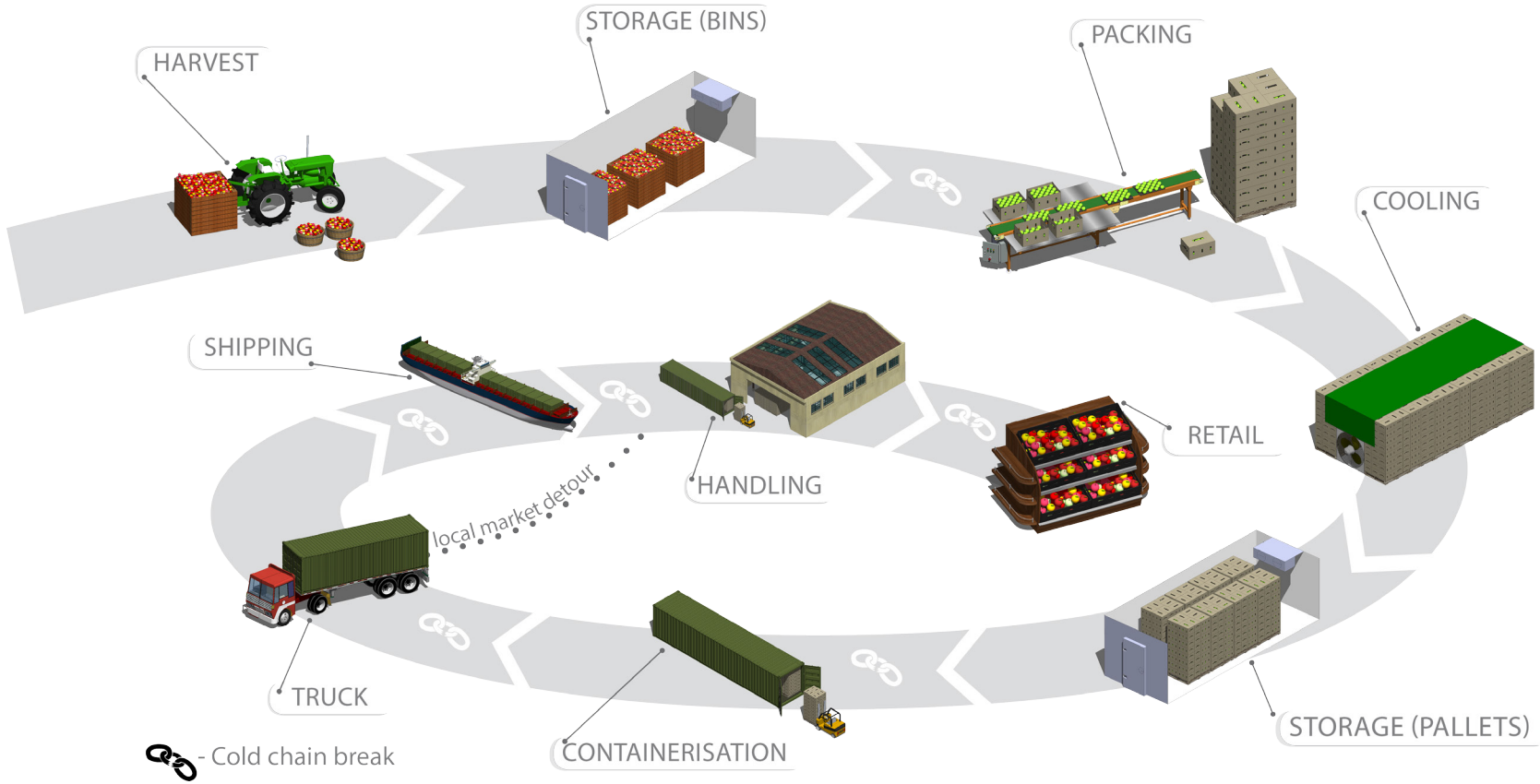

Figure 2.3: Simplified schematic of various steps used in the apple fruit cold chain.

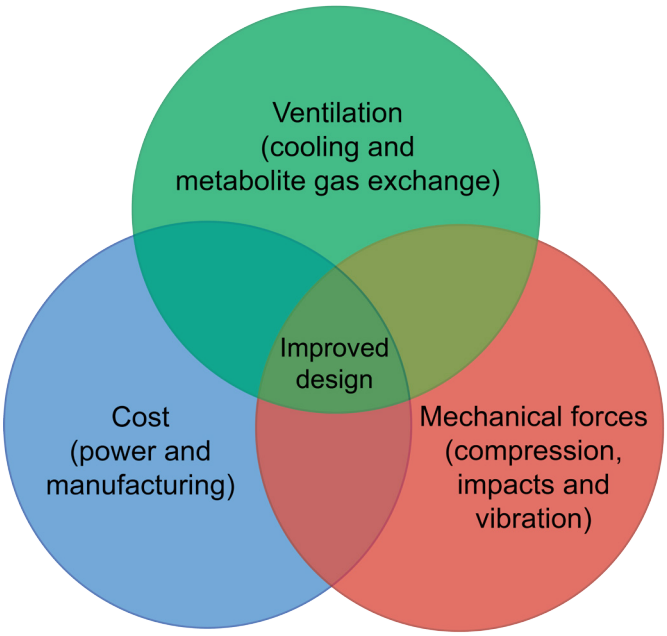

Figure 2.4: Diagram showing overlap between competing design parameters and the improved design niche.

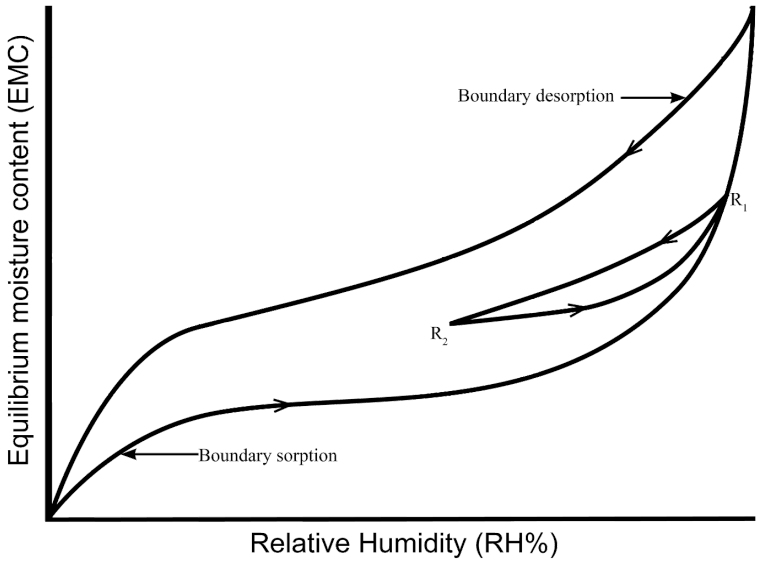

Figure 2.5: Relationship between equilibrium moisture content (EMC) and relative humidity (RH). The boundary absorption and desorption isotherms represent the maximum and minimum EMC per the surrounding RH and, therefore, determine the operating environment of the hysteresis loops. Point R_1 and R_2 represent a desorption and re-adsorption loop. Image adapted from Chatterjee (2001).

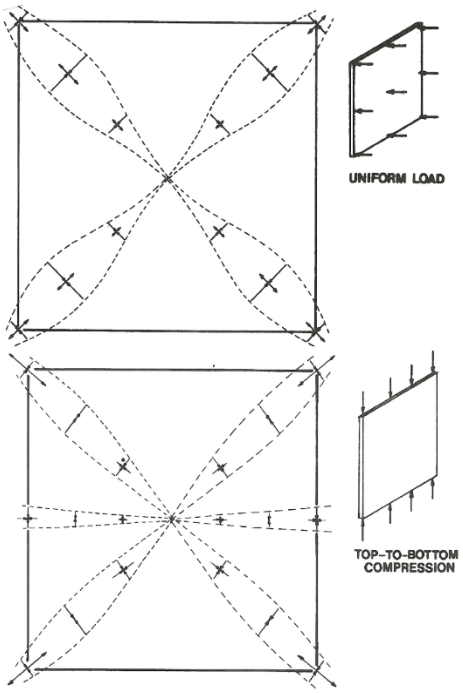

Figure 2.6: Simplified stress distribution across a vertical corrugated fibreboard wall when under side and compression loads (Peterson and Fox, 1989).

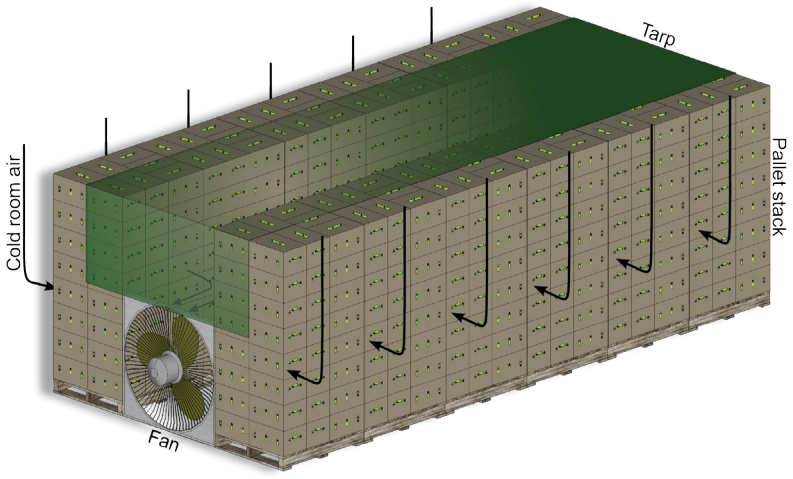

Figure 2.7: Schematic of pallet stacks being cooled using a tunnel-type forced-air cooler.

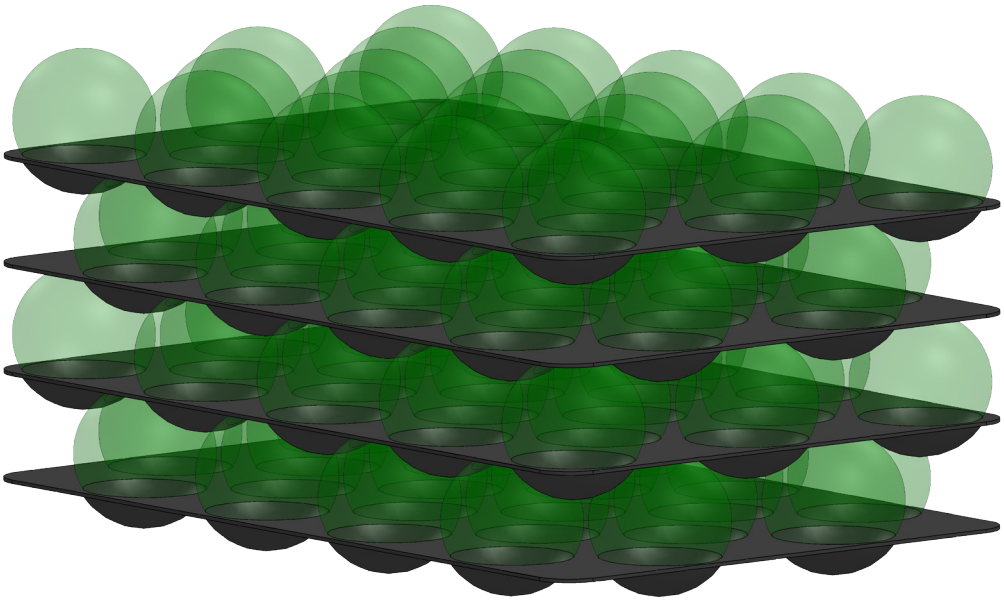

Figure 2.8: Illustration a typical tray packing configuration separating four fruit layers, which is placed inside a carton.

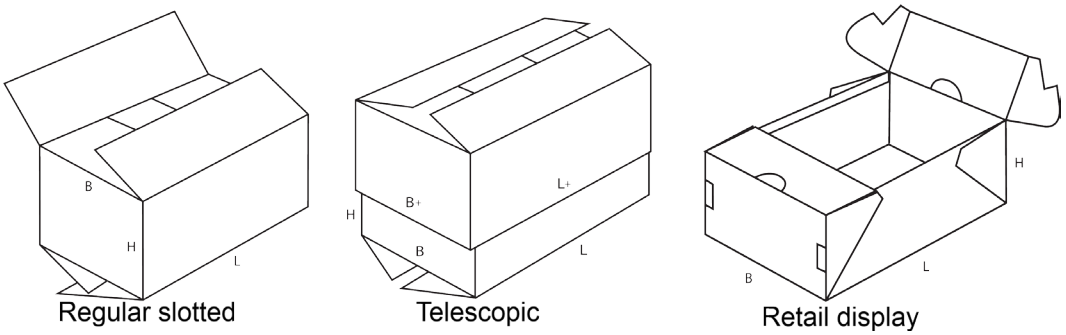

Figure 2.9: Diagram depicting three carton folding/assembly designs (FEFCO and ESBO, 2007).

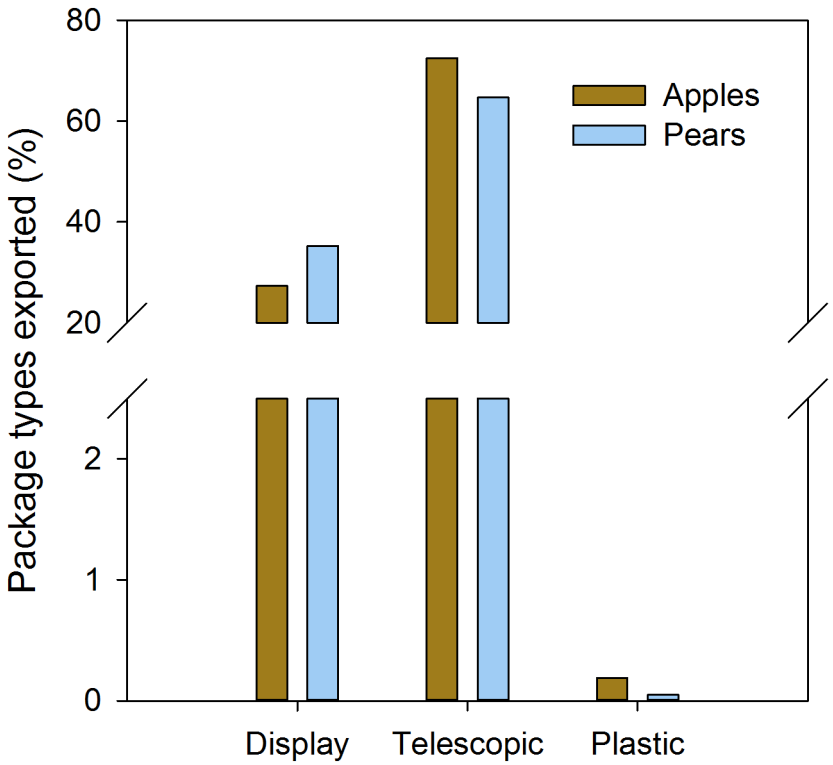

Figure 2.10: Types of horticultural-boxes used to export apples and pears from South Africa between 2008 and 2012. Each category is made up of multiple designs. Display indicates the cartons with open retail display tops, Telescopic indicate closed cartons that make use of an inner and outer component and Plastic indicates boxes made from a plastic material (Berry, 2013; Berry et al., 2015).

Chapter 3. Multi-parameter Analysis of Cooling Efficiency of Ventilated Fruit Cartons using CFD: Impact of Vent Hole Design and Internal Packaging*

Abstract

Forced-air cooling (FAC) efficiency of fruit packed in ventilated cartons can be considerably improved by revising vent hole design and tailoring these openings according to the internal packaging used. Current vent hole designs for fruit cartons, however, often result from trials and errors or are developed in order to improve a specific package functionality, such as fruit cooling rate. This study presents a novel multi-parameter evaluation process for ventilated fruit packaging. This multi-parameter strategy evaluates cooling rate and cooling uniformity, airflow resistance and energy efficiency. Computational fluid dynamics is used to evaluate the impact of internal trays and four vent hole designs. One of the designs investigated is currently used in commercial export of apples, while the other three are new configurations proposed to improve fruit cooling efficiency. Results showed that the addition of trays to the existing commercially used Standard Vent hole design increased ventilation energy consumption by 31% compared to cartons without trays, but in the two newly proposed carton designs (Altvent and Multivent), the energy usage was reduced by 27% and 26%, respectively, as airflow was distributed more evenly between the five fruit layers. The use of the new vent hole designs (Altvent and Multivent) compared to the Standard Vent design, also considerably improved cooling uniformity and energy efficiency during FAC, reducing cooling heterogeneity by 79% and 51%, as well as energy consumption by 48% and 7%, when packed with and without trays, respectively. By simultaneous evaluation of multiple parameters, this analysis approach thus unveiled the benefits and disadvantages of the new ventilated carton designs and can be used to further improve vent hole designs for specific cold chains.

---

*Publication:

Berry, T.M., Defraeye, T., Nicolaï, B.M., Opara, U.L., 2016. Multiparameter analysis of cooling efficiency of ventilated fruit cartons using CFD: Impact of vent hole design and internal packaging. *Food Bioprocess Technol*. 9, 1481–1493.

1. Introduction

Forced-air cooling (FAC) is one of the most prevalent precooling techniques used to remove field heat from produce packed in ventilated packaging (Thompson et al., 2008). The process is achieved by drawing refrigerated air through stacked and packaged fruit with extraction fans which produce a pressure difference across the pallet stack. Cooling rates and uniformity within a carton during FAC are thus determined by the air conditions (temperature, speed) and the airflow distribution through the packaging (Zou et al., 2006a). Inadequate cooling can cause premature senescence, accelerated ripening and spoilage and can be quantified by Van't Hoff's rule. The Van't Hoff's rule states that undamaged, climacteric fruit such as apples will undergo a two to threefold increase in the rate of metabolic reactions for every 10 °C rise in fruit temperature (Salisbury and Ross, 1991). Thus, to better preserve postharvest quality, fruit should be promptly cooled after harvest and maintained at the correct temperatures throughout transport and storage (Ravindra and Goswami, 2008). In addition, FAC needs to be performed within certain time frames to avoid delays in the start of the cold storage, which negatively influences cold chain efficiency and can extend periods that uncooled fruit spend queuing for FAC (Kader, 2002).

Vent holes are added to many packaging types used for horticultural produce to improve cold air penetration and to induce even airflow distribution (Pathare et al., 2012). Recommendations for optimal package vent hole design have long been a priority in the commercial cold chain. Insufficient ventilation can result in excessive energy usage by the fans and extended cooling durations. However, the development of standardised vent hole recommendations can be challenging as many factors can also influence airflow distribution and heat transfer rate (Pathare et al., 2012). Some of these factors include fruit physical properties, packaging geometry and presence of internal packaging, such as trays, liner bags, carry bags or clamshell containers. Nevertheless, several rather general recommendations have been stated. Vigneault & Goyette (2002) recommended a total ventilated area percentage (TVA) per carton wall of 25% or larger for plastic crates, in order to minimise pressure loss and therefore improve cooling efficiency. However, de Castro et al. (2005a) concluded that an overall TVA between 8% and 16% should be used to minimise energy consumption by the FAC fan. When oranges were packed in bulk (without internal packaging), Delele et al. (2013a, 2013b) observed only small increases in fruit cooling rate when TVAs per carton wall exceeded 7%, in comparison with the much larger increases in cooling rate observed for TVAs from 1 to 7%. However, Thompson et al. (2008) recommended a TVA of just 5%, to minimise compression strength loss in the carton. This recommendation coincides with observations by Berry et al. (2015), who reported that the majority of telescopic cartons used for export have an average TVA of 4%.

The presence of internal packaging inside cartons packed with fruit can further influence air distribution and cooling efficiency during precooling. For example, Anderson et al. (2004) demonstrated that airflow distribution to the horticultural produce could be considerably improved if the carton vent hole configuration was designed to work in concert with the geometry of the internal packaging.

The above discussion emphasises the fact that there are several competing parameters determining optimal vent hole design. It is thus necessary to apply a multi-parameter evaluation method to identify an optimal compromise between the different package functionalities. Cold storage efficiency can be evaluated based on several criteria including cooling rate, cooling uniformity and contribution of the package to the FAC fan's energy consumption. In addition, the selected vent hole design has a significant effect on carton mechanical strength (Han and Park, 2007). The vent hole design should, therefore, also be guided by past studies on box strength, or evaluated through an analysis using either experimental tests such as box compression tests (BCTs) or numerically through finite element analysis (Frank, 2014; Pathare and Opara, 2014). Product cooling can be approached either numerically using computational fluid dynamics (CFDs) or experimentally using wind tunnels (Opara and Zou, 2007; Smale et al., 2006; Vigneault and de Castro, 2005; Zou et al., 2006a, 2006b). Product cooling rate and heterogeneity noticeably influences the deterioration rate and spatial distribution of fruit quality in packaging. Another important quality parameter is moisture loss, where the transpiration coefficient indicates the overall rate of moisture loss of a fruit and is a function of the vapour pressure difference between the cellular tissue surface and the surrounding air. However, moisture loss is usually very low during FAC (< 1%) since most FAC procedures occur at high RH values over short durations (Thompson et al., 2008). Energy consumption during FAC is mainly a function of packaging resistance to airflow and the duration of the FAC process (overall cooling time). Fan energy consumption can thus best be reduced by decreasing the pressure drop that needs to be overcome by the FAC fan through improvements in carton design, such as increasing TVA (Thompson et al., 2010).

A wide range of packaging vent design configurations are used in the fresh fruit industry (Berry et al., 2015). In their recent study, Delele et al. (2013a, 2013b) investigated the effects of vent hole design on cooling properties and pressure drop. However, the effect of internal packaging was not included in the designs and the evaluation parameters did not consider package-related energy consumption. Many currently implemented carton designs in the fruit industry have been produced through a process of trial and error and it is expected that significant improvements in performance are still possible (Berry et al., 2015; Cagnon et al., 2013). Future carton design recommendations should, therefore, incorporate the presence of internal packaging (Pathare et al., 2012). In addition, evaluations should integrate the various package performance parameters (e.g., cooling rate) to emphasise carton design effectiveness and energy use efficiency.

The aim of this study was to evaluate the effect of vent hole designs and trays (internal packaging) on the fruit cooling behaviour during FAC of cartons packed with apple fruit. A multi-parameter analysis technique was proposed to evaluate the cooling characteristics of three new vent hole designs against a standard design currently implemented in commercial fruit export. The multi-parameter strategy used CFD simulations to evaluate airflow and cooling parameters.

2. Materials and methods

2.1 Numerical model

2.1.1 Carton geometry

Four vent hole designs, with equal TVA (4%), were evaluated for a telescopic carton (500 × 333 × 270 mm) with the same geometrical dimensions (Figure 3.1). The Standard Vent design, often with the addition of trays, is implemented extensively in the apple fruit export cold chain (Berry et al., 2015). Variations of the Standard Vent design are also frequently observed in other locations and for different produce types, such as pear fruit. The Multivent (MV) and Altvent (AV) designs were proposed in this study as designs that may improve airflow distribution between the packed fruit when trays are present. The Edgevent (EV) design was proposed based on similar recent designs that were successfully tested and implemented for citrus fruit cartons (Defraeye et al., 2014, 2013a; Delele et al., 2013a). In addition, the proposed designs were configured to maximise ventilation alignment during pallet stacking.

2.1.2 Operating conditions

Horizontal airflow, as induced in FAC conditions, was evaluated through the four carton designs (with and without trays) using CFD. The duct and package geometries, as well as the CFD models are shown in Figure 3.2. Some simplifications were introduced to reduce computational cost: (i) only a single carton was used, where in reality several cartons are stacked next to each other on a pallet and (ii) the carton walls and trays were modelled as surfaces with no thickness, but the thickness was included in thermal conductivity predictions. Individual apple fruit were modelled discretely as spheres (Ø 72.36 mm), with each carton holding 150 fruit packed across 5 layers of trays using a staggered packing configuration. Simulations of cartons packed without trays used the same geometrical models as cartons packed with trays; however, the trays were considered permeable to airflow by setting the respective boundary conditions to ‘interior’ as offered from the Fluent solver (ANSYS, 2015). Furthermore, the vent holes in the carton walls were also specified as interior surfaces. Fruit volumes were trimmed by 2.5 mm at points of contact with other fruit, trays and the carton walls to facilitate meshing. The length of the upstream and downstream sections of the domain was determined to limit the influence of the inlet and outlet boundaries.

The inlet boundary condition were set as a uniform velocity inlet, with low turbulence intensity (0.05%). Three airflow rates were evaluated, namely 0.33, 1.00, 3.00 L s^{-1} kg^{-1}, which are representative for FAC flow rates in reality (Brosnan and Sun, 2001; de Castro et al., 2004a; Thompson et al., 2008). Reynolds numbers for flow inside the carton thus ranged between 380 and 4 100, indicating both transitional and turbulent flow regimes (Verboven et al., 2006). The inflow air temperature was set to -0.5 °C, as used in the pome fruit industry. The ambient atmospheric pressure was set at the outlet boundary condition. Thermal properties of the corrugated fibreboard cartons, expanded polystyrene trays and 'Granny Smith' apples were kept constant, irrespective of temperature. Input parameters and boundary layer conditions are listed in Table 3.1. Values for air, 'Granny Smith' apples, corrugated fibreboard and expanded foam polystyrene trays were determined from ASHRAE (2009), Ramaswamy and Tung (1981), Ho et al. (2010) and Margeirsson et al. (2011), respectively.

2.2 **Numerical simulation**

For each carton design a hybrid grid (tetrahedral and hexahedral cells) was created, with 3.90×10^6, 3.89×10^6, 3.89×10^6 and 4.05×10^6 computational cells for the ST, EV, AV and MV designs, respectively. These computational grids were based on a grid sensitivity analysis using Richardson extrapolation (Celik et al., 2008) (Celik et al. 2008). The resulting spatial discretisation error estimate was around 5.0% for the average heat transfer rate across fruit surface and 0.14% for the wall shear stress at the fruit surfaces.

The accuracy of CFD simulations, based on Reynolds-averaged Navier Stokes (RANS), is strongly dependent on the turbulence modelling and boundary-layer modelling approaches used. Regarding turbulence modelling, the shear stress transport (SST) k–ω model (Menter, 1994) was applied in this study as many previous studies presented successful validations for similar cold storage applications with satisfactory agreement with experimental data (Ambaw et al., 2013d; Defraeye et al., 2013a, 2013b, Delele et al., 2013a, 2013b, 2008, Ferrua and Singh, 2011b, 2009a).

Regarding boundary layer modelling, a fine boundary layer mesh is required for low Reynolds number modelling. The complex geometry of most horticultural systems makes such high-resolution meshing around walls such as the cartons and fruit difficult and also entails a large computational cost. Wall functions are, therefore, applied instead of low Reynolds number modelling which significantly reduces computational cost, while still providing satisfactory accuracy (Defraeye et al., 2013b, 2012a; Hu and Sun, 2001). Boundary conditions along the sides of the computational domains leading to the carton (duct) were modelled as symmetry planes (slip walls), which assumed the normal velocity components and normal gradients at the boundary were zero. The carton and tray boundary conditions inside the domain were specified as no-slip walls with zero roughness.

ANSYS-Fluent 15 (ANSYS FLUENT Release 15.0, ANSYS.Inc, Canonsburg, Pennsylvania, USA) CFD software code was used in this study. Second-order discretisation schemes were used throughout and SIMPLE algorithm (Patankar and Spalding, 1972) was used for pressure-velocity coupling. Both buoyancy and radiation were assumed negligible during FAC and were thus not considered in these simulations. Moreover, respiration heat was also considered negligible as apple fruit have relatively low respiration rates (Thompson et al., 2008). Finally, fruit mass loss and the latent heat of evaporation were not explicitly included in this model. Iterative convergence was determined by monitoring the velocity, turbulent kinetic energy, shear stress and temperature along specific boundaries (surface-averaged values) and in the flow field, volume-averaged over the carton.

Steady-state simulations were run prior to transient simulations, in order to obtain flow fields and the initial temperature conditions. The fruit temperature was fixed to the initial condition (20 °C) and the inlet air was set to standard FAC precooling temperatures (-0.5 °C). Flow calculations were disabled during transient simulation, which was possible as the flow field is steady over time and buoyancy was not included in this model. The computational cost was thus reduced, as only the energy equation was solved for the transient cooling. Transient simulations were run for 12 h (real time), with time steps of 2.5 min, as determined from a temporal sensitivity analysis. Simulation time took about 96 h on an Intel® core™ i7-4770 CPU (3.4 GHz) with 32 GB of RAM (Defraeye et al., 2013a, 2013b).

2.3 **Evaluation of package functionalities**

2.3.1 Cooling rate and uniformity

Fruit cooling rate was evaluated using the seven-eighths cooling time (SECT in hours; $t_{7/8}$ in seconds), which is defined as the period needed to cool the produce to seven-eighths of the temperature difference between initial temperature and set air temperature (Becker and Fricke, 2004). The dimensionless temperature (Y) over time (t) is used to determine the cooling curve (Defraeye et al., 2015a, 2015c; Dincer, 1995) using Eq. (3.1). The SECT can thus be identified as the time required for Y to equal 0.125.

$$Y = \left(\frac{T - T_{ref}}{T_i - T_{ref}} \right) = j e^{-Ct} \tag{3.1}$$

where T (°C) is the fruit temperature at a certain time (t), T_i is the initial fruit temperature (20 °C), T_{ref} (-0.5 °C) is the incoming temperature as set for the FAC room, j is the lag factor and C is the cooling coefficient.

The SECT was used in this study as FAC facilities often conclude precooling when the seven-eighths cooling temperature is reached and allows the remaining heat to be removed during storage (static cooling). Temperatures were monitored based on volume-averaged values of each combined fruit layer (30 fruit), as well as point monitors at the core of a centrally positioned fruit of the middle fruit layer (third tray).

Another useful performance parameter is the convective heat transfer coefficient (CHTC) at the surfaces of the apples, which is calculated using Eq. (3.2).

$$h = \text{CHTC} = \frac{q_{c.w}}{T_w - T_{ref}} \tag{3.2}$$

where h (W m^{-2} K^{-1}) is the CHTC, $q_{c,w}$ (J s^{-1} m^{-2}) is the convective heat flux at the air-fruit interface, T_w (°C) is the fruit surface temperature and T_{ref} is the reference or incoming air temperature (T_{ref} = -0.5 °C).

The CHTC serves as a convenient method of quantifying heat exchange at air-material interfaces in complex simulation problems. In this study, the CHTC was only evaluated at the start of FAC (steady-state simulations), so with T_w = 20 °C, which was uniform across all fruit surfaces. This CHTC thus directly reflects the magnitude of the heat flux, as the temperature difference (T_w - T_{ref}) value was constant across all measured surfaces. Furthermore, cooling heterogeneity in each carton was quantified by determining the relative standard deviation (RSD) of the CHTC of each fruit layer; a low percentage indicates homogenous cooling and a high percentage indicates heterogeneous cooling.

2.3.2 FAC energy consumption

Resistance to airflow can be determined by relating the pressure drop over a carton (difference between inlet and outlet) to the flow rate at the inlet. Airflow resistance due to the packaged fruit is often characterised using the Darcy–Forchheimer (DF) equation (van der Sman, 2002). However, the DF equation has two coefficients, namely the Darcy term and the Forchheimer term. The Forchheimer term characterises inertial effects, while the Darcy term characterises the viscous effects. The Darcy term is generally only applicable to flows with Reynolds numbers less than 300 and was therefore ignored in this study (Verboven et al., 2006). The pressure loss coefficient (ξ; kg m^{-7}) was determined from Eq. (3.3) using the pressure differential (ΔP; Pa) and the flow rate (G; m^3 s^{-1}) (Defraeye et al., 2015a):

$$\Delta P = \xi G^2 \tag{3.3}$$

The airflow resistance due to packaging and the operational time of the precooler are the most important factors determining fan energy consumption over the course of a FAC procedure (de Castro et al., 2005a; Defraeye et al., 2015a, 2014). The fan and motor efficiency were ignored as they vary depending on the facility. Eq. (3.4) can then be used to calculate the energy consumption (E; J) by a fan when cooling a single carton packed with fruit. As such, different packaging designs can be directly compared for their package related energy consumption:

$$E = \Delta P G t_{7/8} = \xi G^3 t_{7/8} \tag{3.4}$$

3. Results and discussion

3.1 Cooling characteristics

3.1.1 Cooling rate

Differences between point temperature monitors of a single fruit near the carton centre and volume-averaged temperature monitors using the carton-combined fruit volume were considerably influenced by vent hole design and presence of trays (Figure 3.3). Differences between the temperature values with respect to the various designs and flow rates examined ranged between 4% and 187% when using trays and 1% and 24% without trays. The use and placement of temperature monitors should, therefore, be carefully considered with respect to the carton design and presence of trays, as misleading readings could result in either overly extending or prematurely ending precooling periods. Commercial fruit exports are thus most at risk, as they generally limit the number of temperature sensors used per a pallet, due to the large quantities being handled (Hortgro, 2012).

The cooling rate with respect to the SECT (volume-averaged) and the CHTC (surface-averaged) versus airflow rate are shown in Figure 3.3 and Figure 3.4, respectively. The CHTC is an important determinant of fruit cooling performance during commercial FAC and thus a useful parameter to identify areas of high or low heat exchange and to determine the total heat transfer from fruit (de Castro et al., 2004a). A good correlation ($R^2 = 0.99$) between CHTC and airflow rate was found using a power-law curve, which is consistent with previous studies (Defraeye et al., 2014).

Only small differences between the ST, AV and MV carton vent designs were observed, namely, < 1% for the CHTC and < 7% for SECT. This can be attributed to similar airflow distributions between the fruit and thus comparable convective heat transfer rates (de Castro et al., 2005a). In contrast to the other designs, the EV carton had a 37% ±4% and 17% ±1% lower CHTC, as well as 75% ±12% and 22% ±9% higher SECT compared to the Standard Vent design for the carton packed with and without trays, respectively. The considerably lower cooling rates of the EV

design was due to poor airflow distribution, where the vent holes at the top and bottom of the carton caused airflow to bypass fruit packed near the vertical centre of the carton. The presence of trays further limited heat transfer to fruit packed closer to the vertical centre, thus reducing overall fruit cooling rate.

3.1.2 Cooling heterogeneity

Table 3.2 shows the RSD of the different cartons with and without trays at the three airflow rates tested. The top and bottom air distribution of the EV carton also resulted in high cooling heterogeneity (RSD = 70%), which was on average 3.8 times larger than other carton designs. Figure 3.5 also emphasises the cooling heterogeneity and shows that fruit positioned at the vertical centre of the EV carton were at considerably lower CHTC values when compared to similarly positioned fruit in other carton designs. Additionally, the presence of trays in the EV carton increased heterogeneity (RSD) by 87%, as the trays further restricted vertical airflow movement.

The Standard Vent design produced an RSD half of the EV design's, which was also influenced by the presence of trays and increased the average value by 87% (Table 3.2). In contrast, the AV and MV vent hole designs had the lowest cooling heterogeneity values, producing on average an RSD one third of the Standard Vent design. The addition of trays to the AV and MV cartons slightly improved cooling uniformity compared to the other designs (Table 3.2), by maintaining an even distribution of airflow to each fruit layer. In contrast to the Standard Vent, these results promote the usage of the proposed AV and MV designs, which were specifically configured to evenly distribute airflow across all the fruit, irrespective of tray usage.

An alternative representation of cooling heterogeneity is shown in Figure 3.6, which displays the relative frequency distribution of the average CHTC at each computational cell of the simulated fruit surfaces. Local high $CHTC/CHTC_{ave}$ values indicate rapid cooling compared to the rest of the carton, such as fruit positioned near vent holes with incoming airflow, which may therefore be more susceptible to chilling injury. Conversely, fruit with low $CHTC/CHTC_{ave}$, such as fruit located downwind, in areas with low air speed, may not be sufficiently cooled at the end of the FAC procedure. Improved carton designs should produce relative distribution graphs with large peaks at $CHTC/CHTC_{ave}$ of 1.0 and a smaller spread.

Figure 3.6 shows the distribution became skewed towards low $CHTC/CHTC_{ave}$ at the lowest airflow rate (0.33 L s^{-1} kg^{-1}). The reason for this is the large cooling heterogeneity across the horizontal axis (airflow direction). However, as flow rates increased, the relative frequency distribution progressively developed towards a more normal distribution. Increasing flow rates thus improved cooling heterogeneity (de Castro et al., 2004b) but did not generally affect cooling differences between the five fruit layers (Table 3.2). Figure 3.6 thus shows that all the vent hole designs produced more normal curve distributions at flow rates of

3.00 L s^{-1} kg^{-1}. However, due to improved vent hole design, the AV and MV designs cooled considerably more uniformly than did the Standard Vent and EV designs at lower flow rates (0.33-1.00 L s^{-1} kg^{-1}).

3.2 **Package-related energy consumption**

3.2.1 Resistance to airflow

The resistance to airflow of the four vent hole designs was determined by applying three consecutive airflow rates and monitoring the corresponding pressure drop over the package. The results are shown in Figure 3.7, where the pressure drop ranged between 10 and 1560 Pa for airflow rates between 0.33 and 3.00 L s^{-1} kg^{-1}. Resistance to airflow was then quantified using the pressure loss coefficient (ζ) as shown in Table 3.3, which was calculated by correlating Eq. (3.3) to the respective data points.

Figure 3.7 and Table 3.3 show that the addition of trays did not meaningfully influence (< 1%) the resistance to airflow in the EV carton, as it did in the other carton designs. Moreover, the EV carton had the lowest resistance to airflow of all the carton designs examined. This can again be attributed to the vent hole positions which were located at the top and bottom of the carton. Airflow thus progressed along the top and bottom walls of the carton (Figure 3.5) where apples are less densely packed, resulting in lower resistance to airflow and the circumvention of areas containing trays. These results are similar to observations made by Defraeye et al. (2013a) and Delele et al. (2013a) when using similar EV vent hole designs on smaller citrus cartons (400 × 300 × 270 mm) with no internal packaging (trays).

Furthermore, almost no difference (< 1%) was observed in resistance to airflow between the Standard Vent and AV cartons when packed without trays, but on average the carton designs had a 29% larger pressure loss coefficient than did the EV cartons. The similar Standard Vent and AV results can be explained by the comparable vent hole shapes, which were both vertical oblong. However, the Standard Vent vent holes were positioned near the vertical centre and the AV vent holes were in alternating high and low positions (Figure 3.1). The benefit of the AV vent hole design was, therefore, best observed with the addition of trays, where the pressure loss coefficient of the Standard Vent carton increased by 33% and the AV only increased by 13% (Table 3.3). The vertical staggered positioning of the AV vent holes, thus allowed air to be distributed more evenly across the multiple trays (fruit layers). In contrast, the Standard Vent vent holes distributed a majority of the airflow to only one fruit layer (Figure 3.1).

Finally, the MV carton had a pressure loss coefficient of 35% and 21% smaller than the Standard Vent carton design when packed with and without trays, respectively. However, the MV still had a resistance to airflow slightly larger to the EV cartons (< 13%). Consequently, the MV and EV vent hole designs generated a much lower resistance to airflow compared to the Standard Vent or AV cartons. However, note that these results only target the resistance to airflow, whereas cooling performance should also be accounted for when evaluating package performance.

3.2.2 Package-related energy consumption

The resistance to airflow of packaged fruit determines the FAC equipment's working point and thus the power needed to maintain a specific flow rate during FAC. The MV and EV cartons thus required less power to achieve similar FAC flow rates, compared to the AV and Standard Vent cartons. However, the total energy consumption needed to reach the seven-eighths cooling temperature is a function of both the FAC equipment's power usage (ξG^3; W) and the duration ($t_{⅞}$) of FAC procedure (Eq. (3.4)). It should also be noted, that the package-related power consumption increases non-linearly with the airflow rate and also depends on the fan and motor efficiencies (Defraeye et al. 2015b).

Fruit cooling rate is determined by the temperature difference between the fruit and the neighbouring air. This in turn is dependent on the geometry of the packaging (ventilated carton design, internal packaging and fruit), which influences the air distribution and velocity amongst the packed fruit. The MV carton design (with trays) produced an even airflow distribution across the fruit and therefore averaged a SECT of 3.1 h with a standard deviation between the five fruit layers of 0.1 h. In contrast, the unventilated (Figure 3.1), centrally positioned fruit layers of the EV carton design (with trays) were exposed to less cooling airflow, resulting in a SECT (volume-averaged) of 8.9 hours, compared to the top and bottom fruit layers which cooled at an average SECT of 3.8 h (results not shown). The total fruit cooling rate of the EV carton design was thus extended as a result of uneven airflow distribution.

FAC is utilised in cold storage to decrease fruit cooling durations and should therefore be completed within a set period of time, which is accomplished by adjusting the power usage of the fan (Wang and Muller 2000). The relationship between FAC power consumption and SECT is thus a relevant performance parameter for practitioners in the cold chain, as it quantifies the FAC energy efficiency of a package (Defraeye et al., 2015c; Thompson et al., 2010). To quantify the carton designs FAC efficiency, the curve produced from the package-related power usage (w; W) versus the SECT was plotted in Figure 3.8. The data points were correlated using a power-law curve ($w = \alpha t_{⅞}^{b}$; adjusted $R^2 \geq 0.99$) and the resulting parameters are shown in Table 3.4. The b parameter showed a rather constant value (-6.00), which left the α parameter to be used as the only variable term to collectively quantify the various vent hole designs according to forced-air cooling efficiency.

Although low resistance to airflow values were observed in the EV carton design, without trays the EV design required 65% more energy to reach the necessary seven-eighths cooling temperature compared to the Standard Vent design (Figure 3.8), due to the longer SECT. Furthermore, the addition of trays to the EV carton increased the energy consumption by a factor of 7. Relatively similar energy consumption curves were observed between the Standard Vent and AV designs without trays. However, with the addition of trays, the energy consumption of the Standard Vent carton increased by 31% and the AV carton actually decreased by 27% as a result of the trays more evenly redistributing cool air to the fruit (Figure 3.8). Finally, the MV carton design cooled the most efficiently, reducing energy consumption by 58% and 25% compared to the Standard Vent carton when packed with and without trays, respectively. Use of the MV vent hole design is thus the most promising design to reduce energy consumption during FAC. However, the AV vent hole design may offer an acceptable alternative if the MV carton design is rejected due to other performance parameters.

4. Conclusions

This study implemented a multi-parameter approach to the evaluation of one commercially used and three new horticultural packaging designs with different vent hole configurations. In addition, the effect of trays (internal packaging) on the various packaging designs was also examined. To achieve this, computational fluid dynamics was used to evaluate each carton design during forced-air cooling according to several performance criteria. These included cooling rate, uniformity, resistance to airflow and package-related energy consumption. The relationship between cooling rate and package-related power consumption was also combined into a single performance parameter (forced-air cooling efficiency), on the principle that forced-air cooling needs to meet certain time constraints within the cold chain.

The Altvent vent hole design was proposed in this study as a modification of the commercially used Standard Vent design. Without trays the Standard Vent carton design had a similar forced-air cooling efficiency to the Altvent carton design. However, with trays, the Standard Vent design decreased in forced-air cooling efficiency and cooling uniformity as a result of the upper and lower fruit layers being short circuited from air distribution. Conversely, trays improved cooling uniformity in the Altvent design, as all fruit cooled relatively homogenously since each fruit layer was well ventilated.

A variation of the Edgevent vent hole design is actively used in citrus fruit packaging where it has shown improved performance versus other commercial designs. The Edgevent design mostly distributes air along the top and bottom walls of the carton and therefore bypasses fruit located near the centre of the carton, resulting in low cooling uniformity and forced-air cooling efficiency. Furthermore, the addition of trays considerably increased cooling heterogeneity and the package-related power consumption to force air through by means of fans. The Edgevent vent hole design is therefore not suitable for use in fruit packaging in combination

with trays. However, due to the Edgevent design's low resistance to airflow, it may provide better cold air penetration in large stacking volumes compared to other designs, in situations such as when only low power fans are available.

The Multivent design used multiple vent holes across a carton's wall to distribute air evenly between the fruit. The Multivent carton design cooled more efficiently and uniformly than did any of the other carton designs and demonstrated improved performance with the addition of trays to the cartons. Energy usage and cooling uniformity (relative standard deviation) values compared to the commercially implemented Standard Vent design was thus reduced by 43% and 71%, respectively. The Multivent design therefore offers a favourable alternative over the other examined vent hole designs and emphasised the benefits of matching a carton's vent hole design to the packages internal geometry (internal packaging and fruit). It should be noted however, that other performance parameters may also need to be included into the design's final evaluation before commercial implementation. For example, the vent hole configuration has a significant effect on mechanical strength. Cartons using vent hole configurations that reduce mechanical strength will need to be compensated for with thicker materials, which undesirably increases production costs. Future carton design assessments should therefore extend this multi-parameter evaluation approach to additional performance parameters.

Table 3.1: Boundary conditions and input parameters.

Parameters	Value
Air density (kg m^{-3})	1.185
Air specific heat capacity (J kg^{-1} K^{-1})	1 004.4
Air thermal conductivity (W m^{-1} K^{-1})	0.0261
Granny smith apple density (kg m^{-3})	829
Granny smith apple specific heat capacity (J kg^{-1} K^{-1})	3580
Granny smith apple thermal conductivity (W m^{-1} K^{-1})	0.398
Corrugated fibreboard carton density (kg m^{-3})	145
Corrugated fibreboard carton specific heat capacity (J kg^{-1} K^{-1})	1 338
Corrugated fibreboard carton thermal conductivity (W m^{-1} K^{-1})	0.064
Trays (expanded polystyrene foam) density (kg m^{-3})	23
Trays (expanded polystyrene foam) specific heat capacity (J kg^{-1} K^{-1})	1 280
Trays (expanded polystyrene foam) thermal conductivity (W m^{-1} K^{-1})	0.036
T_{ref} - Inlet cooling temperature (ºC)	-0.5.0
T_w - Initial apple temperature (ºC)	20.0

Table 3.2: Percentage relative standard deviation (heterogeneity) of CHTC between the five fruit layers with respect to airflow rate for the cartons.

Flow rate (L s^{-1} kg^{-1})	With trays				No trays			
	AV	EV	MV	ST	AV	EV	MV	ST
0.33	10.5	97.1	7.2	46.5	14.0	61.0	11.0	26.1
1.00	10.2	89.5	7.9	42.4	12.0	44.4	10.5	22.0
3.00	11.1	88.6	9.7	44.3	11.6	42.1	11.4	23.2

Table 3.3: Pressure loss coefficient (kg m^{-7}) for both cartons packed with and without trays.

Vent hole Design	With trays	No trays
Standard Vent	287 600	215 700
Edgevent	166 100	167 300
Altvent	242 100	214 200
Multivent	187 700	171 200

Table 3.4: Parameters α and b for power-law correlations of the power usage (w; W) versus SECT (hours): $w(t) = \alpha t_{⅛}^{b}$.

Vent hole design		α	b	Adjusted R^2
Standard Vent	With trays	2 366	-6	1.0000
Edgevent		23 760	-6	0.9992
Altvent		1 464	-6	0.9999
Multivent		1 003	-6	0.9998
Standard Vent	No trays	1 806	-6	0.9996
Edgevent		2 976	-6	1.0000
Altvent		2 013	-6	0.9997
Multivent		1 363	-6	0.9993

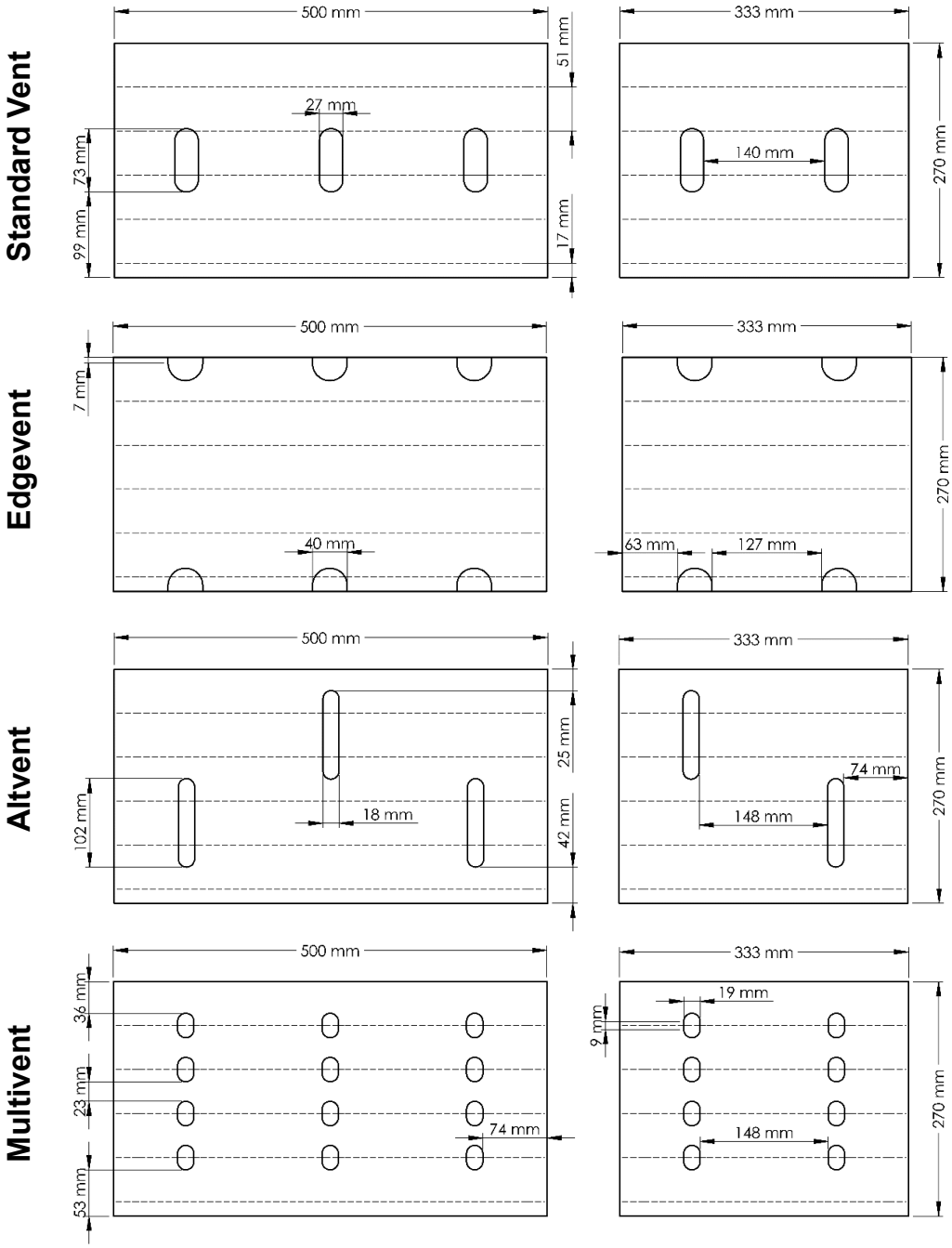

Figure 3.1: Geometry and diagram of the cartons: Standard Vent, Edgevent, Altvent and Multivent. Dashed line indicates positions of the five trays, FAC was examined through the 500 × 270 mm face only.

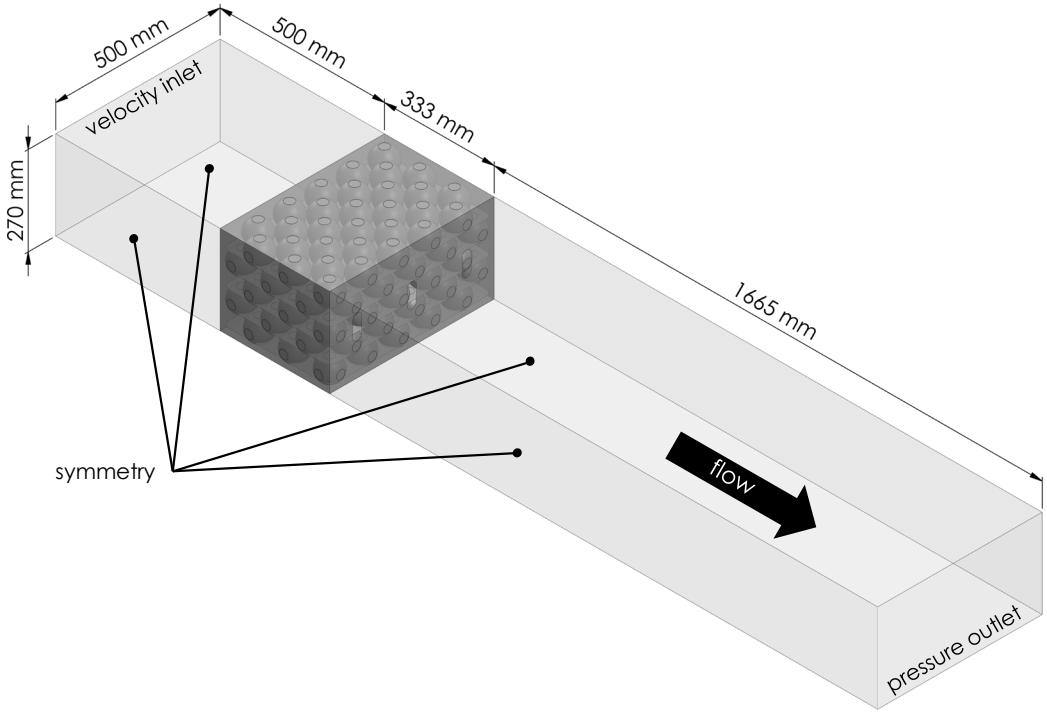

Figure 3.2: Duct, package geometries and boundary conditions for a single carton.

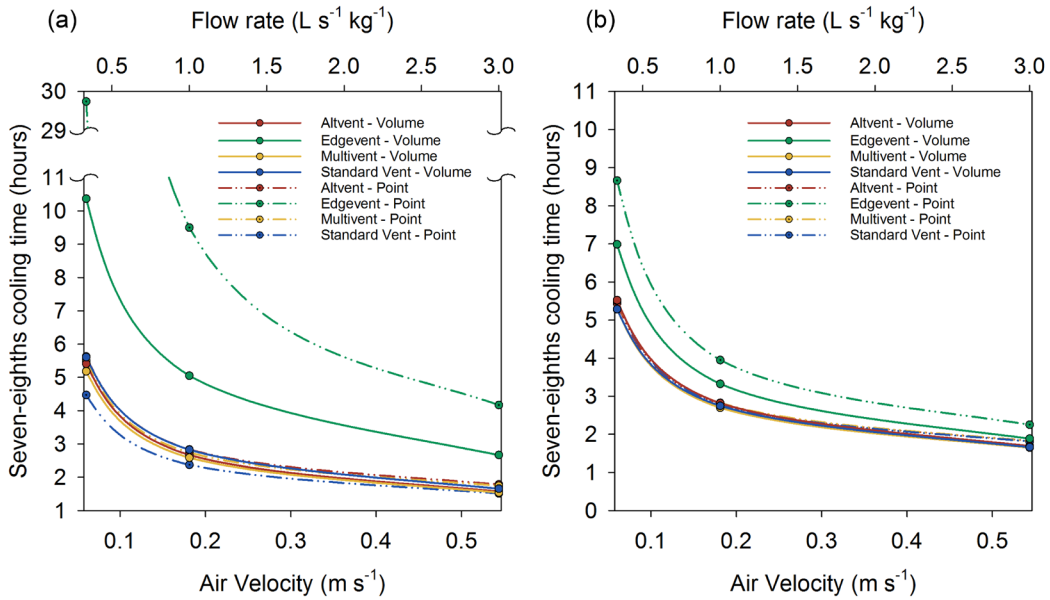

Figure 3.3: Seven-eighths cooling time as a function of air velocity and airflow rate for cartons packed using apples (a) with and (b) without trays. Values were taken using volume-averaged monitors and point monitors placed at the core of centrally positioned fruit (3rd fruit layer).

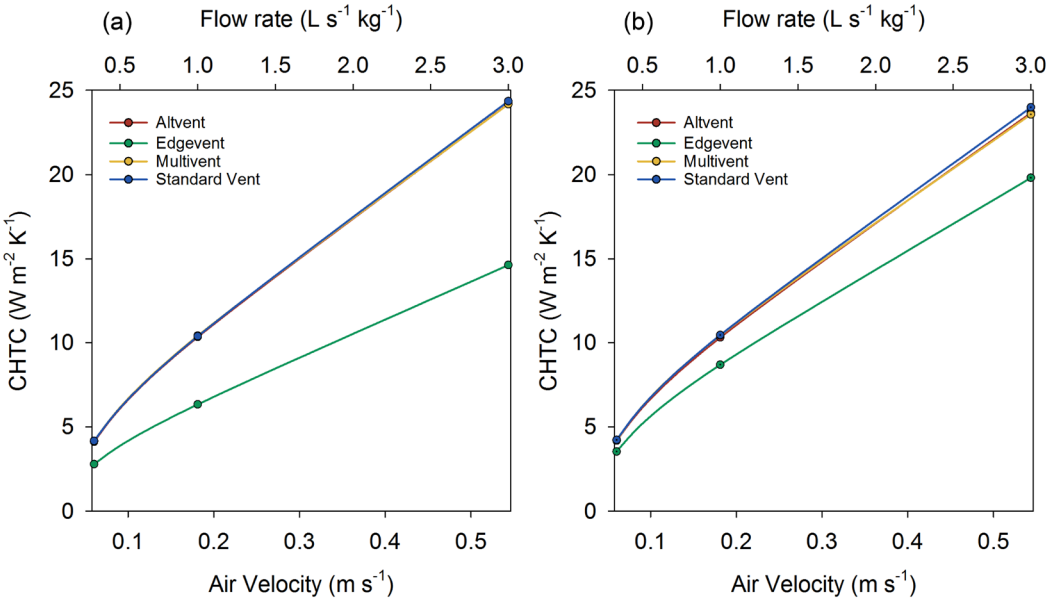

Figure 3.4: Convective heat transfer coefficient with respect to air velocity and airflow rate for cartons packed using apples both (a) with and (b) without trays.

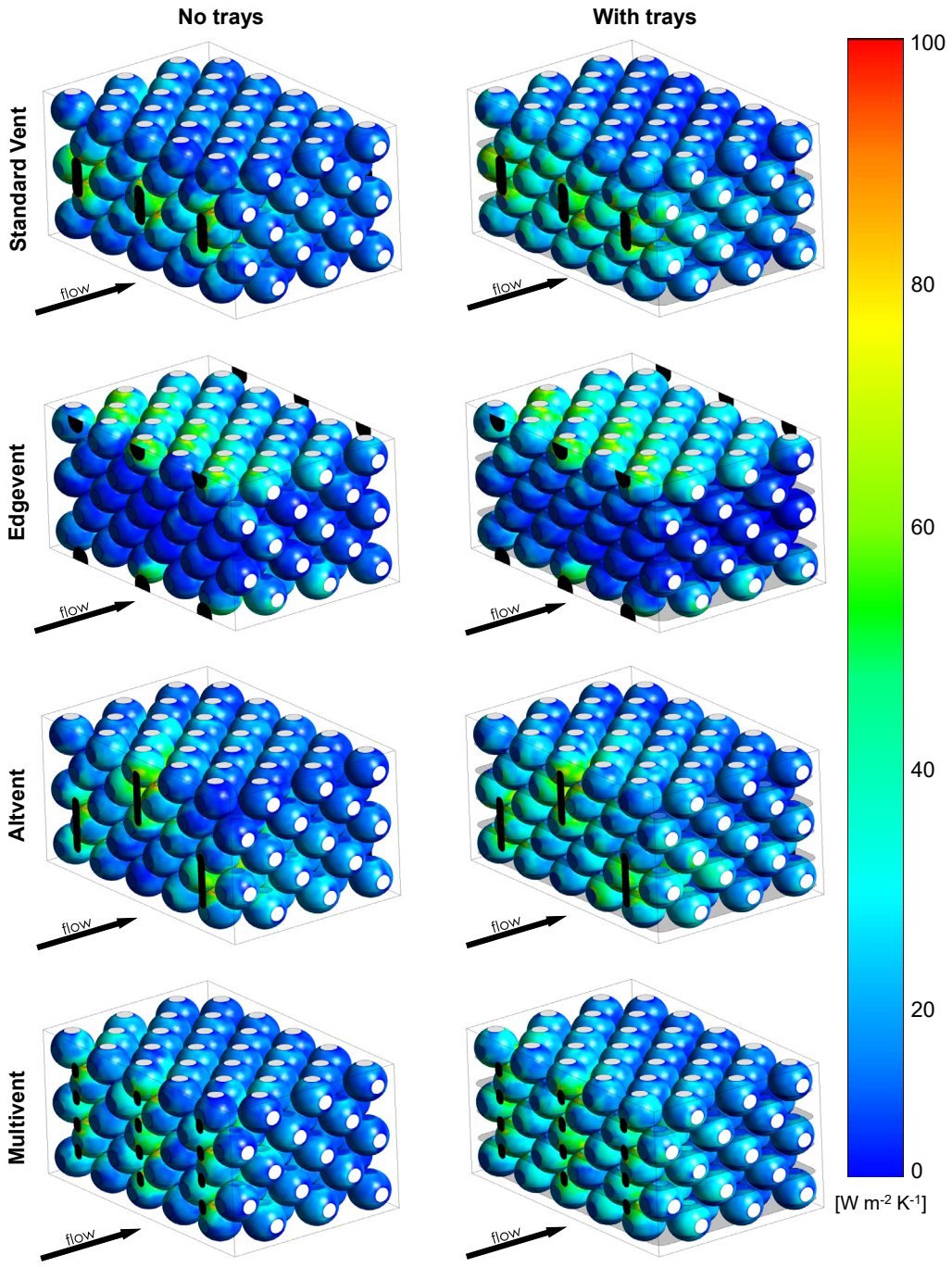

Figure 3.5: Distribution of CHTC values over apple fruit surfaces for the Altvent, Edgevent, Multivent and Standard Vent at 1 L s^{-1} kg^{-1}.

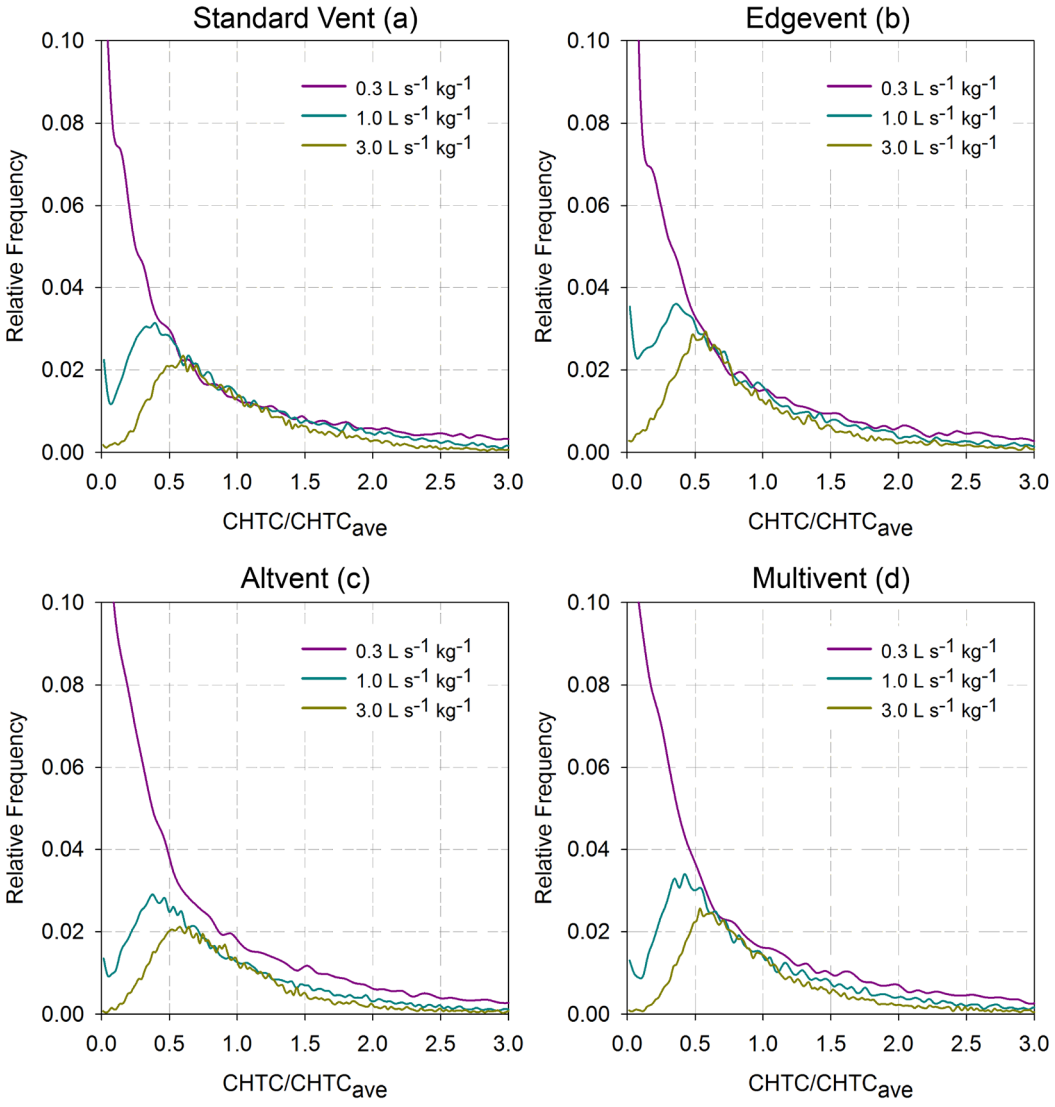

Figure 3.6: Relative frequency distribution of the average CHTC of every cell on the simulated apple fruit for the (a) ST, (b) EV, (c) AV and (d) MV carton designs with trays.

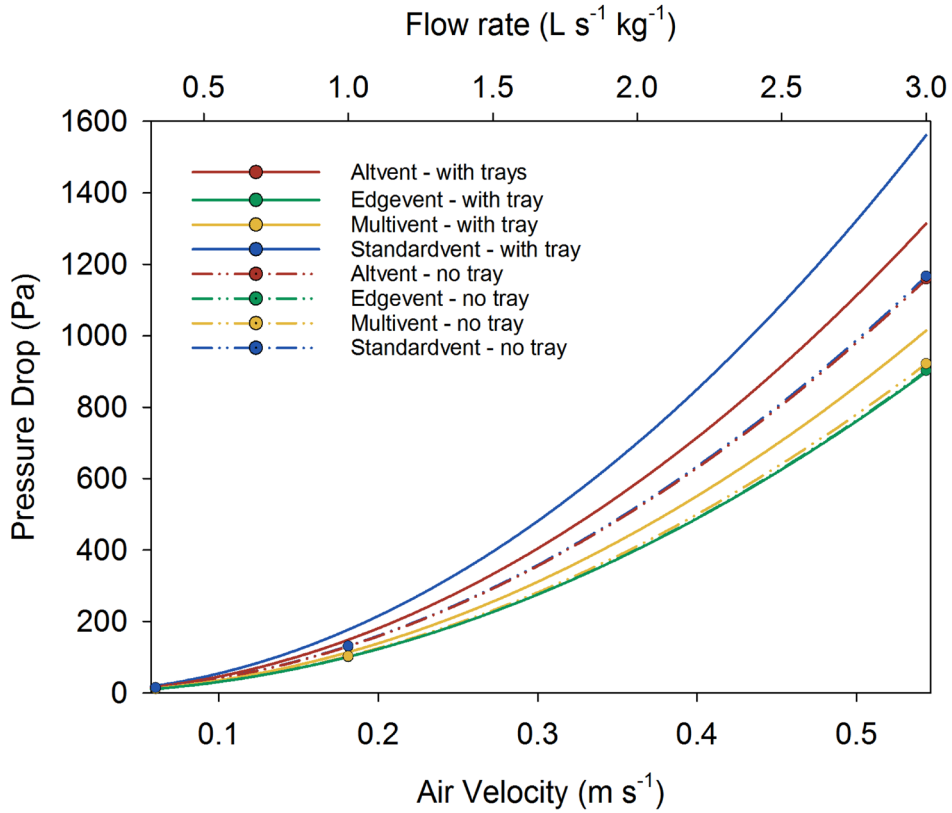

Figure 3.7: Pressure drop as a function of air speed and airflow rate for cartons packed using apples with and without trays.

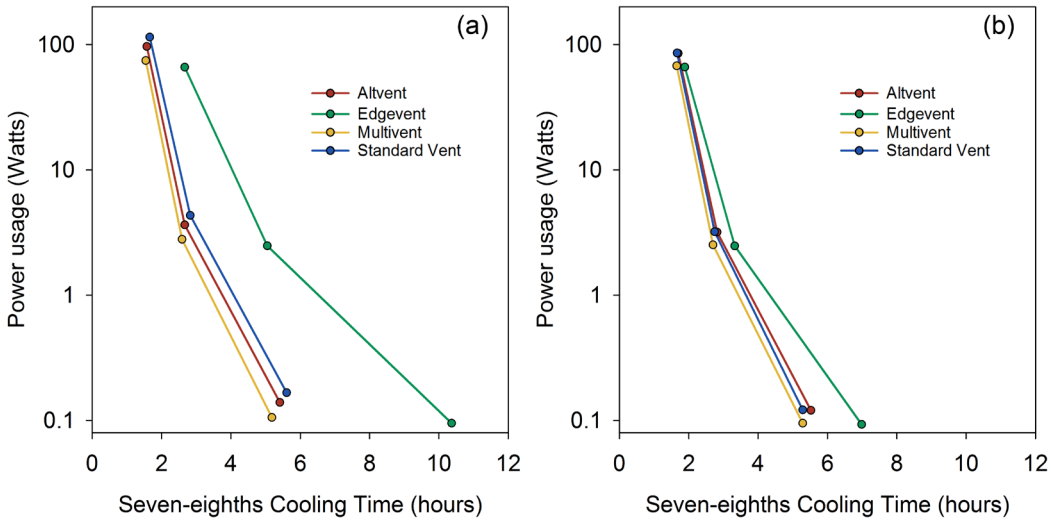

Figure 3.8: Ventilation power usage (logarithmic scale) versus seven-eighths cooling time for cartons packed using apples (a) with and (b) without trays.

Chapter 4. The Role of Horticultural Carton Vent Hole Design on Cooling Efficiency and Compression Strength: A Multi-parameter Approach*

Abstract

Forced-air cooling (FAC) is used to rapidly remove the field heat of horticultural produce to better preserve quality. Cartons are ventilated to promote uniform cooling of the packed produce and to minimise energy used by precooler fans. The resulting cooling efficiency is influenced by the area and configuration of carton vent holes. However, placing vent holes also reduces the carton compression strength, which requires reinforcement using additional fibreboard, thereby increasing carton manufacturing costs. This study, therefore, applied a multi-parameter evaluation approach to assess four carton designs, each for three vent hole areas and three corrugated fibreboard grades. Computational fluid dynamics (CFD) was used to evaluate airflow resistance, cooling rate, uniformity and package related energy consumption. Experiments were used to quantify box compression strength. Results of mechanical strength evaluation showed a negative linear relationship between carton strength and vent hole area. The effect of vent hole configuration on compression strength was dependent on the corrugated fibreboard grade. For cartons packed using trays, the Multivent vent hole design used 58% less FAC energy and also significantly improved cooling uniformity compared to the Standard vent design. The significant improvement in FAC energy efficiency, therefore, enables the Multivent to match or improve the compression strength and FAC energy efficiency of the Standard vent design, by using a considerably smaller ventilation area. This study thus demonstrates the importance of incorporating a multi-parameter approach in developing improved packaging with optimised vent hole designs.

---

* Publication:

Berry, T.M., Fadiji, T.S., Defraeye, T., Opara, U.L., 2017. The role of horticultural carton vent hole design on cooling efficiency and compression strength: A multi-parameter approach. *Postharvest Biol. Technol*. 124, 62–74.

1. Introduction

With the size of the world's population predicted to reach 9.1 billion by 2050, reducing high incidence of postharvest losses, which is estimated at 15-30% globally, is a necessary step in ensuring future food security (FAO, 2009; Munhuweyi et al., 2016; Opara, 2010). Temperature mismanagement and physical damage are considered the most common causes of postharvest losses of fresh fruit (Kader, 2002; Opara and Pathare, 2014) and can be minimised by using packaging and cold chain facilities more efficiently (Gustavsson et al., 2011; Opara and Mditshwa, 2013; Pathare and Opara, 2014). Future packaging will thus be expected to play a greater role in facilitating temperature regulation during precooling processes, as well as protecting produce from physical damage, such as bruising or abrasion (Defraeye et al., 2015a; Thompson et al., 2008). The ventilation design of horticultural packaging, must therefore take into consideration multiple performance parameters so that it functions efficiently across all areas of the cold chain.

Cartons are commonly palletised to simplify handling and to improve packing density during precooling, transport and storage. Packaging containers and pallet structures create barriers between the fruit and the surrounding refrigerated air, which limits cooling and quality preservation. Air penetration is therefore enhanced by adding vent holes to the cartons. Fruit cooling rate and uniformity are typically a function of the airflow rate and cooling air temperature, as well as the resulting airflow distribution in the carton. These aspects are determined by the produce-packaging system, including vent holes, fruit size, fruit shape, packing configuration and internal packaging (Anderson et al., 2004; Han et al., 2015; O'Sullivan et al., 2016; van der Sman, 2002). Conversely, vent holes must be added cautiously as they reduce carton mechanical strength and, therefore, increase susceptibility to mechanical failure, particularly when palletised. Several studies have identified improved vent hole designs for higher mechanical strength using various strategies (Frank et al., 2010; Singh et al., 2008). Jinkarn et al. (2006) examined circular and oblong (elliptical) vent holes and determined that circular vent holes placed near the wall centre reduced mechanical strength less than other designs. Han and Park (2007) also examined circular and oblong vent holes; however, the authors showed that vertical oblong vent holes were preferable to other designs, which is consistent with designs used in commercial environments (Berry et al., 2015).

Vent hole design has been investigated predominantly in the context of forced-air cooling (FAC), with the aim of improving air penetration into the stack of cartons. This is essential to facilitate rapid and uniform fruit cooling during FAC, without creating conditions that induce fruit chilling injury (Alvarez and Flick, 1999a; Kader, 2002; Sevillano et al., 2009). FAC entails a fan system that draws refrigerated air horizontally through pallets and cools the fruit convectively. FAC should also be designed so that the desired temperatures are reached within fixed time frames, to avoid delays in the handling procedure. Prolonged FAC can negatively influence cold chain efficiency and can unnecessarily extend periods that uncooled fruit spend queuing for FAC (Kader, 2002).

Another important aspect in FAC is fan energy consumption, which is a function of the pallet's resistance to airflow (RTA), the working point of the fan, and the overall cooling time (Anderson et al., 2004). Optimising fan selection to match the aerodynamic resistance of a package-produce system will enable the fan to operate more energy-efficiently while still providing a satisfactory produce cooling rate. RTA is determined by the produce geometry (size and shape), surface roughness, packing pattern and porosity inside the carton and the vent hole design (Chau et al., 1985; Eisfeld and Schnitzlein, 2001; Ngcobo et al., 2012a). RTA is characterised by the relationship between pressure drop and airflow rate. At low flow rates, this relationship shows a linear trend (van der Sman, 2002). However, a polynomial equation is usually required at high flow rates, with increased Reynolds numbers (Verboven et al., 2006). Fan systems consume significantly more energy at higher airflow rates than at low airflow rates. Moreover, the use of internal packaging types such as trays or liner bags can considerably influence the RTA of packaged produce, as well as alter the airflow distribution inside a carton (Ngcobo et al., 2012a; O'Sullivan et al., 2016).

Despite the many variables affecting carton performance, most studies have focused on only a single performance parameter, such as mechanical strength or cooling rate (Defraeye et al., 2015a; Pathare et al., 2012). For example, de Castro et al. (2005a) showed that cartons with a total ventilated area percentage (TVA) of 8% to 16% cooled most efficiently. However, due to the negative effect of large vent holes on the mechanical strength of corrugated fibreboard carton, Thompson et al. (2008) recommended a much smaller TVA, namely 5% to 6%. Cartons with larger vent holes can be manufactured however, but then require reinforcement with additional fibreboard materials, which undesirably increases manufacturing costs. For packaging made from stronger materials such as plastic, Vigneault & Goyette (2002) recommended a TVA of 25%, which is possible due to the higher material strength. Most developments in packaging design have primarily occurred within the horticultural industry through a process of trial and error. This current practice to carton design optimisation is therefore missing a guided multi-parameter approach that simultaneously evaluates the effects of vent-hole design and carton material properties on cooling, energy usage and mechanical strength (Defraeye et al., 2015a).

Currently, the most reliable method of evaluating mechanical strength is through box compression tests (BCT), although several studies have made significant progress towards numerical techniques, such as finite element analysis (Frank, 2014). On the other hand, evaluation of cooling efficiency can be determined experimentally or also numerically, through computational fluid dynamics (CFD) (Ambaw et al., 2013a; Zhao et al., 2016; Zou et al., 2006a, 2006b). CFD has the advantage that it can analyse both surface-averaged and volume-averaged quantities, such as convective heat transfer coefficients (CHTC) and produce cooling temperatures (Defraeye et al., 2014, 2013a). CFD can also incorporate the effect of discrete fruit packing and internal packaging geometries (Berry et al., 2016; Delele et al., 2013a; Opara and Zou, 2007; Zou et al., 2006b).

The aim of this study is to develop a vent hole design that performs best with respect to trade-offs between the various performance parameters. The effect of vent hole design (configuration and TVA) on cooling performance, FAC fan energy consumption and carton mechanical strength was thus evaluated. Furthermore, the study also examined the efficacy of using various corrugated fibreboard grades in the carton production to offset the negative effects of vent holes on mechanical strength. A multi-parameter analysis technique was applied on three new vent hole designs as well as on a Standard vent design, which is currently implemented for commercial fruit export. The multi-parameter strategy combines CFD simulations to evaluate airflow characteristics and cooling properties, with experimental BCT assessments used for mechanical strength evaluations. This study is a follow-up of Berry et al. (2016), which investigated the effect of vent hole configuration on FAC performance when packing apple cartons with and without trays.

2. Materials and methods

2.1 Package design

Twelve vent hole designs were investigated for telescopic cartons (500 × 333 × 270 mm) packed ‘Granny Smith’ apple fruit on expanded polystyrene trays. The designs comprised of 4 vent hole configurations (shape and position) as proposed in Berry et al. (2016), each evaluated for three vent hole areas (TVA = 2%, 4% and 8%) as shown in Figure 4.1. The Standard vent (ST) configuration is commonly used for commercial pome fruit export from South Africa (Berry et al., 2015) while the Multivent (MV) and Altvent (AV) configurations were proposed as alternatives to the ST design. These new package designs aimed at better distributing airflow to all fruit layers within a carton when trays are present. The use of trays is common practice in commercial handling apple fruit inside cartons. The Edgevent design (EV) was proposed in a previous study based on superior performance and successful application in the South African citrus industry (Defraeye et al., 2014, 2013a; Delele et al., 2013a).

2.2 Box compression strength

Box compression strength was evaluated experimentally using BCTs, based on protocols recommended by ASTM (2010) and TAPPI (2012). The twelve vent hole designs (Figure 4.1) as well as a design without any vent holes were manufactured into a telescopic (international fibreboard case code: 0320M/A; FEFCO and ESBO 2007) box configuration. The telescopic carton is commonly implemented for export of South African pome fruit (Berry et al., 2015) and consists of an outer and an inner carton that forms a single unit (Figure 4.2). The cartons were fabricated using a corrugated fibreboard cutting machine (KM series 6, Kasemake House, Cheshire, United Kingdom) and then assembled and glued by hand.

Three corrugated fibreboard grades (board grades) were evaluated, namely: (i) 140T2/125B/125M (B, 436 g m^{-2}); (ii) 175T1/175SC/125SC (C, 536 g m^{-2}) and; (iii) 140T2/100B/100FL/100C/100FL (BC, 619 g m^{-2}). The numerical values indicate the paper boards (fluting and liner) densities (g m^{-2}), T2 indicates partly recycled liner board, B indicates B-fluting, M indicates mottled white kraft board, T1 indicates fully recycled board, SC indicates semi-chemical fluting using a C-flute, C indicates C-fluting and FL indicates fluting liner board. Board thickness based on 10 measurements was 2.8 mm, 3.9 mm and 6.2 mm for the B, C and BC boards, respectively. Furthermore, edgewise compression tests (ECT) using the FEFCO No. 8 Standard for rectangular corrugated paperboard samples (TAPPI, 2007b), resulted in ECT values of 4.32 kN/m (SD = 0.09, N = 10), 6.40 kN/m (SD = 0.22, N = 10) and 6.63 kN/m (SD = 0.20, N = 10), for the B, C and BC boards, respectively.

Samples were preconditioned at 30 °C (±1 °C) at 20-30% relative humidity for 24 hours and then conditioned at 23 ± 1 °C and 50% relative humidity for 24 hours prior to testing in accordance with ASTM D4332 recommendations (ASTM, 2006). Eight replications were used for every box compression test, which were conducted using a box compression tester (M500-25CT, Testomatic, Rochdale, United Kingdom). The BCT is a top-to-bottom compression load test between two flat plates, which is performed on individual, empty cartons at a constant deformation rate (12.7 ±2.5 mm/min). The crosshead deformation and compressive load were continuously recorded until failure occurred. A preload of 222.2 N was applied to the cartons before recording compression strength values to ensure proper contact with the top plate. The fixed-plate mode of the compression tester was used for all tests.

Statistical evaluations using the R software package (R Core Team, 2015) were performed based on analysis of variance (ANOVA), with the factors influencing variance being the vent hole size, vent hole configuration and corrugated board grade. Fisher's LSD multiple comparison tests were performed and mean values were considered significantly different at $P \leq 0.05$.

2.3 **Numerical simulations**

2.3.1 Numerical model

Computational fluid dynamics was used to simulate horizontal airflow through carton designs, to represent precooling in commercial practices. The computational models were set up according to Figure 4.3. The individual apple fruit were modelled discretely as spheres with a diameter of 72.4 mm. Each carton contained 150 fruit packed on five trays using a staggered packing configuration, with a total mass of 24.5 kg. Upstream and downstream lengths were set to limit the effect of the inlet and outlet boundaries on flow and cooling conditions near the carton. Several simplifications were used to reduce computational cost: (i) Individual cartons were examined, instead of in a stacked configuration; (ii) The geometry of the carton walls and trays were modelled as surfaces with no thickness, but the surface boundaries included thermal resistance, which was determined from the thermal conductivity and thickness (tray = 3 mm; carton wall = 6 mm) of the respective material; (iii) The surfaces of the fruit were trimmed by 2.5 mm at points of contact between fruit, trays and carton walls. This better represented the contact areas between fruit of a close-fitting packing strategy as used in reality, but also enhanced mesh quality.

A hybrid grid (tetrahedral and hexagonal cells) was built within the computational domain of each carton. The number of computational cells per simulation is listed in Table 4.1. The grid refinement was determined from a grid sensitivity analysis using the Richardson extrapolation method (Celik et al., 2008). The results showed a spatial discretisation error of 0.14% for wall shear stress across the fruit surfaces and 5.0% for average heat transfer rate across fruit surfaces.

The inlet and outlet boundary conditions were set to mimic FAC conditions in the fresh fruit industry (Brosnan and Sun, 2001; de Castro et al., 2004a; Thompson et al., 2008). The inlet boundary condition was, therefore, set as a uniform velocity inlet, with low turbulence intensity (0.05%) at -0.5 °C. Three inlet airflow rates were selected, namely 0.33, 1.00 and 3.00 L s^{-1} kg^{-1} (Brosnan and Sun, 2001), while the outlet boundary condition was set to ambient atmospheric pressure. Boundary conditions along the sides of the computational domain were modelled as symmetry (slip walls), which assumed the normal velocity component and normal gradients at the boundary were zero. The carton and tray boundary conditions inside the domain were specified as no-slip walls with zero roughness. Thermal properties of corrugated fibreboard, expanded polystyrene trays and ‘Granny Smith’ apples were kept constant, i.e. independent of temperature. The thermal properties are listed in Table 4.2 and initial fruit temperature was set to 20 C.

2.3.2 Simulation setup

CFD simulations were based on Reynolds-averaged Navier-Stokes (RANS). The shear stress transport (SST) k–ω model was used for turbulence modelling (Menter, 1994). This RANS turbulence model has been validated extensively in previous studies for flow and cooling of spherical fruit (Ambaw et al., 2013a; Norton et al., 2013; Norton and Sun, 2006; Smale et al., 2006; Verboven et al., 2006; Xia and Sun, 2002; Zhao et al., 2016).

Concerning boundary-layer modelling, wall functions were applied instead of low-Reynolds number modelling. Although low-Reynolds number methods generate more accurate predictions, the complexity of the geometry would have required very high resolution meshes near the fruit surfaces which are difficult to generate for complex geometries as is the case in the present study. Simulations under such conditions would thus entail very large computational costs. Wall functions are therefore often the only practical alternative and have been proven to provide satisfactory results (Defraeye et al., 2013b, 2012b).

The use of this RANS turbulence model in combinations with wall functions was applied in a related study on citrus fruit cooling by Defraeye et al. (2014, 2013b), with satisfactory agreement to experimental data and indicates sufficient accuracy of the CFD simulations. Several other studies performed by the authors have also found good agreement to experiments using this turbulence model with wall functions (Ambaw et al., 2013d; Delele et al., 2013b, 2009).

Simulations were performed using ANSYS-Fluent 15 CFD software code. The SIMPLE algorithm (Patankar and Spalding, 1972) was used for pressure-velocity coupling and second-order discretisation schemes were used throughout. Buoyancy, radiation, heat from respiration, latent heat of evaporation and mass loss were not considered in these simulations, as they were assumed negligible (<1% of total heat load cooled for both respiration heat and latent heat of evaporation) during FAC (Defraeye et al., 2013a). Before performing transient cooling simulations, the flow field and temperature conditions were determined using steady-state simulations, to obtain the initial conditions. Initial fruit and inlet air were fixed to 20 °C and -0.5 °C, respectively, which is typical of commercial precooling temperatures. The flow field was thus disabled during transient simulations, which reduced the computational cost as only the energy equations were solved. Iterative convergence was determined by monitoring the velocity, turbulent kinetic energy, shear stress and temperature in the flow field and along specific boundaries (surface-averaged values). Transient simulations were run for about 12 hours, with time steps of 2.5 minutes, as determined from a temporal sensitivity analysis. Simulation time took about 96 hours on an Intel® core™ i7-4770 CPU (3.4 GHz) with 32 GB of RAM.

2.4 Cooling rate and uniformity

The seven-eighths cooling time (SECT in hours; $t_{7/8}$ in seconds) was used to evaluate fruit cooling rates and is defined as the time needed to cool produce to seven-eighths of the temperature difference between initial temperature and set air temperature (Becker and Fricke, 2004; Defraeye et al., 2015a). Fruit temperatures were monitored during cooling based on the volume-averaged temperature value of each of the five fruit layers, so per 30 fruit. The SECT is representative of precooling times used in commercial fruit export, where the FAC protocol includes cooling the fruit to about seven-eighths of the cold room temperature. Afterwards, precooling is stopped and the remaining heat is removed during cold storage.

In addition to the SECT of each fruit layer, the convective heat transfer coefficient (CHTC; h) was also monitored at the surfaces of fruit to assess cooling heterogeneity between individual fruit (Section 3.2.2). The CHTC expresses the convective heat flux ($q_{c,w}$; J s^{-1} m^{-2}) at the air-material interface, to the difference between the wall temperature (T_w) and a reference temperature (T_{ref}). In this study, T_w was taken at the start of the simulation when fruit were at a constant temperature (20 °C) and T_{ref} was taken as the incoming air temperature (-0.5 °C): $h = q_{c,w}/(T_w - T_{ref})$. CHTC is a defined quantity and is directly proportional to the heat flux at the wall ($q_{c,w}$). The CHTC depends strongly on the selected reference temperature. For the latter, also other values can be chosen, such as the temperature at the vent hole inlets. However, the selection of the reference temperature is less critical, as this study is interested in identifying differences in heat transfer rates. The CHTC is used as a parameter to identify the cooling heterogeneity across individual fruit surfaces.

The CHTC was also used to evaluate cooling heterogeneity between the five fruit layers, by calculating the relative standard deviation (%; RSD), which is the ratio of the standard deviation to the mean. A low RSD thus indicates homogenous cooling and a high percentage indicates heterogeneous cooling. Furthermore, the dimensionless Biot (Bi) number was used to indicate the different ratios of convective and conductive heat transfer in each of the fruit layers (Eq. (4.1)):

$$Bi = \frac{hL}{\lambda} \tag{4.1}$$

where λ is the thermal conductivity (W m^{-1} K^{-1}) in the body, L is the characteristic length (m), which is the quotient between the bodies volume and total surface area.

2.5 FAC energy consumption

The resistance to airflow (RTA) of the packed cartons was determined by relating the pressure drop over the carton to the airflow rate at the inlet. The relationship followed a quadratic curve, which was consistent with other observations in previous studies (Defraeye et al., 2014; Ngcobo et al., 2012a; van der Sman, 2002; Verboven et al., 2006). Such behaviour is characteristic for flow at high Reynolds numbers and can be characterised using Eq. (4.2) (Defraeye et al., 2015a):

$$\Delta P = \xi G^2 \tag{4.2}$$

where ΔP is the pressure drop (Pa), ξ is the pressure loss coefficient (PLC; kg m^{-7}) and G is the airflow rate (m^3 s^{-1}).

The package related energy consumption needed to maintain airflow throughout FAC is a function of the airflow rate, resistance and operational time needed to reach the desired temperature (de Castro et al., 2005a; Defraeye et al., 2015a, 2014). The fan and motor efficiency were ignored in this study as they vary depending on the facility. The package-related power (w; Watts) required to maintain a flow rate through the package was calculated in Eq. (4.3).

$$w = \Delta P G = \xi G^3 \tag{4.3}$$

The total fan energy consumption (E; Joules) was therefore calculated by incorporating Eq. (4.3) into Eq. (4.4), to calculate the theoretical power needed during FAC to maintain a set airflow rate through the package for duration equal the SECT of the produce inside the package.

$$E = \mathrm{w} t_{7/8} \tag{4.4}$$

3. Results and discussion

3.1 Mechanical strength

Table 4.3 and Table 4.4 shows the peak force and respective deformation distance of the examined telescopic carton designs. The vent hole configuration (AV, EV, MV, ST), vent hole TVA (2%, 4%, 8%) and board grade (B, C, BC) factors each had a significant ($p \leq 0.05$) effect on the evaluated cartons' peak compression force. Furthermore, the vent hole configuration and TVA factors both showed a significant interaction ($p \leq 0.05$) with board grade. The interaction indicates that the specific grade of board used in a carton will determine the extent of the influence the vent

hole design (configuration and TVA) will have on peak compression force. The effect of vent hole configuration and TVA were therefore evaluated individually for each board grade. Conversely, no significant ($p > 0.05$) interaction between vent hole TVA and the vent hole configuration was shown, which is in contradiction to findings by Singh et al. (2008). The conflicting findings may be attributed to the evaluation of different ranges of TVAs (10-50%) and the use of a different carton folding type (regular slotted). Instead, the present study investigated TVAs ranging between 0% (control) and 8% using a telescopic folding type, as commonly practised in the horticultural export industry (Berry et al., 2015).

3.1.1 Vent hole area

A negative linear correlation ($R^2 = 0.94$) was observed between the TVA and compression force for each of the vent hole designs. The effect of the vent hole configurations had an influence equivalent to about a 2% change in TVA, making vent hole TVA differences between 2% and 4% TVA less significantly ($p \leq 0.05$) observable, than between the 4% and 8%. Figure 4.4 illustrates the relationship between the board grade (density) and vent hole TVA with respect to peak compression force. The results emphasise the generalised perception or approach by many commercial and academic groups to select a desired compression force by adjusting vent size and board density (properties). However, whereas TVA had a relatively linear relationship with strength, Figure 4.4 illustrates the inconsistent interaction of the board grade with vent hole design in determining peak compression force. For example, small differences were observed between the C and BC boards for the ST cartons. In contrast, the EV designs maintained a consistent gradient, thus indicating that some vent hole designs may be more effective when matched to a specific board grade. The results suggest that vent hole recommendations from past studies should only be considered within the scope of the evaluated board grade (Han and Park, 2007; Jinkarn et al., 2006; Singh et al., 2008). Consequently, future studies should also place more emphasis on better characterising the evaluated boards as well as the individual fibreboard liners.

3.1.2 Mechanism of failure and deformation

The interaction between board grade and vent hole design can be attributed to the influence of the board's material properties on buckling patterns during mechanical failure. During compression, the evaluated carton faces began to bow either inwards or outwards (results not shown). Buckling developed at a critical deformation and was observed both between and through corners, edges or vent holes. Vent holes therefore mainly dictate the mode of failure and as a result determined the peak compression force. Multiple failure modes were observed for each of the evaluated carton designs, producing a spread in the compression versus deformation curves (Figure 4.5).

During individual BCT evaluations, certain failure modes were observed to be more prevalent for specific vent hole designs (results not shown). A possible hypothesis for this phenomena, is that the carton geometry and the vent hole designs predispose compression towards a certain failure pattern. Furthermore, minor inconsistencies in the carton's assembly and natural variation in the board may influence the probability towards a specific failure mode. This hypothesis suggests that failure occurs through a stochastic process and may, therefore, explain the consistent reports of high variability in BCT results in other studies (Frank, 2014; Urbanik and Frank, 2006).

Note, however, that the BCT results measured will differ a bit in reality, due to the lack of fruit inside the boxes. Although the packaging failure modes through the vent holes are expected to be similar, the packed fruit are expected to provide supplementary compression resistance during deformation. The peak force from BCT testing is, therefore, considered a conservative indicator of stacking performance (Frank, 2014; Frank et al., 2010).

Peak compression forces for the B board grade produced the lowest compression force, with the unventilated control cartons leading to a compression force of 4334 N. C and BC board grades were significantly stronger, increasing the carton strength by 68% and 83%, respectively. Regarding deformation at the respective peak compression force, the results do not show any influence by vent hole TVA or vent hole configuration. The board grade, however, had a significant ($p \leq 0.05$) effect, on deformation at peak force, resulting in average values of 8 (±2) mm, 12 (±2) mm and 18 (±3) mm for the B, C and BC board grades, respectively.

Figure 4.5 shows plots of average compression force at different deformations (5, 10, 15, 20 and 25 mm) and illustrates the general compression curve for each of the carton designs. This relationship is of importance as compression past a critical deformation can cause damage to fresh produce. The determination of compression force at the critical deformation, before damage to packed produce occurs, would be a valuable performance parameter compared to peak compression force. However, very few significant ($p > 0.05$) differences were observed between the force versus deformation gradients. This was attributed to the multiple failure modes observed for each design, which resulted in considerable variability between replications. After extensive analysis, it was thus concluded that peak force is the most suitable parameter for evaluation, as conventionally used in previous studies (Frank et al., 2010; Jinkarn et al., 2006; Singh et al., 2008).

3.1.3 Vent hole configuration

Vent hole configuration had a significant effect on the peak compression force. However, different configuration types were found to be superior for each respective board grade (Table 4.3, Table 4.4 and Figure 4.5). For B board, the MV and EV designs showed statistically larger compression forces compared to the AV design, which produce the lowest compression force (Table 4.3). For C board, the

ST design had statistically, the largest peak compression force. The ST design produced a compression force of 5%, 8% and 11% larger than the EV, AV and MV designs, respectively. Finally for BC board, the EV design was significantly stronger than the other designs, with a compression force 6%, 8% and 13% larger than the AV, ST and MV designs, respectively. Vent hole configuration should therefore be carefully selected based on the properties of the board material being used. The Edgevent configuration, offered the strongest compression strength when used on telescopic cartons manufactured from BC board. Furthermore, the Edgevent design also maintained comparatively higher compression strength in cartons made from the B and C boards, respectively.

Another factor to consider is the interaction between the inner and outer components of the telescopic carton (Figure 4.2). In this study both the inner and outer board types were kept constant; however, in the fresh produce industry, it is common practice to mix and match different fluting and liner fibreboard densities to achieve desired carton strength. These combinations would therefore likely further influence the performance of a specific vent hole configuration. Additionally, it is also common practice to maintain fresh produce at high relative humidity (90-100%) in the cold chain. This has a significant effect on the material properties of the board and thus the effectiveness of a specific vent hole configuration (Allaoui et al., 2009a; Singh et al., 2007).

3.2 **Cooling rate and heterogeneity**

3.2.1 Cooling rate

The effect of vent hole TVA and configuration on SECT as a function of airflow rate is shown in Figure 4.6a. The MV configuration had the lowest SECT for each of the vent hole TVAs and flow rates examined. Accordingly, the AV, ST and EV carton configurations cooled on average 6%, 11% and 127% longer, respectively. The high cooling performance of the MV configuration can be attributed to the use of multiple smaller holes, which distributed air more evenly to all fruit layers. Similar to the MV configuration, the AV configuration also distributed air to all fruit layers. However, the lower cooling performance can be attributed to a less even distribution of cooling airflow to the various fruit, as a result of fewer vent-holes (3 versus 12). The total cooling rate was therefore reduced as some fruit located in a low airflow region, were not adequately cooled.

Figure 4.6a also shows that the effect of increasing vent hole TVA from 2% to 8%, improved the EV carton design's SECT by 34%. Conversely, improvements of only 1% to 5% were observed for the ST, AV and MV carton designs. The large cooling rate improvement of the EV configuration, with respect to increasing vent hole TVA, can be attributed to improved airflow distribution. At a TVA of 2%, the EV carton only distributed air above the top and below the bottom fruit layers. Compared to the top fruit layer, fruit at the bottom layer cooled at a slower rate due to the thermal resistance of the tray (Figure 4.6b). With increasing TVA (4% and

8%), cold airflow was additionally distributed above the bottom fruit layer, hence the large effect on cooling rate. Furthermore, the effect of TVA on SECT at low flow rates (0.33 L kg^{-1} s^{-1}) was more pronounced (8.4% decrease) than at higher flow rates (4.7% decrease at 3.00 L kg^{-1} s^{-1}). The phenomenon was attributed to a higher degree of heat transport between the fruit, from low TVAs to higher TVAs. FAC at low airflow rates results in slightly higher mean air temperatures inside the carton, due to the extended duration of the air in the carton. For example, at the onset of FAC the AV carton had a mean air temperature of 14 °C at 0.33 L s^{-1} kg^{-1} versus 7 °C at 3 L s^{-1} kg^{-1}.

The CHTC is an important indicator of cooling rate and is primarily influenced by the air velocity and distribution around the produce. Figure 4.7 shows the total CHTC across the fruit surfaces for each of the package designs as a function of airflow rate. In contrast to the other designs, the EV carton showed an increase in CHTC with larger TVAs (Figure 4.6c), which was attributed to an improved airflow distribution between the fruit layers as vent holes extended towards the carton centre (Figure 4.7 and Figure 4.6b). Larger CHTC differences at high (3 L s^{-1} kg^{-1}) airflow rates were observed between the different vent-hole TVAs than at lower airflow rates. Furthermore, quite similar CHTC values were observed for the AV, MV and ST configurations at each of the vent hole TVAs. This is attributed to the effect of the air jets at the vent holes, which lead to highly increased air speeds, since air at the vent holes must accelerate as a function of the inlet velocity and the TVA. For example, when the AV carton's vent hole TVA was decreased from 8% to 2%, the volume-average air velocity in the carton increased by 0.06 m s^{-1} and 0.59 m s^{-1} for inlet flow rates of 0.33 L s^{-1} kg^{-1} and at 3.00 L s^{-1} kg^{-1}, respectively. The cooling effect by the air jets is depicted in Figure 4.7 and shows higher CHTC values at fruit near vent holes. A higher incidence of chilling injury could be expected in chilling sensitive fruit, if cooling exceeded tolerable rates at these location (Lukatkin et al., 2012).

3.2.2 Cooling heterogeneity

The effect of TVA and airflow rate on the cooling heterogeneity for each of the carton designs is shown in Table 4.5. The results emphasise a distinct relationship between increasing TVA and a reduction in cooling heterogeneity in each of the carton designs. This finding is consistent with observations by de Castro et al. (2004b) and Tutar et al. (2009), who both examined the effect of TVA and flow rates on cooling characteristics in fruit packed using a simplified configuration (simple cubic) and without the presence of internal packaging. Increasing TVA will therefore also improve cooling uniformity in more complex packaging systems. However, the magnitude of the achieved improvement is dependent on the geometry and decreases at larger vent hole TVAs.

The dimensionless Biot number is shown for each fruit layer in Figure 4.6b and represents the ratio between convective and conductive heat transport. Fruit layers near vent holes had larger ratios of convective versus conductive heat transport

(Figure 4.7). The AV and MV vent hole designs had Biot numbers between 1.0 and 1.5 across all fruit layers, indicating a fairly even convective heat transfer across the fruit layers. However, the ST designs had larger values (1.0 - 2.5) at the centre tray and values less than one at the top and bottom fruit layers. Conversely, the EV design had large values (1.5) at the top and bottom fruit layers and values less than one at the middle layers. Biot numbers larger than one indicate the heat conduction rate in the fruit is the limiting factor for cooling. However, it should be noted that the calculated values may be influenced by heat conduction into adjacent fruit through contact points (area = 3% of the fruit surface per contact).

Both increases and decreases in cooling heterogeneity were observed with increasing flow rate (Table 4.5). At a TVA of 2%, the AV, MV and EV showed an increase in cooling heterogeneity with increasing flow rates (1 to 3 L s^{-1} kg^{-1}). Conversely, the 4% and 8% EV designs showed an improved cooling heterogeneity with increasing flow rate, whereas the other vent hole designs showed no relationship between flow rate and cooling uniformity. The effect of TVA on cooling uniformity is thus dependent on the airflow distribution, which is a function of the vent hole configuration and carton's internal geometry (fruit on trays). These findings can be attributed to the explicit design of the geometry in the model, where airflow that is directed either into or between fruit as a result of vent hole placement. For example, high flow rates would be distributed more broadly when focused into an obstacle, versus an air stream that entered into the carton without being obstructed. The 2% EV design directed the majority of the air stream across the top of the uppermost fruit layer and the bottom of the bottommost fruit layer (Figure 4.6b), as depicted by the high CHTC in Figure 4.7. However, when the TVA was increased to 4% and 8%, a portion of the airflow was directed into the fruit centre, resulting in better air distribution inside the package (Figure 4.6c). The EV vent hole placement at the top and bottom of the carton resulted in an average relative standard deviation twice as large as the ST configuration and seven times larger than the AV and MV configurations. The AV and MV vent hole designs thus improved cooling uniformity compared to the commercially used ST carton design.

3.2.3 Energy efficiency

Differences between the carton designs with respect to cooling rate values, such as SECT, do not necessarily indicate similar FAC energy consumption values. The energy required to maintain a certain flow rate will be different in each carton design due to the unique RTA produced (Pathare et al., 2012). An analysis of the pressure loss as a function of air velocity for the various cartons designs is shown in Figure 4.6d. These data were used to calculate the pressure loss coefficient (Table 4.6), which quantifies the RTA of each of the cartons.

Figure 4.6d shows that within the examined range, vent hole size had a larger influence on RTA compared to the vent hole configuration. Increasing the TVA from 2% to 4% and 4% to 8%, consequently reduced the pressure loss coefficient by 70% and 61% (Table 4.6), respectively. The ST carton design had the largest resistance

to airflow for each of the respective TVAs, while AV, MV and EV carton designs were on average 21%, 35% and 47% smaller, respectively. Interestingly, although the EV carton produced the highest SECT, it also produced the lowest RTA. Whereas, the AV and MV carton designs generated the lowest SECT values, but their RTA values were higher than the EV carton, but were still lower than the ST carton design.

Precooling rates are usually selected to optimise produce quality preservation and to meet cold chain time constraints. From a cold chain logistical perspective, cooling rate (SECT) is therefore, a determining variable that should be met to handle horticultural produce efficiently with minimum or no product loss (Defraeye et al., 2015c; Thompson et al., 2010). To quantify the carton designs FAC inefficiency, the curve produced from the package-related power usage (w; Eq (4.3)) versus the SECT are plotted in Figure 4.8 and were also correlated using a power-law curve ($w = \alpha t_{7/8}^{b}$; adjusted $R^2 \geq 0.99$). The b parameter showed a rather constant value (-6.00), which left the α parameter to be used as an indicator of FAC energy inefficiency (FACEI).

Figure 4.8 thus shows this relation between the FACEI (α and the SECT for each of the carton designs. The results show that the EV package design with 2% TVA had the most inefficient vent hole design, requiring 57 times more energy to precool than the ST design with 2% TVA, while the EV with 4% TVA used 10 times more energy than the ST design with 4% TVA. Furthermore, the AV and MV carton designs on average improved cooling efficiency (Figure 4.8) by 38% and 58% (averaged over the three vent hole areas), respectively, compared to the ST carton design.

3.3 **Multi-parameter analysis and design**

A multi-parameter approach in package design is required to take into account the importance of each performance parameter during development, so that the final design is functionally balanced at each of the various areas in the cold chain (Defraeye et al., 2015a). Commercially, carton designs are typically benchmarked according to manufacturing costs. A design that meets the minimal performance requirements and uses the most economical board is thus superior, as it improves cold chain cost efficiency.

Figure 4.9 shows the effect of vent hole design on compression strength and FACEI (α) for each of the board grades. Superior carton designs therefore have plotted curves located nearer the top left corner of the graph (high compression resistance and energy efficient FAC) and inferior carton designs have plotted curves nearer to the bottom right (low compression resistance and energy inefficient FAC). Based on this criterion, the EV design was thus the most unfavourable vent hole configuration for cartons packed using trays. However, the EV configuration is more commonly used in citrus fruit (Defraeye et al., 2015a), which are typically

packed in bulk (no trays). A more energy efficient FAC process would thus be expected in these circumstances (Berry et al., 2017).

The Standard vent design had an inferior performance compared to the AV and MV in the B and BC board grades. However, in the C board grade, the Standard vent design was the most superior design at compression forces larger than 6000 N. The close competition between the Standard design and the AV/MV designs can be attributed to a slightly larger setback in FACEI (section 3.2.3), compared to the benefit in compression strength (section 3.1.3) by the respective vent hole configuration.

The Multivent design had comparatively superior results for the B and BC board grades, as well as for compression strengths below 6000 N for the C board grade. Although, it should be noted, that the Altvent design produced nearly equivalent results to the MV design for the C and BC board grades. It is thus the Multivent design that can be used as a generalised recommendation for cartons packed with trays. Although the selected designs compatibility should always be matched to the board material properties, by selecting an appropriate board grade.

An important observation in this study was the interactive effect that board material properties have on the relationship between vent hole design and compression strength (section 3.1.2). However, corrugated fibreboard does not maintain consistent material properties at varying environmental conditions. Instead, moisture sorption in the fibreboard influences the bonds between the cellulose fibres, causing significant reductions in strength and thus entirely different corrugated fibreboard material properties (Paunonen and Gregersen, 2010; Sørensen and Hoffmann, 2003). Future multi-parameter evaluations should therefore include the effects of cold chain conditions, to further improve ventilated packaging designs.

4. Conclusions

This study examined the effects of four vent hole configurations and three vent hole areas on cooling performance and mechanical strength of ventilated packaging using a multi-parameter evaluation approach. Some of the proposed vent hole designs were selected to represent similar packages used in commercial practice. Furthermore, new configurations were designed that should induce better ventilation alignment during stacking, as well as promote more even airflow distribution in the cartons.

CFD was used to evaluate the effects of the vent hole designs and total ventilated area (TVA) on cartons packed with apples on trays, under forced-air cooling conditions. Cooling performance parameters investigated included cooling rate, cooling uniformity, resistance to airflow and package-related forced-air cooling energy inefficiency (FACEI). Both the configuration and TVA of the vent holes had a considerable influence on FACEI. With respect to vent hole configuration, the Altvent and Multivent reduced power consumption by 38% and 58% (for all vent hole areas) compared to the Standard vent design, respectively. Furthermore, vent hole configuration and TVA also had a significant effect on cooling uniformity. In this case, the Multivent and Altvent also generated more homogenous cooling patterns compared to the Standard vent and Edgevent designs.

The effect of vent hole design on mechanical strength was evaluated experimentally using box compression tests. Examinations were performed on telescopic cartons manufactured from three corrugated fibreboard grades. Vent hole configuration, TVA and corrugated fibreboard grade had a significant effect on carton mechanical strength. Peak compression strength decreased linearly with increasing vent hole size. Corrugated fibreboard grade had a significant interaction with both the configuration and TVA of the vent holes. The effectiveness of the vent hole designs was therefore dependent on the material properties of the selected corrugated fibreboard.

This study thus emphasised the importance of a multi-parameter evaluation approach to packaging design, by highlighting the interactions and effects that vent hole designs have on the package performance parameters. For cartons packed with fruit on trays, the Multivent design was generally the most superior. However, the considerable influence of the corrugated fibreboard grade on compression strength of the carton raised concerns regarding the consistency of performance across various environmental conditions, which in turn exert significant effects on the properties of the board material. Future multi-parameter studies should thus also aim at quantifying packaging performance across cold chain conditions.

Table 4.1: Number of mesh elements used for the various CFD domains.

Vent configuration	TVA	Number of elements
Altvent	2%	3.9×10^6
	4%	$3\ 9 \times 10^6$
	8%	4.0×10^6
Edgevent	2%	3.9×10^6
	4%	3.9×10^6
	8%	4.0×10^6
Multivent	2%	4.5×10^6
	4%	4.1×10^6
	8%	4.2×10^6
Standard Vent	2%	$3\ 9 \times 10^6$
	4%	$3\ 9 \times 10^6$
	8%	4.0×10^6

Table 4.2: Thermal and physical material properties used for numerical models.

Material	Density (kg m^{-3})	Specific heat capacity (J kg^{-1} K^{-1})	Thermal conductivity (W m^{-1} K^{-1})	Reference
Air	1.185	1 004.4	0.0261	(ASHRAE, 2013)
Granny smith apple fruit	829	3 580.0	0.3980	(Ramaswamy and Tung, 1981)
Corrugated fibreboard carton	145	1 338.0	0.0640	(Ho et al., 2010)
Trays (expanded polystyrene foam)	23	1 280.0	0.0360	(Margeirsson et al., 2011)

Table 4.3: Average peak force of box compression tests for each of the vent hole designs.

Vent configuration	TVA	B flute Average peak force (N)	C flute Average peak force (N)	BC flute Average peak force (N)
Control	0%	4 334 ±85^{e}	7 268 ±158^{d}	7 945 ±261^{f}
Altvent	2%	3 547 ±52^{bcd}	6 230 ±183^{bc}	7 504 ±331^{ef}
	4%	3 515 ±18^{bcd}	6 061 ±127^{abc}	6 727 ±260^{cde}
	8%	3 163 ±54^{a}	5 827 ±167^{ab}	5 788 ±144^{ab}
Edgevent	2%	3 799 ±99^{d}	6 741 ±124^{cd}	7 538 ±188^{ef}
	4%	3 598 ±52^{cd}	6 187 ±66^{abc}	7 097 ±200^{def}
	8%	3 234 ±93^{ab}	5 707 ±174^{ab}	6 486 ±149^{bcd}
Multivent	2%	3 862 ±111^{d}	5 943 ±77^{ab}	7 029 ±158^{def}
	4%	3 588 ±66^{cd}	6 089 ±39^{abc}	6 289 ±211^{abcd}
	8%	3 301 ±80^{abc}	5 485 ±184^{a}	5 439 ±83^{a}
Standard Vent	2%	3 642 ±41^{d}	6 770 ±270^{cd}	6 981 ±204de
	4%	3 755 ±38^{d}	6 797 ±124^{cd}	6 716 ±204^{bcd}
	8%	3 158 ±89^{a}	5 952 ±233^{ab}	5 861 ±80^{abc}

Data shown are mean ± standard deviation of the mean. Different superscript letters indicate statistically significant differences ($p < 0.05$) between the various carton designs within each of the three board grades (B, C and BC).

Table 4.4: Deformation distance at the peak compression force (box compression tests) for each of the vent hole designs.

Vent configuration	TVA	B flute Deformation (mm)	C flute Deformation (mm)	BC flute Deformation (mm)
Control	0%	8.8 ±0.2	11.6 ±0.2	18.0 ±0.8
Altvent	2%	7.6 ±0.2	12.1 ±0.4	19.2 ±0.4
	4%	8.3 ±0.1	11.8 ±0.3	18.7 ±0.5
	8%	7.1 ±0.2	10.8 ±0.4	15.0 ±0.7
Edgevent	2%	7.9 ±0.2	15.3 ±1.2	19.5 ±0.6
	4%	8.7 ±0.3	12.3 ±0.3	18.1 ±0.7
	8%	7.7 ±0.1	13.0 ±0.5	17.6 ±0.6
Multivent	2%	8.8 ±0.4	11.8 ±0.4	17.0 ±0.5
	4%	8.2 ±0.2	12.4 ±0.3	17.1 ±1.3
	8%	6.9 ±0.3	10.4 ±0.6	14.2 ±0.8
Standard Vent	2%	8.4 ±0.1	12.8 ±0.4	20.3 ±0.9
	4%	7.7 ±0.1	13.2 ±0.2	16.4 ±0.7
	8%	8.5 ±0.5	11.3 ±0.3	17.5 ±0.6

Table 4.5: Relative standard deviation (heterogeneity, in percentage) of the CHTC between the five fruit layers within the respective cartons for each of the vent hole designs and airflow rates (L s^{-1} kg^{-1}). High values indicate heterogeneous cooling.

Vent TVA	Airflow rate	AV	EV	MV	ST
2%	0.33	19.5	98.3	15.8	64.0
	1.00	20.3	104.9	16.8	61.4
	3.00	23.3	112.4	19.7	63.8
4%	0.33	10.5	97.1	7.2	46.5
	1.00	10.2	89.5	7.9	42.4
	3.00	11.1	88.6	9.7	44.3
8%	0.33	11.0	85.1	7.1	38.7
	1.00	10.0	72.4	5.8	34.6
	3.00	10.3	67.5	7.4	35.7

Table 4.6: Pressure loss coefficient (kg m^{-7}) for the examined cartons.

Vent configuration	TVA	Pressure loss coefficient (ξ)
Altvent	2%	462
	4%	146
	8%	56
Edgevent	2%	311
	4%	100
	8%	37
Multivent	2%	389
	4%	113
	8%	43
Standard Vent	2%	591
	4%	174
	8%	74

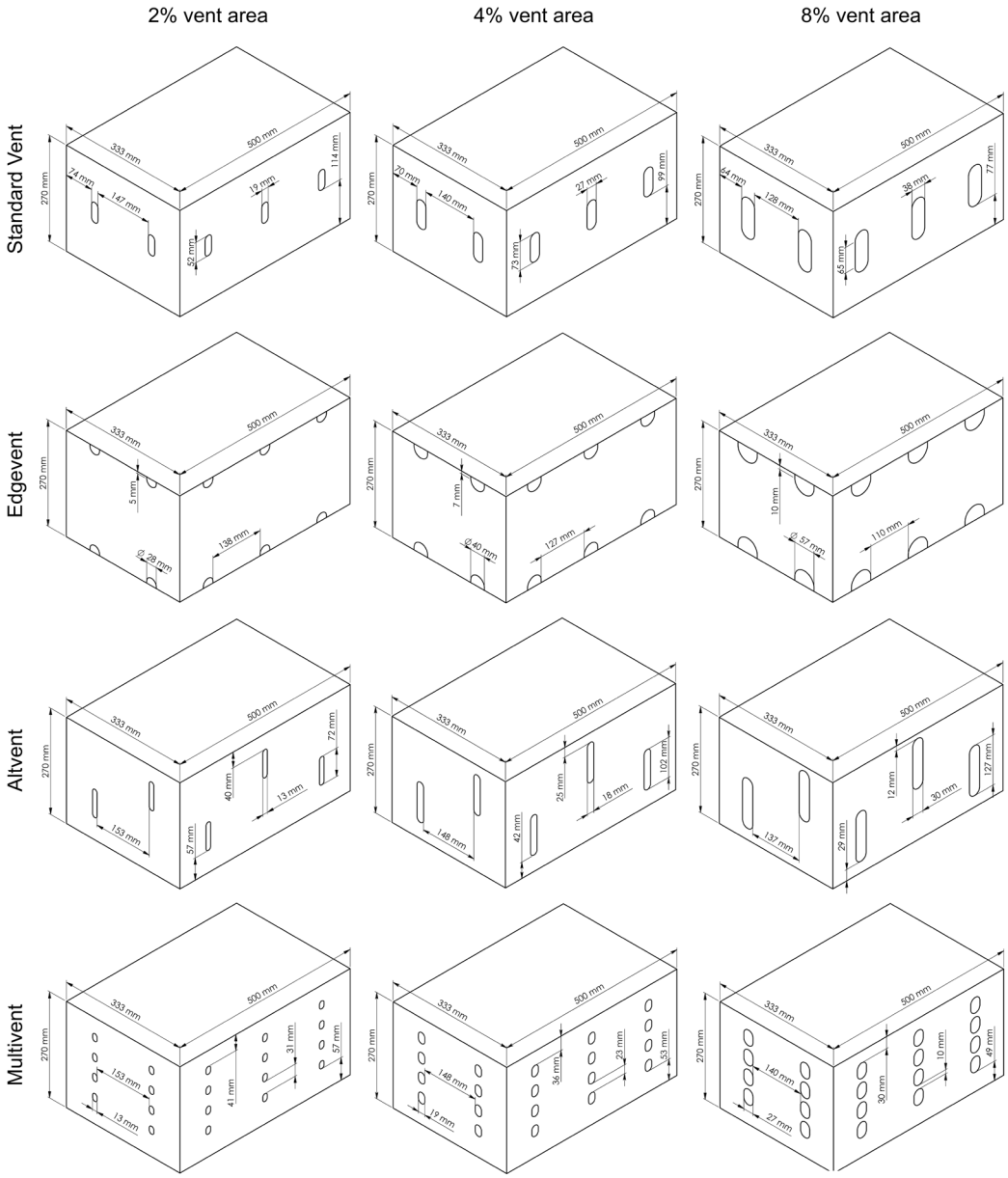

Figure 4.1: Geometry and diagram of the corrugated fibreboard cartons: Standard Vent, Edgevent, Altvent and Multivent.

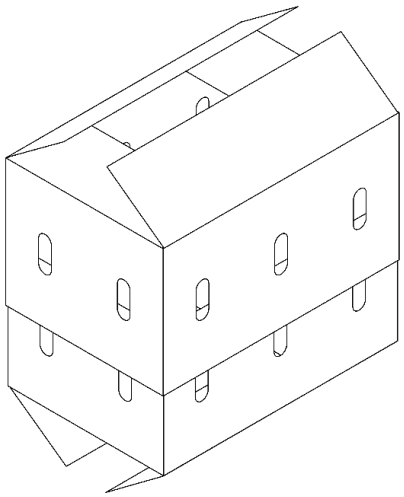

Figure 4.2: Geometry of a telescopic carton (Standard Vent).

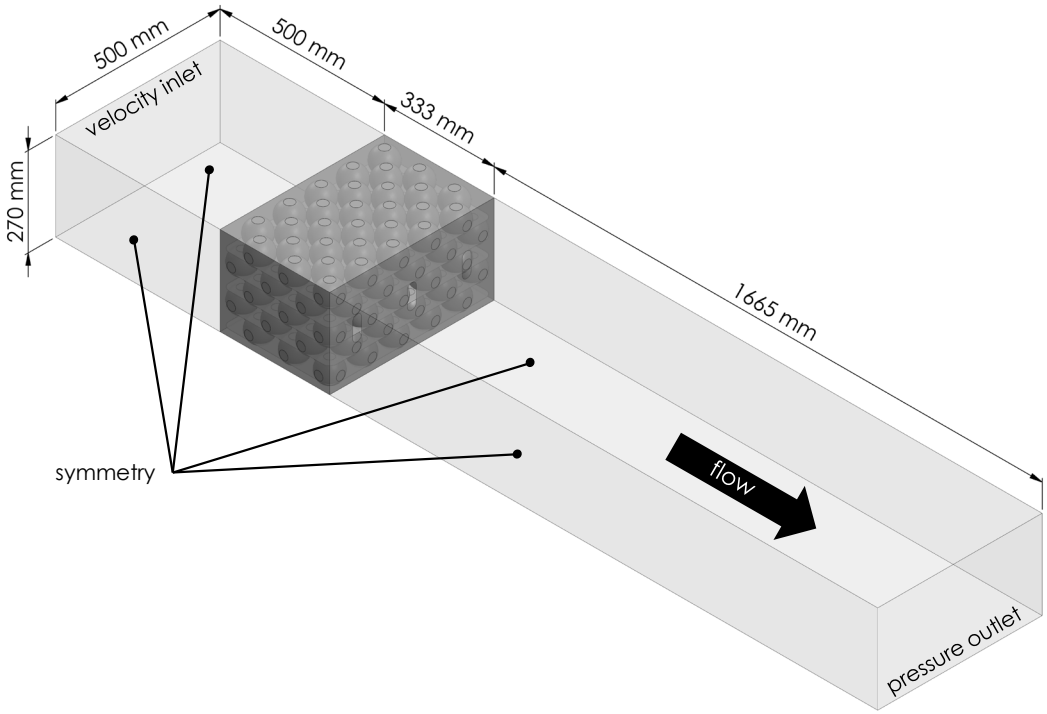

Figure 4.3: Computational model and boundary conditions for a single carton.

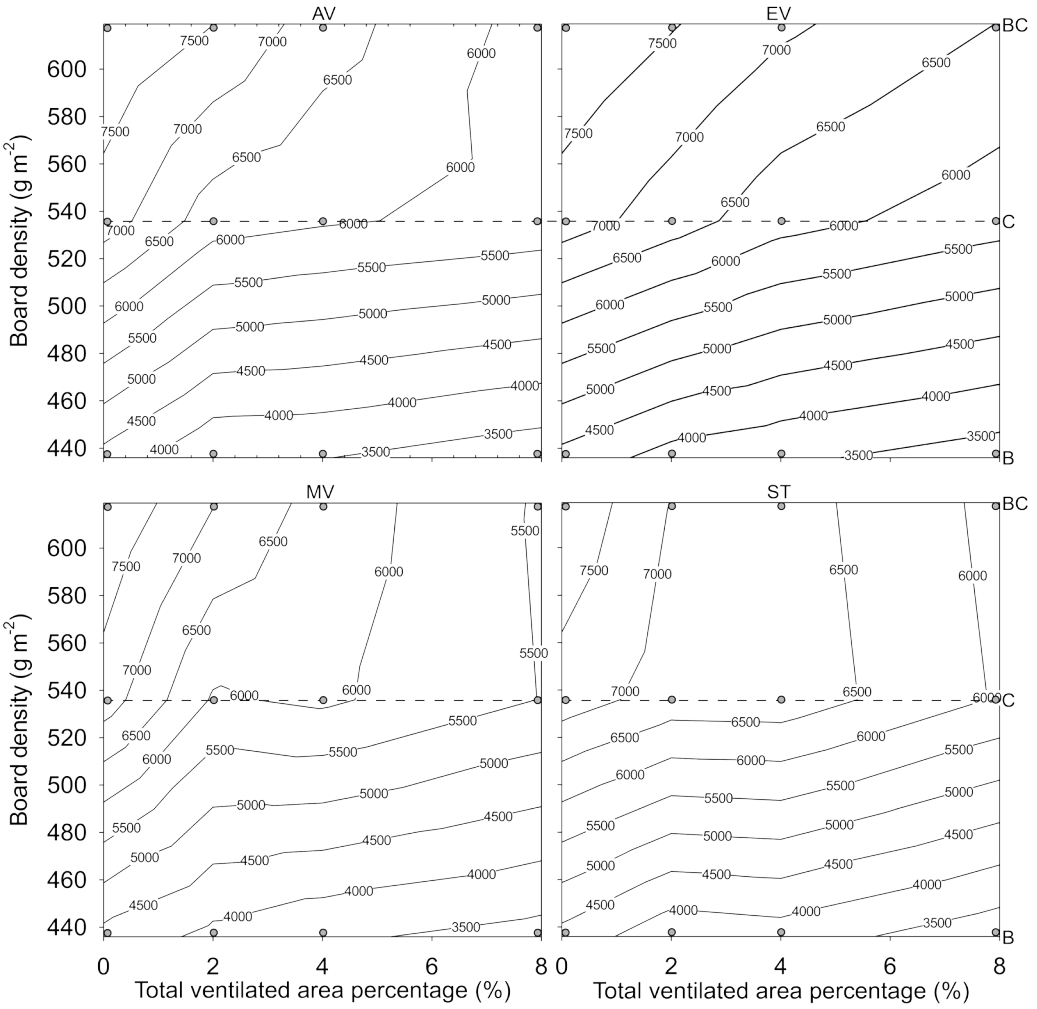

Figure 4.4: Relationship between board grade (density), TVA and peak compression force (N). B, C and BC along the right axis indicate corrugated fibreboard grade. Grey dots indicate data points.

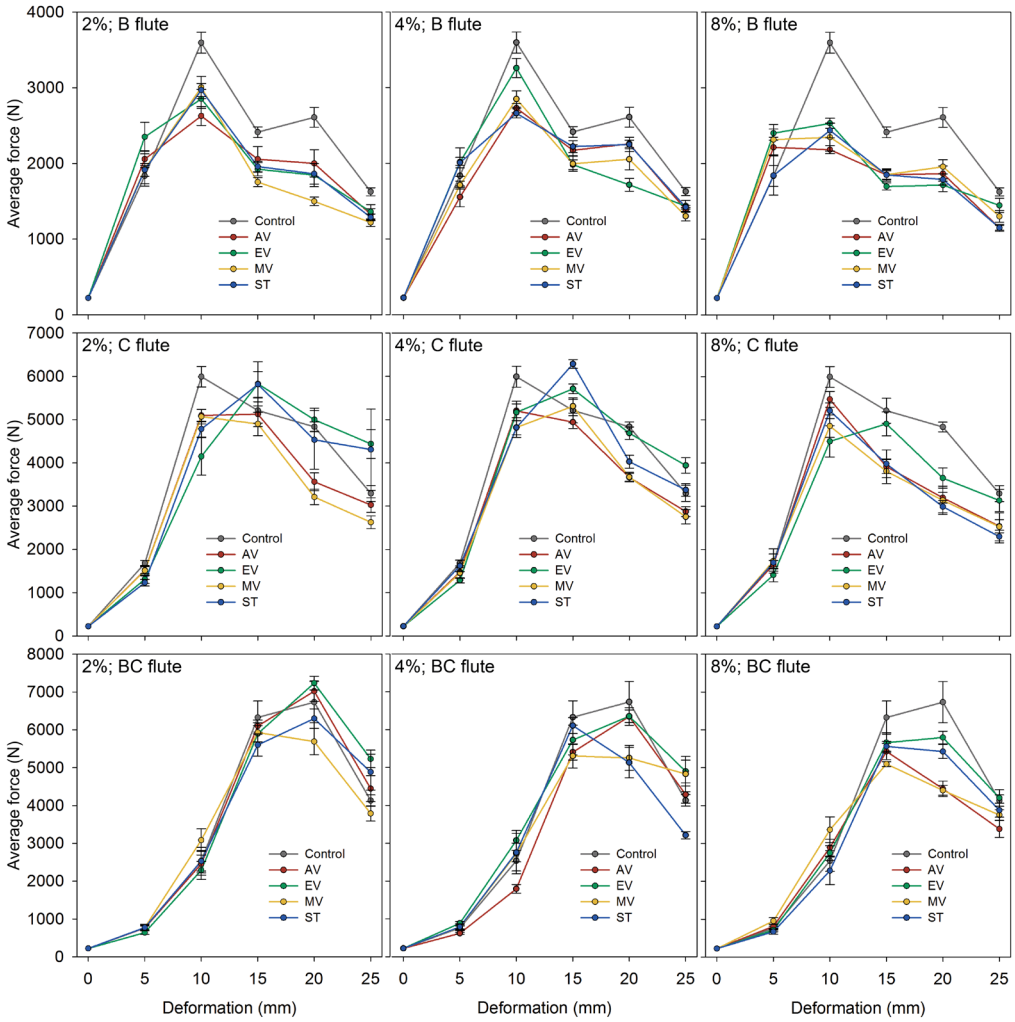

Figure 4.5: Average compression force versus deformation (at 5 mm increments) for the B, C and BC board grade. Error bars indicate standard error of the mean.

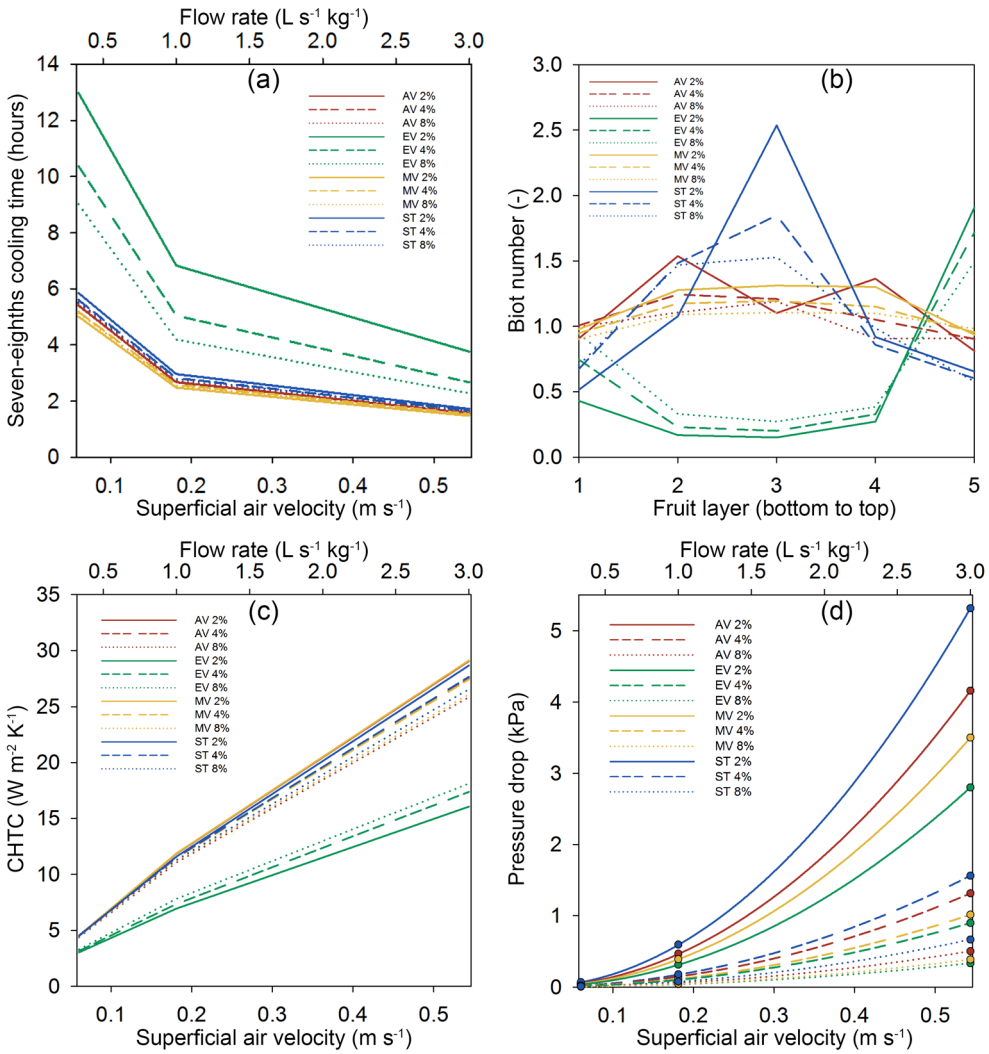

Figure 4.6: Plots expressing the various airflow and cooling performance parameters during FAC, for different package designs and TVAs. (a) Seven-eighths cooling time with respect to air velocity and airflow rate; (b) Biot number of each fruit layer; (c) convective heat transfer coefficient with respect to air velocity and airflow rate; and (d) pressure drop as a function of air speed and airflow rate.

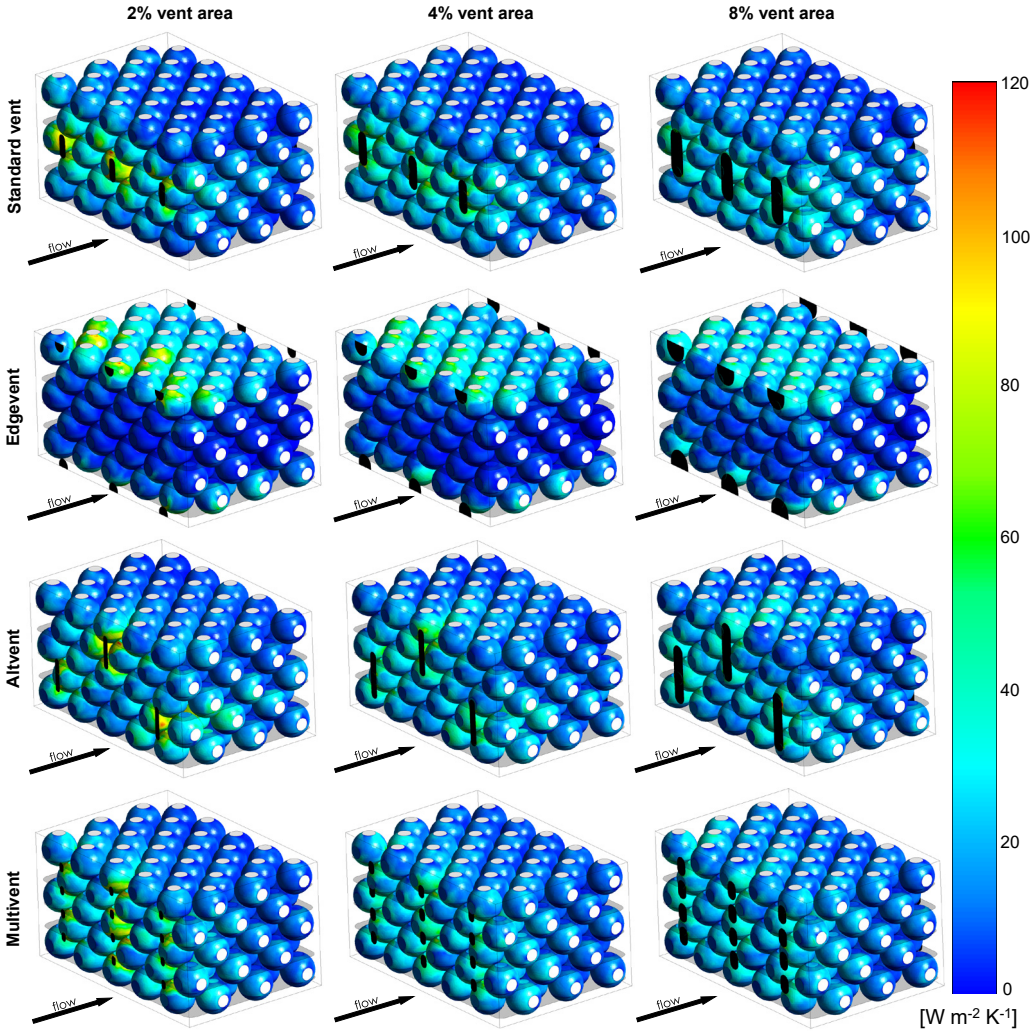

Figure 4.7: Distribution of CHTC values over apple fruit surfaces using 2%, 4% and 8% TVA for the Altvent, Edgevent, Multivent and Standard Vent cartons at 1 L s^{-1} kg^{-1}.

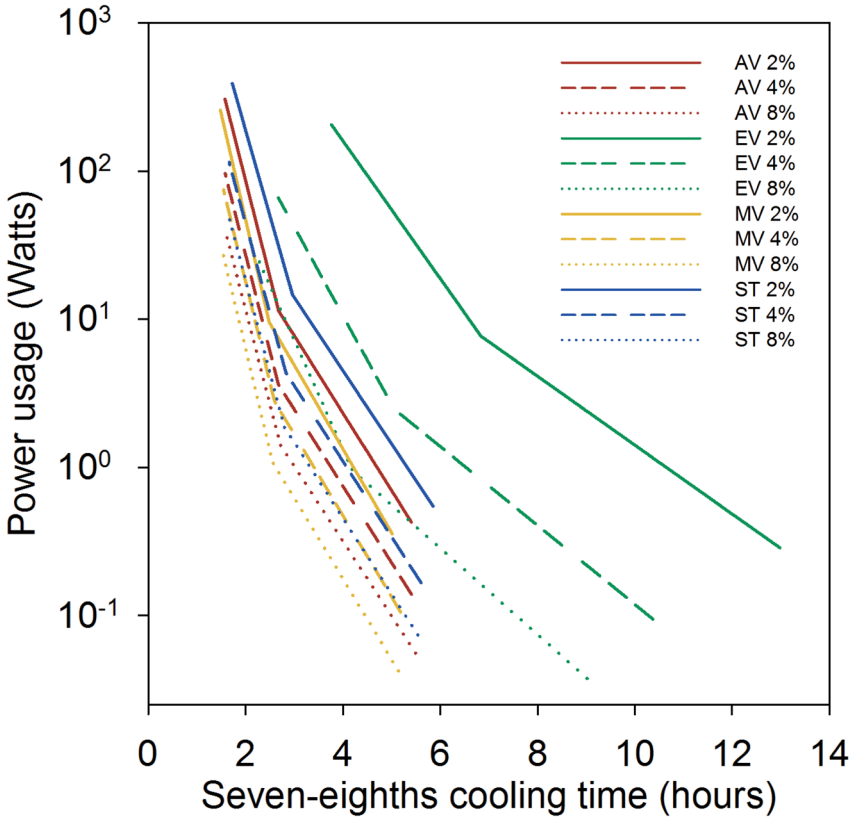

Figure 4.8: Ventilation power usage (logarithmic scale) versus seven-eighths cooling time for the Altvent, Edgevent, Multivent and Standard Vent cartons using 2%, 4% and 8% TVA.

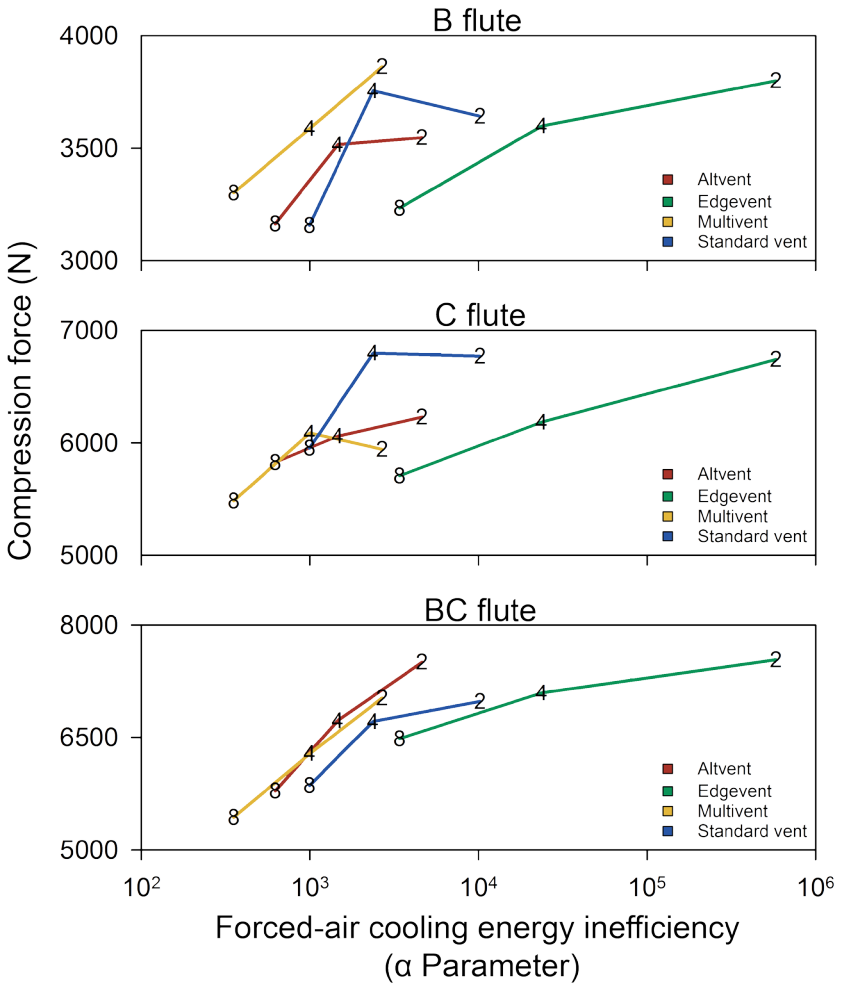

Figure 4.9: Summary of the multi-parameter evaluation with respect to effect of vent hole design on compression strength and forced-air cooling energy inefficiency. Numerical symbols (2, 4, 8) on the plotted curves indicate TVA. The α is the coefficient of a power-law correlation between FAC power usage and SECT ($w = \alpha t^{7/8} b$; adjusted $R^2 \geq 0.99$).

Chapter 5. Impact of Moisture Adsorption in Palletised Corrugated Fibreboard Cartons under Shipping Conditions: CFD Modelling and Experimental Validation

Abstract

Corrugated fibreboard packages (cartons) must support considerable mechanical loads during long term transport of fresh produce in refrigerated freight containers (RFCs). Fresh produce are transported at high relative humidities to preserve quality and reduce moisture loss. However, these conditions can progressively reduce carton mechanical strength over the long transit time as a result of (mechano-sorptive) creep. Currently, little is known regarding the actual moisture distributions and moisture content values of stacked cartons in RFCs, which makes detailed assessment of mechanical strength of cartons difficult. To this end, a computational fluid dynamics (CFD) model was used to study the moisture transport in the air and corrugated fibreboard in a part of a fully loaded RFC. The model investigated a standard RFC voyage and included the effects of loading, defrost cycles, respiration and transpiration. Experiments were conducted to characterise the relevant properties of paperboard material and environmental conditions inside a commercial RFC, as well as to generate data to validate the CFD model, which compared well to model predictions. Results showed relatively low board moisture content gradients through the stack, indicating the conditions will not substantially accelerate the normal creep process. The effect of the daily defrost cycles did not significantly affect board moisture content. However, the initial RFC activation (refrigeration started after loading) considerably accelerated the development of moisture content gradients in the cartons. Finally the most significant factor influencing spatial moisture content gradients (1.3 g/100 $g_{dry\ fibre}$) through the cartons was a temperature gradient caused by heat conduction from outside through the container wall. The change in board moisture content over time (temporal distribution) was about 1.4 g/100 $g_{dry\ fibre}$. The study therefore unveiled relatively small moisture content gradients in stacked cartons during ideal RFC shipping. Future studies can use this model to investigate less desirable shipping conditions. Additionally, the model can be used to provide detailed moisture boundary conditions for future creep investigations.

1. Introduction

Corrugated fibreboard boxes (cartons) are used extensively (> 90%) to transport fresh produce from growers to consumers and therefore play an essential role in fresh produce quality preservation (Berry et al., 2015). Corrugated fibreboard (CF or board) is generally preferred over other materials as it conveys several unique advantages. For example, (i) CF can be manufactured safely and sustainably from cellulose based products (e.g. wood and recycled materials) and is essentially made from paper, glued together with cornstarch; (ii) CF is completely recyclable and biodegradable; (iii) CF is lightweight; (iv) CF has high rigidity for its density; and (v) CF has a dampening effect when fruit are exposed to impacts. However, an important challenge which influences carton design is to maintain carton mechanical strength under cold chain conditions over extended time periods, which include high humidity environments and large compression forces.

During storage and shipping, compression forces occur as a result of pallet stacking, whereby cartons are palletised to form ~2 m high pallet stacks (pallet base/ footprint area ≈ 1.2 m^2) and cartons near the bottom of the stack must support the full pallet load (~1000 kg). High humidity conditions are necessary to minimise fruit moisture loss and preserve fruit quality. Fruit such as apples are therefore maintained at -0.5 °C and 90-95% relative humidity (RH) for periods between 1 and 6 weeks (Thompson et al., 2008), depending on the fruit type, market preferences and export destination (Robertson, 2013). These high RH conditions result in large moisture contents (Parker et al., 2006) in the corrugated fibreboard, which adversely affect board strength, due to water molecules breaking hydrogen bonds in the cellulose fibres (Allaoui et al., 2009b). For instance, Pathare et al. (2016) observed a 47% reduction in carton compression strength after just two days storage at 90% RH.

High moisture contents also influence the material properties of the corrugated fibreboard (Parker et al., 2006; Sørensen and Hoffmann, 2003), which can affect the mode of failure during compression. Previous work by the authors (Berry et al., 2017), examining the effect of vent hole design on carton strength, showed that certain vent hole designs are superior when matched to a particular board type (material properties). This has considerable implications to the assessment of new designs, since most box compression tests are performed at 23 °C and 50% RH. However, in reality the outcome of these evaluations may not be applicable to cold chain conditions. Before these concerns can be addressed, more information is needed regarding the carton spatio-temporal moisture content distribution in the cold chain.

An equally important and often overlooked factor is the effect of creep. In this context, creep is defined as a relatively slow process, whereby corrugated board materials permanently deform under the influence of mechanical stress (load). An important subcategory of creep is mechano-sorptive creep, whereby the deformation process is significantly accelerated by varying humidity. Mechano-sorptive creep has been documented in both wood (Armstrong and Christensen,

1961; Armstrong and Kingston, 1960) and paper materials (Byrd, 1972a, 1972b), with many processes behind mechano-sorptive creep being proposed (Gibson, 1965; Haslach, 1994; Söremark and Fellers, 1993). However, more recent studies suggest a process of nonlinear creep due to transient stresses from changes in board moisture contents (Alfthan, 2004, 2003; Alfthan et al., 2002; Habeger and Coffin, 2000). The resulting stresses (heterogeneous hygro-expansion and pallet weight) are, therefore, continuously redistributed and relaxed over time as the board deforms and moisture gradients change.

Mechano-sorptive creep plays a significant role in the mechanical strength of horticultural cartons and therefore influences the potential of the carton to protect fresh produce from mechanical forces (compression, impacts and vibration). A common challenge reported in many fruit industries is the unexpected failure of one or more pallet stacks after an extended sea voyage in a refrigerated freight container (RFC). This is only discovered at the destination end and is very costly due to the damaged fresh produce and investments for repacking. Furthermore, the conditions in the RFC are often reported to be normal. An improved understanding of the conditions in RFCs leading to creep is, therefore, an important step towards improved horticultural carton designs and reduced postharvest losses. However, most studies have focused on mechanisms of creep in wood (Olsson et al., 2007) and paper (Haslach, 2000; Rahman et al., 2006), and little is known regarding the transient moisture distributions and concentrations in cartons during shipping, specifically hygrothermal conditions and mechanical loads, which directly governs the rate and degree of creep.

Mathematical models could be very useful for studying moisture transport during shipping, as they can help to identify and understand the potential challenges, and therefore to better design cartons and optimise performance evaluation methods. Numerical approaches, specifically computational fluid dynamics (CFD), have become increasingly successful in recent years to simulate flow and scalar transfer in horticultural systems (Ambaw et al., 2013a; Delele et al., 2010; Norton et al., 2007; Zhao et al., 2016). This information could also be used to model creep in cartons (Rahman et al., 2006) and to improve carton strength evaluation procedures. More informed decisions regarding carton design and the consequential reduction in both postharvest losses and material costs would be possible. To the best knowledge of the authors, a coupling of simulations of heat and mass transfer in the airflow to the hygrothermal transport in cartons has not been performed for postharvest cold chain operations, in particular for long-haul transport using RFC.

The aim of this study was to quantify the presence of moisture content gradients in corrugated fibreboard cartons stored in a RFC during shipping. The study first validated the CFD model in a sealed glass-chamber under diffusion only conditions. Next, the model was validated in a larger controlled atmosphere chamber (CATTS-chamber) under convective conditions. Finally, the hygrothermal response of a part of a RFC, loaded with packaged apple fruit, was simulated. The simulation

incorporates a realistic airflow distribution as well as the effects of loading, defrost cycles, respiration and transpiration. These factors were selected to represent a normal shipping scenario and are some of the main factors influencing RH variability inside a RFC.

2. Materials and methods

2.1 Fruit

Apple fruit (cv. Golden Delicious) were purchased directly after harvest from a local grower in South Africa (March 2016). Fruit had an average diameter of 62 mm (±8 mm; d), were free of visual defects and were stored at -0.5 °C for a few days before experiments were conducted. The thermal and material properties with respect to fruit density (ρ), thermal conductivity (K) and specific heat (C_p) were 845 kg m^{-3} (ρ_f), 0.427 W m^{-1} K^{-1} (K_f) and 3 690 m^2 s^{-2} K^{-1} ($C_{p,f}$), respectively (Ramaswamy and Tung, 1981).

2.2 Corrugated fibreboard cartons

2.2.1 Corrugated fibreboard material

The corrugated fibreboard used throughout this study was supplied by APL Cartons (APL Cartons (Pty) Ltd, Worcester, South Africa) and is commonly used to manufacture cartons for fresh produce export. The CF was 4.2 mm thick (H), had a density of 167.5 kg m^{-3} (ρ_q), with specifications of 250K/175C/250K (250 g m^{-2} Kraft Paper/175 g m^{-2} Tugela C-Flute/ 250 g m^{-2} Kraft Paper) and an edge compression test value of 9.06 kN/m. The supplied CFs were in visually good condition and were stored at 20 °C ±1 °C and 50% (±5%) RH before the experiments.

2.2.2 Samples used in glass and CATTS-chamber experiments

Experiments performed in the glass-chamber made use of square CF samples, with dimension of 9.0 × 9.0 cm (volumes and masses were equal). Conversely, a single-walled, bottomless carton was manufactured (APL Cartons) for use in all CATTS-chamber experiments and is depicted in Figure 5.1a. The size of the cartons were reduced to 18% (with respect to footprint area) of a standard apple fruit carton, as used in the RFC simulations.

2.2.3 Carton design in RFC simulation

Cartons used in the RFC simulations represent a telescopic design (FEFCO and ESBO, 2007), which is formed from both an inner and outer carton (total wall thickness = 8.5 mm). The cartons size and ventilation (area and positioning) were further based on standard apple fruit cartons, as used in South African exports (Mark 4; 500 × 333 × 270 mm), with a total ventilation area percentage (TVA) of 2.2% and 3.7% along the top/bottom and side walls, respectively (Berry et al., 2015).

2.3 Experiments

2.3.1 Moisture diffusivity

A diffusion cup setup was used to estimate the effective moisture diffusivity (D_{eff}) through the CF (Figure 5.2). To achieve this, a constant moisture concentration gradient was maintained across a CF sample using saturated salt solutions for a set time period. Total moisture transfer into the cup was then used to calculate the D_{eff}.

The diffusion cup was suspended in an air-tight 3 L glass chamber (glass-chamber) above a saturated salt solution (Potassium nitrate; KNO_3; 94.6% RH), which provided a constant source of moisture to the chamber and was kept at 20 °C (±0.5 °C). The inside of the diffusion cup was maintained at a slightly lower moisture concentration, by filling the inner volume with Sodium Chloride (NaCl; 75.5%). Consequently, a moisture content gradient is expected between the saturated salt solution (bottom of chamber) and the board sample. RH sensors (Tinytag TV- 4500, Hastings Data Loggers, Australia) were therefore placed 5 mm above the CF board samples, to exactly derive the moisture concentration across the board over the experimental period.

Circular CF samples were preconditioned (84% RH for 3 days) prior to the experiment and placed over the diffusion cup (Figure 5.2) to separate the chamber and inner cup regions with different moisture concentrations. A threaded ring was attached over the sample to compress the board into the rubber seals so that moisture transport was limited to diffusion through the board region only. Fully assembled, the board sample exposed area (A_d; m^2) had a diameter of 55 mm. The experiment was performed in triplicate and run over 24 days. The cup setup was weighed before and after the experiment to determine total moisture transport over the experimental period (G_d; kg s^{-1}). The D_{eff} value was then calculated using Eq. (5.1) (Radhakrishnan et al., 2000).

$$D_{eff} = G_d H / A_d \Delta c \tag{5.1}$$

where H is the board thickness (m) and Δc is the moisture content gradient across the board (kg m^{-3}).

2.3.2 Sorption isotherms

The equilibrium CF moisture content is a factor of the surrounding RH, which is represented in the sorption isotherm (Parker et al., 2006). To characterise this relationship, board samples were equilibrated and measured for a range of RH conditions (11-95%). Both dry and wet samples were examined, since equilibrated moisture content values are higher during desorption (drying from high moisture content) than adsorption (hygroscopic loading from low moisture content). This phenomenon is commonly referred to as moisture hysteresis and is characteristic of

the cellulose fibres in the CF (Chatterjee, 2001; Mualem, 1973; Peralta and Bangi, 1998). Moisture hysteresis can be defined as a time-based dependence of the moisture content in the CF, whereby the previous board moisture content history influences the current equilibrium moisture content (Chatterjee, 2001).

Due to the uncertain initial moisture content in the board (moisture hysteresis can influence the final equilibrium moisture content), samples were first preconditioned for 9 days by cycling the samples successively between 0% RH (silica gel) and 100% RH (deionised water solution), with 3 day periods for each RH. Samples used for the adsorption measurements, were concluded at 0% RH conditioning and then further oven dried to remove any potential remaining moisture. The remaining samples used for board desorption experiments, finalised conditioning with a 100% RH step and were then soaked in deionised water.

CF samples were then individually suspended at the centre of the sealed glass-chambers containing saturated salt solutions (Greenspan, 1977), to create a constant RH environment of 11%, 36%, 43%, 67%, 84% and 95% RH (±0.1%) around the sample. All experiments were repeated in triplicate at 20 °C (±1 °C) over a period of 72 hours. Moisture content ($g/100g_{dry\ fibre}$) values were determined by immediately weighing the sample on a balance (NewClassic MF: ML104/01, Mettler Toledo, Switzerland) after the experiment and then taking the difference from the weight after oven-drying (100 °C, 48 hours).

2.3.3 Measuring moisture adsorption and desorption inside a glass-chamber

Validation experiments measuring the rate of moisture adsorption and desorption in a CF sample were performed in glass-chambers (Figure 5.1b) under diffusion only conditions and compared to numerical simulations. To remove any potential influence of hysteresis, samples were first preconditioned and then oven-dried, initial moisture content was therefore zero at the start of the experiments. From here, board samples were suspended in glass-chambers containing KNO_3 (94.6% RH) and weighed successively (in triplicate) over a period of 29 hours (every ~3.5 hours). Multiple glass-chamber/sample setups were run simultaneously (33 chambers in total), since the weighing process is disruptive to the experiment and can therefore only be performed once. After the 29 hours, all remaining samples were then relocated to new chambers (15 chambers total) containing K_2CO_3, which modified the glass-chamber RH to 43.2%. The relocation process took about 1-2 seconds and was performed at a RH of 50%. Very little effect from the environment was therefore expected. Samples were then again weighed successively (in triplicate) over a period of 21 hours (every ~3.5 hours).

2.3.4 Measuring humidity distribution in a controlled atmosphere container

A second complimentary validation experiment investigating board moisture adsorption and desorption was performed under forced convective conditions. Experiments were performed in a laboratory-scale CATTS (Controlled

Atmosphere/Temperature Treatment System) chamber, manufactured by Techni-Systems (USA). To this end, corrugated fibreboard cartons were conditioned in the climate controlled CATTS room (25 °C and 40% RH) for 48 hours prior to the experiments. After conditioning, four cartons were placed centrally in the CATTS-chamber (Figure 5.1c). The CATTS-chamber is a flow through, airtight system with temperature and humidity control. The inlet to the chamber was fitted with a meshed plastic crate (external dimension of 57 × 38 × 40 cm with ±60% open area), which supports the cartons in position to allow vertical flow of air. Air entered the chamber vertically from the bottom. The inlet air velocity was measured (in triplicate) using 56 unidirectional velocity sensors (TVS-1100, Omega, USA). The air in the chamber is humidified by micro-misting nozzles. The conditioning regime inside the CATTS-chamber was pre-set on the device and the resulting conditions at the inlet, which changed gradually over time, were recorded using three temp/RH loggers (Tinytag TV- 4500).

At the start of the experiment, the temperature and RH inside the chamber were 25 °C and 59% RH, respectively. Then temperature and RH in the chamber was first increased to 33 °C and 94% over 7.9 hours, decreased to 25 °C and 47% RH (for 4.3 hours), then increased again to 32 °C and 95% RH (for 5.1 hours) and finally decreased to 25 °C and 32% RH (for 4.1 hours). After every conditioning period (7.9, 12.3, 17.3 and 21.4 h), square samples (3 × 3 cm) were cut from each of the carton faces and weighed (immediately and after oven-drying) to determine moisture content. The resulting holes due to sampling were sealed with paper-based adhesive tape to maintain the carton's profile with respect to air distribution. The conditioning periods between sampling were selected to capture significant portions of the adsorption and desorption dynamics. Additional sampling between the adsorption and desorption curves were not possible, as this would have vented the sealed chamber and irrevocably disturbed the conditions around the sample cartons.

2.3.5 Determining conditions in refrigerated freight container during overseas transport

Temperature inside a RFC packed with apple fruit was characterised over time to develop more realistic operating conditions for the CFD model. Temperatures at different positions inside a fully loaded RFC carrying apple fruit were measured over time. Three temperature loggers (LogTag Recorders Ltd., Auckland, New Zealand) were placed in the bottom, middle and top cartons of a single apple fruit pallet stack. With respect to the horizontal plane, loggers were positioned inside cartons, at the centre of the stack. Loggers were added during the container loading process (August 2015) and the respective pallet stack was situated near the RFC door. The container was then transported via truck from a Grabouw pack house to the Cape Town docks (70 km; South Africa) and then shipped to the United Kingdom (UK) over a period of 18-days. The temperature data was used to obtain realistic boundary conditions for the CFD model.

Additionally, two RH loggers were also placed at the centre of the pallet stack. However, these sensors were misplaced during the container unloading phase (UK). It was therefore necessary to estimate the moisture concentration values for the simulation boundary conditions. Fresh produce exporters reported relatively small changes in the air moisture concentration, which is mainly a function of condensation on the evaporative coils (refrigeration unit) and transpiration from the packed fruit. To confirm, humidity data from five horticultural cold rooms packed with apple fruit was investigated (data not shown). Analysis showed that at 1 °C and 90% RH, moisture concentrations gradually alternated by about 5.0×10^{-4} kg m^{-3} per day, which is equivalent to about 1% RH.

2.4 **Numerical model**

2.4.1 Model Concept and Assumptions

A mathematical model describing moisture adsorption, desorption and diffusion through fibreboard sheets was obtained from Radhakrishnan et al. (2000) and Bandyopadhyay et al. (2002, 2000). The model was extended in this study to predict moisture transport through corrugated fibreboard under RFC conditions. Convection was included in the moisture diffusion-adsorption process by modelling airflow in a RFC packed with cartons filled with fruit.

Fruit were assumed spherical and the corresponding fruit volume and surface area were calculated using the average fruit diameter. Fruit were also assumed to be homogenous with constant material properties throughout. The Corrugated fibreboard material was assumed to be a composite solid material with spatially uniform air-to-fibre ratio. Material properties (density, thermal and moisture diffusion properties) were assumed uniform and estimated based on the air-to-fibre ratio. The volume inside the cartons consisting of loose fruit (solid) and air (fluid) was treated as a porous domain. The two phases in these volumes are therefore assumed to form a continuum. The respective interfaces are therefore not resolved geometrically, but are instead parameterized through the volume averaging procedure (Hassanizadeh and Gray, 1979). The airflow resistance of the porous medium was described using an isotropic loss model with linear coefficients, which were previously determined in a dedicated wind tunnel experiment (similar to the experimental setup described by Berry (2013)). Moisture transport in the air zones was described using a passive scalar transport equation, since the moisture content in the air is very dilute and thus has an almost negligible effect on the air properties.

2.4.2 Governing equations

Reynolds-averaged Navier Stokes (RANS) equations were used to solve airflow, energy and scalar (moisture) transport in the air with the shear stress transport (SST) k–ω turbulence model (Menter, 1994). This particular turbulence model performed best compared to other turbulence models in postharvest cooling of spherical produce in similar cases and has been validated extensively in previous work (Ambaw et al., 2014, 2013b, Delele et al., 2012, 2009; Hoang et al., 2015).

In the porous domain (stacked fruit), the moisture transport was described by Eq. (5.2) and (5.3) (Chourasia and Goswami, 2007).

$$\varepsilon_a \frac{\partial c_a}{\partial t} + \varepsilon_a \frac{\partial}{\partial x_i}\left(u_i c_a\right) = \frac{\partial}{\partial x_i}\left(D_a \frac{\partial c_a}{\partial x_i}\right) + S_c \tag{5.2}$$

$$S_c = -\frac{\partial c_f}{\partial t} = k_m A_f \left(c_f - c_a\right) \tag{5.3}$$

where ε_a is the porosity (0.57), c_a (kg m^{-3}) is the moisture content in the air zone, A_f is the specific area of the fruit in the air zone (63.8 m^2 m^{-3}), c_f (kg m^{-3}) is the fruit moisture content and S_c (kg m^{-3} s^{-1}) is the moisture loss as a result of transpiration.

Transpiration from fruit is assumed to create a constant source of moisture at the air-fruit interface. Fruit flesh is saturated with moisture containing various dissolved minerals and sugars, resulting in a vapour pressure lowering effect, where the intercellular moisture concentration (c_f) is slightly below saturation (c_{sat}). The resultant saturation moisture content of apple fruit (c_f) was determined to be 98% of the c_{sat} value (Chau et al., 1987). k_m (m s^{-1}) is the effective interfacial moisture transfer coefficient, and is determined from properties of the air layer over fruit surface and skin of the fruit as: $k_m = (1/k_a + 1/k_f)^{-1}$, where k_a, and k_f are the resistance of the air film and the fruit skin to moisture transfer, respectively. The corresponding k_f value was obtained (1.06×10^{-4} m s^{-1}) from Kessler and Stoll (1953) and k_a was determined from the Sherwood number which was calculated using the Sherwood-Reynolds-Schmidt correlation (Becker et al., 1996; Chau et al., 1987; Geankoplis, 1978) as shown in Eq. (5.4).

$$Sh = \frac{k_a d}{D_a} = 2.0 + 0.552\,\mathrm{Re}^{0.53}\, Sc^{0.33} \tag{5.4}$$

where d is the fruit diameter (m), Re is the Reynolds number ($(\rho_a v d)/\mu_a$), ρ_a is the air density (kg m^{-3}), v is the air velocity (m s^{-1}), D_a is the moisture diffusivity in the air, μ_a is the air dynamic viscosity (Pa s) and Sc is the Schmidt number ($\mu_a/(\rho_a D_a)$).

Two phase volume-averaged equations (Eq. (5.5) and (5.6)) were used to model the heat transfer inside the porous domain (Smale et al., 2006; Zhao et al., 2016):

$$\varepsilon_a \rho_a C_{p.a} \frac{\partial T_a}{\partial t} + \varepsilon_a \rho_a C_{p.a} \frac{\partial}{\partial x_i}\left(u_i T_a\right) = \frac{\partial}{\partial x_i}\left(K_a \frac{\partial T_a}{\partial x_i}\right) + h_{conv} A_f \left(T_f - T_a\right) \tag{5.5}$$

$$\left(1-\varepsilon_a\right) \rho_f C_{p.f} \frac{\partial T_f}{\partial t} = \frac{\partial}{\partial x_i}\left(K_f \frac{\partial T_f}{\partial x_i}\right) + h_{conv} A_f \left(T_a - T_f\right) + S_e \tag{5.6}$$

where $C_{p,a}$ (J kg^{-1} K^{-1}) is the air heat capacity at constant pressure, K_a (W m^{-1} K^{-1}) is the effective thermal conductivity in the air, h_{conv} (W m^{-2} K^{-1}) is the convective heat transfer coefficient, T_a (K) is the air temperature, T_f (K) is the fruit temperature and u (m s^{-1}) is the air velocity.

The interfacial heat transfer between fluid and solid phases in the porous domain is assumed to be affected only by the resistance of the air film around fruit surfaces. In this case, heat conduction in the solid region (fruit) was larger than convective interfacial heat transfer under the examined flow (Biot ≈ 0.6). For larger Biot numbers, the thermal resistance of the fruit flesh must also be included (van der Sman, 2003). The corresponding heat transfer coefficient is calculated from Eq. (5.7), which is the Nusselt-Reynolds-Prandtl ($Pr = (\mu_a C_{p,a})/(\rho_a K_a)$) correlation (Becker et al., 1996). This is similar in form to Eq. (5.4), except the Sherwood and Schmidt numbers are replaced with the Nusselt and Prandtl numbers, respectively:

$$Nu = \frac{h_{conv} d}{K_a} = 2.0 + 0.552\,\mathrm{Re}^{0.53}\,\mathrm{Pr}^{0.33} \tag{5.7}$$

The heat source term (S_e) in the fruit region of the porous medium (Eq. (5.6)) was determined as the sum heat loss from transpiration ($Q_{lat} = L_s S_c$; W m^{-3}) and the respiration heat (Q_{resp}) generated by the apple fruit ($S_e = Q_{resp} + Q_{lat}$). The latent heat of evaporation (L_s = 2499.1 J kg^{-1}) was determined at 0.8 °C as the average temperature during shipping (ASHRAE, 2009). Respiration heat was calculated from Eq. (5.8) as taken from USDA (1986) and Becker et al. (1996) for apples:

$$Q_{resp} = \left(1-\varepsilon_f\right) \rho_f \left(2.778 \times 10^{-3} \left(f\left(1.8 T_f + 32\right)^g\right)\right) \tag{5.8}$$

where the f and g coefficients are determined from USDA (1986) to be 5.5671 × 10^{-4} and 2.5977, respectively; ρ_f is the apple fruit density and T_f (°C) is the fruit temperature.

The corrugated fibreboard was modelled as a solid domain with two concentration fields. One for the moisture concentration within the void (c_p; i.e. air gaps between the corrugations and the air-filled inter-fibre regions) and one for the moisture content in the fibres (c_q; fibreboard). The model expressed board moisture contents as a concentration value (c; kg m^{-3}), however, this value can also be expressed as a weighted average value (g/100g$_{\text{dry fibre}}$): $q = c_q / (100\rho_q)$. The model for moisture transport in the two regions for the board is given by Eq. (5.9) and Eq. (5.10) (Bandyopadhyay et al., 2002, 2000):

$$\frac{dc_p}{dt} = -D_{eff.p}\nabla^2 c_p - r_s \tag{5.9}$$

$$\frac{dc_q}{dt} = -D_{eff.q}\nabla^2 c_q + r_s \tag{5.10}$$

$$r_s = k_i\left(c_x - c_q\right) \tag{5.11}$$

where r_s accounts the adsorption and desorption of moisture inside the corrugated fibreboard (Eq. (5.11)), k_i is the intra-fibre mass-transfer coefficient or a local moisture exchange coefficient (0.0035 s^{-1}) as determined by (Bandyopadhyay et al., 2002, 2000) and c_q is the moisture content in the fibres of the board.

The c_x in Eq. (5.11) is the equilibrium moisture content (EMC) in the fibres of the board (kg m^{-3}) as determined by the Guggenheim–Anderson–deBoer (GAB; Eq. (5.12) and (5.13)) model (Labuza and Altunakar, 2007; Marcondes, 1996).

$$c_x = 100 q_x \rho_q \tag{5.12}$$

$$q_x = \frac{q_o G_c G_K a_w}{\left(1 - G_K a_w\right)\left(1 - G_K a_w + G_C G_K a_w\right)} \tag{5.13}$$

where G_K and G_C are dimensionless coefficients, q_x (g/100g$_{\text{dry fibre}}$) is the weighted average value for the EMC, a_w is water activity (-) and q_o is the monolayer moisture content (g/100g$_{\text{dry fibre}}$), which represents the moisture content when all primary adsorption sites in the fibreboard are saturated by one water molecule.

2.5 Geometry and computational domains

Geometries corresponding to the three models are shown in Figure 5.1b, Figure 5.1c and Figure 5.3b. The computational mesh was a hybrid grid (tetrahedral and hexahedral cells). The spatial discretisation error was evaluated by means of a grid sensitivity analysis together with a generalised Richardson extrapolation (Celik et al., 2008; Roache, 1994). The grid size used in the pallet stack simulation was 1 002 267 cells, where the average discretisation error in estimated moisture content in board was 1%.

2.5.1 Boundary and initial conditions

The computational domain corresponding to the glass-chamber validation experiment consists of the board region (solid domain) as submerged in the free air region (fluid domain). The surface of the board sample was a no-slip wall to airflow and a conservative flux for moisture transfer (c_p). The glass wall was modelled as no-slip adiabatic wall. The bottom boundary (Figure 5.1b), which represented the saturated salt solution, was set as a no-slip adiabatic wall with a fixed additional moisture value equal to 95% and 43% RH (16.2 g m^{-3} and 8.1 g m^{-3}) for 29 hours and then 20 hours, respectively.

Similar to the glass-chamber case, the computational domain for the CATTS experiment consists of the carton region (board material, solid domain) and a free air region (fluid domain). The computational domain was reduced by imposing a symmetry plane (slip walls) vertically through the domains (Figure 5.1c), which assumed normal velocity components and normal gradients at the boundary are zero. The surface of the cartons was set as a no-slip wall for airflow and a flux boundary condition was applied for heat and moisture transfer. The walls of the chamber were modelled as no-slip adiabatic walls. Zero static pressure was imposed at the outlet boundary and the inlet boundary was set according to the velocity profile as determined in section 2.3.4. Furthermore, the temperature and moisture content values at the velocity inlet boundary were set to match the experimental conditions as reported in section 3.2.2.

Figure 5.3b shows the model geometry for the RFC pallet stack case, which represents a portion of a fully packed RFC (Figure 5.3a). Similar to the validation cases, the cartons are explicitly accounted. The geometry of the individual cartons is shown in Figure 5.3c and are each packed (loose) with 21.6 kg of ‘Golden Delicious’ apple fruit. The apple fruit were modelled as a porous medium domain and the pallet base region under the cartons was modelled as an air domain. A symmetry plane was imposed half way through the pallet stack to reduce computational grid size and thus simulation time. The surface of the cartons was set as a no-slip wall to airflow and a conservative flux for heat and moisture transfer. A pressure profile was imposed at the pressure openings (Figure 5.3a) to generate a realistic flow field in the pallet stack, which was attained from a validated full scale simulation of a RFC packed with fruit (Getahun, 2016). Temperature and

moisture conditions at the pressure openings were determined from experimental results, as discussed in section 3.3.1. Heat entering the RFC from the outside of the container (T_O; temperature varied with time) was included along the pallet boundary wall exposed to the RFC side. The sensible heat gain ($q_{r,w}$; W) through the wall was calculated as Eq. (5.14) and the corresponding overall coefficient of heat transfer (U_w) of the RFC wall was estimated using Eq. (5.15) as determined from ASHRAE (2006). For this study, the U_w was determined to be 0.13 W m^{-2} K^{-1}.

$$q_{r,w} = U_w A_w \Delta T \tag{5.14}$$

$$U_w = \frac{1}{h_{i,w} + x_w / k_w + h_{o,w}} \tag{5.15}$$

where A_w is the RFC wall area (m^2), ΔT (K) is the temperature difference between the outside and inside of the RFC wall, $h_{i,w}$ is the inside surface conductance (1.6 W m^{-2} K^{-1}; (ASHRAE, 2006)) for the trapped pockets of air between the pallet stack and the RFC wall, x_w is the RFC wall thickness (0.15 m), k_w is the thermal conductivity of the RFC wall (polyurethane; 0.022 W m^{-1} K^{-1}; (ASHRAE, 2006)) and $h_{o,w}$ is the outside surface conductance (6 W m^{-2} K^{-1}; (ASHRAE, 2006)), which assumes the outer RFC wall was exposed to an average wind speed of 25 km h^{-1} over the shipping duration.

2.5.2 Simulation setup

Simulations were performed using Ansys-CFX 16.2 CFD (Ansys Inc., Canonsburg, PA, USA) code, which uses the finite volume method. The simulations used second order backward Euler, high resolution spatial differencing (i.e. a blend between central differencing and upwind differencing locally) and second order schemes for the transient, advection and turbulent term. Before performing transient moisture and heat simulations, the initial flow field conditions was determined using steady-state simulations (CATTS and Pallet stack). The flow field was then disabled during transient simulations, which reduced computational cost as only the scalar and energy equations were solved. Several time step sizes (900, 300, 45, 5, 1, 0.1 s) were examined for sensitivity and were assessed with respect to accuracy, convergence history and computing time. A time step of 45 s with 13 iterations was selected as optimal and showed good predictions compared to experimental results. Under the selected optimum solver format, a one day simulation (pallet stack) took about 80 h on an Intel® core™ i7-4770 CPU (3.4 GHz) with 32 GB of RAM.

3. Results and discussion

3.1 Board properties

3.1.1 Board diffusivity

Table 5.1 summarises the moisture diffusivity and physical properties of the board and its respective components. The total effective moisture diffusivity (D_{eff}) was calculated using Eq. (5.1), with the moisture gradient (Δc) using the measured inner and outer RH values in the experimental cup setup (Figure 5.2). The inner RH at the board surface was taken to be equal to the NaCl solution (75.5% RH), since the air gap (< 5 mm) has a much higher diffusivity compared to the CF sample (Radhakrishnan et al., 2000). The outer surface had an average RH of 84.8% (±1.4%), as determined by the data logger. This value includes the initial lower RH (< 10 hours), before moisture transport reached a steady state and is thus representative of the total moisture transport.

The two regions of moisture transport in the corrugated fibreboard were modelled, namely, along the cellulose fibres ($D_{eff,q}$) and through the air components ($D_{eff,p}$). Bronlund et al. (2014) showed that $D_{eff,p}$ can be estimated from the sum of the total resistances, which includes the inter-fibre regions (D_p; Table 5.1) and the air gaps (D_a; Table 5.1) of the CF board and the respective board component thicknesses (fibreboard = H_p; air = H_a) using Eq. (5.16):

$$D_{eff.p} = \frac{H}{\left(\frac{H_p}{D_p} + \frac{H_a}{D_a}\right)} \tag{5.16}$$

Moisture diffusion through the fibre component of the CF ($D_{eff.q}$) occurs in parallel to the $D_{eff.p}$ (air components) and can therefore be estimated as: $D_{eff} = D_{eff.p} + D_{eff.q}$ (Table 5.1). For corrugated fibreboard, Bronlund et al. (2014) showed that diffusion through the fibre component is less critical to moisture transport than in non-corrugated fibreboard (thicker paperboard). This is due to the fluted geometry in the board, which considerably slows diffusion as a result of the tortuous path.

It should be noted that diffusivity of moisture in corrugated fibreboard is a somewhat complex mechanism, as the rate of transport is dependent on the direction of travel, due to the non-uniform geometry. However, lateral moisture transport along the board is considered less critical under the conditions examined in the study. This is due to local differences in board moisture content being quite low, as a result of the relatively even air moisture gradients across the board surfaces. The moisture diffusion rate normal to the board surface was thus used uniformly in this study.

3.1.2 Board moisture content

The adsorption and desorption curves with respect to water activity are shown in Figure 5.4. The adsorption curve was obtained by hygroscopically loading a sample from a dry state and the curve of desorption was obtained by drying a sample from a high humidity state. This was done to fully capture the desorption and adsorption curves, which differ as a result of the moisture hysteresis phenomenon. Specifically, the board equilibrium moisture content values are higher during desorption than adsorption. The adsorption and desorption curves in Figure 5.4, represent the minimum and maximum EMC values at each respective a_w. Equilibrium board moisture content values will therefore always lie within these two boundary curves (Chatterjee et al., 1997). The resulting curves followed a sigmoidal trend and each respective curve (adsorption, desorption, average of the two) were characterised using the Guggenheim–Anderson–deBoer (GAB; Eq.(5.13)) model (Labuza and Altunakar, 2007; Marcondes, 1996). The resulting GAB coefficients are shown in Figure 5.4.

The GAB model emphasises the fact that moisture content is a factor of the temperature dependent water activity (equivalent to the relative humidity), which is equal to the quotient between the water vapour content (c_p; kg m^{-3}) and the saturated water vapour content (c_{sat}; kg m^{-3}). The board q_x value is therefore influenced by both board temperature and water vapour content (c_p).

Due to the relatively small range of RH (90.0-94.5% RH; section 3.3.1) used in the RFC, which is within the ranges examined, moisture hysteresis is not expected to have a critical effect on EMC (q_x) values inside the RFC. Hysteresis was therefore not included within the scope of this study and the average of the two curves (Figure 5.4) was used in the CFD model.

It should be noted, that moisture adsorption and desorption isotherm curves, may potentially vary slightly at different temperatures (Parker et al., 2006). According to Sørensen and Hoffmann (2003) these differences can range from 3% to 4% at high relative humidity values (2-25 °C), which is consistent with the findings from earlier studies (Darling and Belding, 1946; Skogman and Scheie, 1969; Wahba and Nashed, 1957). The examined sorption isotherms (Figure 5.4) were therefore assumed constant within the examined temperature ranges in this study.

3.2 **Model validation**

The CFD model was validated using experimental results at two separate scales. At small scale, moisture diffusion adsorption/desorption dynamics were examined in a single CF sample, which was suspended in a sealed glass-chamber. Next, at medium scale, the convection-diffusion adsorption-desorption dynamics of moisture transport of the model is validated in a CATTS-chamber packed with four cartons. Finally, the model is extended to predict moisture transport in a fully loaded RFC using a simplified geometry and boundary conditions.

3.2.1 Moisture transport in glass-chamber

Figure 5.5 compares simulated and measured moisture content values versus time for an adsorption process followed by desorption inside the glass-chamber holding a CF sample. There is good agreement between predicted and measured values. A slight discrepancy between the model and experimental results was observed at the end of the adsorption and desorption curves. However, overall, the validation study at this scale demonstrated the models capacity to accurately predict moisture transport between the air and board domains.

3.2.2 Moisture transport in CATTS-chamber

Figure 5.6a shows the temperature and RH treatment regime used in the CATTS-chamber. The resulting volume-averaged moisture content in the cartons is further shown in Figure 5.6b, as determined from experimental measurements and CFD predictions. Based on the similar moisture adsorption and desorption trends and values, acceptable agreement between the experimental and predicted values was observed, indicating model validity. Some variability was observed in the first experimental readings (7.9 hours), which can be ascribed to differences in initial carton moisture contents, due to different weather conditions before each experiment. Although, variability was significantly reduced after the first desorption curve.

The EMC value (g/100$g_{dry\ fibre}$), as calculated from the experimentally determined GAB equation (Eq. (5.13)); Figure 5.4) and the RH in the chamber (Figure 5.6a) are shown in Figure 5.6b. The EMC indicates the final moisture content towards which the board was adsorbing or desorbing. Figure 5.6 therefore shows that experimental measurements were taken before (~13% of total moisture change) the cartons had reached the equilibrium moisture content. The CFD model, consequently, provided satisfactory predictions of large moisture adsorption/desorption ranges under convective conditions.

Figure 5.7a shows the predicted flow field along the symmetry plane of the CATTS-chamber. The CATTS inlet has a higher air velocity along the left side (door), which was characterised in the model using an experimentally determined velocity profile and had an average velocity of 5.9 m s^{-1}. For the bottom portion of the chamber (volume near the cartons), the CFD simulations showed a volume-averaged velocity of 6.6 m s^{-1} and a Reynolds number of 1.9 $\times 10^5$. Flow in the CATTS-chamber was thus turbulent, which consequently minimised moisture gradients in the chamber and across the carton surfaces (standard deviation of 0.5% RH).

The moisture gradients present in the cartons were mainly a factor of the convective mass transfer coefficient (CMTC) and board thickness. The walls parallel to the symmetry plane were the location of highest moisture heterogeneity (2-5% different to carton average), due to the additional thickness (two boards) and the low CMTC (1.39×10^{-2} m s^{-1}), where the average CMTC along the carton surfaces was 2.28×10^{-2} m s^{-1}.

3.3 **Moisture distribution inside refrigerated freight containers**

3.3.1 Conditions in pallet stack

Figure 5.8a shows the air temperature logger data as recorded at the bottom of the pallet stack during shipping from South Africa to the UK. The results showed an uneventful voyage, with ideal temperature regulation throughout the shipping duration. A slight temperature increase (< 1%) was observed between the temperature of the various loggers. The initial temperature conditions inside the RFC simulation were consequently set uniformly across the pallet domains as 0.8 °C.

Analysis of the results showed three prominent contributors to temperature variability. The initial large peak in temperature ($T_{P;}$ Figure 5.8) on the 1st day was due to the container refrigeration unit and fan system being activated on the vessel after an extended period without power. Heat that had collected in the air near the RFC's walls was thus first gradually forced up into the pallet stacks and then over time (about 6 hours) replaced with cool refrigerated airflow. Short (45 minutes) temperature peaks occurred daily and are a result of defrost cycles ($T_{D;}$ Figure 5.8a), whereby the refrigeration unit's evaporation coils are heated to eliminate ice build-up (ASHRAE, 2000b). Finally, the main bell shaped temperature curve ($T_{M;}$ Figure 5.8a) over the whole shipping duration is attributed to the outside temperatures ($T_{O;}$ Figure 5.8a), which were lowest at the start (South Africa) and end (UK), and highest half way through the journey (Earth's equator). It was possible to estimate the T_O (outside temperature) using sea surface temperature (SST) data from NASA JPL (Jet Propulsion Laboratory) ROMS (Regional Ocean Modelling System) group (Figure 5.9), which ranged between 13 °C and 27 °C over the 18-day period. Correlating T_M and T_O, showed that T_O can be expressed in terms of T_M: $T_O = T_M \times 23 + 4$ °C ($R^2 = 0.94$).

Simulating a full 18-day voyage (Figure 5.8a) would require considerable computational resources. The 18-day shipping duration was therefore reduced to 7-days (Figure 5.8b). Specifically, the T_M curve was scaled (with respect to the time domain), the T_P peak was left unchanged (~1 day) and the daily occurrence period, range and domain of the individual of the T_D defrost cycles were kept constant. The temperature and moisture content of air entering the simulated pallet at the pressure openings was set uniformly, as indicated in Figure 5.8a, whereas the outside temperature was set to T_O. The initial moisture concentration set in the RFC simulations was set as 4.97×10^{-3} kg m^{-3} in the air domains and inter-fibre air regions and 22.2 g/100$_{\text{dry fibre}}$ in the fibre regions of the carton domains.

The airflow distribution along the middle of the domain (parallel to the RFC length) is shown in Figure 5.7b. The volume-averaged air speed in the cartons and pallet base regions was 0.02 m s^{-1} and 0.63 m s^{-1}, respectively. Inside the cartons, air flowed in a mainly diagonal direction (up and left = towards the RFC doors; Figure 5.3b). Air entered the cartons at the bottom (pallet base) and from the right (right = refrigeration unit side) vent holes and then exited at the top boundary and left vent holes (Figure 5.7b). With respect to the pallet base, air was flowing mainly from the right side of the pallet base and up the T-bar floor to the left side of the pallet base, with a small portion entering the cartons.

3.3.2 Carton moisture content over the shipping duration

Conditions in the RFC represent an ideal shipping journey, without any cold chain breaks or equipment failures. The resulting CF moisture content values and distributions are therefore typical of desirable shipping conditions and provides a valuable baseline against which future studies incorporating cold chain breaks can be compared. The volume-averaged temperature and relative humidity in the cartons and air/fruit (porous) regions are shown in Figure 5.10a and b. The temperature in the carton region generally followed a similar trend to the air temperature profile (0.8-1.9 °C). A slightly larger (0.3 °C) average temperature was predicted in the cartons compared to the air region, due to the heat conduction into the cartons from the RFC wall. Furthermore, the three temperature features (T_P, T_D, T_M) were clearly present in the cartons, but were attenuated compared to the inlet conditions (Figure 5.8b).

As expected, the range of RH in the stacked cartons were rather small, which is a desirable goal during RFC shipping. The RH curve in the cartons had a more linear profile than in the air region (Figure 5.10b). The RH in the porous region is mainly a function of the inlet temperature and moisture concentration. Specifically, RH values in the porous region ranged between 90.9% and 94.5% RH (Δ3.6%), whereas the carton inter-fibre (air) region ranged between 92.9% and 93.2% RH (Δ0.3%). The relative uniformity in the carton RH can be attributed to the fibreboard acting as a buffer to changes in RH. Fibreboard has a large moisture content capacity and its equilibrium value (q_x) is a function of the RH in the board (Eq.(5.13)). Consequentially, an increase or decrease in board RH results in a rapid decrease or

increase in air moisture concentration, respectively, as moisture is transported between the air and fibres. Conditions inside the cartons were therefore more influenced by the long term T_P and T_M curves, than by the smaller defrost cycles (T_D). The impact of defrost cycles on mechano-sorptive creep has been a topic of speculation in the fresh produce industry, however, these findings indicate it may be a minor contributor.

Figure 5.10c shows the average moisture content in the cartons over the shipping duration. The trend of the board moisture content was a clear function of the difference in RH between the carton and air regions (Figure 5.10b). The initial moisture content value was set at 22.2 g/100$g_{dry\ fibre}$ (equivalent to 225.5 g H_20 per a carton), based on the initial temperature and air moisture conditions. However, the heat gain from the RFC wall lowered the overall RH and thus the equilibrium moisture content. A generally negative moisture content trend was consequently observed, with volume-averaged values ranging between 21.3 g/100$g_{dry\ fibre}$ and 22.2 g/100$g_{dry\ fibre}$. This is expected to be a relatively realistic scenario, since pallet stacks are first stored as higher RH conditions (90-95% RH) before being loaded into the RFC. Furthermore, the loading temperature peak (T_P) and general equatorial temperature trend (T_M) also significantly influenced board moisture content over the journey.

3.3.3 Moisture content gradients in cartons

Figure 5.11 show the distribution of moisture in the stacked cartons at one day intervals. A uniform board moisture content value was initially set across the stacked cartons (Day 0), which then gradually developed over the simulated shipping duration. The development of a moisture content gradient across the stacked carton between the RFC wall and opposite pallet side is visible. The evolution in moisture content distribution in the stacked cartons between day 1 and day 7 suggests the distribution may further develop if a longer shipping duration is used. The transient change in moisture content inside a RFC is therefore a long term process and could potentially last several weeks.

Figure 5.12 depicts the board moisture content values along vertical lines throughout the stacked cartons after 7-days. The graph shows a generally even board moisture content gradient through the stack. The small variations can be attributed to different board volume to surface area ratios. For instance, larger moisture content values (peaks) occurred near the carton corners and edges.

The board moisture content distributions in the stack were mainly a function of differences in RH, which in this study were relatively small. Total moisture transpiration at the examined shipping temperature (1.5 °C for fruit) was about 460 g over the 7-days (0.28% of fruit mass) and therefore did not have a large influence on moisture RH gradients between the individual cartons. However, larger effects are expected across an entire RFC, at higher temperatures (cold chain breaks, larger transpiration rates) or when using fruit with higher transpiration rates (e.g. stone fruit). Similarly, respiration heat (6 W across examined domain) was also not significant under the examined conditions.

The main moisture content gradients across the stacked cartons were attributed to the corresponding temperature gradient as depicted in Figure 5.13b. In this case, temperature gradients were therefore a significant factor driving changes in moisture content across the pallet stack. This is due to the dependence of the board EMC (q_x) on water activity, which is a factor of temperature. It should be noted that in this study the cartons were assumed to be an equal distance from the RFC wall, resulting in a constant rate of heat conduction into the stacked cartons. Although this is often the case, slight differences in pallet loading can also result in varying gaps and contact areas with the RFC walls. Furthermore, contact between neighbouring pallet stacks follows a similar pattern, resulting in direct or partial contact between pallet stacks.

Temperatures in RFC can also vary in reality, depending on the time of year and quality of the RFC, whereas breaks in the cold chain can result in more substantial temperature and RH variations. For example, when refrigeration is halted (power break); large temperature differences between pallet stacks due to in adequate forced-air cooling (Brosnan and Sun, 2001); ambient loading, whereby pallet stacks are loaded warm and cooled over the shipping duration (Defraeye et al., 2015b); and intermittent warming treatments, where the packed fruit are continuously heated and cooled during shipping to reduce incidence of chilling injury (Xi et al., 2012). Follow-up studies should therefore focus on these aspects.

The CMTC is depicted in Figure 5.13a and shows the potential rate of moisture transport between the board and air regions as determined by the flow properties near the board surface. It should be noted, however, the mass transfer Biot number was about 100, indicating a low dependence on convective transport. The average CMTC was 5.1×10^{-3} m s^{-1} for the carton surfaces in contact with the pallet base (bottom surface), where flow was highest and 3.8×10^{-3} m s^{-1} at the inner carton surfaces, which had comparatively lower flow rates. The CMTC was relatively evenly distributed along the carton surfaces (Figure 5.13a), except near the vent holes, where CMTC values were considerably larger (2.5×10^{-2} m s^{-1} to 6.3×10^{-2} m s^{-1}).

An important consideration is that there are three moisture related factors influencing carton strength. First, the high board moisture contents, which weaken the board by breaking hydrogen bonds in the cellulose. Second, the heterogeneous moisture content gradients throughout the cartons at any moment (Δ0.9 g/100$g_{dry\ fibre}$), resulting in inhomogeneous hygroexpansion throughout the stack. Third, the transient changes in moisture content over time (Δ1.4 g/100$g_{dry\ fibre}$) in combination with the large compression forces result in a process of mechano-sorptive creep. The study, therefore, showed generally small moisture content gradients in the pallet stack, which is not expected to substantially accelerate the creep process, although some contribution to carton strength loss is still expected (Alfthan, 2004; Bandyopadhyay et al., 2000; Dong et al., 2010; Söremark and Fellers, 1993). This study, therefore, has shown the RFC studied can provide relatively stable environmental conditions, which can help maintain carton mechanical strength as long as possible in the cold chain.

4. Conclusions

Stacked corrugated fibreboard cartons are transported in refrigerated freight containers (RFC) at low temperatures and high humidity conditions. The resulting presence of high moisture contents and moisture gradients in the corrugated fibreboard cartons can have a substantial effect on carton mechanical strength. This study therefore characterises moisture properties in stacked cartons under standard shipping conditions. To achieve this, a CFD model was developed to predict moisture transport through stacked cartons under convective airflow conditions. The CFD model was validated using two experimental approaches and compared well to predictions. The study incorporated the presence of respiration, transpiration, defrost cycles, initial RFC activation and temperature changes over the geographical voyage (South Africa to United Kingdom).

Results revealed relatively small spatio-temporal changes in moisture content under standard shipping conditions, with the board moisture content decreasing by 1.4 g/100$g_{dry\ fibre}$ over the simulation period (7-days). Almost no significant effect by the daily defrost cycles was observed on board moisture content. The initial RFC activation (refrigeration is powered on), whereby the warm air around the container walls was forced up into the pallet stack, caused a rapid change in RH and therefore accelerated the development of a heterogeneous moisture content distribution. The temperature gradient caused by heat conduction from outside through the container wall was the most significant factor affecting spatio-temporal changes in moisture content. By day 7, a moisture content gradient of 1.3 g/100$g_{dry\ fibre}$ was observed across the domain (3 cartons), which is equivalent to about 8% of the total board moisture content change between 50% and 95% RH. Although relatively small, these gradients are expected to contribute to the creep process and should be quantified with respect to mechanical strength in future studies. The model can therefore be used to provide detailed moisture boundary conditions for these creep evaluations.

In future follow-up work, the model will be used to investigate various cold chain breaks (temperature and humidity conditions vary drastically), where the findings in this study can be used as a base line. Furthermore, the model can be used to develop improved carton conditioning treatments for box compression tests, for which there is currently little information available.

Table 5.1: Physical and diffusivity parameters of the C-flute corrugated board.

Parameter	Value
Liner fibreboard (outer) thickness	407 µm
Liner fibreboard (inner) thickness	357 µm
Fluting fibreboard thickness	317 µm
Effective thickness of air component in CF	3 023 µm
Corrugated fibreboard (CF) thickness	4 244 µm
Ratio between the areas of the fluting fibreboard and liner fibreboard	1.44
Diffusivity of air (D_a)[a]	2.18×10^{-5} m^2 s^{-1}
Inter-fibre (pore regions) diffusivity through liners/fluting (D_p)[b]	5.07×10^{-7} m^2 s^{-1}
Total effective diffusivity across CF (D_{eff})[c]	1.76×10^{-6} m^2 s^{-1}
Effective diffusivity across CF inter-fibre regions and air gaps ($D_{eff,p}$)	1.66×10^{-6} m^2 s^{-1}
Effective diffusivity across CF fibre regions ($D_{eff,q}$)	1.09×10^{-6} m^2 s^{-1}

[a] As taken from ASHRAE (2009) at 1 °C;
[b] As taken from Bandyopadhyay et al. (2002);
[c] Experimentally determined, SD = 4% (relative standard deviation).

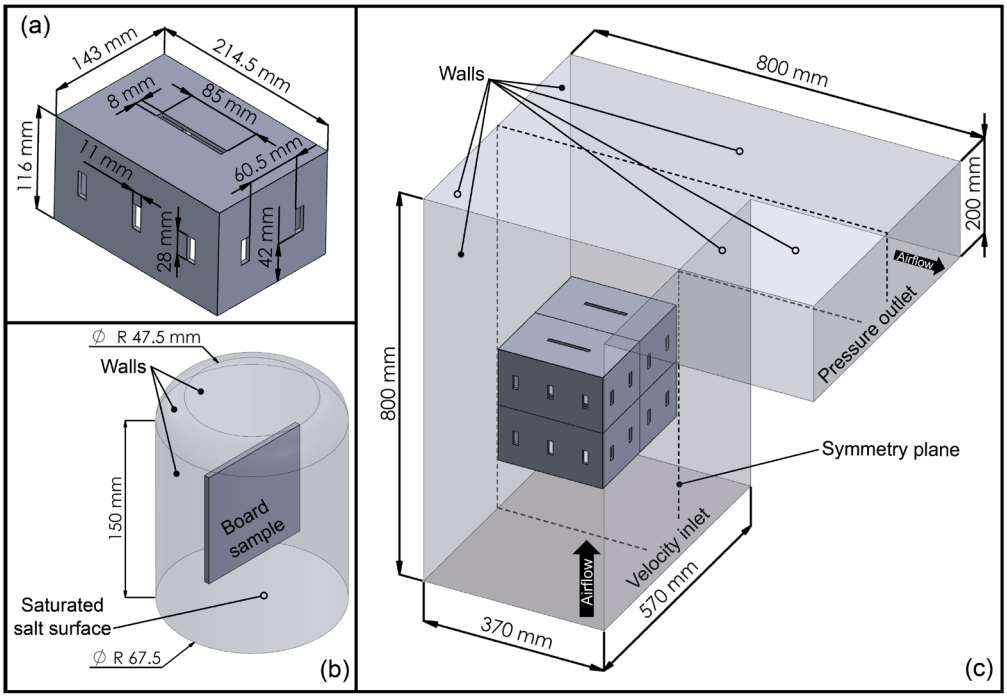

Figure 5.1: Schematic diagram showing geometry and boundary conditions of the (a) small scale carton, (b) glass-chamber and (c) CATTS-chamber, dashed line indicates symmetry plane.

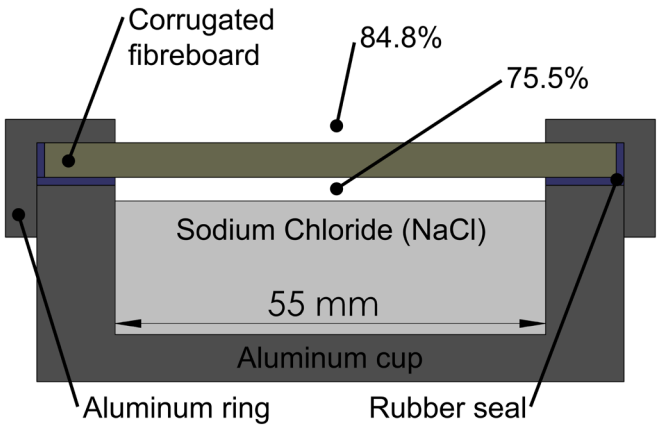

Figure 5.2: Cross section diagram of the diffusion cup setup. An average relative humidity (RH) of 84.4% was maintained just above the board sample, by holding the diffusion cup in a sealed glass-chamber containing a solution saturated with Potassium nitrate (KNO_3; 94.6% RH) at 20 °C.

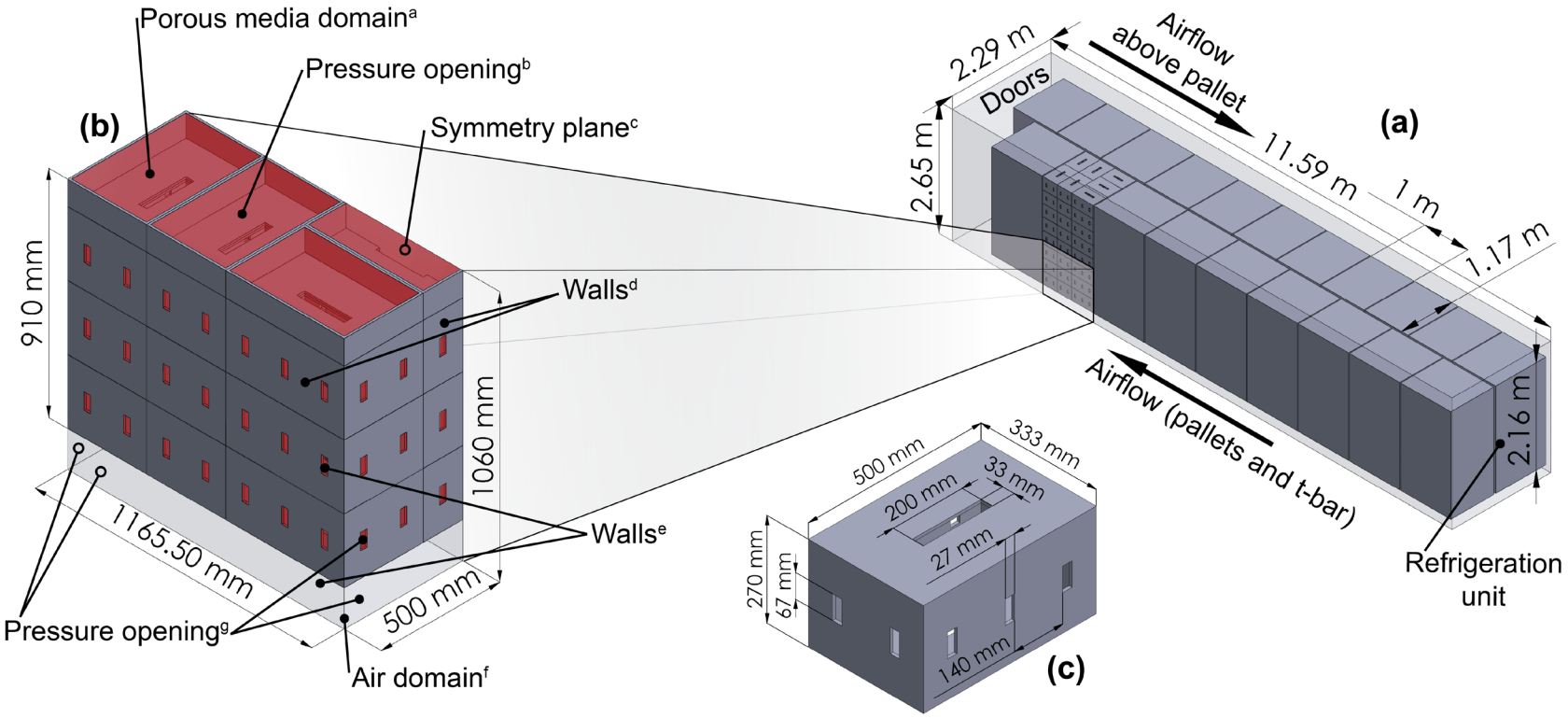

Figure 5.3: Schematic diagram of the (a) refrigerated shipping container, which depicts the (b) simulation domain used in this study. Superscript letters indicate: [a] air and fruit filled volume (red region); [b] top boundaries along the porous media domain; [c] vertical boundaries (carton and porous media) through the pallet; [d] all outer carton surfaces; [e] vertical boundaries along the reefer container wall at vent holes and air domain; [f] air volume (under cartons) representing pallet; [g] front, back and bottom boundaries along the air domain. Diagram (c) shows geometric specification of the ventilated carton used in the pallet stack.

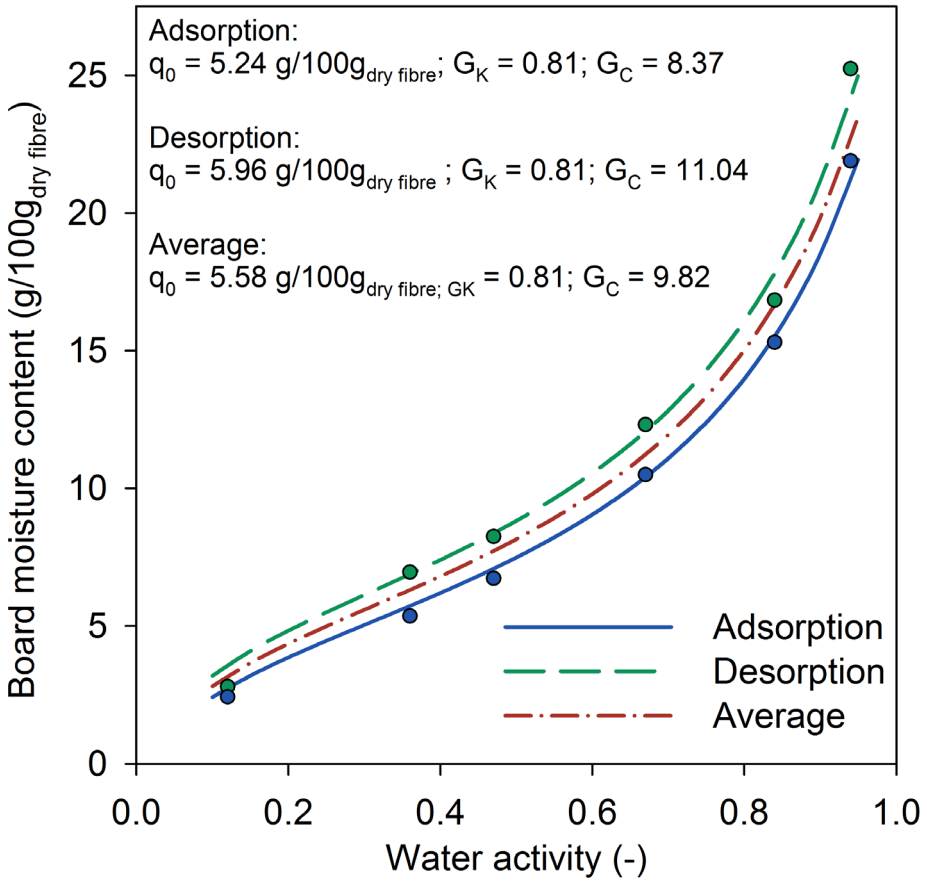

Figure 5.4: Equilibrium moisture content (EMC) for the corrugated fibreboard used in this study, with respect to the water activity (equivalent to relative humidity) for the adsorption, desorption and average (of the two) curves.

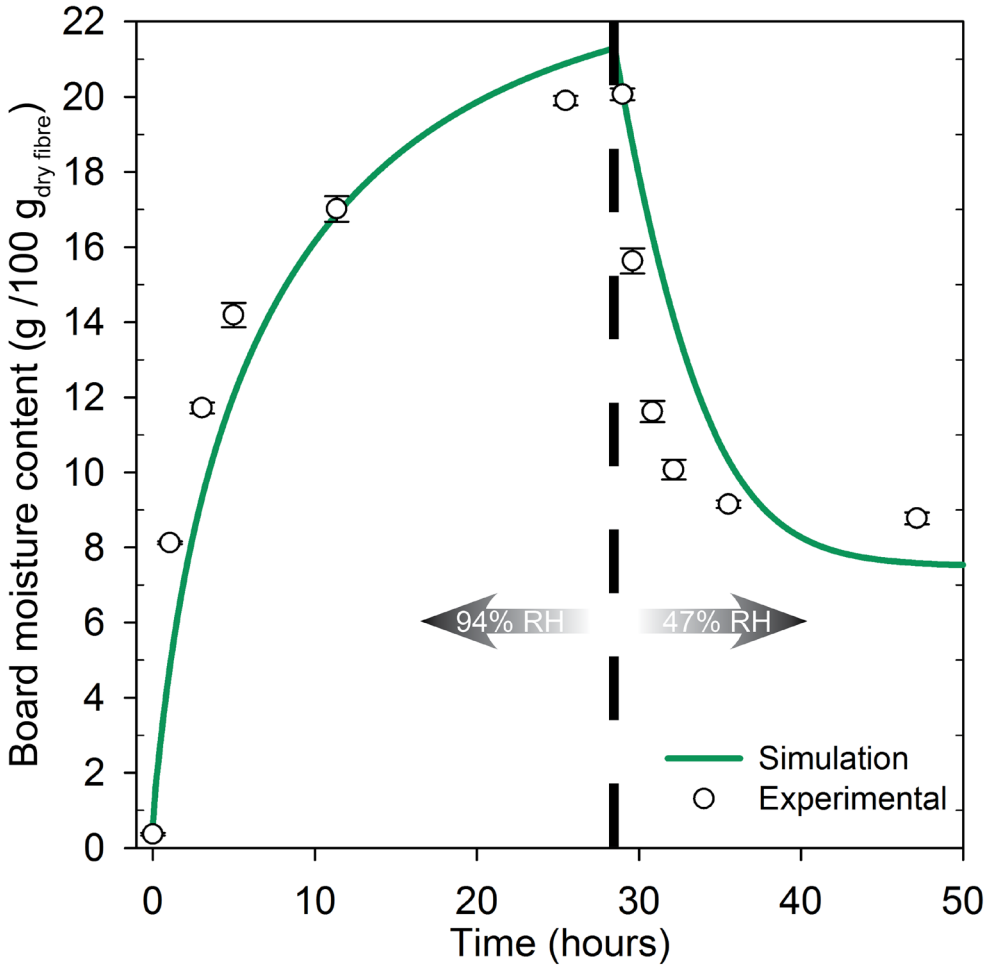

Figure 5.5: Comparison between experimental and numerical moisture content values of a corrugated fibreboard sample stored in the glass-chamber over time. All error bars indicate standard deviation of the mean.

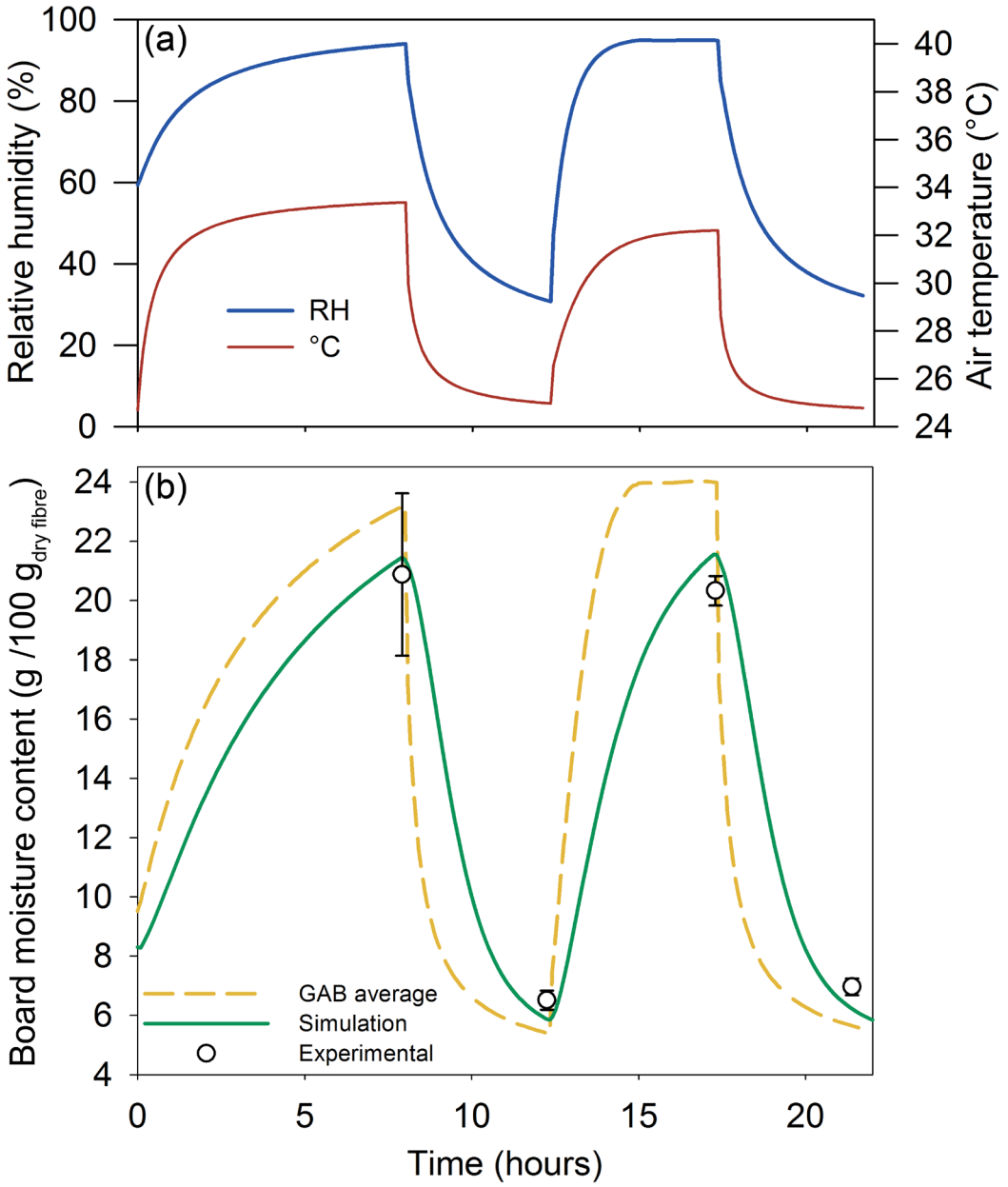

Figure 5.6: (a) Applied temperature and relative humidity conditions and (b) comparisons between experimental and simulation results for the CATTS validation experiment. The yellow (dashed) line indicates the equilibrium moisture content (EMC) of the cartons, based on the GAB model and the RH at the inlet. Error bars indicate standard deviation of the mean.

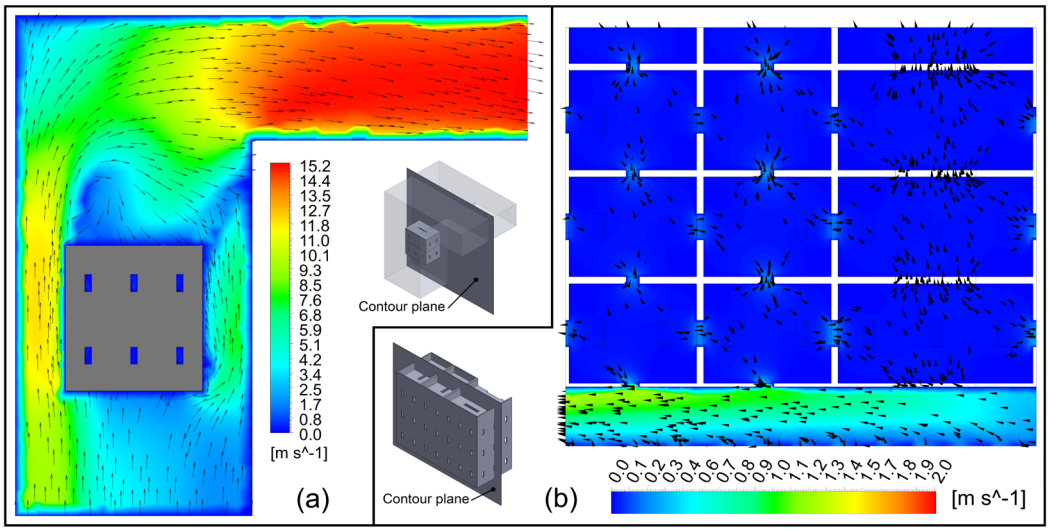

Figure 5.7: Simulated contours of velocity profile along the (a) symmetry plane of the CATTS-chamber and (b) through the centre plane of the pallet domain.

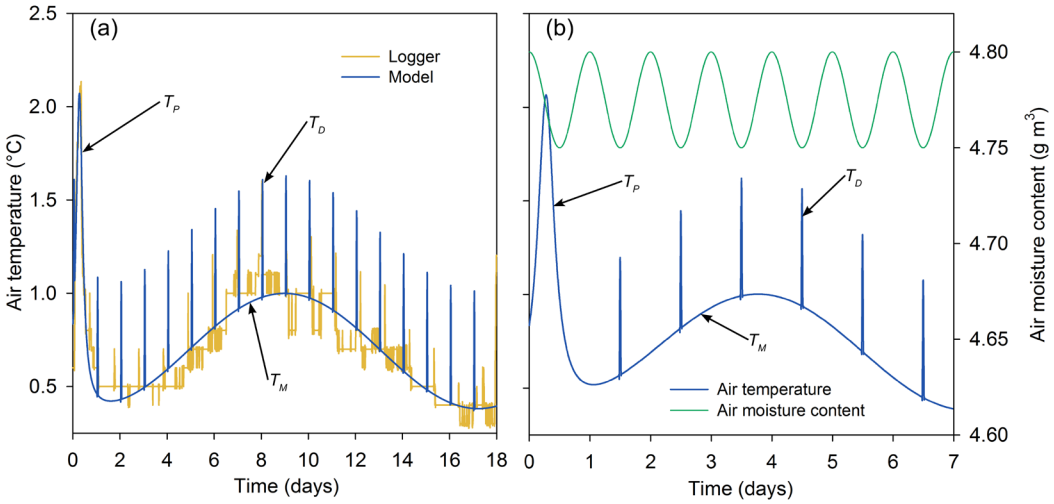

Figure 5.8: (a) Average logger and model air temperature inside a pallet shipped from South Africa to the United Kingdom over 18-days. (b) Shows the seven day simplification of the full (18-day) shipping duration and indicates the temperature and moisture values used at the pressure openings of the pallet stack over the RFC simulation period.

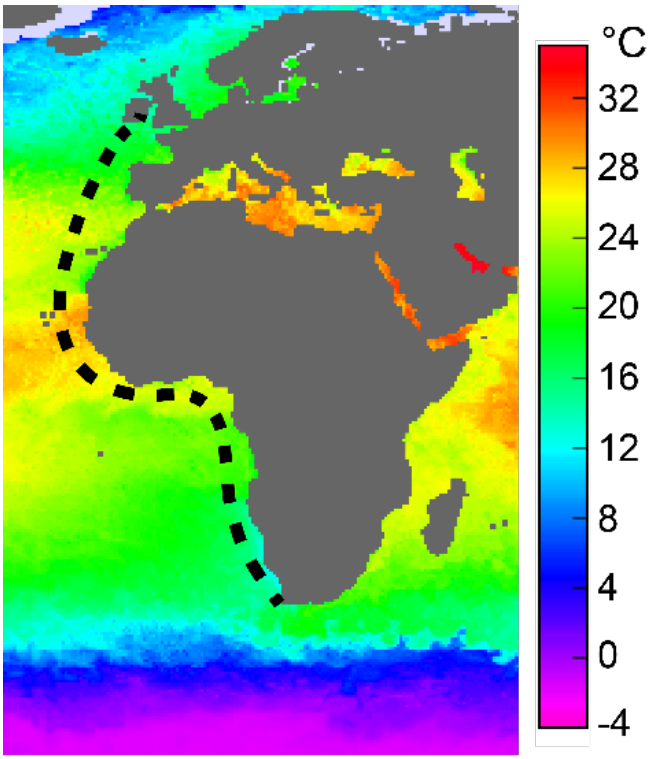

Figure 5.9: Sea Surface Temperature (SST) data produced for the 24th of August 2015. Dashed line indicates the shipping journey between South Africa and UK, each dash represents one of the 18 travel days. Data acquired from the NASA Jet propulsion laboratory ROMS (Regional Ocean Modelling System) group (http://ourocean.jpl.nasa.gov/SST).

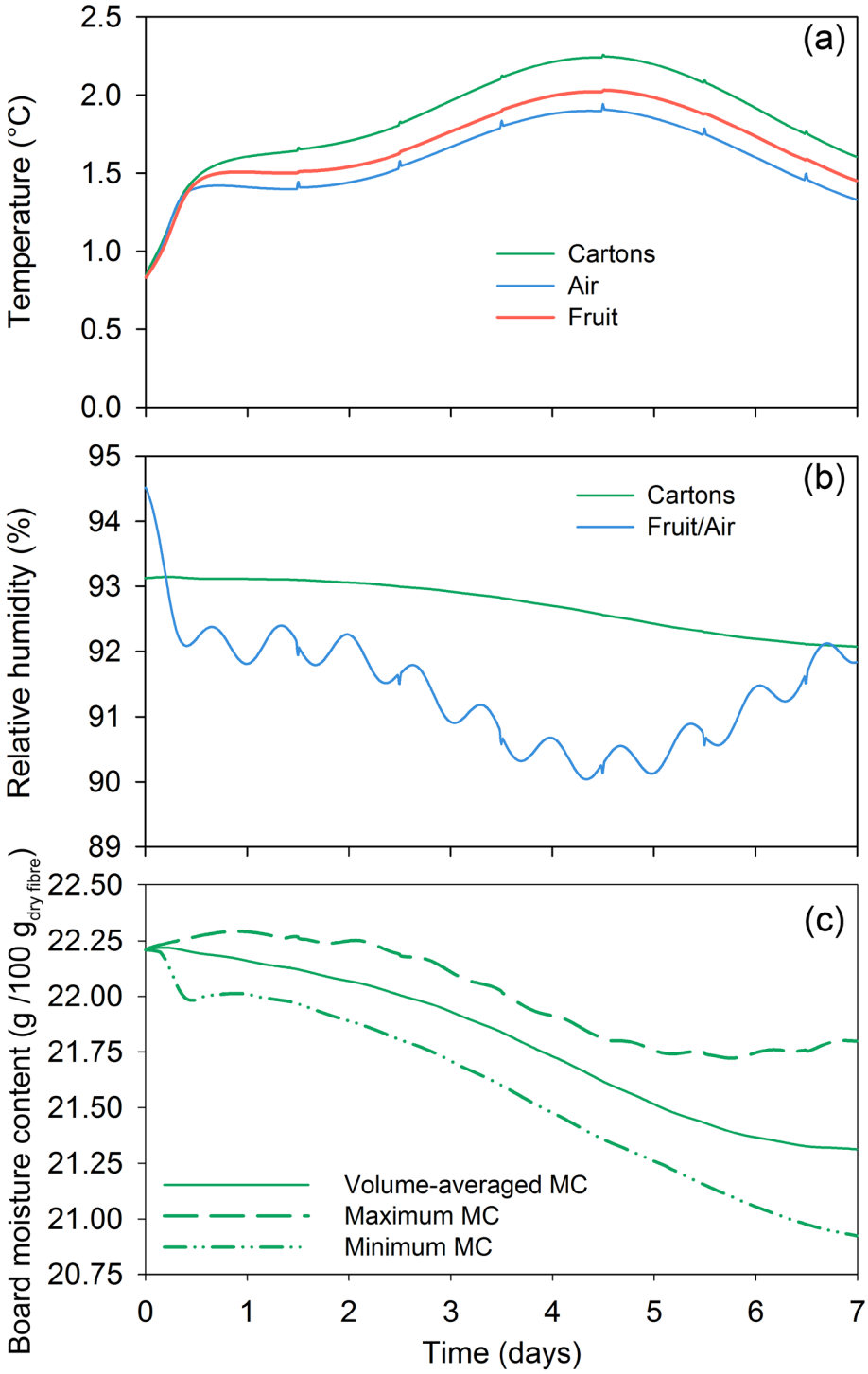

Figure 5.10: (a) Average temperature, (b) relative humidity and (c) moisture content (MC) in cartons and porous regions over the 7-day shipping period.

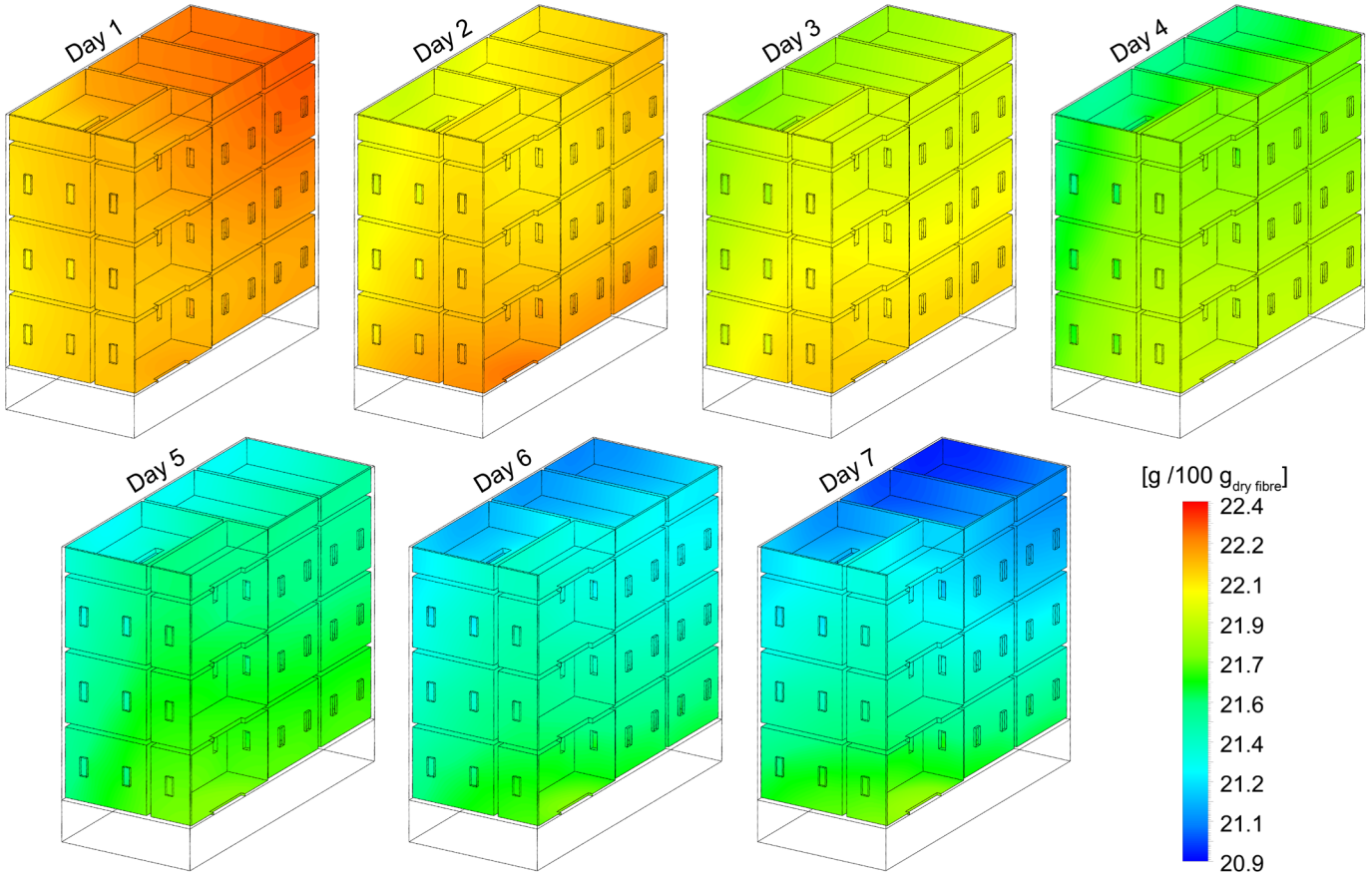

Figure 5.11: Simulated contours of carton moisture content profiles across carton surfaces for each day of the shipping period.

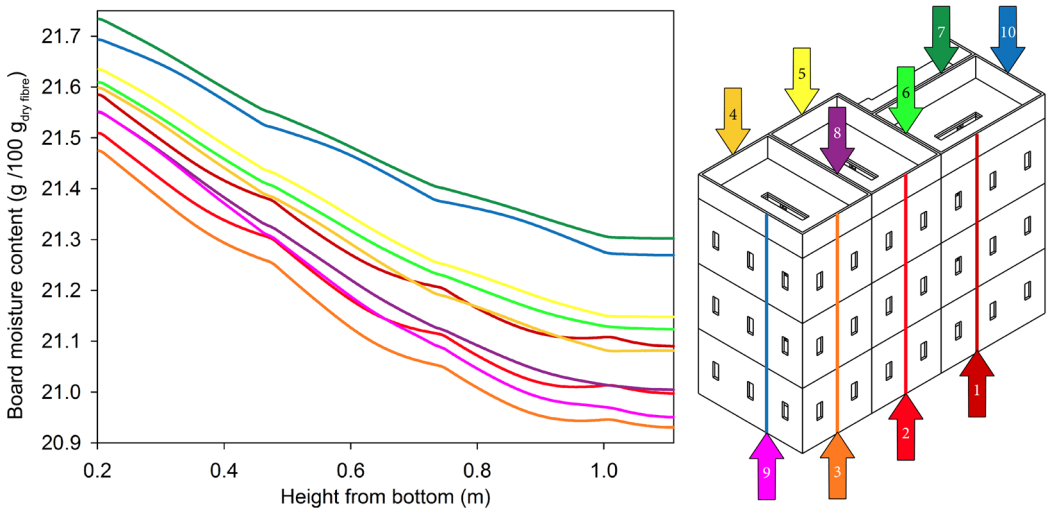

Figure 5.12: Moisture content along vertical lines through the corrugated fibreboard cartons showing moisture gradients on day 7. Colour coded arrows are correlated to the graph line colours.

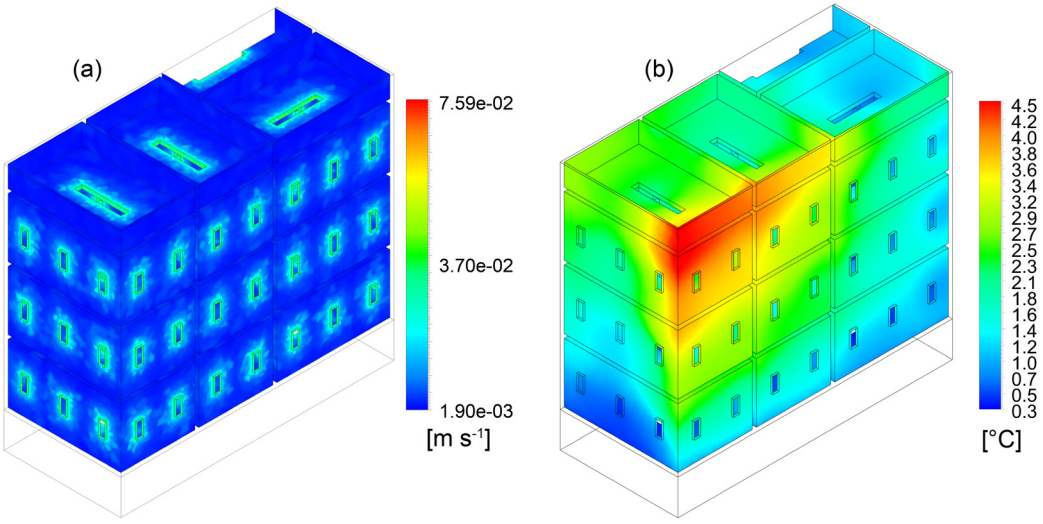

Figure 5.13: Simulated contours of (a) convective mass transfer coefficient profile across carton surfaces and (b) the temperature profile on day 7.

Chapter 6. Optimising Fresh Produce Carton Design: Exploring Improved Refrigerated Container Space Usage

Abstract

Large quantities of fresh produce, such as pome fruit, are exported every year to international markets across the world using refrigerated freight containers (RFCs; length = 40 feet or 12.2 m). However, current packaging systems typically employ 1.2 × 1.0 m pallets, which leave about 10% of the RFC unused. The introduction of an improved packaging system that better utilises RFC volume and improves cooling efficiency could enable a significant reduction in transport costs, carbon emissions and postharvest losses. This study therefore investigated two new packaging systems under forced-air cooling (FAC; horizontal airflow) and RFC (vertical airflow) conditions using computational fluid dynamics. The Tes packaging system consists of a novel pallet and carton design, which occupies 98.9% of the RFC floor area. The Hex packaging system, on the other hand, uses an isosceles trapezoid carton, which forms a hexagonal shape when placed back to back. The complimentary Hex pallet results in a 97.4% RFC floor area usage. For FAC, the Hex design produced a low airflow resistance, but reduced cooling rate compared to the standard (STD) design, resulting in a somewhat similar cooling efficiency. Conversely, compared to the STD design, the Tes packaging system improved cooling efficiency by 29%. For RFC, relatively heterogeneous cooling was observed in all cases. This was attributed to the presence of trays, which substantially restricted vertical airflow. The results showed that RFC performance is primarily a factor of the number of cartons vertically stacked in a line. Findings further suggest that improved vent hole designs on the top and bottom of the cartons could significantly improve cooling performance in all designs. Further work is recommended here. Overall, the Tes packaging system is able to facilitate the largest fruit packing density and the most energy efficient pre-cooling. Additionally, the characteristics of the Tes packaging system are relatively similar to current packaging systems, which provides several practical benefits if it is ever adopted. Future studies will need to address the stability and mechanical strength of these packaging systems under pallet stack conditions.

1. Introduction

Transport of fresh produce between producers and retailers is a critical component of the horticultural cold chain and often includes the use of refrigerated containers, which have become the standard mechanism for long distance freight. In the 2014/2015 season, South Africa (SA) exported about 28 000 refrigerated freight containers (RFCs) packed with pome fruit. This represented around 16% of the total SA fresh fruit exports (PPECB, 2015). However, recent concerns relating to rising fuel costs and a high carbon footprint have highlighted a need for new innovations to more efficiently transport fresh produce. One feasible solution is to make more effective use of the space inside RFCs. For example, current fresh produce packaging designs are packed on standard ISO pallets (1.2 × 1.0 m), by which about 10% of the RFC floor area is left unused. An improved carton and pallet design (packaging system) that fully utilizes this area, would therefore enable the SA pome fruit industry to use about 2 800 fewer RFCs each year. Since exporters typically lease refrigerated containers (one-way) from third party suppliers to transport produce to international markets, freight costs could potentially be reduced by approximately 18 million USD (based on quotations for container shipping between Cape Town and Felixstowe ≈ $6500; value does not include levies or tax).

Refrigerated freight containers have grown considerably over the last 50 years and their use is expected to increase with the rising demand for year round fruit supply (Eyring et al., 2005; Opara, 2009). The 12.2 m or 40 feet RFC (model type: 40RF/RH), commonly used for refrigerated transport of fresh produce, have internationally standardised (ISO 668:2013) exterior dimensions. The internal dimensions are mainly a factor of the remaining space after the addition of insulated walls and the refrigeration unit, resulting in dimensions of about 11.59 × 2.29 × 2.56 m (L × W × H). Cartons packed with fresh produce are normally stacked on pallets and then loaded into the RFC. Currently there is no universally accepted pallet base design, with many regions and industries using their own standard. However, the most common pallet base used for fruit export is 1.2 × 1.0 m (P-120) and many facilities have thus been equipped to transport and store this pallet type. Consequently, a major challenge to the introduction of a new pallet base is that both parties (producer and recipient) would have to modify equipment simultaneously. It should be noted, that retrofitting at this scale could be very costly and would require tremendous cooperation between the various partners. Any design proposed for this scenario would therefore have to offer significant financial and practical benefits with respect to compensation for the initial investments.

The design of a new packaging system (pallet base in combination with a matching carton design) must be performed within the context of several important practical requirements. (i) The pallet base should have relatively similar dimensions to a P-120 pallet, to aid in compatibility with current equipment (e.g. forklifts and doorways). (ii) Cartons are typically pallet stacked into tall (~2.2 m) structures and are thus somewhat unstable. Pallet stack stability should therefore be a priority and must optimally include some form of interlocking pattern, allowing cartons to lean into each other for additional support and to resist tipping over. (iii) Carton stacking strategies should facilitate vent hole alignment, for uniform airflow distribution and low air resistance. (iv) Finally, the pallet stack design should enable efficient container loading, with some tolerance for variations in pallet stack size.

A significant advantage of implementing an improved packaging system is the opportunity to optimise RFC space utilisation and to address challenges relating to high cooling heterogeneity, which is often observed in the cold chain. RFC systems predominantly make use of vertical airflow. However, due to the positioning of the refrigeration unit, some horizontal airflow parallel to the container length is also expected (Jiménez-Ariza et al., 2014; Rodríguez-Bermejo et al., 2007; Smale et al., 2006). These complex airflow patterns can lead to cold or hot spots throughout the container, which may result in chilling/freezing injury, undesirable ripening, accelerated senescence and conditions prone to decay. Significant contributors to this phenomenon are inadequate ventilation schemes and the presence of gaps between the pallets that short-circuit airflow around the pallets stacks (Defraeye et al., 2015b; Jedermann et al., 2013). The improved usage of RFC floor area to eliminate gaps between packed fresh produce and improve cooling efficiency is therefore a significant motivator for an improved packaging system.

The introduction of an improved packaging system could further enable the use of various advanced temperature treatments. Depending on the destination, marine transport takes between 3 to 5 weeks, which represents a significant period of the fresh produce life span spent in transit. Circumventing precooling processes, which are normally performed after packing, and instead cooling the produce to the set temperature using the RFC refrigeration system is referred to as ambient loading. This technique is highly desirable for many resilient fruit types (e.g. citrus), as it accelerates the start of transit and thus shortens the overall cold chain (Defraeye et al., 2016, 2015b, 2015c; Jedermann et al., 2013). Ambient loading makes use of the RFC's vertical airflow system to precool the produce and is also applicable when forced-air cooling (FAC) facilities are not available or are occupied due to high turnover at the packhouse.

Another treatment that requires rapid fruit cooling for successful quality preservation is intermittent warming, which is practiced for fruit sensitive to chilling injury. This temperature treatment is mainly applied to stone fruit produce, which are susceptible to chilling injury at the low temperatures needed to adequately preserve fruit quality over the long transit periods. For example, in the case of peaches, storage temperatures are increased from 5 °C to 20 °C for 24 hour periods (Xi et al., 2012). This short temperature increase can both relieve damage as a result of chilling injury and improve the fruit cell membrane resistance against further damage (Wang, 1990). However, rapidly heating and cooling fruit is often challenging under RFC conditions and its potential use through the introduction of an improved package system would significantly reduce postharvest losses in chilling injury sensitive fruit.

An important packaging functionality in any new design, is the pallet stack's porosity to horizontal airflow for efficient FAC. Forced-air cooling is commonly applied after packing to rapidly remove excess heat, so as to reduce fruit respiration rates and therefore better preserve quality (Thompson et al., 2008). The packaging system should therefore facilitate rapid and uniform fruit cooling, without creating conditions that induce fruit chilling injury (Alvarez and Flick, 1999b; Kader, 2002). The effect of the packaging on FAC energy consumption should also be considered in any design, which is a function of the overall cooling time, the pallet stack's resistance to airflow (RTA) and the respective working point of the fan (Anderson et al., 2004). A pallet stacks airflow resistance is significantly influenced by the carton design, which affects tortuosity of flow pathways and can result in misalignment of ventilation holes (Delele et al., 2008; Ngcobo et al., 2012a). Cartons should consequently be designed to facilitate vent alignment during stacking.

Although the above-mentioned practices are of critical importance to the fresh produce industry, very little has been done with respect to investigating new packaging systems to optimally achieve these goals. Furthermore, to the best knowledge of the authors, no prior work has been reported to optimise pallet stacking in transport containers. In the past, the main challenges facing such an investigation have been the large cost associated with experimentally evaluating new designs. Computational fluid dynamics (CFD) is thus a suitable tool to efficiently explore new designs and has been applied extensively to evaluate refrigerated transport (Defraeye et al., 2016, 2015b, 2015c; James et al., 2006; Moureh et al., 2009a, 2002; Moureh and Flick, 2004; Tapsoba et al., 2007) and FAC performance (Defraeye et al., 2014, 2013a, Dehghannya et al., 2012, 2011, 2010, Delele et al., 2013a, 2013b; Ferrua and Singh, 2011b; Han et al., 2015; O'Sullivan et al., 2016; Zou et al., 2006a, 2006b).

The aim of this study was to explore innovative packaging systems, which included new package and pallet design approaches, that better utilises RFC floor area and also improve cooling efficiency. As a case study, two new carton designs were proposed and compared to a currently implemented design. The cooling performance was evaluated for both horizontal (FAC) and vertical (RFC cooling) airflow to achieve a multi-parameter analysis.

2. Materials and methods

2.1 Packaging design strategies

2.1.1 The standard packaging system

The standard packaging system (STD), which uses a 500 × 333 × 270 mm (L × W × H) carton design is applied in the commercial export of apple fruit and is typically stacked on the P-120 (1 200 × 1 000 mm) pallet, 7 cartons per a layer. The subsequent footprint of the stacked cartons is 1 165 × 999 mm (on top of the P-120), resulting in a 35 mm unused gap along the pallet length. Various industries occasionally make use of a smaller 1 165 × 999 mm pallet (P-STD, area = 1.16 m^2), to avoid this wasted space. The P-STD pallet is therefore considered in this study, as it represents a more optimal version of the P-120, with respect to fruit packing.

Figure 6.1a-c shows three possible pallet-RFC loading strategies using P-STD. In this case, loading 20 pallets (Figure 6.1a and b) results in an 87.7% usage of the RFC floor, whereas the smaller P-STD pallet (not possible using the P-120 pallet) further enables a 21 pallet loading approach (Figure 6.1c) for a 92.1% floor area usage.

2.1.2 Tes carton design

The Tes pallet (P-TES; 1 157 × 1 135 mm) is a novel design proposed in this study, with similar dimensions to the P-120. The Tes pallet base uses 99% of the RFC shipping containers floor area, with 20 pallets (two rows) loaded per RFC as shown in Figure 6.1e. A 1% opening (floor area) is intentionally left unoccupied to facilitate the loading process and equates to a 2 cm gap between the pallet stacks and RFC walls. A consequence of the P-TES footprint is that the normal interlocking stacking patterns used on the P-STD/P-120 are not possible. The two available carton stacking options are therefore a linear three by three arrangement (grid) or the stacking pattern shown in Figure 6.2 (Tes). The latter option was selected in this study, using the Tes carton design (Figure 6.3c). The Tes design stacks nine cartons per layer and has an arrangement that forms a partial interlocking pattern, whereby each row is interlocked with the adjacent row. A tipping motion in one of the stacked rows would thus potentially be resisted by the adjacent row, providing some additional support compared to a simple linear arrangement.

A consequence of the Tes stacking pattern are two 2.2 × 2.2 cm unused openings were the corners of the cartons meet (Figure 6.2). It is envisaged that a square paperboard bar could be placed in these channels, to improve stacking stability. This support bar could be manufactured from the same material used in the cornering strips (Figure 6.4), which are already used in combination with pallet straps to improve pallet stack stability. When considering the lost area from the open channels in each P-TES (P-TES; area = 1.31 m^2), the Tes packaging system takes up 98.9% of the RFC container. Additionally, the vent hole design of the Tes carton is not symmetrical and has unique vent hole positions on each horizontal face, to enable vent alignment during stacking. Correctly orientating the cartons during stacking is therefore critical to achieve vent hole alignment. Nonetheless, one of the carton faces in the stack does not align (Figure 6.2, Tes), although, FAC can simply be performed through the aligned orientation. Furthermore, vent hole alignment will be present parallel to the RFC length, which is desirable, considering some horizontal airflow is expected in RFC containers.

2.1.3 Hex carton design

The hex packaging system is also proposed in this study as an entirely new approach to carton stacking and RFC container usage. Hexagons are valued for their efficient tessellating structures (stacking efficacy), as they use the least wall area per a volume enclosed, compared to other shapes. In this study, the Hex carton design is an isosceles trapezoid (quadrilateral), which when placed back to back against another Hex carton forms a hexagonal shape (Figure 6.2). The Hex carton design is packed 6 per a pallet (P-HEX; area = 1.17 m^2). A total of twenty two P-HEX pallets can be loaded into each RFC, resulting in a floor area usage of 97.4%, where 2 cm gap is again purposefully left open along the sides to aid in loading. The pallet loading strategy is shown in Figure 6.1d and illustrates that the unused floor area is concentrated at the door and refrigeration unit of the RFC, as a result of the uneven pallet wall at the front and back of the P-HEX pallets.

A considerable advantage of the Hex packaging system is the inherent vent hole alignment between the individual cartons and interlocking pallet stacks between the loaded pallets. Furthermore, the diagonal intersections between the stacked cartons is expected to provide supplementary stability, compared to a similar rectangular carton design.

2.2 **Numerical model**

2.2.1 Carton design and fruit packing geometry

For cooling simulations, each carton design was given the same total ventilated area percentage (TVA = 4%) on each face as depicted in Figure 6.3(a-c). Commercially, the STD carton design uses centrally positioned oblong vent holes. However, in a previous study the Multivent vent hole design was shown to improve both cooling energy efficiency (43%) and cooling uniformity (71%) compared to central oblong ventilation for FAC of fruit packed on trays (Berry et al., 2016). The Multivent vent

hole design was therefore used in each carton design, so that comparisons are more a factor of the packaging system than a specific vent hole design. The top and bottom vent holes in this study followed the approach used in most commercial pome fruit cartons (SA), which is a single, centrally positioned vent hole. These vent holes are accomplished using the carton flaps that do not extend far enough to meet at the middle (Berry et al., 2015). Ventilation openings along the carton top and bottom sides are therefore more a consequence of the carton folding pattern and are rarely from punched holes.

The cartons were packed with 'Granny Smith' apples on expanded polystyrene trays, as shown in Figure 6.3(d-f) and the respective physical properties of each packed carton is shown in Table 6.1. An effort was made to maintain a similar fruit radius (Mean = 37.6 mm; SD = 1.4 mm) and fruit packing ratio (packing ratio = (fruit volume)/(inner box volume); Mean = 54.1%; SD = 0.35%) for each carton (Table 6.1). However, it should be noted, that fruit packing can still be improved or reduced in each carton design by modifying the fruit radius in combination with carton height. For each design, fruit were packed on four trays using a staggered packing configuration for the STD and Tes designs and a hexagonal close packing (HCP) configuration for the Hex design. No contact was present between the individual fruit in STD and Tes designs. However, the HCP packing (Hex design) resulted in a 0.5 mm fruit overlap in fruit rows parallel to the carton length, but not in other directions. A 4 mm gap was set in all designs between the trays edges and the carton walls, which was determined from measurements of commercially packed cartons in SA. Several small simplifications were included into the geometry to improve grid quality: (i) Individual apple fruits were modelled discretely as spheres. (ii) Fruit were trimmed by 1 mm at locations where the trays are resting on the top of fruit. (iii) A 2 mm gap was set between the carton walls and fruit surfaces, as well as between the bottom tray and bottom carton wall. As these simplifications are rather small, they will have a limited impact on the convective heat transfer calculations.

2.2.2 Operating conditions

Computational fluid dynamics was used to model the airflow and cooling profiles for both FAC and RFC cooling operations of a commercial setting. The two settings have different direction of flow of the cooling air with respect to the stack of produce to be cooled. In the FAC operation, the cooling airflow is horizontal, while RFC airflow is essentially vertical.

Solving the heat transfer problem requires a very fine mesh to accurately capture the interfacial heat fluxes. Modelling this problem on the full stack was computationally difficult and time consuming. Hence, to reduce the computational cost, the models were based on a single horizontal layer of cartons for the FAC and a single vertical column of cartons for the RFC (Figure 6.5 and Figure 6.6). The inlet boundary condition was set as a uniform velocity inlet, with low turbulence intensity (1%). Three airflow speeds were evaluated for the FAC and RFC

simulations, namely 0.2, 0.4 and 0.6 m s^{-1}, for the FAC and 0.02, 0.04 and 0.06 m s^{-1} for the RFC cases, which are within the expected ranges as used in the South African export industry (Brosnan and Sun, 2001; Defraeye et al., 2015b). The inflow air temperature was set to -0.5 °C, as used in the South African pome fruit industry. Ambient atmospheric pressure was set at all outlet boundary conditions. Initial fruit temperature were 20 °C and 5 °C for the FAC and RFC operations, respectively. Thermal and physical material properties are listed in Table 6.2.

For the FAC setup (Figure 6.5), the length of the upstream and downstream sections of the domain was taken sufficiently long to limit the influence of the inlet and outlet boundaries. The RFC ducts (Figure 6.6) have a total length equal to a RFCs internal height (2.56 m), with a 15 cm air domain below the bottom carton, to represent the pallet base. The inlet was set at the bottom of the domain to represent the T-bar floor, which delivers air vertically up into the pallet stacks. The air domain above the top carton represents the air gap between the top of the stack and the RFC ceiling that is left open as a path for air to return back to the refrigeration unit. The outlet region of the computational domain was therefore set along the sides of the top air domain and the top boundary was set as a no-slip adiabatic wall. Boundary conditions along the remaining sides of the RFC and along the top, bottom and sides of the FAC computational domains (air and carton) were modelled as symmetry (slip walls), which assumed the normal velocity component and normal gradients at the boundary were zero. The carton and tray boundary conditions inside the domain were specified as no-slip walls with zero roughness.

A respiration heat source term ($Q_{resp;}$ W m^{-3}) was included in the apple fruit domains. Respiration heat was calculated from Eq. (6.1) as taken from USDA (1986) and Becker et al. (1996) for apples:

$$Q_{resp} = \rho_f \left(2.778\times10^{-3}\left(f\left(1.8T_f + 32\right)^g\right)\right) \tag{6.1}$$

where the f and g coefficients are determined from USDA (1986) to be 5.5671×10^{-4} and 2.5977, respectively, ρ_f is the apple fruit density (Table 6.2) and T_f is the fruit temperature in °C.

A tetrahedral grid was built within the computational domain of each case. The number of computational cells per simulation is listed in Table 6.3. The grid refinement was determined from a grid sensitivity analysis using the Richardson extrapolation method (Celik et al., 2008; Roache, 1994). The results showed a spatial discretisation error of 2.6% for seven-eighths cooling time, 0.3% for pressure drop across the domain (FAC) and 0.7% for average speed inside the carton.

2.3 Numerical simulations

2.3.1 Simulation setup

CFD simulations were based on the Reynolds-averaged Navier-Stokes equations (RANS). The shear stress transport (SST) k–ω model was used for turbulence modelling (Menter, 1994). This RANS turbulence model has been discussed and validated extensively in previous studies for flow and cooling of spherical fruits (Ambaw et al., 2013a; Norton et al., 2013; Norton and Sun, 2006; Smale et al., 2006; Verboven et al., 2006; Xia and Sun, 2002; Zhao et al., 2016).

Concerning boundary-layer modelling, wall functions were applied instead of low-Reynolds number modelling. Although low Reynolds number modelling are inherently more accurate for momentum and heat transfer predictions, the complexity of the current geometry would have required very high resolution meshes near the fruit surfaces, which are difficult to generate for complex geometries as is the case in the present study. Simulations under such conditions would thus entail a very large computational cost. Wall functions are therefore often the only practical alternative and have been proven to provide satisfactory results (Defraeye et al., 2013b, 2012b).

The use of this RANS turbulence model in combinations with wall functions was applied in a related study on citrus fruit cooling by Defraeye et al. (2013a), with satisfactory agreement with experimental data, which indicates sufficient accuracy of the CFD simulations. Several other studies performed by the authors have also found good agreement to experiments using this turbulence model with wall functions (Ambaw et al., 2013b; Delele et al., 2013b, 2008).

Simulations were performed using ANSYS-CFX 16 CFD software code (ANSYS, 2015). The effect of buoyancy was considered negligible in the simulations. The influence of flow driven by air temperature-density differences was therefore not included, since forced-convective flow is considered a much more significant factor (Norton et al., 2007) and heat is therefore treated as a passive scalar. Radiation was further neglected in the simulations, as the temperature differences between the various surfaces are fairly small, particularly compared to convective heat transfer rates. Finally, the latent heat of evaporation and mass (moisture) loss were not considered in the model, as apple fruit moisture loss values are generally quite low (< 1%) during commercial FAC and refrigerated transport (high relative humidity) conditions (Maguire et al., 2001). Before performing transient cooling simulations, the flow field and temperature conditions were determined using steady-state simulations, to obtain the initial conditions. Initial fruit and inlet air temperatures were fixed. The flow field was then disabled during transient simulations, which reduced the computational cost as only the energy equation was solved.

The simulation used second order backward Euler, high-resolution spatial differencing (i.e. a blend between central differencing and upwind differencing locally) and second order schemes for solving the transient cooling process, advection and turbulent terms, respectively. Iterative convergence was determined by monitoring the velocity, turbulent kinetic energy, shear stress and temperature in the flow field and along specific boundaries (surface-averaged values). The simulation time for the transient FAC and RFC simulations was about 12 hours and 55 hours respectively, with time steps of 60 seconds, as determined from a temporal sensitivity analysis. Simulations took about 5 days on an Intel® core™ i7-4770 CPU (3.4 GHz) with 32 GB of RAM.

2.4 **Evaluation of package functionalities of cooling**

2.4.1 Cooling rate and uniformity of fruit temperature

Fruit cooling rates were determined from the simulated time-temperature histories. Then from this data seven-eighths cooling time (SECT) was calculated, which is the time needed to cool produce to seven-eighths of the difference between initial produce temperature and the cooling air temperature (Defraeye et al., 2015a). The SECT is representative of precooling times used in commercial fruit export, where fruit are often considered sufficiently cooled after reaching about seven-eighths of the desired temperature change.

In addition to the SECT of each fruit layer, the convective heat transfer coefficient (CHTC; h) was also calculated at fruit surfaces to assess cooling heterogeneity within the stack. The CHTC expresses the convective heat flux ($q_{c,w}$; J s^{-1} m^{-2}) at the air-material interface, to the difference between the fruit surface temperature (T_w) and a reference temperature (T_{ref}). In this study, T_w was taken to be the produce temperature at the start of the simulation and T_{ref} was taken as the incoming cooling air temperature (-0.5 °C): $h = q_{c,w}/(T_w - T_{ref})$. CHTC is a defined quantity and is proportional to the heat flux at the wall ($q_{c,w}$). The CHTC depends strongly on the selected reference temperature T_{ref}. Other values can also be chosen, such as the temperature at the vent hole inlets. However, the selection of the reference temperature is less critical, as this study is interested in identifying differences in heat transfer rates.

The CHTC was also used to evaluate cooling heterogeneity, by calculating the relative standard deviation (%; RSD) of CHTC across the fruit surfaces, which is the ratio of the standard deviation to the mean. The data set used to calculate the RSD made use of about 15 CHTC monitoring points per fruit and were evenly distributed across the stack. A low RSD thus indicates homogenous cooling and a high percentage indicates heterogeneous cooling.

2.4.2 Package-related power consumption and cooling throughput

The resistance to airflow (RTA) of the packed cartons was determined by relating the pressure drop over the carton to the airflow rate at the inlet. The relationship followed a quadratic curve, which is consistent with other observations in previous studies (Defraeye et al., 2014; Ngcobo et al., 2012a; van der Sman, 2002; Verboven et al., 2006) and can be characterised using Eq. (6.2) (Defraeye et al., 2015a). The packaging, packed produce and internal packaging (e.g. trays) are some of the main components that contribute to a systems resistance to airflow.

$$\Delta P = \xi G^2 \tag{6.2}$$

where ΔP is the pressure drop (Pa), ξ is the pressure loss coefficient (PLC; kg m^{-7}) and G is the airflow rate (m^3 s^{-1}).

The fan related power needed to maintain airflow during cooling is a function of both the airflow rate and air resistance to the system (de Castro et al., 2005a; Defraeye et al., 2015a, 2014). The fan and motor efficiency were ignored in this study as they vary depending on the facility.

The package-related power (w; Watts) required to maintain a flow rate through the package was calculated in Eq. (6.3). In addition, the package system also affects fruit cooling rates, which influences overall throughput in the cold chain, namely the amount of fruit that can be cooled over a certain amount of time. The cooling throughput thus indicates the fan related power needed in a system to cool equivalent quantities of fruit with respect to time. Alternatively, the total power consumption (E) can be calculated as the product between the cooling duration ($t_{⅞}$ in seconds; SECT) and power usage (Eq. (6.4)).

$$w = \Delta P G = \xi G^3 \tag{6.3}$$

$$E = \Delta P G t_{⅞} = \xi G^3 t_{⅞} \tag{6.4}$$

3. Results and discussion

3.1 Cooling characteristics

3.1.1 Fruit cooling rate

The cooling rate with respect to the SECT (volume-averaged) is depicted in Figure 6.7a and b. Cooling values were compared against the mass averaged flow rate (L s^{-1} kg^{-1}) to account for differences in total fruit mass (Table 6.1) and thus heat load between the various cases. The contribution of fruit respiration to the total heat load cooled during the FAC and RFC cases ranged between 0.4%-0.8% and 4.6-11.3%, respectively. Respiration was therefore not significant to cooling under the FAC conditions examined, which can be attributed to the short cooling periods. Conversely, the much longer RFC durations resulted in substantially larger heat loads. Respiration rates are expected to increase further if fruit are stressed (e.g. physical damage and ethylene exposure). Cooling took between 2.2 and 4.6 hours under FAC and between 16.6 and 51.4 hours in RFC cooling. The Hex carton design cooled the slowest, with about a 10% larger SECT compared to the STD design during both FAC and RFC cooling. The Tes packaging system facilitated a slightly reduced cooling rate (< 5% during RFC cooling), but improved the cooling rates (9%) under FAC. Differences in SECT can be explained by the respective carton design's effect on airflow properties (Table 6.4) and distributions between the packed fruit and the resultant heat transfer rates, which can be identified as well by considering the CHTC.

Figure 6.8a shows the surface-average CHTC on fruit during FAC as a function of airflow rate (L s^{-1} kg^{-1}) and Figure 6.8b shows the average CHTC across fruit surfaces in each individual carton during RFC cooling. The CHTC is a defined parameter in this study and provides some valuable insight with respect to the causes for differences in cooling rates. As expected, the average CHTC values followed a similar pattern to the SECT (Figure 6.7a). For FAC, the Hex and Tes carton designs were characterised by a 10% lower and 6% larger CHTC values than the STD design, respectively. Compared to the FAC, the RFC had much lower CHTC values. Although both the FAC and RFC simulations had similar fruit loads, a significant advantage of the FAC approach is that cartons are stacked side-by-side, which reduces stack depth and improves airflow distribution compared to the RFC cooling cases. Figure 6.8b shows a rapidly diminishing CHTC in cartons between the inlet and outlet. This is attributed to a combination of the lined arrangement of cartons and low airflow rates. Airflow was also considerably restricted vertically by the presence of trays in the cartons, which limited air to pass through a 4 mm gap between the edges of the trays and the carton walls. Although detrimental to airflow, trays are a critical component of pome fruit packaging, as they substantially reduce bruising damage from vibration and impact forces (Fadiji et al., 2016c). The air retention period per individual carton is quite large, allowing more time for the air to heat up before reaching the next consecutive carton. A much

smaller temperature difference is, therefore, present between the fruit and air higher up in the stack, resulting in low heat flux values.

Similar challenges were reported by Defraeye et al. (2015b), who examined ambient cooling of citrus fruit using vertical airflow through pallet stacks (RFC conditions). Defraeye et al. (2015b) showed that the inclusion of air gaps next to the column of carton significantly improved cooling uniformity, since the cooling air partially bypassed the lower cartons and directly reached cartons higher up in the stack. However, the study suggests that the presence of gaps in the RFC can increase total SECT periods, encouraging the closure of gaps when at all possible.

3.1.2 Cooling heterogeneity

The relative standard deviation representing cooling heterogeneity for each examined case is shown in Table 6.5 and the CHTC distributions across the fruit surfaces are shown in Figure 6.9 and Figure 6.10. The vertical CHTC distribution in the RFC was highly non-uniform (average RSD of 282%), which is about 3.5 times larger than in the FAC cases (RSD = 81%). The Hex design produced the most uniform cooling distribution during RFC cooling (Figure 6.9). The average RSD of the design was 7% and 5% lower than the STD and Tes designs, respectively. Compared to the overall average, these differences can be considered relatively small. However, the lower RSD value is credited to the Hex stack having one less vertically stacked carton layer than the STD and Tes stacks, due to the slightly taller individual cartons. From an air distribution perspective, all the RFC stacks had somewhat similar air distributions, with air mainly flowing along the carton wall sides and between the top and bottom vent holes (Figure 6.9b).

With respect to FAC (Figure 6.10), the newly proposed Hex and Tes carton designs cooled somewhat less evenly than the STD design, with a 14% and 10% larger RSD value, respectively. The more uniform cooling pattern of the STD carton design can be ascribed to an additional column of vent holes (Figure 6.2; four vertical holes) on each stack face (Figure 6.2). Airflow was thus more uniformly distributed throughout the carton. An important consideration here, is that although the STD carton design (geometry) is used commercially, the vent hole design is not. A much poorer performance would therefore be expected from a commercially used STD packaging system (Berry et al., 2016).

With respect to the Hex and Tes designs during FAC, the Hex design has the least number of cartons per a row and consequently less walls separating the air stream. This caused a generally lower air speed than the other carton stacks with more carton walls separating flow, since air must accelerate at each of the respective vent holes, forming air jets into each packed carton. Findings from Berry et al. (2016), reported differences in RSD as large as 9 times, between different vent hole configuration. The respective differences in this study are thus much smaller. This is primarily due to the use of the recommended vent hole design (Multivent; size and configuration) from Berry et al. (2016) in each carton design, as well as the

same internal packaging configurations (tray number, fruit size and porosity). The observed differences are therefore a consequence of the cartons geometry and stacking patterns only, which have a more subtle effect than ventilation design.

3.2 **Package-related energy consumption**

3.2.1 Resistance to airflow

Figure 6.11 depicts the pressure drop across the stacked cartons for each air flow rate (m^3 s^{-1}) examined during FAC and RFC conditions, as well as the corresponding pressure loss coefficient (ξ) which were determined by correlating ($R^2 > 0.99$) each curve to Eq. (6.2). The resistance to airflow is an important parameter that indicates the power (ΔPG; watts) required to maintain a specific airflow rate through stacked cartons. FAC pressure drops ranged between 69 to 1163 Pa for air speeds between 0.2 to 0.6 m s^{-1}. The much slower 0.02 to 0.06 m s^{-1} air speeds used during RFC cooling resulted in pressure drops ranging between 13 Pa to 112 Pa.

Carton walls significantly restrict air movement and are an important contributor to airflow resistance during convective cooling processes (Ngcobo et al., 2012a). The number of cartons stacked between the inlet and outlet of an airflow system thus considerably influences the power needed to achieve a desired flow rate. A row of STD cartons have three cartons (four carton walls) on the one side and two cartons (three carton walls) on the other (Figure 6.2), producing a ξ value of 23 936 (Figure 6.11a). The Tes packaging system on the other hand stacks nine cartons per pallet stack row, three cartons (four carton walls) thus separate the inlet and outlet, producing a 61% larger ξ value than the STD carton stack. Conversely, the Hex stacking pattern separates the airflow system with just two cartons (three carton walls), reducing airflow resistance across the stack by 33% (ξ value) compared to the STD design.

A much higher airflow resistance was observed during vertical cooling, with an average airflow resistance (ξ value) 42 times larger than FAC. Similar to the CHTC, this difference can be attributed to the number of successive cartons stacked in the airflow direction. Specifically, the RFC cases have 7 to 8 cartons stacked consecutively, versus the two or three cartons during horizontal flow (FAC). Additionally, air porosity is much higher in the horizontal direction, since trays are parallel to the airflow, but perpendicular to vertical airflow. FAC cases further make use of a Multivent ventilation design along the carton sides, which more evenly distributes airflow throughout the system. In contrast, the single vent hole at the top and bottom of the cartons (for vertical flow), as is commonly used in commercial practice (Figure 6.3a-c), concentrates airflow to a single point of the packed fruit. In the case of the Tes design, which had the largest airflow resistance (Figure 6.11b), the nearly square vent hole directed most of the airflow between three fruit (Figure 6.9b). The STD top/bottom vent hole, on the other hand, has a more elongated vent hole, which more evenly distributed air out of and into the cartons. Lastly, the Hex

design produced the lowest airflow resistance during vertical cooling. Partly, due to a similar elongated vent to the STD design, but also from the stack using one less carton (7 cartons).

These findings highlight the importance of minimising packaging use in the fresh produce cold chain (Ferrua and Singh, 2009a; Ngcobo et al., 2012a; Thompson et al., 2010). However, a major priority in carton design is mechanical strength. Carton stacking systems need to be resilient enough to support a fully loaded pallet stack for extended periods. A reduction in packaging material, would therefore make it necessary to improve the existing individual carton strength, using stronger materials. In the case of cartons, this would involve thicker and higher quality fibreboard as well as improved fluting structures, which could substantially increase manufacturing costs.

3.2.2 Power usage

Figure 6.12 shows the relationship between the power required by fans to maintain a certain airflow rate versus fresh produce cooling throughputs. The graphs emphasises the carton designs influence on power usage to cool equivalent quantities of fruit within the same time period. As expected, significantly larger quantities of energy are needed to decrease cooling durations. In the case of FAC, an average energy consumption of 658 kJ was required, versus just 36 kJ during RFC cooling. This is consistent with current cold chain strategies, whereby relatively large quantities of power are available to rapidly cool produce in the packhouse, while the limited power in the RFC is used to maintain fresh produce temperatures and to cool away small temperature differences (e.g. cold chain breaks). It should be noted, however, the actual working point of a system and thus the resulting power consumption, is facility/equipment dependant. A packaging system with a theoretically high airflow resistance (ξ value), may therefore in reality operate at a more efficient working point compared to other packaging systems.

The curves in Figure 6.12 followed a power law relationship ($f(x) = ax^{-b}$), where the b coefficient was consistently equal to -6.2 (Figure 6.12a; $R^2 > 0.99$) and -3.2 (Figure 6.12b; $R^2 > 0.99$) for FAC and RFC cases, respectively. The a coefficient is thus a convenient parameter to compare differences in power consumption (within the FAC and RFC cases), irrespective of the desired cooling period. With respect to FAC, the Hex carton design had very similar (2%) cooling efficiency properties to the STD design, whereas the Tes design decreased power consumption by 29%. Conversely, under RFC conditions, the Hex and Tes carton designs increased power consumption by 21% and 90% compared to the STD design, respectively. However, the RFC power consumption values where substantially influenced by vent hole configuration, and could all be significantly enhanced with an improved design that more evenly distributes airflow around the carton sides. The study therefore suggests that RFC cooling performance is more a factor of the number of cartons consecutively stacked on a pallet (individual carton height) and air distribution into the respective carton (internal packaging and vent hole configuration), than by the

carton/pallet design and stacking pattern used for each layer. In contrast, the FAC cases were already using enhanced vent hole designs and power consumption values are therefore mainly a factor of the carton design (Figure 6.3) and stacking configuration used.

3.3 Mechanical aspects

An important factor influencing package design is ergonomics with respect to being safe to handle by manual labour (human workers). The final weight and size of a carton is therefore critical for cold chain efficiency. Although no regulatory standardisations exist in this regard, most guidelines recommend carrying weights smaller than 23 kg (Cal/OSHA, 2007). However, depending on the lifting frequency and height, Waters et al. (1994) recommend package weights of between 8 kg and 15 kg. The mass of a fully packed Hex carton (21 kg; Table 6.1) is therefore at the limit of acceptable carrying weight. In contrast, the fully packed Tes carton (14 kg; Table 6.1) is within advised weight tolerances (Waters et al., 1994). A key factor to further consider in this discussion, is the current movement towards mechanisation. In which case manual labour may not be necessary in terms of lifting cartons in the near future, thus allowing far more flexibility in carton size and weight.

Additionally, pallet stack stability and mechanical strength are important performance parameters that can be included in future evaluations. For instance, after palletisation, pallet stacks are often exposed to dynamic forces and impulses as a result of tilting during transit (truck, ship and rail) and sudden impacts when being conveyed by forklifts. To improve stability, the STD packaging system is often stacked using an alternating pattern (cross stacking), whereby each successive row is orientated 180° to the previous row, however, this can reduce stack compression strength by 40% (Koning and Moody, 1989). This significantly reduces vent hole alignment and is also expected to reduce cooling efficiency. However, in the case of the Hex and Tes cartons, the stacking pattern remains the same irrespective of cross stacking, removing the possible use of this technique.

Other methods to improve stability include pallet straps and pallet sheets. Pallet sheets are ventilated fibreboard covers that are placed in between the various layers and overlap along the sides to resist the individual carton columns from separating. Finally, cornering strips are also often added to the pallet stack edges to resist the various stacked rows from separating.

3.4 Packing density and multi-parameter analysis

Table 6.6 shows the fruit packing/loading properties inside a RFC for the packaging systems discussed above (studied). The height of the respective package designs were set so as to maintain a similar fruit load between the various simulations. However, as a consequence, each pallet stack design has a different height, which makes comparisons with respect to fruit packing density in a RFC challenging. For the sake of an impartial comparison, Table 6.6 (listed as “same height”) also

presents the same loading properties for the STD, Hex and Tes packaging systems when using an identical carton height (270 mm) and fruit packing porosity (52.3% of the cartons inner volume). In this case, fruit packing density is a combination of both the floor area used and quantity of packaging material used. The results show a similar packing density between the Hex and Tes systems and a 10.6% or 6.2% larger packing density than the STD packaging system using 20 and 21 pallets. respectively. The Hex and Tes designs therefore offer a substantial and relatively equivalent benefit with respect to potential packing density. It should also be noted, that the Tes design uses about 7% more packaging material than the Hex design (Table 6). This will influence the selection of corrugated fibreboard material used for each design. For instance, a stronger and more costly board for the Hex, whereas the Tes packaging system can make use of a slightly weaker and less expensive board, but in larger quantities.

From a multi-parameter performance perspective, the Tes packaging system generally out performed both the STD and Hex packaging systems. Specifically, the Tes design shows a substantially improved RFC fruit packing density compared to the STD design. For cooling properties, the Tes design had a comparable cooling uniformity under both FAC and RFC conditions to the other packaging systems. However, the Tes design considerably improved FAC cooling throughput efficiency, by reducing the fan-related power needed to cool equivalent quantities of fruit over set durations. Primarily, this was due to the significantly larger cooling rates in the Tes design, compared to the slightly larger airflow resistance. Logistically, the P-TES pallet has similar characteristics to the P-120 pallet, making its reception by industry easier than if the P-Hex was used. Lastly, the Tes carton is more ergonomic and would likely be easier to manufacture using current facilities than the Hex carton. Within the scope of this study, the Tes packaging system is therefore preferable. However, before adoption in industry, future studies will need to first evaluate the design with respect to pallet stack stability and mechanical strength.

4. Conclusions

This study examined the potential use of two innovative new packaging systems with improved vent hole design to increase the usage of refrigerated freight container (RFC) floor area. Computational fluid dynamics (CFD) modelling were used to compare the new designs to a standard packaging system (STD) used in South African pome fruit export. A multi-parameter evaluation approach was applied by examining the three carton types under both forced-air cooling (FAC; horizontal airflow) and RFC (vertical airflow) conditions. The performance parameters considered in this study were fruit cooling rate, cooling heterogeneity, resistance to airflow inside the container, power consumption and RFC packing density (floor usage).

Commercially used pallet designs (1.2 × 1.0 m; P-120) utilise about 89.9% of the RFC floor area. In contrast, the proposed Hex and Tes packaging systems reported in this study significantly improved usage to 97.4% and 98.9% of the RFC floor area, respectively. Specifically, the Hex design is an isosceles trapezoid shaped carton that forms a hexagon shape when placed back to back with another Hex carton. The resulting stacking pattern thus potentially provides additional stability during pallet stacking. The Tes carton has a standard rectangular carton shape and is stacked using an atypical pattern to accommodate the respective TES pallet, which fully utilises the whole RFC floor area.

With respect to FAC, the Hex design facilitated very similar cooling energy efficiency to the STD design (2% improvement). This was attributed to a combination of low airflow resistance and reduced cooling rate. The Tes design on the other hand, considerably improved cooling energy efficiency (29%) compared to the STD design, due to an improvement in cooling rate against a slight increase in airflow resistance.

Mixed performances with respect to cooling throughput energy efficiency were observed for the three packaging systems during RFC cooling, with similarly high cooling heterogeneity in each case. Overall, the STD design facilitates more energy efficient cooling. However, analysis of the various RFC cases indicate the use of an improved vent hole configuration at the top and bottom of the cartons could significantly improve cooling performance in all cases. Results further indicated RFC cooling performance is less a function of pallet and carton design, but more a factor of the carton vent hole design and the number of cartons stacked vertically in a line (carton height).

Although the Hex packaging system performed better compared to the STD design, it was the Tes packaging system that generally outperformed both the Hex and STD designs, with respect to cooling efficiency (FAC) and packing density. In conclusion, this study has demonstrated the significant benefits of implementing a new fresh produce packaging system, using a multi-parameter approach, which combines experimental validation with the computational power of modern predictive modelling. The next step here, is to extensively evaluate the design with respect to mechanical strength and pallet stack stability, under typical storage and long term cold chain shipping conditions.

Table 6.1: Physical and geometrical properties of the STD, Hex and Tes carton designs packed with apple fruit on trays.

Packaging properties	STD	Hex	Tes
Total box volume	44.91 L	56.78 L	37.23 L
Inner box volume	38.93 L	49.67 L	32.03 L
Box height	270.0 mm	290.0 mm	255.3 mm
Box width	333.0 mm	378.0 mm	393.0 mm
Box length	499.5 mm	518.0 mm[†]	371.0 mm
Carton wall thickness[a]	8.0 mm	8.0 mm	8.0 mm
Fruit radius	37.8 mm	38.9 mm	36.2 mm
Fruit count	90	104	84
Total fruit mass	16.9 kg	21.2 kg	13.8 kg
Fruit packing density (total box)	45.3%	45.2%	44.8%
Fruit packing density (inside box)	52.3%	51.6%	52.1%
Tray number	4	4	4
Tray thickness	2 mm	2 mm	2 mm

[a] Carton walls are a combination of both the inner and outer cartons (telescopic carton design) each 4 mm thick. [b] Value is an average of top and bottom widths (345.0 mm and 691.0 mm).

Table 6.2: Thermal and physical material properties used for numerical models.

Material	Density (ρ; kg m^{-3})	Specific heat capacity (J kg^{-1} K^{-1})	Thermal conductivity (W m^{-1} K^{-1})	Reference
Air	1.184	1 003.8	0.02428	(ASHRAE, 2009)
Granny smith apple	829	3 580	0.398	(Ramaswamy and Tung, 1981)
Corrugated fibreboard carton	145	1 338	0.064	(Ho et al., 2010)
Trays (expanded polystyrene foam)	23	1 280	0.036	(Margeirsson et al., 2011)

Table 6.3: Number of mesh elements used for the CFD cases.

Carton design	Cooling conditions	Number of elements
STD	FAC	7.8×10^6
	RFC	7.4×10^6
Hex	FAC	8.6×10^6
	RFC	10.1×10^6
Tes	FAC	8.6×10^6
	RFC	8.1×10^6

Table 6.4: Flow rate, superficial air velocity at inlet, average air speed in carton for the STD, Hex and Tes carton designs during FAC and RFC conditions.

		STD		Hex		Tes	
	Air velocity (m s-1)	Average air speed (m s-1)	Air flow (L s-1 kg-1)	Average air speed (m s-1)	Air flow (L s-1 kg-1)	Average air speed (m s-1)	Air flow (L s-1 kg-1)
FAC	0.20	0.81	0.53	0.77	0.52	0.81	0.47
	0.40	1.62	1.07	1.56	1.03	1.63	0.93
	0.60	2.44	1.60	2.34	1.55	2.45	1.40
RFC	0.02	0.17	0.03	0.18	0.03	0.17	0.03
	0.04	0.35	0.05	0.38	0.05	0.36	0.05
	0.06	0.54	0.08	0.58	0.08	0.55	0.08

Table 6.5: Percentage relative standard deviation (heterogeneity) of CHTC across the fruit surfaces with respect to air velocity.

Air velocity (m s^{-1}; FAC / RFC)	STD		Hex		Tes	
	FAC	RFC	FAC	RFC	FAC	RFC
0.2/0.02	83	377	96	343	94	365
0.4/0.04	72	273	81	254	79	267
0.6/0.06	69	225	78	214	75	224

Table 6.6: Loading properties, fruit packing density and packaging material used in a RFC.

Loading properties	STD (20)	STD (21)	Hex	Tes
Pallets per RFC	20	21	22	20
Floor area usage ratio	87.8%	92.1%	97.4%	98.9%
Studied[a] packaging volume in RFC (and ratio of RFC)	6.7 m^3 (10%)	7.0 m^3 (10%)	6.3 m^3 (9%)	7.7 m^3 (11%)
Studied fruit density in RFC	278 kg m^{-3}	292 kg m^{-3}	289 kg m^{-3}	293 kg m^{-3}
Same height[b] - packaging volume in RFC (and ratio of RFC)	6.7 m^3 (10%)	7.0 m^3 (10%)	7.2 m^3 (11%)	7.7 m^3 (11%)
Same height - packing density in RFC	278 kg m^{-3}	292 kg m^{-3}	310 kg m^{-3}	312 kg m^{-3}

[a] Studied: Properties for the packaging system used in this study.
[b] Same height: Properties for the packaging system (STD, Hex and Tes), but with the same individual carton height (270 mm) and packing density (52.3%).

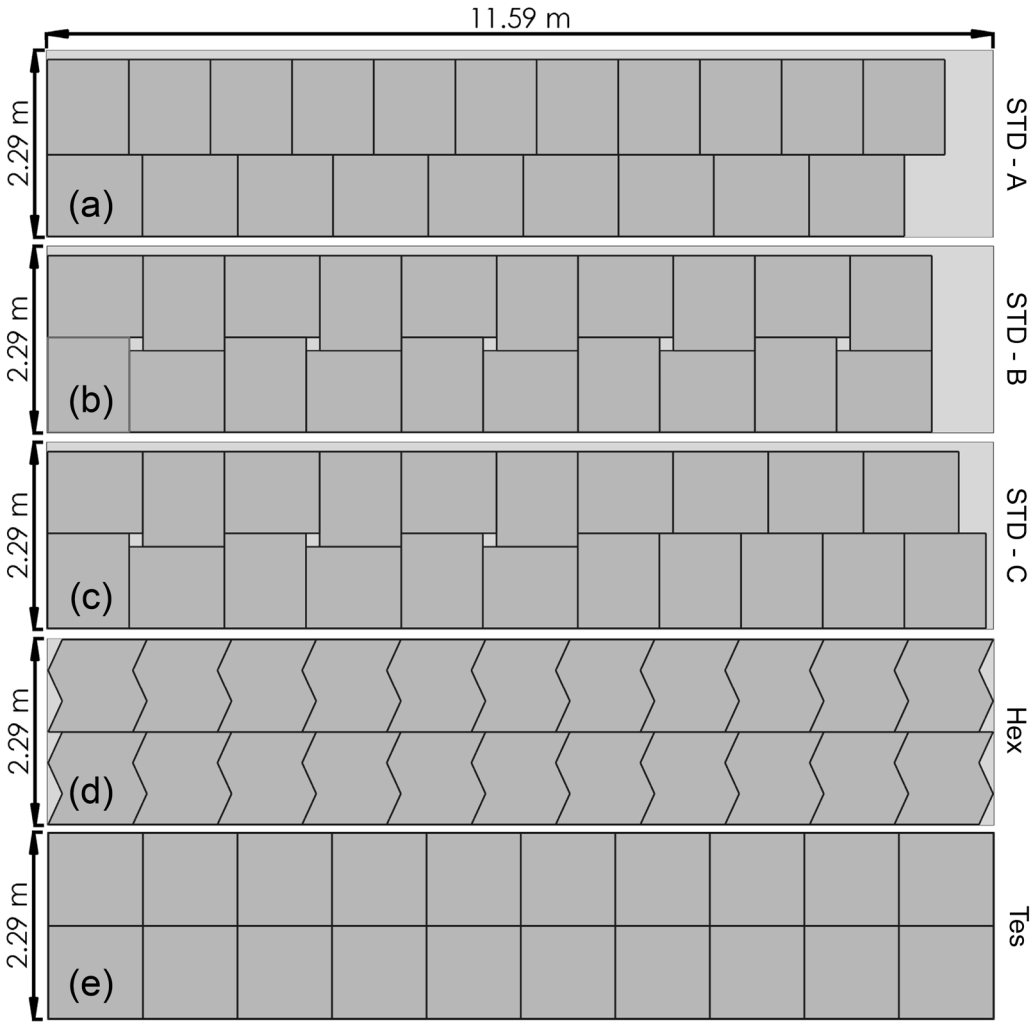

Figure 6.1: Top view of a RFC container showing pallet stack loading strategies.

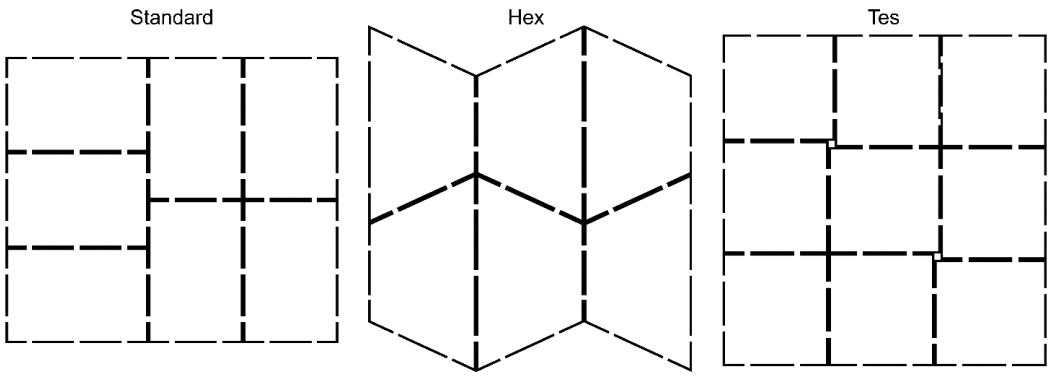

Figure 6.2: Horizontal carton vent hole alignment during stacking.

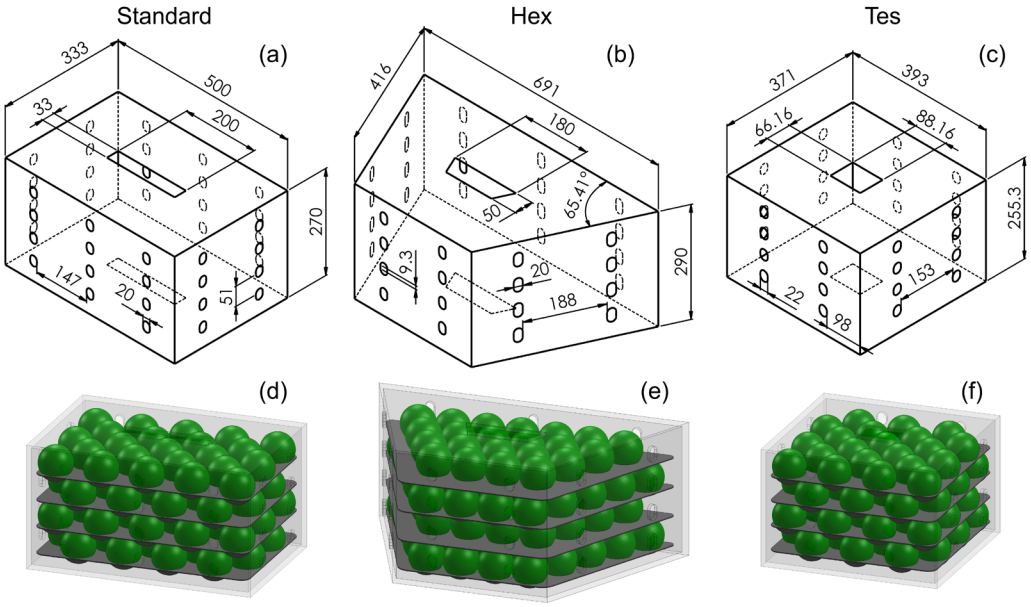

Figure 6.3: The STD, Hex, and Tes designs showing (a-c) the geometry and diagram of each, as well as (d-e) the fruit and tray packing configurations used.

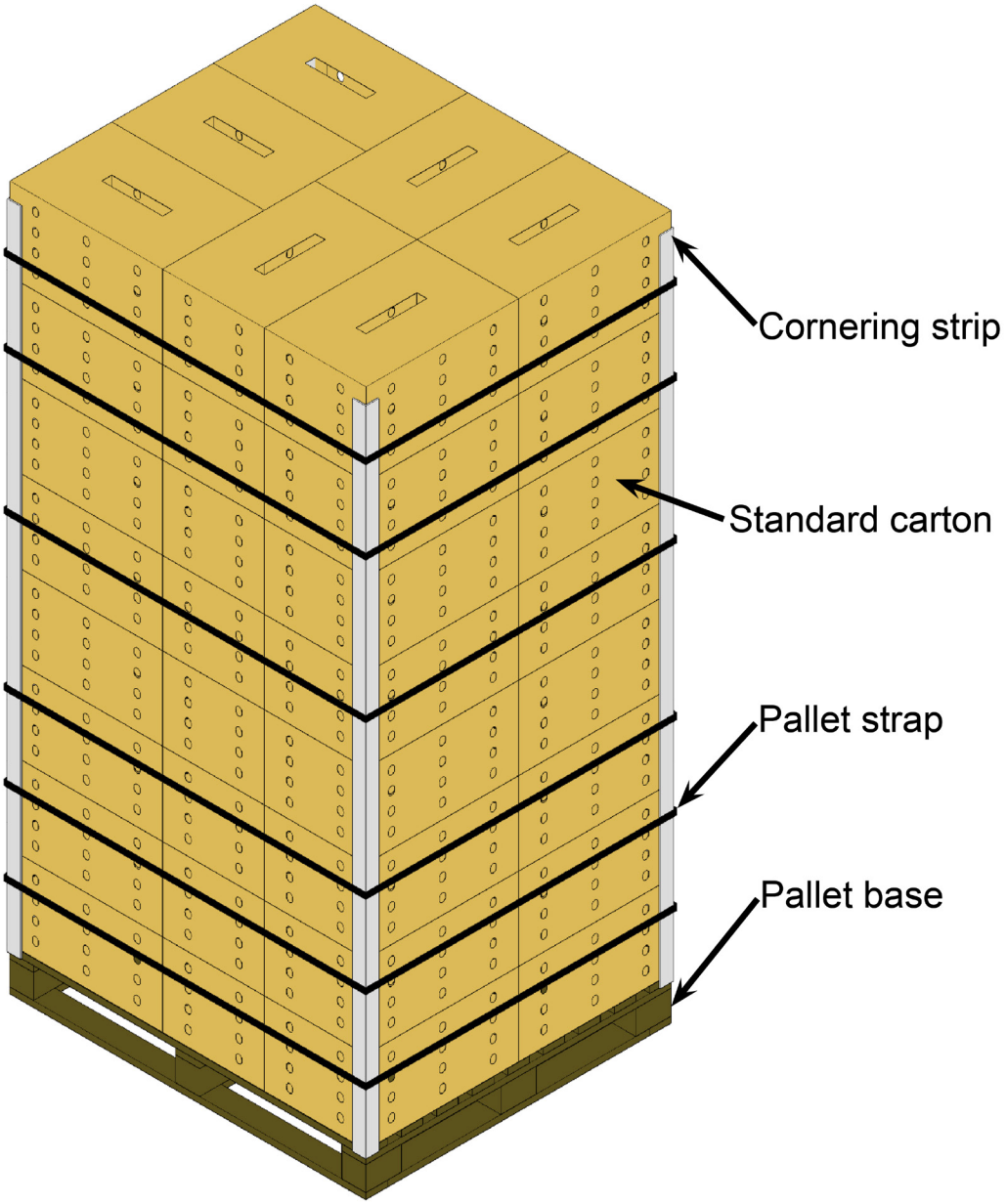

Figure 6.4: Schematic diagram of a fully assembled pallet stack comprised of the STD carton design from the present study and also in Berry et al. (2017, 2016).

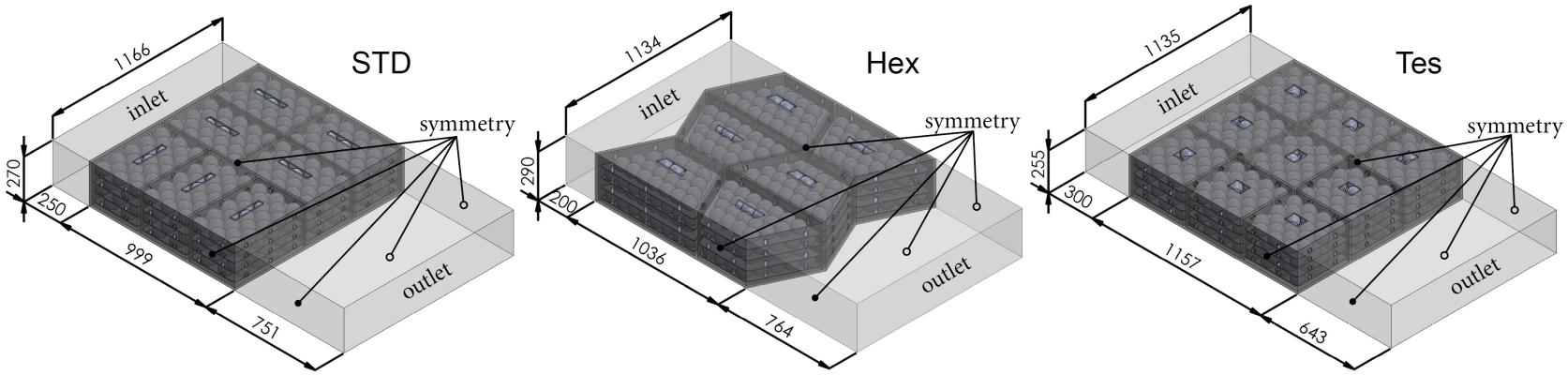

Figure 6.5: Duct, package geometries, and boundary conditions for stacked cartons during FAC (values in mm).

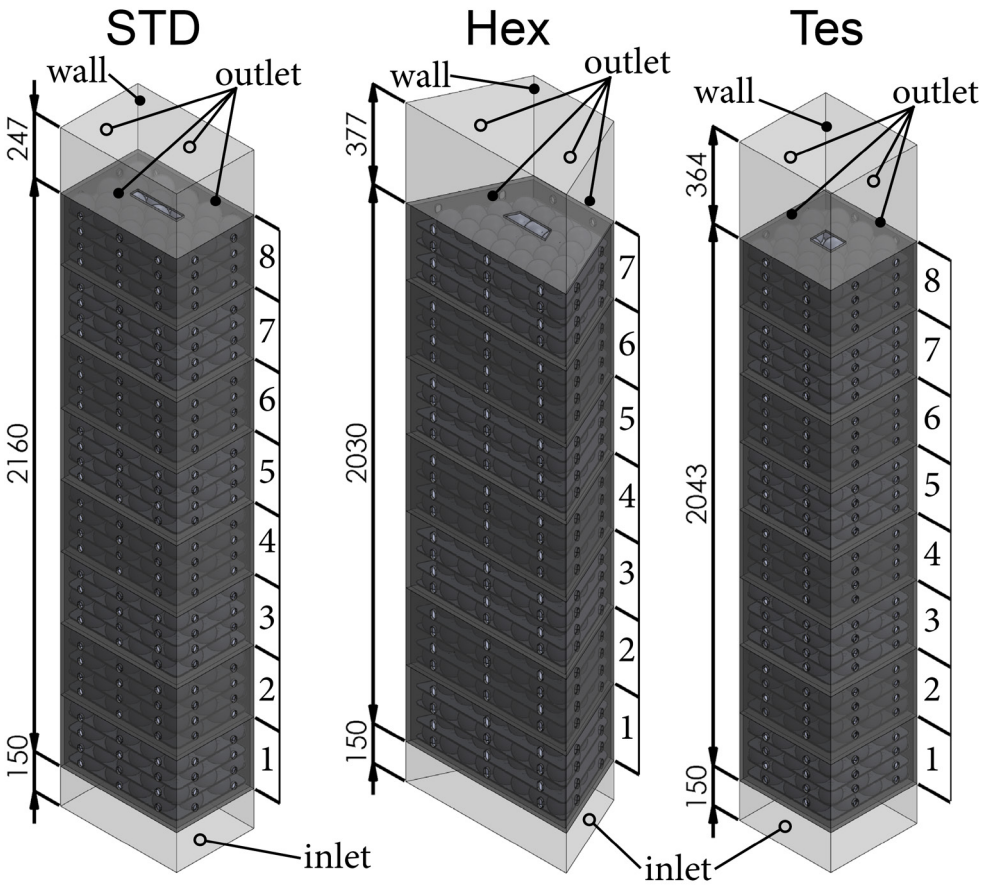

Figure 6.6: Duct, package geometries, and boundary conditions for stacked cartons during RFC cooling (values in mm).

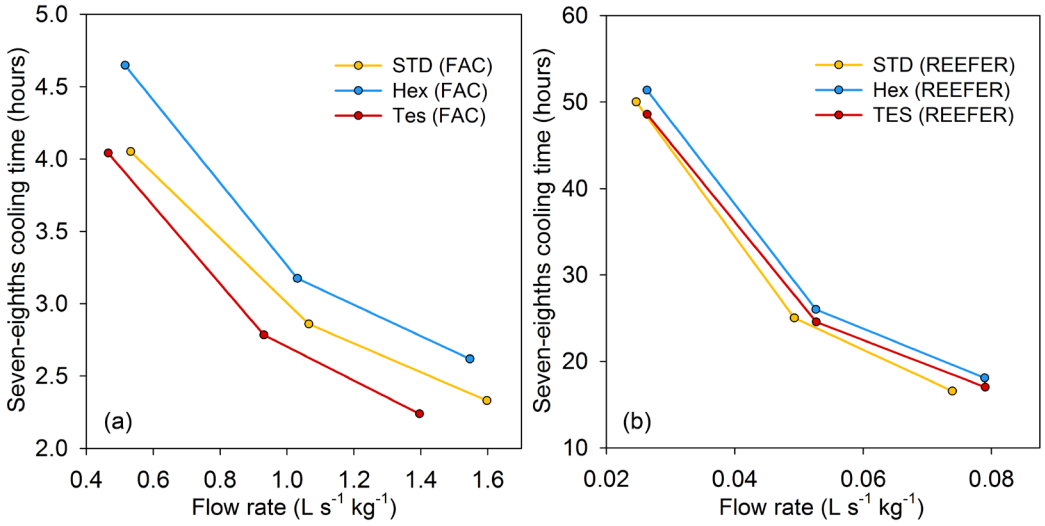

Figure 6.7: Seven-eighths cooling time as a function of airflow rate for the three cartons designs under (a) FAC and (b) RFC conditions.

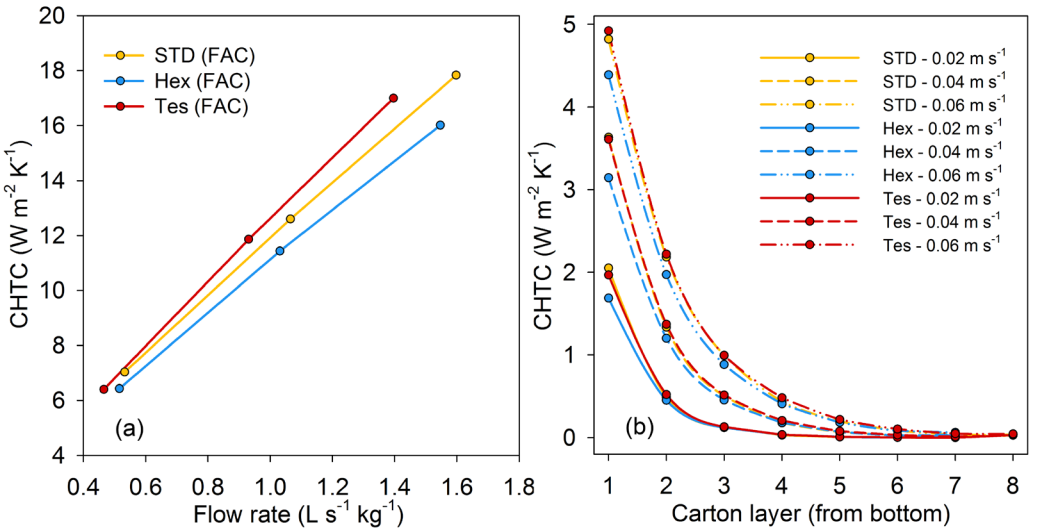

Figure 6.8: Convective heat transfer coefficient with respect to air velocity for the three carton designs under (a) FAC and (b) RFC conditions.

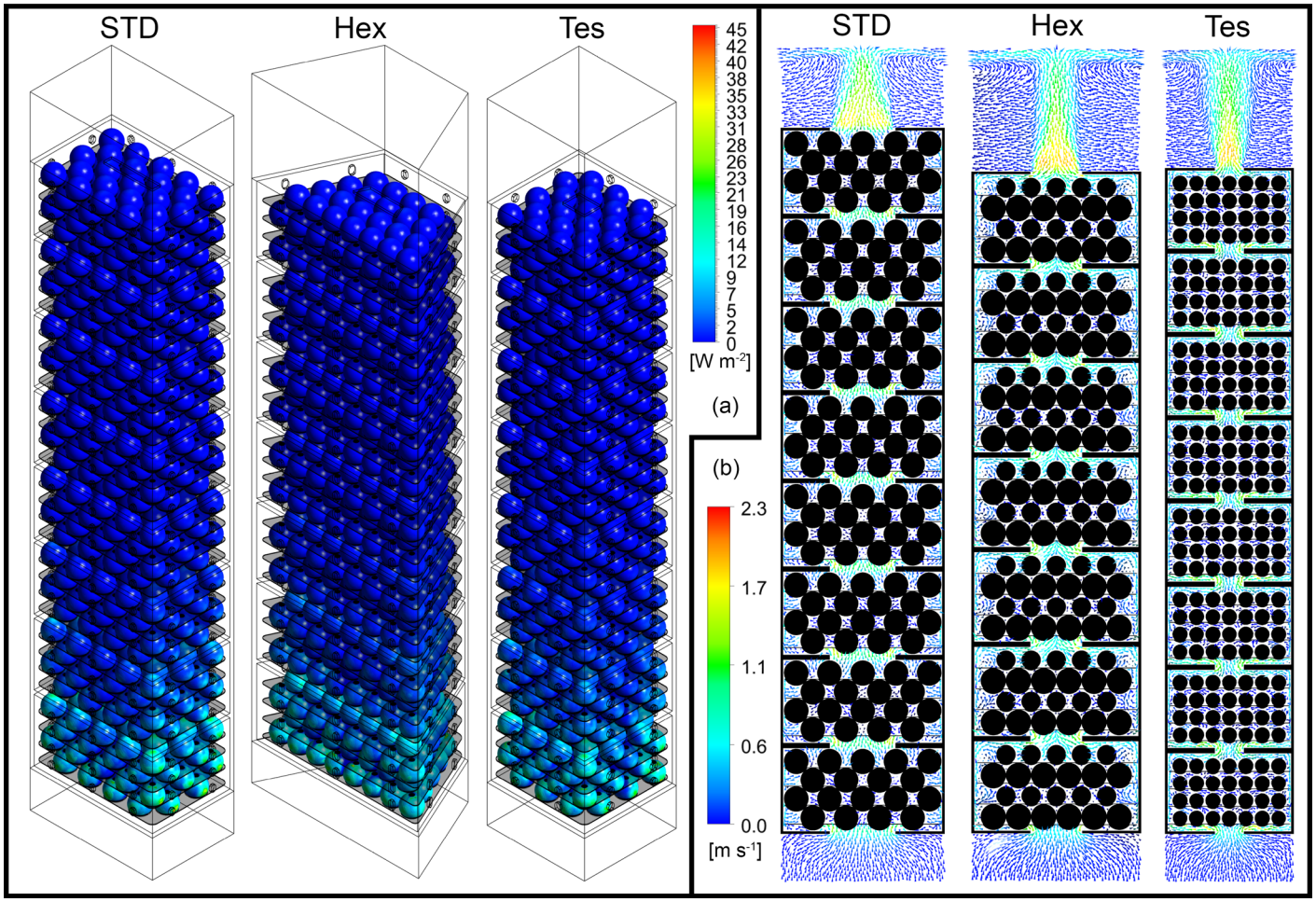

Figure 6.9: (a) Distribution of CHTCs over surfaces and (b) vector plot through a centre plane for the three packaging designs at 4 m s^{-1} (velocity at inlet) during RFC conditions.

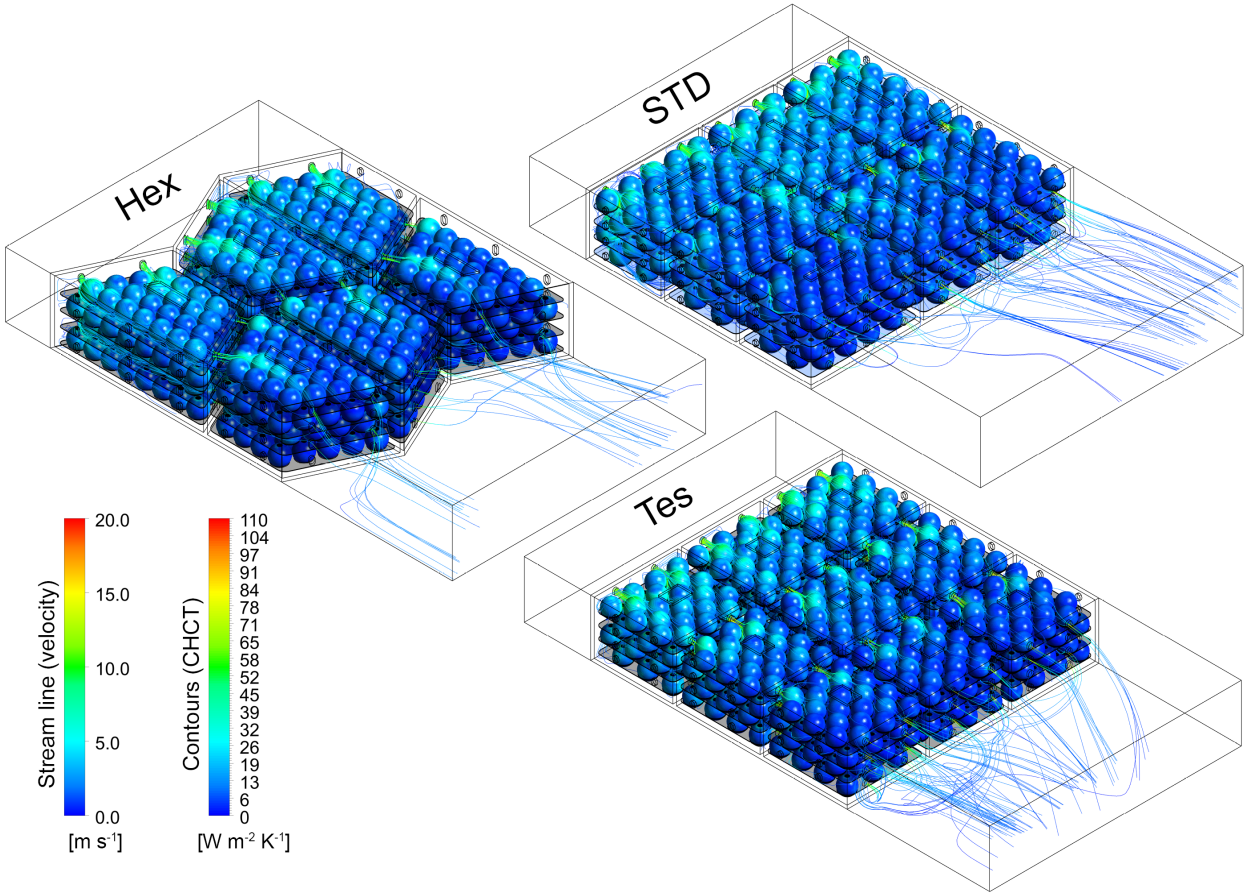

Figure 6.10: Velocity streamlines and distribution of CHTCs over surfaces of apple fruit for the three packaging designs at 4 m s^{-1} (velocity at inlet) during FAC conditions.

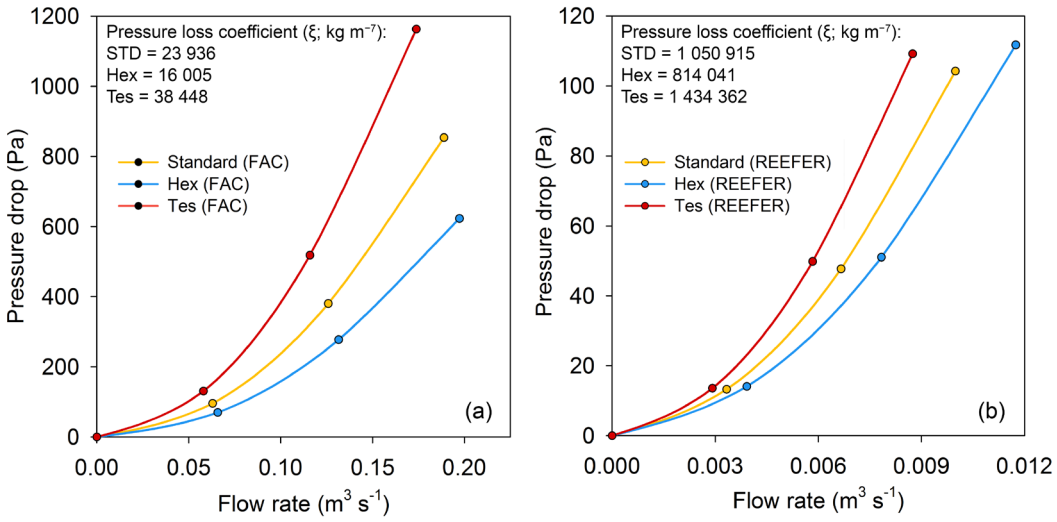

Figure 6.11: Pressure drop as a function of airflow rate for the three carton designs under (a) FAC and (b) RFC cooling conditions.

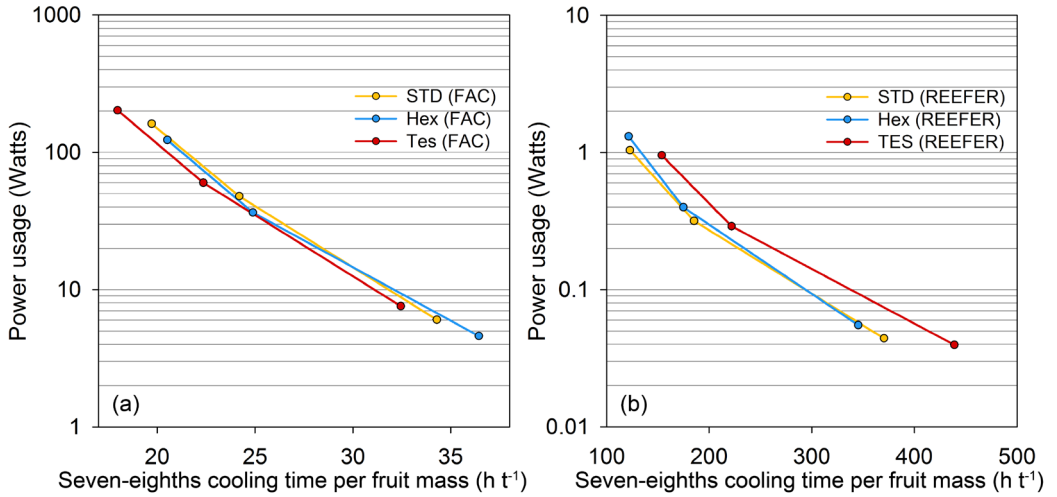

Figure 6.12: Ventilation power usage (logarithmic scale) versus seven-eighths cooling time per ton of fruit for the three cartons under (a) FAC and (b) RFC conditions.

Chapter 7. General Conclusions

This research study presents a novel approach to fresh produce package design using a multi-parameter method, within the scope of a multi-scale system. Following an extensive review (Chapter 2) of the factors affecting design of fresh produce packaging systems, four stand-alone research articles addressing the thesis objectives are presented in chapter format. Chapters 3 and 4 investigate the potential implementation of alternative vent hole designs for improved performance in the cold chain. Chapter 5 proposes a computational fluid dynamics (CFD) model to characterise moisture content values and distributions in stacked corrugated fibreboard cartons during refrigerated shipping conditions. Lastly, Chapter 6 considers the challenge of refrigerated freight container (RFC) loading and proposes an improved package design for fresh produce export. A comparison of the results and findings of these individual studies show that the aim and objectives set out in this thesis have been successfully achieved. The sections below provide a synthesis of the contributions in this thesis and briefly discuss future research directions.

1. A synthesis of the primary contributions of the thesis

An important contribution in this work was the clear delineation of packaging functionalities in the horticultural cold chain. Specifically, packaging systems must perform very different roles in three distinct components of the cold chain, namely, precooling (forced-air cooling; FAC), storage and refrigerated transport. Some examples include facilitating temperature control for quality preservation, removal of unwanted atmospheres (ethylene, CO_2), intermittent-warming (to treat chilling injury), phytosanitary treatments (either chemical or temperature related) and mechanical protection (to protect fruit from vibration, impact and compression forces).

Another major contribution in this thesis, was the elucidation and implementation of a multi-parameter evaluation approach for designing and assessing the performance of horticultural packaging, which is in contrast with previous work that based performance evaluations on just one or two parameters (e.g. cooling or airflow resistance). For example, a new performance parameter that combines the two main concerns facing FAC operators was introduced. Specifically, package performance was quantified with respect to cooling throughput (power usage versus cooling duration). Within this context, three new vent hole designs were proposed, using positioning schemes to ensure alignment during stacking (multi-scale). This positioning approach is applicable to many other packaging systems with different geometries, making the findings applicable to other packaging systems (e.g. citrus and stone fruit packages).

The influence of trays versus loose fruit packing was also examined. This provides a vital link to the many previous studies investigating packaging packed with loose produce. Findings demonstrated that cartons packed with trays do not require larger vent hole areas and that significant improvements (48%) in cooling efficiency (energy consumption) are possible using alternative vent hole configurations.

Next, the study examined the relationship between vent hole size, configuration and corrugated fibreboard material. This is an important component of carton design, since manufacturers often attempt to balance the ventilation size and fibreboard strength to achieve a desirable mechanical strength. Results showed that significant improvements in mechanical strength are possible, without decreasing cooling efficiency, using either different board types or different vent hole configurations in combination with smaller holes. The broad scope of this assessment further showed the effects of vent hole features (size, shape, position) are considerably more complex than previously assumed in literature. Increases in vent hole area generally resulted in a linear reduction in carton mechanical strength, which was consistent with previous work. However, the extent of improvement was dependent on which vent hole configuration was used. Curiously, the effect of both vent hole configuration and size on mechanical strength were also shown to have a significant interaction with the type of fibreboard used.

A key contribution in this study, was therefore: The observation that optimal vent hole design on cartons is affected by the type of fibreboard materials used, which has not been reported in literature before. This effect was shown to be related to the material properties of the corrugated fibreboard (e.g. thickness, rigidity and elasticity), which determined the mode of failure (buckling locations) of the carton. The implications of these findings are significant, since the material properties in corrugated fibreboard change throughout the lifetime of a carton, as moisture is adsorbed as a result of the high humidity conditions during cold storage (90-95% relative humidity; RH). Additionally, humidity cycles in the storage environment can also result in mechano-sorptive creep. However, most studies have only evaluated cartons using a single board type and at standard conditions (23 °C and 50% RH). A note of caution is that previous recommendations for a carton design based on these findings should, therefore, only be accepted within the examined range of materials and cold chain conditions investigated. Recommendations can therefore not be extrapolated to other cold chain conditions. Furthermore, these findings provide some explanation for the large discrepancies in carton performance, often reported between laboratory tests and field performance of new package designs. The results in this study clearly indicate that an improved mechanical testing approach, which incorporates the high moisture content distributions of cartons (during cold chain conditions) is critical for future evaluations. However, very little information is currently available in this area.

Another contribution in this thesis is the development and validation of a CFD model to predict moisture transport in corrugated fibreboard under RFC shipping conditions. Discussions with industry role players suggested that stacked cartons can fail even under optimal RFC conditions. The model was therefore used to characterise moisture contents and distributions in a pallet stack under these ideal transit conditions. Findings showed that the respective spatio-temporal moisture content gradients were relatively small. Furthermore, the main influence to moisture gradients was the presence of gradual long term temperature changes, whereas smaller factors (e.g. defrost cycles) were relatively insignificant. These conditions can be used as groundwork for future box compression test conditioning protocols, whereby the RFC conditions are replicated in a humidity chamber or in a well-controlled cold room. Additionally, the detailed simulation results can be used as boundary condition inputs for future numerical models evaluating carton mechanical strength.

A further contribution in this thesis, was the optimisation of RFC container space usage, which previously has not been considered in other studies. Current packaging systems (complimentary carton and pallet base design) do not use about 10% of the RFC floor area, representing a significant opportunity to improve cold chain efficiency. Two new improved packaging systems were proposed, where the optimal vent hole designs were guided based on findings from the preceding sections. The study extended the multi-parameter approach, by evaluating both horizontal (FAC) and vertical airflow (RFC) cooling. Although both designs showed promise, the “Tes” design, which stacks nine rectangular cartons per pallet (1 157 × 1 135 mm) was identified as a viable alternative to current package designs, showing improved cooling performance and 98.9% RFC floor area usage.

2. Future research directions

The work and concepts introduced in this study have formed a basis for improved package evaluation methods towards the next-generation of future fresh produce package design. Additionally, it is intended that the approaches presented in this thesis be adapted and applied to other fresh produce packaging systems within the agricultural engineering and postharvest research communities.

The multi-parameter approach used to evaluate carton performance packed loose and with trays now needs to be extended to cartons packed with other internal packaging types (e.g. liner bags, carry bags and clam-shells). This will enable packhouses to tailor packaging designs to the respective contents, which is often determined by the destination and expected conditions during transit. Additionally, similar to vent holes on the horizontal axis, improvements in vent holes along the vertical axis also need to be explored using a multi-parameter approach as presented in this thesis. Currently, this aspect has been largely overlooked and the potential for improvements was raised during RFC evaluations (vertical airflow).

The work in this thesis also identified the need for a new performance parameter to quantify pallet stack stability. Pallet stacks are relatively tall structures that must resist tipping over when being handled by forklifts or during the swaying of a ship at sea. Stability is often improved using additional packaging materials or using more complex stacking patterns, which can negatively affect cooling performance. The incorporation of a stability performance parameter to future multi-parameter evaluations is therefore recommended.

Quantifications of carton moisture content and distributions under various desirable and undesirable conditions are needed, which can then be related to mechanical pallet stack failures in real world conditions. Additionally, more information is needed regarding the physics behind moisture transport in fibreboard and mechano-sorptive creep, particularly at ultra-high humidity conditions (98-100% RH), which is relevant to certain fresh produce types. Much has already been speculated in these areas, however, more reliable empirical relationships are needed at these conditions.

The development of a refined experimental box compression test protocol is another critical issue identified in this thesis. A promising direction, is the inclusion of protocols that evaluate the effects of both static and dynamic loads. Future box compression tests should also include conditioning treatments that can replicate the high moisture content conditions found in the cold chain. Furthermore, another possibility for future conditioning protocols is to include long term compression forces to replicate the effects of creep (mechano-sorptive). Finally, inclusion of mechanical calculation to current CFD models and the use of improved finite element models is also expected to play an important role in future mechanical strength evaluations. Detailed quantification of spatio-temporal moisture contents will thus be an important resource to these approaches.

Lastly, future goals include the development of numerical tools to evaluate packaging systems at much larger scales, while still including details of the individual fruit and internal packaging. This includes cooling assessments in fully loaded holding areas (FAC, RFC and cold rooms). Additionally, further developments in finite element models are required, which include the effects of pallet stacking and environmental factors (handling damage, high humidity and mechano-sorptive creep).

This thesis therefore provides some foundations and direction for realizing these ambitious goals and has addressed many research questions raised by the horticultural industry. Significant progress was made towards the advancement and implementation of a multi-parameter evaluation approach that is applicable for packaging horticultural fresh produce. Furthermore, a strong case has been made for the introduction of a new and novel packaging system that facilitates enhanced RFC space utilisation, improved cooling efficiency and increased mechanical strength.

References

Alfthan, J., 2004. The effect of humidity cycle amplitude on accelerated tensile creep of paper. *Mech. Time-Dependent Mater.* 8, 289–302.

Alfthan, J., 2003. A simplified network model for mechano-sorptive creep in paper. *J. Pulp Pap. Sci.* 29, 228–234.

Alfthan, J., Gudmundson, P., Östlund, S., 2002. A micro-mechanical model for mechano-sorptive creep in paper. *J. Pulp Pap. Sci.* 28, 98–104.

Allaoui, S., Aboura, Z., Benzeggagh, M.L., 2009a. Effects of the environmental conditions on the mechanical behaviour of the corrugated cardboard. *Compos. Sci. Technol.* 69, 104–110.

Allaoui, S., Aboura, Z., Benzeggagh, M.L., 2009b. Phenomena governing uni-axial tensile behaviour of paperboard and corrugated cardboard. *Compos. Struct.* 87, 80–92.

Alvarez, G., Flick, D., 1999a. Analysis of heterogeneous cooling of agricultural products inside bins Part I: aerodynamic study. *J. Food Eng.* 39, 227–237.

Alvarez, G., Flick, D., 1999b. Analysis of heterogeneous cooling of agricultural products inside bins Part II: thermal study. *J. Food Eng.* 39, 239–245.

Ambaw, A., Beaudry, R.M., Bulens, I., Delele, M.A., Ho, Q.T., Schenk, A., Nicolaï, B.M., Verboven, P., 2011. Modeling the diffusion–adsorption kinetics of 1-methylcyclopropene (1-MCP) in apple fruit and non-target materials in storage rooms. *J. Food Eng.* 102, 257–265.

Ambaw, A., Delele, M.A., Defraeye, T., Ho, Q.T., Opara, U.L., Nicolaï, B.M., Verboven, P., 2013a. The use of CFD to characterize and design post-harvest storage facilities: Past, present and future. *Comput. Electron. Agric.* 93, 184–194.

Ambaw, A., Verboven, P., Defraeye, T., Tijskens, E., Schenk, A., Opara, U.L., Nicolaï, B.M., 2013b. Porous medium modeling and parameter sensitivity analysis of 1-MCP distribution in boxes with apple fruit. *J. Food Eng.* 119, 13–21.

Ambaw, A., Verboven, P., Defraeye, T., Tijskens, E., Schenk, A., Opara, U.L., Nicolaï, B.M., 2013c. Effect of box materials on the distribution of 1-MCP gas during cold storage: A CFD study. *J. Food Eng.* 119, 150–158.

Ambaw, A., Verboven, P., Delele, M.A., Defraeye, T., Tijskens, E., Schenk, A., Nicolaï, B.M., 2013d. CFD modelling of the 3D spatial and temporal distribution of 1-methylcyclopropene in a fruit storage container. *Food Bioprocess Technol.* 6, 2235–2250.

Ambaw, A., Verboven, P., Delele, M.A., Defraeye, T., Tijskens, E., Schenk, A., Verlinden, B.E., Opara, U.L., Nicolaï, B.M., 2014. CFD-based analysis of 1-MCP distribution in commercial cool store rooms: Porous medium model application. *Food Bioprocess Technol.* 7, 1903–1916.

Anderson, B.A., Sarkar, A., Thompson, J.F., Singh, R.P., 2004. Commercial-scale forced-air cooling of packaged strawberries. *Trans. ASAE* 47, 183–190.

ANSYS, C., 2015. ANSYS CFX-solver theory guide. ANSYS Inc, Canonsburg, PA.

Armstrong, L.D., Christensen, G.N., 1961. Influence of moisture changes on deformation of wood under stress. *Nature* 191, 869–870.

Armstrong, L.D., Kingston, R.S.T., 1960. Effect of moisture changes on creep in wood. *Nature* 185, 862–863.

ASHRAE, 2009. *ASHRAE Handbook - Fundamentals (SI edition)*. American Society of Heating, Refrigerating and Air Conditioning Engineers, Inc, Atlanta, GA, USA.

ASHRAE, 2006. Refrigeration Load, in: *ASHRAE Handbook Refrigeration (SI)*. American Society of Heating, Refrigerating and Air Conditioning Engineers, Inc, Atlanta, GA, USA, p. 13.1-13.8.

ASHRAE, 2000a. *ASHRAE Handbook - Refrigeration: systems and applications (SI edition)*. American Society of Heating, Refrigerating and Air Conditioning Engineers, Inc, Atlanta, GA, USA.

ASHRAE, 2000b. *ASHRAE Handbook - HVAC systems and Equipment (SI edition)*. American Society of Heating, Refrigerating and Air Conditioning Engineers, Inc, Atlanta, GA, USA.

ASTM, 2010. *ASTM D642: Standard Test Method for Determining Compressive Resistance of Shipping Containers, Components, and Unit Loads*. American Society of Testing and Materials International, West Conshohocken, PA.

ASTM, 2006. *D4332-01: Standard Practice for Conditioning Containers, Packages , or Packaging Components for Testing*. American Society of Testing and Materials International, West Conshohocken, PA.

Babalis, A., Ntintakis, I., Chaidas, D., Makris, A., 2013. Design and development of innovative packaging for agricultural products. *Procedia Technol.* 8, 575–579.

Bandyopadhyay, A., Radhakrishnan, H., Ramarao, B. V, Chatterjee, S.G., 2000. Moisture sorption response of paper subjected to ramp humidity changes: Modeling and experiments. *Ind. Eng. Chem. Res.* 39, 219–226.

Bandyopadhyay, A., Ramarao, B. V, Ramaswamy, H.S., 2002. Transient moisture diffusion through paperboard materials. *Colloids Surfaces A Physicochem. Eng. Asp.* 206, 455–467.

Becker, B.R., Fricke, B.A., 2004. Heat transfer coefficients for forced-air cooling and freezing of selected foods. *Int. J. Refrig.* 27, 540–551.

Becker, B.R., Misra, A., Fricke, B.A., 1996. Bulk refrigeration of fuits and vegatables part I : Theoretical consideration of heat. *HVAC&R Res.* 2, 122–134.

Berardinelli, A., Donati, V., Giunchi, A., Guarnieri, A., Ragni, L., 2005. Damage to pears caused by simulated transport. *J. Food Eng.* 66, 219–226.

Berry, T.M., 2013. Resistance to airflow and the effects on cooling efficiency of multi-scale ventilated pome fruit packaging, MSc thesis, Stellenbosch University, Stellenbosch.

Berry, T.M., Defraeye, T., Nicolaï, B.M., Opara, U.L., 2016. Multiparameter analysis of cooling efficiency of ventilated fruit cartons using CFD: Impact of vent hole design and internal packaging. *Food Bioprocess Technol.* 9, 1481–1493.

Berry, T.M., Delele, M.A., Griessel, H., Opara, U.L., 2015. Geometric design characterisation of ventilated multi-scale packaging used in the South African pome fruit industry. *Agric. Mech. Asia, Africa, Lat. Am.* 46, 1–19.

Berry, T.M., Fadiji, T.S., Defraeye, T., Opara, U.L., 2017. The role of horticultural carton vent hole design on cooling efficiency and compression strength: A multi-parameter approach. *Postharvest Biol. Technol.* 124, 62–74.

Biancolini, M.E., Brutti, C., 2003. Numerical and experimental investigation of the strength of corrugated board packages. *Packag. Technol. Sci.* 16, 47–60.

Birla, S.L., Wang, S., Tang, J., Fellman, J.K., Mattinson, D.S., Lurie, S., 2005. Quality of oranges as influenced by potential radio frequency heat treatments against Mediterranean fruit flies. *Postharvest Biol. Technol.* 38, 66–79.

Boyette, M.D., Sanders, D., Rutledge, G., 2000. *Packaging requirements for fresh fruits and vegetables*, Agricultural Extension publication, AG-418-8. The North Carolina State University.

Bronlund, J.E., Redding, G.P., Robertson, T.R., 2014. Modelling steady-state moisture transport through corrugated fibreboard packaging. *Packag. Technol. Sci.* 27, 193–201.

Brosnan, T., Sun, D.-W., 2001. Precooling techniques and applications for horticultural products—a review. *Int. J. Refrig.* 24, 154–170.

Byrd, V.L., 1972a. Effect of relative humidity changes on compressive creep response of paper. *Tappi* 55, 1612–1613.

Byrd, V.L., 1972b. Effect of relative humidity changes during creep on handsheet paper properties. *Tappi* 55, 247–252.

Cagnon, T., Méry, A., Chalier, P., Guillaume, C., Gontard, N., 2013. Fresh food packaging design: A requirement driven approach applied to strawberries and agro-based materials. *Innov. Food Sci. Emerg. Technol.* 20, 288–298.

Çakmak, B., Alayunt, F.N., Akdeniz, R.C., Aksoy, U., Can, H.Z., 2010. Assessment of the quality losses of fresh fig fruits during transportation. *J. Agric. Sci.* 16, 139–224.

Cal/OSHA, 2007. Ergonomic Guidelines for Manual Material Mandling, California Department of Industrial Relations.

Caleb, O.J., Mahajan, P. V, Al-Said, F.A.J., Opara, U.L., 2013. Modified atmosphere packaging technology of fresh and fresh-cut produce and the microbial consequences-A review. *Food Bioprocess Technol.* 6, 303–329.

Caleb, O.J., Opara, U.L., Witthuhn, C.R., 2012. Modified atmosphere packaging of pomegranate fruit and arils: A review. *Food Bioprocess Technol.* 5, 15–30.

Cargo Systems International, 1989. *Guide to Food Transport: Fruit and Vegetables*. Mercantila Publishers, Copenhagen, Denmark.

Celik, I.B., Ghia, U., Roache, P.J., Freitas, C.F., Coleman, H., Raad, P.E., 2008. Procedure for estimation and reporting of uncertainty due to discretization in CFD applications. *J. Fluids Eng.* 130, 1–4.

Chatterjee, S.G., 2001. Comparison of domain and similarity models for characterizing moisture sorption equilibria of paper. *Ind. Eng. Chem. Res.* 40, 188–194.

Chatterjee, S.G., Ramarao, B. V, Tien, C., 1997. Water-vapour sorption equilibria of a bleached-kraft paperboard - A study of the hysteresis region. *J. Pulp Pap. Sci.* 23, J366–J373.

Chau, K. V, Gaffney, J.J., Baird, C.D., Church, G.A., 1985. Resistance to air flow of oranges in bulk and in cartons. *Trans. ASAE* 28, 2083–2088.

Chau, K. V, Romero, R.A., Baird, C.D., Gaffney, J.J., 1987. Transpiration Coefficients of Fruits and Vegetables in Refrigerated Storage. *ASHRAE Reports* 370–380.

Chourasia, M.K., Goswami, T.K., 2007. Three dimensional modeling on airflow, heat and mass transfer in partially impermeable enclosure containing agricultural produce during natural convective cooling. *Energy Convers. Manag.* 48, 2136–2149.

Crofts, B.W., 1989. The Effect of Simulated Handling on the Compression Performance of Corrugated Fibreboard Containers, MSc thesis, Michigan State University, Lansing.

Darling, R.C., Belding, H., 1946. Moisture adsorption of textile yarns at low temperatures. *J. Textle Inst.* 38, 524–529.

de Castro, L.R., Vigneault, C., Cortez, L.A.B., 2005a. Effect of container openings and airflow rate on energy required for forced-air cooling of horticultural produce. *Can. Biosyst. Eng.* 47, 1–9.

de Castro, L.R., Vigneault, C., Cortez, L.A.B., 2005b. Cooling performance of horticultural produce in containers with peripheral openings. *Postharvest Biol. Technol.* 38, 254–261.

de Castro, L.R., Vigneault, C., Cortez, L.A.B., 2004a. Effect of container opening area on air distribution during precooling of horticultural produce. *Trans. ASAE* 47, 2033–2038.

de Castro, L.R., Vigneault, C., Cortez, L.A.B., 2004b. Container opening design for horticultural produce cooling efficiency. *J. Food, Agric. Environ.* 2, 135–140.

de Vries, P., Huysamer, M., Hurndall, R., 2003. *Picking, Storage and Handling Protocol for Pome fruit*. Hortec, Ceres.

Defraeye, T., Blocken, B., Derome, D., Nicolaï, B.M., Carmeliet, J., 2012a. Convective heat and mass transfer modelling at air–porous material interfaces: Overview of existing methods and relevance. *Chem. Eng. Sci.* 74, 49–58.

Defraeye, T., Herremans, E., Verboven, P., Carmeliet, J., Nicolaï, B.M., 2012b. Convective heat and mass exchange at surfaces of horticultural products: A microscale {CFD} modelling approach. *Agric. For. Meteorol.* 162–163, 71–84.

Defraeye, T., Lambrecht, R., Delele, M.A., Tsige, A.A., Opara, U.L., Cronjé, P., Verboven, P., Nicolaï, B.M., 2014. Forced-convective cooling of citrus fruit: Cooling conditions and energy consumption in relation to package design. *J. Food Eng.* 121, 118–127.

Defraeye, T., Lambrecht, R., Tsige, A.A., Delele, M.A., Opara, U.L., Cronjé, P., Verboven, P., Nicolaï, B.M., 2013a. Forced-convective cooling of citrus fruit: Package design. *J. Food Eng.* 118, 8–18.

Defraeye, T., Verboven, P., Nicolaï, B.M., 2013b. CFD modelling of flow and scalar exchange of spherical food products: Turbulence and boundary-layer modelling. *J. Food Eng.* 114, 495–504.

Defraeye, T., Cronjé, P., Berry, T.M., Opara, U.L., East, A.R., Hertog, M.L.A.T.M., Verboven, P., Nicolaï, B.M., 2015a. Towards integrated performance evaluation of future packaging for fresh produce in the cold chain. *Trends Food Sci. Technol.* 44, 201–225.

Defraeye, T., Cronjé, P., Verboven, P., Opara, U.L., Nicolaï, B.M., 2015b. Exploring ambient loading of citrus fruit into reefer containers for cooling during marine transport using computational fluid dynamics. *Postharvest Biol. Technol.* 108, 91–101.

Defraeye, T., Verboven, P., Opara, U.L., Nicolaï, B.M., Cronjé, P., 2015c. Feasibility of ambient loading of citrus fruit into refrigerated containers for cooling during marine transport. *Biosyst. Eng.* 134, 20–30.

Defraeye, T., Nicolaï, B.M., Kirkman, W., Moore, S., van Niekerk, S., Verboven, P., Cronjé, P., 2016. Integral performance evaluation of the fresh-produce cold chain: A case study for ambient loading of citrus in refrigerated containers. *Postharvest Biol. Technol.* 112, 1–13.

Dehghannya, J., Ngadi, M., Vigneault, C., 2012. Transport phenomena modelling during produce cooling for optimal package design: Thermal sensitivity analysis. *Biosyst. Eng.* 111, 315–324.

Dehghannya, J., Ngadi, M., Vigneault, C., 2011. Mathematical modeling of airflow and heat transfer during forced convection cooling of produce considering various package vent areas. *Food Control* 22, 1393–1399.

Dehghannya, J., Ngadi, M., Vigneault, C., 2010. Mathematical modeling procedures for airflow, heat and mass transfer during forced convection cooling of produce: A review. *Food Eng. Rev.* 2, 227–243.

Dehghannya, J., Ngadi, M., Vigneault, C., 2008. Simultaneous aerodynamic and thermal analysis during cooling of stacked spheres inside ventilated packages. *Chem. Eng. Technol.* 31, 1651–1659.

Delele, M.A., Ngcobo, M.E.K., Opara, U.L., Meyer, C.J., 2012. Investigating the effects of table grape package components and stacking on airflow, heat and mass transfer using 3-D CFD modelling. *Food Bioprocess Technol.* 6, 2571–2585.

Delele, M.A., Ngcobo, M.E.K., Getahun, S.T., Chen, L., Mellmann, J., Opara, U.L., 2013a. Studying airflow and heat transfer characteristics of a horticultural produce packaging system using a 3-D CFD model. Part II: Effect of package design. *Postharvest Biol. Technol.* 86, 546–555.

Delele, M.A., Ngcobo, M.E.K., Getahun, S.T., Chen, L., Mellmann, J., Opara, U.L., 2013b. Studying airflow and heat transfer characteristics of a horticultural produce packaging system using a 3-D CFD model. Part I: Model development and validation. *Postharvest Biol. Technol.* 86, 536–545.

Delele, M.A., Ngcobo, M.E.K., Opara, U.L., Pathare, P.B., 2013c. CFD modelling to study the effects of table grape packaging and stacking on fruit cooling and moisture loss. *Acta Hortic.* 1008, 105–112.

Delele, M.A., Schenk, A., Tijskens, E., Ramon, H., Nicolaï, B.M., Verboven, P., 2009. Optimization of the humidification of cold stores by pressurized water atomizers based on a multiscale CFD model. *J. Food Eng.* 91, 228–239.

Delele, M.A., Tijskens, E., Atalay, Y.T., Ho, Q.T., Ramon, H., Nicolaï, B.M., Verboven, P., 2008. Combined discrete element and CFD modelling of airflow through random stacking of horticultural products in vented boxes. *J. Food Eng.* 89, 33–41.

Delele, M.A., Verboven, P., Ho, Q.T., Nicolaï, B.M., 2010. Advances in mathematical modelling of postharvest refrigeration processes. *Stewart Postharvest Rev.* 6, 1–8.

Dieter, G.E., Schmidt, linda C., 2009. *Engineering Design*, 4th ed. McGraw Hill, New York.

Dincer, I., 1995. Air flow precooling of individual grapes. *J. Food Eng.* 26, 243–249.

Djilali Hammou, A., Duong, P.T.M., Abbes, B., Makhlouf, M., Guo, Y.Q., 2012. Finite-element simulation with a homogenization model and experimental study of free drop tests of corrugated cardboard packaging. *Mech. Ind.* 13, 175–184.

Dong, F., Olsson, A.-M., Salmén, L., 2010. Fibre morphological effects on mechano-sorptive creep. *Wood Sci. Technol.* 44, 475–483.

Duret, S., Hoang, H.-M., Flick, D., Laguerre, O., 2014. Experimental characterization of airflow, heat and mass transfer in a cold room filled with food products. *Int. J. Refrig.* 46, 17–25.

Eagleton, D.G., Marcondes, J., 1994. Moisture-sorption isotherms for paper-based components of transport packaging for fresh produce. *Tappi J.* 77, 75–81.

East, A.R., Trujillo, F.J., Winley, E.L., 2007. Modelling the incidence of decay development in “B74” mangoes as a function of supply chain temperature. *Acta Hortic.* 877, 1815–1820.

Eisfeld, B., Schnitzlein, K., 2001. The influence of confining walls on the pressure drop in packed beds. *Chem. Eng. Sci.* 56, 4321–4329.

Everett, D.H., 1967. Adsorption hysteresis, in: Flood, E.A. (Ed.), *The Solid Gas Interface, Vol 2*. Marcel Dekker, New York, pp. 1055–1113.

Eyring, V., Köhler, H.W., van Aardenne, J., Lauer, A., 2005. Emissions from international shipping: 1. The last 50 years. *J. Geophys. Res.* 110, 1–12.

Fadiji, T.S., Coetzee, C., Chen, L., Chukwu, O., Opara, U.L., 2016a. Susceptibility of apples to bruising inside ventilated corrugated paperboard packages during simulated transport damage. *Postharvest Biol. Technol.* 118, 111–119.

Fadiji, T.S., Coetzee, C., Opara, U.L., 2016b. Compression strength of ventilated corrugated paperboard packages: Numerical modelling, experimental validation and effects of vent geometric design. *Biosyst. Eng.* 151, 231–247.

Fadiji, T.S., Coetzee, C., Pathare, P.B., Opara, U.L., 2016c. Susceptibility to impact damage of apples inside ventilated corrugated paperboard packages: Effects of package design. *Postharvest Biol. Technol.* 111, 286–296.

FAO, 2013. *Food wastage footprint: Impacts on natural resources*. Food and Agriculture Organization, Rome.

FAO, 2009. *How to Feed the World in 2050*. Food and Agriculture Organization, Rome.

FEFCO, ESBO, 2007. *International fibreboard case code.* FEFCO, Belgium.

Ferrua, M.J., Singh, R.P., 2011a. Improved airflow method and packaging system for forced-air cooling of strawberries. *Int. J. Refrig.* 34, 1162–1173.

Ferrua, M.J., Singh, R.P., 2011b. Improving the design and efficiency of the forced-air cooling process of fresh strawberries using computational modeling. *Procedia Food Sci.* 1, 1239–1246.

Ferrua, M.J., Singh, R.P., 2009a. Modeling the forced-air cooling process of fresh strawberry packages, Part I: Numerical model. *Int. J. Refrig.* 32, 335–348.

Ferrua, M.J., Singh, R.P., 2009b. Design guidelines for the forced-air cooling process of strawberries. *Int. J. Refrig.* 32, 1932–1943.

Ferrua, M.J., Singh, R.P., 2009c. Modeling the forced-air cooling process of fresh strawberry packages, Part II: Experimental validation of the flow model. *Int. J. Refrig.* 32, 349–358.

Ferrua, M.J., Singh, R.P., 2009d. Modeling the forced-air cooling process of fresh strawberry packages, Part III: Experimental validation of the energy model. *Int. J. Refrig.* 32, 359–368.

Ferrua, M.J., Singh, R.P., 2008. A nonintrusive flow measurement technique to validate the simulated laminar fluid flow in a packed container with vented walls. *Int. J. Refrig.* 31, 242–255.

Fox, T., Fimeche, C., 2013. *Global food: Waste not, want not*. Institute of Mechanical Engineers, London, UK.

Frank, B., 2014. Corrugated box compression—a literature survey. *Packag. Technol. Sci.* 27, 105–128.

Frank, B., Gilgenbach, M., Maltenfort, M., 2010. Compression testing to simulate real-world stresses. *Packag. Technol. Sci.* 23, 275–282.

Fraser, H.W., Eng, P., 1998. *Tunnel forced-air coolers for fresh fruits & vegetables*. Ministry of Agriculture, Food and Rural Arrairs, Ontario.

Galotto, M., Ulloa, P., 2010. Effect of high-pressure food processing on the mass transfer properties of selected packaging materials. *Packag. Technol. Sci.* 23, 253–266.

GDV, 2014. Gesamtverband der Deutschen Versicherungswirtschaft : Container Handbook.

Geankoplis, C.J., 1978. *Transport Processes and Unit Operations*. Allyn and Bacon, Boston, Massachusetts.

Getahun, S.T., 2016. Computational Fluid Dynamic Model-Based Quantification of Energy Utilization and Identification of Strategies to Improve Savings and Reduce Waste in the Fruit Cold Chain, PhD thesis, Stellenbosch University, Stellenbosch.

Gibson, E.J., 1965. Role of water and effect of a changing moisture content. *Nature* 206, 213–215.

Greenspan, L., 1977. Humidity fixed points of binary saturated aqueous solutions. *J. Res. Natl. Bur. Stand. (1934).* 81A, 89–96.

Groenewald, D., Bester, H., 2010. *Packaging Material Specifications and Palletisation Protocols for the 2013 Citrus Export Season*. Citrus Cold Chain forum, Ceres, South Africa.

Guo, Y., Xu, W., Fu, Y., Wang, H., 2011. Dynamic shock cushioning characteristics and vibration transmissibility of X-PLY corrugated paperboard. *Shock Vib.* 18, 525–535.

Guo, Y., Xu, W., Fu, Y., Zhang, W., 2010. Comparison studies on dynamic packaging properties of corrugated paperboard pads. *Engineering* 2, 378–386.

Gustavsson, J., Cederberg, C., Sonesson, U., van Otterdijk, R., Meybeck, A., 2011. *Global food losses and food waste - extent, causes and prevention*. Food and agriculture organization, Rome, Italy.

Habeger, C.C., Coffin, D.W., 2000. The role of stress concentrations in accelerated creep and sorption induced physical aging. *J. Pulp Pap. Sci.* 26, 145–157.

Han, J., Park, J.M., 2007. Finite element analysis of vent/hand hole designs for corrugated fibreboard boxes. *Packag. Technol. Sci.* 20, 39–47.

Han, J.-W., Zhao, C.-J., Yang, X.-T., Qian, J.-P., Fan, B.-L., 2015. Computational modeling of airflow and heat transfer in a vented box during cooling: Optimal package design. *Appl. Therm. Eng.* 91, 883–893.

Hanhijarvi, H.D., 1998. Experimental indication of interaction between viscoelastic and mechano-sorptive creep. *Wood Sci. Technol.* 32, 57–70.

Haslach, H.W., 2000. The moisture and rate-dependent mechanical properties of paper : A review. *Mech. Time-Dependant Mater.* 4, 169–210.

Haslach, H.W., 1994. The mechanics of moisture accelerated tensile creep in paper. *TAPPI J.* 70, 179–186.

Hassanizadeh, M., Gray, W.G., 1979. General conservation equations for multi-phase systems: 1. Averaging procedure. *Adv. Water Resour.* 2, 131–144.

Heap, R.D., 2006. Cold chain performance issues now and in the future. *Innov. Equip. Syst. Comf. Food Preserv.* 86, 2–24.

Hellström, D., Saghir, M., 2007. Packaging and logistics interactions in retail supply chains. *Packag. Technol. Sci.* 20, 197–216.

Henriod, R.E., 2006. Postharvest characteristics of navel oranges following high humidity and low temperature storage and transport. *Postharvest Biol. Technol.* 42, 57–64.

Hinsch, R.T., Slaughter, D.C., Craig, W.L., Thompson, J.F., 1993. Vibration of fresh fruits and vegetables during refrigerated truck transport. *Trans. ASAE* 36, 1039–1042.

Ho, Q.T., Carmeliet, J., Datta, A.K., Defraeye, T., Delele, M.A., Herremans, E., Opara, U.L., Ramon, H., Tijskens, E., van der Sman, R.G.M., Liedekerke, P. Van, Verboven, P., Nicolaï, B.M., 2013. Multiscale modeling in food engineering. *J. Food Eng.* 114, 279–291.

Ho, S.H., Rahman, M.M., Sunol, A.K., 2010. Analysis of thermal response of a food self-heating system. *Appl. Therm. Eng.* 30, 2109–2115.

Hoang, H.-M., Duret, S., Flick, D., Laguerre, O., 2015. Preliminary study of airflow and heat transfer in a cold room filled with apple pallets: Comparison between two modelling approaches and experimental results. *Appl. Therm. Eng.* 76, 367–381.

Hoang, H.-M., Laguerre, O., Moureh, J., Flick, D., 2012. Heat transfer modelling in a ventilated cavity loaded with food product: Application to a refrigerated vehicle. *J. Food Eng.* 113, 389–398.

Holt, J.E., Schoorl, D., Luca, C., 1981. Prediction of bruising in impacted multilayered apple packs. *Trans. ASAE* 24, 242–247.

Hortgro, 2013. South African Pome Fruit Industry Packaging Material Guidelines 2013.

Hortgro, 2012. South African Pome Fruit Industry Packaging Material Guidelines 2012.

Hu, Z., Sun, D.-W., 2001. Predicting the local surface heat transfer coefficients by different turbulent k–e models to simulate heat and moisture transfer during air-blast chilling. *Int. J. Refrig.* 24, 702–717.

Hung, D. Van, Nakano, Y., Tanaka, F., Hamanaka, D., Uchino, T., 2010. Preserving the strength of corrugated cardboard under high humidity condition using nano-sized mists. *Compos. Sci. Technol.* 70, 2123–2127.

Hung, D. Van, Tong, S., Tanaka, F., Yasunaga, E., Hamanaka, D., Hiruma, N., Uchino, T., 2011. Controlling the weight loss of fresh produce during postharvest storage under a nano-size mist environment. *J. Food Eng.* 106, 325–330.

Hunt, D.G., Gril, J., 1996. Evidence of a physical ageing phenomenon in wood. *J. Mater. Sci. Lett.* 15, 80–82.

James, S.J., James, C., Evans, J.A., 2006. Modelling of food transportation systems – a review. *Int. J. Refrig.* 29, 947–957.

Jarimopas, B., Singh, S.P., Saengnil, W., 2005. Measurement and analysis of truck transport vibration levels and damage to packaged tangerines during transit. *Packag. Technol. Sci.* 18, 179–188.

Jarimopas, B., Singh, S.P., Sayasoonthorn, S., Singh, J., 2007. Comparison of package cushioning materials to protect post-harvest impact damage to apples. *Packag. Technol. Sci.* 20, 315–324.

Jedermann, R., Geyer, M., Praeger, U., Lang, W., 2013. Sea transport of bananas in containers – Parameter identification for a temperature model. *J. Food Eng.* 115, 330–338.

Jedermann, R., Nicometo, M., Uysal, I., Lang, W., 2014. Reducing food losses by intelligent food logistics. *Philos. Trans. A. Math. Phys. Eng. Sci.* 372, 1–20.

Jiménez-Ariza, T., Correa, E.C., Diezma, B., Silveira, A.C., Zócalo, P., Arranz, F.J., Moya-González, A., Garrido-Izard, M., Barreiro, P., Ruiz-Altisent, M., 2014. The phase space as a new representation of the dynamical behaviour of temperature and enthalpy in a reefer monitored with a multidistributed sensors network. *Food Bioprocess Technol.* 7, 1793–1806.

Jinkarn, T., Boonchu, P., Bao-ban, S., 2006. Effect of carrying slots on the compressive strength of corrugated board panels. *Kasetsart J. Nat. Sci.* 40, 154–161.

Kader, A.A., 2002. *Postharvest Technology of Horticultural Crops*, 3rd ed. University of California Department of Agriculture and Natural Resources, Davis, California.

Kellicutt, K.Q., 1963. Effect of contents and load bearing surface on compressive strength and stacking life of corrugated containers. *TAPPI J.* 46, 151A–154A.

Kessler, H., Stoll, K., 1953. Versuchsergebnisse bei der kaltlagerung von apfelsorten. *Landw. Jb. Schweiz* 1157–1184.

Kondjoyan, A., 2006. A review on surface heat and mass transfer coefficients during air chilling and storage of food products. *Int. J. Refrig.* 29, 863–875.

Koning, J.K., Moody, R.C., 1989. Slip pads, vertical alignment increase stacking strength 65%, in: Maltenfort, G.G. (Ed.), *Performance and Evaluation of Shipping Containers*. Jelmar Publishing Co, Plainview, NY.

Kratsch, H.A., Wise, R.R., 2000. The ultrastructure of chilling stress. *Plant, Cell Environ.* 23, 337–350.

Labuza, T.P., Altunakar, B., 2007. Water Activity Predictions and Moisture Sorption Isotherms, in: Barbosa-Canovas, G. V, Fontana, A.J., Schmidt, S.J., Labuza, T.P. (Eds.), *Water Activity in Foods*. Blackwell Publishing, Carlton, Australia.

Ladaniya, M.S., 2008. Preparation for Fresh Fruit Market, in: *Citrus Fruit: Biology, Technology and Evaluation*. Elsevier Inc., San Diego, Burlington and London, pp. 229–286.

Ladaniya, M.S., Singh, S., 2000. Influence of ventilation and stacking pattern of corrugated fibre board containers on forced-air pre-cooling of "Nagpur" Mandarins. *J. Food Sci. Technol.* 37, 233–237.

Laguerre, O., Hoang, H.-M., Flick, D., 2013. Experimental investigation and modelling in the food cold chain: Thermal and quality evolution. *Trends Food Sci. Technol.* 29, 87–97.

Laniel, M., Émond, J.P., Altunbas, A.E., 2011. Effects of antenna position on readability of RFID tags in a refrigerated sea container of frozen bread at 433 and 915MHz. *Transp. Res. Part C Emerg. Technol.* 19, 1071–1077.

Larsen, H., Måge, I., Børve, J., Vangdal, E., 2015. Plum fruit packed in flow packs with absorbent pads and stored at different temperatures. *Acta Hortic.* 1079, 695–700.

Linke, M., Geyer, M., 2013. Condensation dynamics in plastic film packaging of fruit and vegetables. *J. Food Eng.* 116, 144–154.

Lu, F., Ishikawa, Y., Kitazawa, H., Satake, T., 2010. Impact damage to apple fruits in commercial corrugated fiberboard box packaging evaluated by the pressure-sensitive film technique. *J. Food, Agric. Environ.* 8, 218–222.

Lu, L.-X., Chen, X., Wang, J., 2016. Modelling and thermal analysis of tray-layered fruits inside ventilated packages during forced-air precooling. *Packag. Technol. Sci.* 29, 105–119.

Lukatkin, A.S., Brazaityte, A., Bobinas, C., Duchovskis, P., 2012. Chilling injury in chilling-sensitive plants: a review. *Agriculture* 99, 111–124.

Maguire, K.M., Banks, N.H., Opara, U.L., 2001. Factors affecting weight loss of apples. *Hortic. Rev. (Am. Soc. Hortic. Sci).* 25, 197–234.

Maltenfort, G.G., 1996. *Corrugated Shipping Containers: An Engineering Approach*. Jelmar Publishing Co, Plainview, NY.

Maltenfort, G.G., 1989. *Performance and Evaluation of Shipping Containers: A Collection of Seminal Articles and Technical Papers in the Corrugated Container Industry*. Jelmar Publishing Co, Plainview, NY.

Marcondes, J., 1996. Corrugated fibreboard in modified atmospheres : Moisture sorption/desorption and shock cushioning. *Packag. Technol. Sci.* 9, 87–98.

Margeirsson, B., Gospavic, R., Pálsson, H., Arason, S., Popov, V., 2011. Experimental and numerical modelling comparison of thermal performance of expanded polystyrene and corrugated plastic packaging for fresh fish. *Int. J. Refrig.* 34, 573–585.

McKee, R.C., Gander, J.W., Wachuta, J.R., 1963. Compression strength formula for corrugated boxes. *Pap. Packag.* 48, 149–159.

McKee, R.C., Gander, J.W., Wachuta, J.R., 1962. Flexural stiffness of corrugated board. *Pap. Packag.* 47, 111–118.

Melo, O., Engler, A., Nahuehual, L., Cofre, G., Barrena, J., 2014. Do sanitary, phytosanitary, and quality-related standards affect international trade? Evidence from Chileanf fruit exports. *World Dev.* 54, 350–359.

Menter, F.R., 1994. Two-equation eddy-viscosity turbulence models for engineering applications. *AIAA J.* 32, 1598–1605.

Moureh, J., Flick, D., 2004. Airflow pattern and temperature distribution in a typical refrigerated truck configuration loaded with pallets. *Int. J. Refrig.* 27, 464–474.

Moureh, J., Menia, N., Flick, D., 2002. Numerical and experimental study of airflow in a typical refrigerated truck configuration loaded with pallets. *Comput. Electron. Agric.* 34, 25–42.

Moureh, J., Tapsoba, M., Flick, D., 2009a. Airflow in a slot-ventilated enclosure partially filled with porous boxes: Part I – Measurements and simulations in the clear region. *Comput. Fluids* 38, 194–205.

Moureh, J., Tapsoba, S., Derens, E., Flick, D., 2009b. Air velocity characteristics within vented pallets loaded in a refrigerated vehicle with and without air ducts. *Int. J. Refrig.* 32, 220–234.

Mualem, Y., 1974. A conceptual model of hysteresis. *Water Resour. Res.* 10, 514–520.

Mualem, Y., 1973. Modified approach to capillary hysteresis based on a similarity hypothesis. *Water Resour. Res.* 9, 1324–1331.

Munhuweyi, K., Opara, U.L., Sigge, G., 2016. Postharvest losses of cabbages from retail to consumer and the socio-economic and environmental impacts. *Br. Food J.* 118, 286–300.

Navi, P., Pittet, V., Plummer, C.J.G., 2002. Transient moisture effects on wood creep. *Wood Sci. Technol.* 36, 447–462.

Ngcobo, M.E.K., Delele, M.A., Opara, U.L., Zietsman, C.J., Meyer, C.J., 2012a. Resistance to airflow and cooling patterns through multi-scale packaging of table grapes. *Int. J. Refrig.* 35, 445–452.

Ngcobo, M.E.K., Delele, M.A., Pathare, P.B., Chen, L., Opara, U.L., Meyer, C.J., 2012b. Moisture loss characteristics of fresh table grapes packed in different film liners during cold storage. *Biosyst. Eng.* 113, 363–370.

Ngcobo, M.E.K., Opara, U.L., Thiart, G.D., 2012c. Effects of packaging liners on cooling rate and quality attributes of table grape (cv. Regal Seedless). *Packag. Technol. Sci.* 25, 73–84.

Ngcobo, M.E.K., Delele, M.A., Opara, U.L., Meyer, C.J., 2013a. Performance of multi-packaging for table grapes based on airflow, cooling rates and fruit quality. *J. Food Eng.* 116, 613–621.

Ngcobo, M.E.K., Delele, M.A., Opara, U.L., Thiart, G.D., Meyer, C.J., 2013b. Heat transfer and external quality attributes of “regal seedless” table grapes inside multi layered packaging during postharvest cooling and storage. *Acta Hortic.* 1007, 189–196.

Ngcobo, M.E.K., Pathare, P.B., Delele, M.A., Chen, L., Opara, U.L., 2013c. Moisture diffusivity of table grape stems during low temperature storage conditions. *Biosyst. Eng.* 115, 346–353.

Norton, T., Sun, D.-W., 2006. Computational fluid dynamics (CFD) – an effective and efficient design and analysis tool for the food industry: A review. *Trends Food Sci. Technol.* 17, 600–620.

Norton, T., Sun, D.-W., Grant, J., Fallon, R., Dodd, V., 2007. Applications of computational fluid dynamics (CFD) in the modelling and design of ventilation systems in the agricultural industry: A review. *Bioresour. Technol.* 98, 2386–2414.

Norton, T., Tiwari, B., Sun, D.-W., 2013. Computational fluid dynamics in the design and analysis of thermal processes: a review of recent advances. *Crit. Rev. Food Sci. Nutr.* 53, 251–75.

O’Sullivan, J., Ferrua, M.J., Love, R., Verboven, P., Nicolaï, B., East, A., 2016. Modelling the forced-air cooling mechanisms and performance of polylined horticultural produce. *Postharvest Biol. Technol.* 120, 23–35.

Oelofse, S.H., Nahman, A., 2013. Estimating the magnitude of food waste generated in South Africa. *Waste Manag. Res.* 31, 80–86.

Olsson, A.-M., Salmén, L., Eder, M., Burgert, I., 2007. Mechano-sorptive creep in wood fibres. *Wood Sci. Technol.* 41, 59–67.

Opara, U.L., 2011. From hand holes to vent holes: what's next in innovative horticultural packaging? Inaugural Lecture. South Africa: Stellenbosch University.

Opara, U.L., 2010. High incidence of postharvest food losses is worsening global food and nutrition security. *Int. J. Postharvest Technol. Innov.* 2, 1–3.

Opara, U.L., 2009. Quality Management: An Industrial Approach to Produce Handling, in: Florkowski, W.J., Shewfelt, R.L., Brueckner, B., Prussia, S.E. (Eds.), *Postharvest Handling*. Academic Press, San Diego, pp. 153–204.

Opara, U.L., Mditshwa, A., 2013. A review on the role of packaging in securing food system : Adding value to food products and reducing losses and waste. *African J. Agric. Res.* 8, 2621–2630.

Opara, U.L., Pathare, P.B., 2014. Bruise damage measurement and analysis of fresh horticultural produce—A review. *Postharvest Biol. Technol.* 91, 9–24.

Opara, U.L., Zou, Q., 2007. Sensitivity analysis of a CFD modelling system for airflow and heat transfer of fresh food packaging: Inlet air flow velocity and inside-package configurations. *Int. J. Food Eng.* 3, 1–13.

Parker, M.E., Bronlund, J.E., Mawson, A.J., 2006. Moisture sorption isotherms for paper and paperboard in food chain conditions. *Packag. Technol. Sci.* 193–209.

Parsons, R.A., Mitchell, F.G., Mayer, G., 1972. Forced-air cooling of palletized fresh fruit. *Trans. ASAE* 15, 729–731.

Parvini, M., 2011. Packaging and Material Handling, in: Farahani, R., Rezapour, S., Kardar, L. (Eds.), *Logistics Operations and Management*. Elsevier Inc., Amsterdam, pp. 155–180.

Patankar, S. V, Spalding, D.B., 1972. A calculation procedure for heat, mass and momentum transfer in three-dimensional parabolic flows. *Int. J. Heat Mass Transf.* 15, 1787–1806.

Pathare, P.B., Berry, T.M., Opara, U.L., 2016. Changes in moisture content and compression strength during storage of ventilated corrugated packaging used for handling apples. *Packag. Res.* 1, 1–6.

Pathare, P.B., Opara, U.L., 2014. Structural design of corrugated boxes for horticultural produce: A review. *Biosyst. Eng.* 125, 128–140.

Pathare, P.B., Opara, U.L., Vigneault, C., Delele, M.A., Al-Said, F.A.J., 2012. Design of packaging vents for cooling fresh horticultural produce. *Food Bioprocess Technol.* 5, 2031–2045.

Paunonen, S., Gregersen, Ø., 2010. The effect of moisture content on compression strength of boxes made of solid fiberboard with polyethylene coating - An experimental study. *J. Appl. Packag. Res.* 4, 223–242.

Peralta, P.N., 1995. Modeling wood moisture sorption hysteresis using the independent-domain theory. *Wood fiber Sci.* 27, 250–257.

Peralta, P.N., Bangi, A.P., 1998. Modeling wood moisture sorption hysteresis based on similarity hypothesis. Part 2. Capillary_Radii approach. *Wood Fiber Sci.* 30, 148–154.

Peters, C.C., Kellicutt, K.Q., 1965. *Effect of ventilating and handholes on compressive strength of fiberboard boxes.* Forest Products Laboratory, Madison, Wisconsin.

Peterson, W.S., Fox, T.S., 1989. Workable theory proves how boxes fail in compression, in: Maltenfort, G.G. (Ed.), *Performance and Evaluation of Shipping Containers*. Jelmar Publishing Co, Plainview, NY.

PPECB, 2015. PPECB - Annual Report 2014/2015. Cape Town.

PPECB, 2013. PPECB - Annual Report 2012/2013. Cape Town.

R Core Team, 2015. R: A Language and Environment for Statistical Computing. R Foundation for Statistical Computing, Vienna, Austria. URL http://www.R-project.org.

Radhakrishnan, H., Chatterjee, S.G., Ramarao, B. V, 2000. Steady-state moisture transport in a bleached kraft paperboard stack. *J. pulp Pap. Sci.* 26, 140–144.

Rahman, A.A., Abubakr, S., 2004. A finite element investigation of the role of adhesive in the buckling failure of corrugated fiberboard. *Wood Fiber Sci.* 36, 260–268.

Rahman, A.A., Urbanik, T.J., Mahamid, M., 2006. FE analysis of creep and hygroexpansion response of a corrugated fiberboarad to a moisture flow: A transient nonlinear analysis. *Wood Fiber Sci.* 38, 268–277.

Ramaswamy, H.S., Tung, M.A., 1981. Thermophysical properties of apples in relation to freezing. *J. Food Sci.* 46, 724–728.

Ravindra, M.R., Goswami, T.K., 2008. Comparative performance of precooling methods for the storage of mangoes (mangifera indica l. Cv. Amrapali). *J. Food Process Eng.* 31, 354–371.

Roache, P.J., 1994. Perspective: a method for uniform reporting of grid refinement studies. *J. Fluids Eng.* 116, 405–413.

Robertson, G.L., 2013. *Food Packaging: Principles and Practice*, 2nd ed. CRC Press, Boca-Raton, Florida

Rodríguez-Bermejo, J., Barreiro, P., Robla, J.I., Ruiz-García, L., 2007. Thermal study of a transport container. *J. Food Eng.* 80, 517–527.

Rojas, F., Kornhauser, I., Felipe, C., Cordero, S., 2001. Everett's sorption hysteresis domain theory revisited from the point of view of the dual site-bond model of disordered media. *J. Mol. Catal. A Chem.* 167, 141–155.

Saha, K., Harte, B., Burgess, G., Adudodla, S., 2010. Effect of freeze-thaw cycling on compression strength of folding cartons made from different materials. *J. Appl. Packag. Res.* 4, 257–269.

Salisbury, F.B., Ross, C.W., 1991. *Plant Physiology*, 4th ed. Belmont, CA.

Schoorl, D., Holt, J.E., 1982. Impact bruising in 3 apple pack arrangements. *J. Agric. Eng. Res.* 27, 507–512.

Schuur, C.C.M., 1988. *Packaging for fruits, vegetables and root crops*. Food and Agriculture Organization of the United Nations, Bridgetown, Barbados.

Seaborg, C.O., Simmonds, F.A., Baird, P.K., 1936. Sorption of water vapor by papermaking materials. *Ind. Eng. Chem.* 28, 1245–1250.

Sevillano, L., Sanchez-Ballesta, M.T., Romojaro, F., Flores, F.B., 2009. Physiological, hormonal and molecular mechanisms regulating chilling injury in horticultural species. Postharvest technologies applied to reduce its impact. *J. Sci. Food Agric.* 89, 555–573.

Simko, I., Jimenez-Berni, J.A., Furbank, R.T., 2015. Detection of decay in fresh-cut lettuce using hyperspectral imaging and chlorophyll fluorescence imaging. *Postharvest Biol. Technol.* 106, 44–52.

Singh, J., Bainbridge, P., Singh, S.P., Olsen, E., 2007. Variability in compression strength and deflection of corrugated containers as a function of positioning, operators, and climatic conditions. *J. Appl. Packag. Res.* 2, 89–102.

Singh, J., Olsen, E., Singh, S.P., Manley, J., Wallance, F., 2008. The effect of ventilation and hand holes on loss of compression strength in corrugated boxes. *J. Appl. Packag. Res.* 2, 227–238.

Skogman, R.E.T., Scheie, C.E., 1969. The effect of temperature on the moisture adsorption of kraft paper. *Tappi J.* 52, 489–490.

Smale, N.J., Moureh, J., Cortella, G., 2006. A review of numerical models of airflow in refrigerated food applications. *Int. J. Refrig.* 29, 911–930.

Söremark, C., Fellers, C., 1993. Mechano-sorptive creep and hygroexpansion of corrugated board in bending. *J. Pulp Pap. Sci.* 19, J19–J26.

Sørensen, G., Hoffmann, J., 2003. Moisture sorption in moulded fibre trays and effect on static compression strength. *Packag. Technol. Sci.* 16, 159–169.

Sousa-Gallagher, M.J., Mahajan, P. V, Mezdad, T., 2013. Engineering packaging design accounting for transpiration rate: Model development and validation with strawberries. *J. Food Eng.* 119, 370–376.

TAPPI, 2012. T804: Compression test of fiberboard shipping containers. International Safe Transit Association.

TAPPI, 2007a. T881: Edgewise compressive strength of corrugated fiberboard (short column test).

TAPPI, 2007b. T412: Edgewise compressive strength of corrugated fiberboard (short column test).

Tapsoba, M., Moureh, J., Flick, D., 2007. Airflow patterns in a slot-ventilated enclosure partially loaded with empty slotted boxes. *Int. J. Heat Fluid Flow* 28, 963–977.

Tapsoba, M., Moureh, J., Flick, D., 2006. Airflow patterns in an enclosure loaded with slotted pallets. *Int. J. Refrig.* 29, 899–910.

Thompson, J.F., 2004. *Pre-cooling and storage facilities, Agriculture Handbook Number 66: The Commercial Storage of Fruits, Vegetables, and Florist and Nursery Stocks.* University of California Department of Agriculture and Natural Resources, Davis, California.

Thompson, J.F., Mejia, D.C., Singh, R.P., 2010. Energy use of commercial forced-air coolers for fruit. *Appl. Eng. Agric.* 26, 919–924.

Thompson, J.F., Mitchell, F.G., Kasmire, R.F., 2002. Cooling Horticultural Commodities, in: Kader, A.A. (Ed.), *Postharvest Technology of Horticultural Crops*. University of California Department of Agriculture and Natural Resources, Davis, California, p. 101.

Thompson, J.F., Mitchell, F.G., Rumsey, T.R., Kasmire, R.F., Crisosto, C.H., 2008. *Commercial Cooling of Fruits, Vegetables, and Flowers*, Revised. ed. University of California Department of Agriculture and Natural Resources, Oakland, California.

Tutar, M., Erdogdu, F., Toka, B., 2009. Computational modeling of airflow patterns and heat transfer prediction through stacked layers' products in a vented box during cooling. *Int. J. Refrig.* 32, 295–306.

Twede, D., Selke, S.E.M., 2005a. *Cartons, crates and corrugated board: Handbook of paper and wood packaging technology*. DEStech Publications, Inc., Lancaster, Pennsylvania.

Twede, D., Selke, S.E.M., 2005b. Corrugated fibreboard structure and properties, in: *Cartons, Crates and Corrugated Board: Handbook of Paper and Wood Packaging Technology*. DEStech Publications, Inc., Lancaster, Pennsylvania, p. 517.

United Nations, 2015. World population prospects: The 2015 revision.

Urbanik, T.J., Frank, B., 2006. Box compression analysis of world-wide data spanning 46 years. *J. Wood Fiber Sci.* 38, 399–416.

USDA, 1986. commercial storage of fruits vegetables and florist and nursery stocks, in: *Agricultural Handbook Number 66*. United States Department of Agriculture.

van der Sman, R.G.M., 2003. Simple model for estimating heat and mass transfer in regular-shaped foods. *J. Food Eng.* 60, 383–390.

van der Sman, R.G.M., 2002. Prediction of airflow through a vented box by the Darcy-Forchheimer equation. *J. Food Eng.* 55, 49–57.

Van Zeebroeck, M., Tijskens, E., Dintwa, E., Kafashan, J., Loodts, J., De Baerdemaeker, J., Ramon, H., 2006. The discrete element method (DEM) to simulate fruit impact damage during transport and handling: Case study of vibration damage during apple bulk transport. *Postharvest Biol. Technol.* 41, 92–100.

Van Zeebroeck, M., Van linden, V., Ramon, H., De Baerdemaeker, J., Nicolaï, B.M., Tijskens, E., 2007. Impact damage of apples during transport and handling. Postharvest Biol. Technol. 45, 157–167.

Veraverbeke, E.A., Verboven, P., Van Oostveldt, P., Nicolaï, B.M., 2003. Prediction of moisture loss across the cuticle of apple (Malus sylvestris subsp. mitis (Wallr.)) during storage Part 1. Model development and determination of diffusion coefficient. *Postharvest Biol. Technol.* 30, 75–88.

Verboven, P., Flick, D., Nicolaï, B.M., Alvarez, G., 2006. Modelling transport phenomena in refrigerated food bulks, packages and stacks: basics and advances. *Int. J. Refrig.* 29, 985–997.

Vigh, L., Maresca, B., Harwood, J.L., 1998. Does the membrane's physical state control the expression of heat shock and other genes? *Trends Biochem. Sci.* 23, 369–374.

Vigneault, C., de Castro, L.R., 2005. Produce-simulator property evaluation for indirect airflow distribution measurement through horticultural crop package. *J. Food, Agric. Environ.* 3, 93–98.

Vigneault, C., de Castro, L. R., Gautron, G. 2004a. Effect of the presence of openings as container handles on cooling efficiency of horticultural package. In ASAE Annual Meeting, (paper no. 04e6105).

Vigneault, C., de Castro, L.R., Goyette, B., Markarian, N.R., Charles, M.T., Bourgeois, G., Foot, E.T.L., Cortez, L.A.B., 2007. Indirect airflow distribution measurement method for horticultural crop package design. *Can. Biosyst. Eng.* 49, 13–22.

Vigneault, C., Goyette, B., 2003. Effect of tapered wall container on forced-air circulation system. *Can. Biosyst. Eng.* 45, 3.23-3.26.

Vigneault, C., Goyette, B., 2002. Design of plastic container opening to optimize forced-air precooling of fruits and vegetables. *Appl. Eng. Agric.* 18, 73–76.

Vigneault, C., Markarian, N.R., Da Silva, A., Goyette, B., 2004b. Pressure drop during forced-air ventilation of various horticultural produce in containers with different opening configurations. *Trans. ASAE* 47, 807–814.

Wahba, M., Nashed, S., 1957. Moisture relations of cellulose. *J. Textle Inst.* 48, T1–T20.

Wang, C.Y., 1990. *Chilling Injury of Horticultural Crops*. CRC Press, Boca Raton, Florida.

Wang, D., 2009. Impact behavior and energy absorption of paper honeycomb sandwich panels. *Int. J. Impact Eng.* 36, 110–114.

Wang, J.Z., Dillard, D.A., Kamke, F.A., 1991. A review of transient moisture effects in materials. *J. Mater. Sci.* 26, 5113–5126.

Wang, S., Tang, J., Cavalieri, R.P., 2001. Modeling fruit internal heating rates for hot air and hot water treatments. *Postharvest Biol. Technol.* 22, 257–270.

Waters, T.R., Putz-Anderson, V., Garg, A., 1994. *Applications Manual for the Revised NIOSH Lifting Equation,* U.S. Department of Health and Human Services. Cincinnati, Ohio.

Xi, W., Zhang, B., Shen, J., Sun, C., Xu, C., Chen, K., 2012. Intermittent warming alleviated the loss of peach fruit aroma-related esters by regulation of AAT during cold storage. *Postharvest Biol. Technol.* 74, 42–48.

Xia, B., Sun, D.-W., 2002. Applications of computational fluid dynamics (cfd) in the food industry: a review. *Comput. Electron. Agric.* 34, 5–24.

Zhao, C.-J., Han, J.-W., Yang, X.T., Qian, J.P., Fan, B.L., 2016. A review of computational fluid dynamics for forced-air cooling process. *Appl. Energy* 168, 314–331.

Zou, Q., Opara, U.L., McKibbin, R., 2006a. A CFD modeling system for airflow and heat transfer in ventilated packaging for fresh foods: II. Computational solution, software development, and model testing. *J. Food Eng.* 77, 1048–1058.

Zou, Q., Opara, U.L., McKibbin, R., 2006b. A CFD modeling system for airflow and heat transfer in ventilated packaging for fresh foods: I. Initial analysis and development of mathematical models. *J. Food Eng.* 77, 1037–1047.